Intracranial Pressure Monitoring in Cerebrospinal Fluid Dynamics Disturbances

By

Linda D'Antona

Submitted in accordance with the requirements for the degree of

Doctor of Philosophy (PhD)



University College London

Queen Square Institute of Neurology

2022

Declaration

I, Linda D'Antona confirm that the work presented in this thesis is my own. Where information has been derived from other sources, I confirm that this has been indicated in the thesis.

Dr Linda D'Antona

Abstract

There are numerous gaps in the knowledge of Intracranial Pressure (ICP) physiology and Cerebrospinal Fluid (CSF) dynamics. This PhD answers some of the research questions posed by these gaps, through the use of invasive ICP monitoring in patients with suspected CSF dynamics disturbances.

Research on CSF dynamics disturbances has mainly focused on conditions that cause high ICP, whilst only sparse attention has been centred on low CSF pressure/volume states. Chapter 3 and chapter 4 of this thesis are focused on Spontaneous Intracranial Hypotension (SIH). Chapter 3 is a comprehensive systematic review and meta-analysis of the clinical presentation, investigation findings and treatment outcomes of this disease. Chapter 4 is an observational study that investigated the utility of invasive ICP monitoring when there is diagnostic uncertainty for SIH. This study demonstrates that, in selected cases, ICP monitoring can be useful and confirm a low-pressure state in 8% of the patients and identify a paradoxical clinical presentation with an underlying high-pressure state in 16% of the patients.

Chapters 5 and 6 provide evidence on the way that ICP and brain compliance respond to external variables, such as changes in posture and shunt setting adjustments. Chapter 5 is a retrospective observational study

that describes the changes of ICP and pulse amplitude with different postures. Chapter 6 is a retrospective observational study investigating the effect of valve setting adjustments on ICP. This study demonstrates that paradoxical changes in ICP following differential pressure valves setting changes can occur.

Chapters 7 and 8 investigate the possibility of replacing invasive ICP monitoring with non-invasive biomarkers of raised ICP. Chapter 7 demonstrated the association between higher ICP measurements and the absence of spontaneous retinal venous pulsations detected with infrared video recordings. Chapter 8 demonstrates the utility of integrating ophthalmic and imaging biomarkers to predict raised ICP.

Impact Statement

This PhD thesis has improved the knowledge on various aspects of cerebrospinal fluid dynamics, providing information that is (or could be) useful for clinical practice, academia and for the development of new technologies.

Firstly, while most research on intracranial pressure monitoring and cerebrospinal fluid dynamics has traditionally been conducted in patients affected by acute diseases with suspected intracranial hypertension (e.g., traumatic brain injury), this PhD has focused on patients affected by chronic symptoms and managed in the elective setting. In addition, this thesis also includes studies dedicated to the less studied low cerebrospinal fluid pressure syndromes. The conduction of this experimental work has raised many new research questions, and this will hopefully help other clinicians and researchers to identify future research targets.

In particular, the systematic review on spontaneous intracranial hypotension has revealed a profound heterogeneity in the way that this disease is diagnosed and managed. Since the publication of this work, a national patient survey has revealed the experiences of patients with this disease, further highlighting the need for optimisation and standardisation of the management protocols for this disease. In addition, a national special interest group was created with the aim of producing national guidelines for the

management of spontaneous intracranial hypotension; these guidelines have the potential to improve the path of patients diagnosed with this disease in the future. In addition, the systematic review has highlighted specific aspects of the diagnosis and treatment of spontaneous intracranial hypotension that should be investigated by future research.

The use of cerebrospinal fluid shunts is relatively common in neurosurgery, but despite the technological advances of the last decades (e.g., gravitational valves, telemetric intracranial pressure readers), we are still far from the creation of a closed-loop shunt and the success of shunt systems still relies on the ability of the clinician to correctly interpret the patient's signs and symptoms and adjust the shunt accordingly. Two experimental chapters of this thesis (chapters 5 and 6) describe the influence that external factors, such as posture and valve settings adjustments, have on cerebrospinal fluid dynamics. In addition to its clinical relevance, the information derived from these studies may be commercially useful for the future development of programmable closed-loop shunts that are able to provide automated patient-tailored treatment.

Finally, this thesis has also provided new information on imaging and ophthalmic biomarkers of intracranial pressure that has the potential to reduce the need for invasive cerebrospinal pressure measurements and to improve the triage of patients with suspected raised intracranial pressure. This work has had a clinical impact in our hospital where the assessment of

these ophthalmic and imaging biomarkers now occurs routinely. In addition, this work could have an impact outside of academia with the development of technologies that allow automated analyses of these biomarkers.

Acknowledgements

First of all, I would like to thank all the patients that have participated in this research, for the incredible patience and cooperativeness they demonstrated during such a delicate time of their lives. The thought that my research could, in any way, bring any improvement to the experience of future patients was the main drive for my work.

I am immensely grateful to my PhD supervisors for their continued support, dedication and encouragement throughout these years. Thank you, Mr Toma, Mr Bremner and Prof Matharu, I could not have dreamed of better supervisors and mentors!

I would also like to thank Mr Watkins and Mr Thorne, who have been essential for the development of my academic skills and have supported my research with interest and enthusiasm.

During this time, I have had the opportunity to work within a phenomenal clinical and academic environment, therefore I would like to thank all the exceptional colleagues for their support and for making my academic journey a special experience. In particular, thanks to Simon Thompson, Joana Ramos, Jim McHugh, Junie Koay, Victoria Fleming, Vanessa Bassan, Ben Thomas and all the members of the Queen Square Hydrocephalus Group. Thanks to B.Braun for funding my research fellowship. A special

acknowledgement goes to Claudia Craven, in addition to her immeasurable support in my research activities, she has been an inspiring example of an academic neurosurgeon and colleague.

The help of my mentors and colleagues was of vital importance, however, I could not have completed this PhD without the support of my friends and family. *Mamma e papà, grazie per aver sempre creduto in me*. Elisa, Tore, Sissy, Enrico, Emanuele, Sara e Giulio, *grazie per esserci sempre stati*.

Finally, I would like to dedicate this thesis to Nina and Josè. Josè, words are not enough to express my love and gratitude. *Vi amo infinitamente*.

Publications

The following publications are the result of the work conducted during the period of my PhD study. The publications marked with an asterisk (*) are part of the work presented in this thesis, the remaining publications describe other collaborative work not included in this thesis.

Journal articles

- (*) D'Antona L, Craven CL, Bremner F, Matharu MS, Thorne L, Watkins LD, Toma AK. Effect of position on intracranial pressure and compliance: a cross-sectional study including 101 patients. J Neurosurg. 2021 Oct 29:1-9.
- (*) D'Antona L, Asif H, Craven CL, McHugh JA, Vassiliou A, Thorne L, Matharu MS, Watkins LD, Bremner F, Toma AK. Brain MRI and Ophthalmic Biomarkers of Intracranial Pressure. Neurology. 2021 Apr 13;96(22):e2714–23.
- (*) D'Antona L, Jaime Merchan MA, Vassiliou A, Watkins LD, Davagnanam I, Toma AK, Matharu MS. Clinical Presentation, Investigation Findings, and Treatment Outcomes of Spontaneous Intracranial Hypotension Syndrome: A Systematic Review and Meta-analysis. JAMA Neurol. 2021 Mar 1;78(3):329-337.
- (*) D'Antona L, Craven CL, Merchan MAJ, Thompson SD, Bremner F, Thorne L, Matharu MS, Watkins LD, Toma AK. Paradoxical response

of intracranial pressure to shunt valve setting adjustments. Acta Neurochir (Wien). 2020 Oct;162(10):2451-2458.

- (*) McHugh JA, D'Antona L, Toma AK, Bremner FD. Spontaneous Venous Pulsations Detected With Infrared Videography. J Neuroophthalmol. 2020 Jun;40(2):174-177.
- (*) D'Antona L, McHugh JA, Ricciardi F, Thorne LW, Matharu MS, Watkins LD, Toma AK, Bremner FD. Association of Intracranial Pressure and Spontaneous Retinal Venous Pulsation. JAMA Neurol. 2019 Sep 9;76(12):1502–5.
- D'Antona L, Craven CL, Haq H, Thorne L, Matharu MS, Toma AK, Watkins LD. A case of recurrent flight-induced cerebrospinal fluid shunt overdrainage. Br J Neurosurg. 2022 May 13:1-4.
- Goel A, Asif H, Craven C, D'Antona L, Das P, Thorne L, Toma A. Regional Scalp Blockade for Painless Removal ofIntracranial Pressure Bolts: Technical Note and Patient-Reported Outcomes. World Neurosurg. 2022 Mar 12;162:43-46.
- Luoma AMV, Douglas DR, D'Antona L, Toma AK, Smith M. Using the Postoperative Morbidity Survey to Measure Morbidity After Cranial Neurosurgery. J Neurosurg Anesthesiol. 2022 Apr 1;34(2):201-208.
- McHugh JA, D'Antona L, Toma AK, Bremner FD. Spontaneous Venous Pulsations Detected With Infrared Videography: Response. J Neuroophthalmol. 2021 Dec 28.
- Palasz J, D'Antona L, Farrell S, Elborady MA, Watkins LD, Toma AK. External ventricular drain management in subarachnoid haemorrhage:

a systematic review and meta-analysis. Neurosurg Rev. 2022 Feb;45(1):365-373.

- Funnell JP, D'Antona L, Craven CL, Thorne L, Watkins LD, Toma AK. Ultra-low-pressure hydrocephalic state in NPH: benefits of therapeutic siphoning with adjustable antigravity valves. Acta Neurochir (Wien). 2020 Dec;162(12):2967-2974.
- D'Antona L, Thompson SD, Thorne L, Watkins LD, Toma AK. Letter: Thirty-Day Hospital Readmission and Surgical Complication Rates for Shunting in Normal Pressure Hydrocephalus: A Large National Database Analysis. Neurosurgery. 2020;87(6):E707-e8.
- D'Antona L, Palasz J, Haq H, Usher I, De-Saram S, Curtis C, Thorne L, Watkins LD, Toma AK. Letter to the Editor: Risk of Hospital-Acquired Coronavirus Disease 2019 (COVID-19) Infection During Admission for Semiurgent Neurosurgical Procedures. World Neurosurg. 2020 Aug;140:486-488.
- Pradini-Santos L, Craven CL, Usher I, Mullins S, D'Antona L, Al-Ahmad S, Abuhusain H, Sayal PP. A Novel Neurosurgery Referral Course: Feasibility, Validation, and Inferences for Patient Care. J Surg Educ. 2020 Nov-Dec;77(6):1615-1622.
- Craven CL, Asif H, Curtis C, Thompson SD, D'Antona L, Ramos J, Thorne L, Watkins LD, Toma AK. Interpretation of lumbar cerebrospinal fluid leukocytosis after cranial surgery: The relevance of aseptic meningitis. J Clin Neurosci. 2020 Jun;76:15-19.

- D'Antona L, Blamey SC, Craven CL, Sewell D, Manohara S, Leemans M, Worby S, Thompson SD, Golahmadi AK, Funnell JP, Thorne L, Watkins LD, Luoma AMV, Toma AK. Early Postoperative Outcomes of Normal Pressure Hydrocephalus: Results of a Service Evaluation. J Neurosurg Anesthesiol. 2021;33(3):247-53.
- D'Antona L, Matharu M. Identifying and managing refractory migraine: barriers and opportunities? J Headache Pain. 2019 Aug 23;20(1):89.
- Craven CL, Ramkumar R, D'Antona L, Thompson SD, Thorne L, Watkins LD, Toma AK. Natural history of ventriculomegaly in adults: a cluster analysis. J Neurosurg. 2019 Feb 8:1-8.
- Dasgupta D, D'Antona L, Aimone Cat D, Toma AK, Curtis C, Watkins LD, Thorne L. Simulation workshops as an adjunct to perioperative care bundles in the management of external ventricular drains: improving surgical technique and reducing infection. J Neurosurg. 2018 Oct 1:1-5.
- Funnell JP, Craven CL, Thompson SD, D'Antona L, Chari A, Thorne L, Watkins LD, Toma AK. Pulsatile versus non-pulsatile tinnitus in idiopathic intracranial hypertension. Acta Neurochir (Wien). 2018 Oct;160(10):2025-2029.
- Funnell JP, Craven CL, D'Antona L, Thompson SD, Chari A, Thorne L, Watkins LD, Toma AK. Intracranial pressure in patients with papilloedema. Acta Neurol Scand. 2018 Aug;138(2):137-142.

- Craven CL, Chapman MD, D'Antona L, Thompson SD, Lakdawala N, Zetterberg H, Watkins LD, Toma AK. Lumbar drains can affect CSF biomarker levels. J Clin Pathol. 2019 Jan;72(1):91-92.
- Mallucci CL, Jenkinson MD, Conroy EJ, Hartley JC, Brown M, Dalton J, Kearns T, Moitt T, Griffiths MJ, Culeddu G, Solomon T, Hughes D, Gamble C; BASICS Study collaborators. Antibiotic or silver versus standard ventriculoperitoneal shunts (BASICS): a multicentre, single-blinded, randomised trial and economic evaluation. Lancet. 2019 Oct 26;394(10208):1530-1539.
- Fernández-Méndez R, Richards HK, Seeley HM, Pickard JD, Joannides AJ; UKSR collaborators. Current epidemiology of cerebrospinal fluid shunt surgery in the UK and Ireland (2004-2013). J Neurol Neurosurg Psychiatry. 2019 Jul;90(7):747-754.
- Piper RJ, Afshari FT, Soon WC, Kolias AG, Dyson EW, Watkins L, Laing R, Lo WB, Jayamohan J; British Neurosurgical Trainee Research Collaborative (BNTRC). UK Chiari 1 Study: protocol for a prospective, observational, multicentre study. BMJ Open. 2021 Apr 12;11(4):e043712.

Book chapters

- D'Antona L, Matharu MS. Headache in Postural Tachycardia Syndrome. In: Gall N, Kavi L, Lobo M, editors. Postural Tachycardia

Syndrome: A Concise and Practical Guide to Management and Associated Conditions. Switzerland: Springer Nature; 2020. p. 93-102.

- D'Antona L, Cecchini AP, Leone M, Matharu M. Neuromodulation in Cluster Headache. In: Lambru G, Lanteri-Minet M, editors. Neuromodulation in Headache and Facial Pain Management. Headache. Switzerland: Springer; 2019. p. 173-90.

Table of Contents

LIST OF TABLES……24

LIST OF FIGURES……..26

LIST OF ABBREVIATIONS……..35

CHAPTER 1. INTRODUCTION 40

1.1. PHYSIOLOGY OF CEREBROSPINAL FLUID DYNAMICS..... 40

1.1.1. Cerebrospinal fluid function..... 41

1.1.2. Cerebrospinal fluid production and the role of the choroid plexus 42

1.1.3. Cerebrospinal fluid movement: bulk flow versus pulsatile flow 45

1.1.4. Cerebrospinal fluid absorption 48

1.1.5. The glymphatic system 49

1.2. INTRACRANIAL PRESSURE MONITORING..... 52

1.2.1. Intracranial pressure physiology: importance of the intracranial compliance 52

1.2.2. Intracranial pressure waveform: mean ICP and markers of compliance 56

1.2.3. Effect of posture on CSF dynamics: hydrostatic indifferent point and jugular vein collapse 62

1.2.4. Methods of intracranial pressure monitoring 63

1.3. CEREBROSPINAL FLUID DYNAMICS DISTURBANCES AND APPLICATIONS OF ELECTIVE CONTINUOUS INTRACRANIAL PRESSURE MONITORING 70

1.3.1. Hydrocephalus 71

1.3.2. Idiopathic Intracranial Hypertension (IIH) 72

1.3.3. Chiari Malformation type I 79

1.3.4. Normal Pressure Hydrocephalus 85

1.3.5. Low CSF pressure/volume syndromes 92

1.4. AIMS OF THIS THESIS 97

CHAPTER 2. METHODS: ELECTIVE 24-HOUR INTRACRANIAL PRESSURE MONITORING AT THE NATIONAL HOSPITAL FOR NEUROLOGY AND NEUROSURGERY 100

2.1. INDICATIONS FOR ELECTIVE ICP MONITORING 101

2.2. ICP MONITORING EQUIPMENT 105

2.3. DESCRIPTION OF THE SURGICAL PROCEDURE 107

2.4. DURATION OF 24-HOUR ICP MONITORING 108

2.5. PATIENTS' ACTIVITIES DURING ICP MONITORING 109

2.6. DATA ANALYSIS AND ICP MONITORING REPORT 110

2.7. ICP MONITORING RESULTS 116

2.8. LIMITATIONS 116

CHAPTER 3. SPONTANEOUS INTRACRANIAL HYPOTENSION SYNDROME: A SYSTEMATIC REVIEW AND META-ANALYSIS 120

3.1. ABSTRACT 120

3.1.1. Background 120

3.1.2. Methods 120

3.1.3. Results 121

3.1.4. Conclusion 121

3.2. INTRODUCTION 122

3.3. METHODS 124

3.3.1. Search strategy 124

3.3.2. Selection criteria 124

3.3.3. Risk of bias 125

3.3.4. Data extraction 126

3.3.5. Statistical analysis 128

3.4. RESULTS 130

3.4.1. Demographic characteristics 133

3.4.2. Risk factors and associated factors 135

3.4.3. Clinical presentation 137

3.4.4. Assessment and Diagnosis 157

3.4.5. Treatments and outcomes 183

3.5. DISCUSSION 192

3.5.1. Demographics and phenotype of spontaneous intracranial hypotension 192

3.5.2. The role of imaging in the diagnosis of spontaneous intracranial hypotension 193

3.5.3. The role of lumbar punctures in the diagnosis of spontaneous intracranial hypotension 195

3.5.4. Treatment outcomes 196

3.5.5. Proposed algorithm for the diagnosis and management of spontaneous intracranial hypotension 198

3.5.6. Limitations 200

3.6. CONCLUSIONS 200

CHAPTER 4. INTRACRANIAL PRESSURE MONITORING IN PATIENTS WITH SPONTANEOUS ONSET OF ORTHOSTATIC HEADACHE 201

4.1. ABSTRACT 201

4.1.1. Introduction 201

4.1.2. Methods 201

4.1.3. Results 202

4.1.4. Conclusions 202

4.2. INTRODUCTION 203

4.3. METHODS 205

4.3.1. Ethics 205

4.3.2. Patients' selection 205

4.3.3. Intracranial pressure monitoring methods 207

4.3.4. Data extraction 208

4.3.5. Interpretation of ICP monitoring results 208

4.3.6. Statistical analysis 209

4.4. RESULTS 209

4.4.1. Clinical presentation 210

4.4.2. Investigations and treatments prior to ICP monitoring 213

4.4.3. ICP monitoring results 222

4.5. DISCUSSION 229

4.6. CONCLUSIONS 234

CHAPTER 5. EFFECT OF POSITION ON INTRACRANIAL PRESSURE AND BRAIN COMPLIANCE 235

5.1. ABSTRACT 235

5.1.1. Background 235

5.1.2. Methods 235

5.1.3. Results 236

5.1.4. Conclusions 236

5.2. INTRODUCTION 237

5.3. METHODS 239

5.3.1. ICP monitoring method 240

5.3.2. Short exercise battery 241

5.3.3. Variables 241

5.3.4. Statistical analysis 242

5.4. RESULTS 244

5.4.1. Effect of position on ICP 246

5.4.2. Effect of position on PA 254

5.4.3. Effect of day/night cycle on ICP and pulse amplitude in patients without shunts 257

5.4.4. Effect of day/night cycle on ICP and pulse amplitude in patients with shunts 259

5.4.5. Subgroup analysis of ICP monitoring results in 'normal', 'abnormal' and 'shunt' groups 259

5.5. DISCUSSION 262

5.6. CONCLUSIONS 267

CHAPTER 6. PARADOXICAL RESPONSE OF INTRACRANIAL PRESSURE TO SHUNT VALVE SETTING ADJUSTMENTS 268

6.1. ABSTRACT 268

6.1.1. Background 268

6.1.2. Methods 268

6.1.3. Results 268

6.1.4. Conclusion 269

6.2. INTRODUCTION 269

6.3. METHODS 271

6.3.1. Patients selection 271

6.3.2. ICP monitoring 272

6.3.3. Data collection 272

6.3.4. Statistical analysis 273

6.4. RESULTS 275

6.5. DISCUSSION 283

CHAPTER 7. ASSOCIATION OF INTRACRANIAL PRESSURE AND SPONTANEOUS RETINAL VENOUS PULSATION 289

7.1. ABSTRACT 289

7.1.1. Background 289

7.1.2. Methods 289

7.1.3. Results 290

7.1.4. Conclusions 290

7.2. BACKGROUND 291
7.3. METHODS 292
7.3.1. Patient selection 293
7.3.2. ICP monitoring methods 293
7.3.3. Ophthalmology assessments and IR video recording of SVP 294
7.3.4. Data collection 294
7.3.5. Statistical analysis 295
7.4. RESULTS 296
7.5. DISCUSSION 302
7.6. CONCLUSIONS 306
CHAPTER 8. BRAIN MRI AND OPHTHALMIC BIOMARKERS OF INTRACRANIAL PRESSURE 308
8.1. ABSTRACT 308
8.1.1. Background 308
8.1.2. Methods 308
8.1.3. Results 309
8.1.4. Conclusions 309
8.2. INTRODUCTION 309
8.3. METHODS 311
8.3.1. Participants 311
8.3.2. ICP monitoring 312
8.3.3. Brain MRI imaging assessment 313

8.3.4. Ophthalmic Assessment 315

8.3.5. Statistical analysis 316

8.4. RESULTS 317

8.4.1. ICP monitoring results by normal/abnormal biomarker 321

8.4.2. Time-ICP burden analysis 325

8.4.3. Time-PA burden analysis 331

8.4.4. Biomarkers and their association with ICP 337

8.4.5. Positive and negative predictive value of the 6 biomarkers .. 340

8.4.6. A comparison of brain MRI and ophthalmic biomarkers domains 342

8.5. DISCUSSION 345

8.6. CONCLUSIONS 351

CHAPTER 9. DISCUSSION 353

9.1. EVIDENCE ON SPONTANEOUS INTRACRANIAL HYPOTENSION 353

9.2. THE ROLE OF ICP MONITORING IN SPONTANEOUS INTRACRANIAL HYPOTENSION 356

9.3. EFFECT OF POSITION AND VALVE SETTING CHANGES ON CSF DYNAMICS 357

9.4. OPHTHALMIC AND IMAGING MARKERS OF RAISED ICP 359

9.5. FUTURE DIRECTIONS 360

CHAPTER 10. APPENDICES 363

CHAPTER 11. BIBLIOGRAPHY 373

List of Tables

Table 1-1: Diagnostic criteria for a definite diagnosis of idiopathic intracranial hypertension by Friedman *et al.* (2013). 73

Table 3-1: Variables included in the systematic review 126

Table 3-2: Inclusion criteria for meta-analyses 129

Table 3-3: Diagnostic criteria used to make diagnosis of spontaneous intracranial hypotension in the selected articles 133

Table 3-4: Risk factors associated with spontaneous intracranial hypotension 136

Table 3-5: Clinical presentation of spontaneous intracranial hypotension patients 138

Table 3-6: Treatment of spontaneous intracranial hypotension and outcomes 184

Table 4-1: Central location of orthostatic headache 211

Table 4-2: Summary of patients' investigation findings, treatment outcomes and intracranial pressure monitoring results 214

Table 4-3: Clinical presentation and investigation findings of patients with orthostatic headache stratified by intracranial pressure monitoring results 227

Table 5-1: Patients' characteristics and underlying diagnoses. 245

Table 5-2: Twenty-four-hour and exercise battery intracranial pressure (ICP) monitoring results stratified by type of monitor in patients without shunts 248

Table 5-3: Twenty-four-hour and exercise battery intracranial pressure (ICP) monitoring results stratified by type of monitor in patients with CSF diversion shunts 250

Table 5-4: Adjusted multiple regression models testing the association between position and pulse amplitude (PA) stratified by monitor type.256

Table 5-5: ICP monitoring results of 20 patients in the 'normal' group 261

Table 6-1: Population baseline characteristics 276

Table 6-2: Comparison of baseline demographic, clinical, shunt and intracranial pressure characteristics between three groups of patients with different response to valve setting adjustment: ‘expected’, ‘paradoxical’ and ‘no effect’ groups. 279

Table 7-1: Results of ICP monitoring and ophthalmic assessments 298

Table 8-1: Baseline patients' characteristics..... 319

Table 8-2: Intracranial pressure monitoring results (in mmHg) stratified by imaging and ophthalmic biomarkers..... 321

Table 8-3: Sensitivity, specificity, Positive Predictive Value (PPV) and Negative Predictive Value (NPV) of the biomarkers for the identification of raised intracranial pressure. 342

Table 10-1: Diagnostic criteria for spontaneous intracranial hypotension .. 363

Table 10-2: List of selected studies and inclusion for meta-analyses..... 364

List of Figures

Figure 1-1: Cerebral autoregulation 53

Figure 1-2: Intracranial pressure-volume curve. 54

Figure 1-3: Intracranial pressure waveform components 57

Figure 1-4: Intracranial pressure-volume curve and pulse amplitude changes 58

Figure 1-5: Presentation of different B waves sub-classification patterns. Each is illustrated by two computer-generated examples: column A simulating ICP recordings and column B showing an artistic rendering.61

Figure 1-6: Sites of cranial invasive intracranial pressure monitoring 65

Figure 2-1: Flowchart of 10 steps ICP monitoring at NHNN 102

Figure 2-2: Raumedic NEUROVENT-P (A) and Spiegelberg (B) ICP monitoring sensors 105

Figure 2-3: MPR 1 Raumedic (A) and Spiegelberg (B) ICP monitors..... 105

Figure 2-4: Procedure of ICP monitor insertion at NHNN. A: equipment; B: Burr hole with hand drill in the right frontal area; C: Insertion of ICP monitoring sensor; D: Final result; E: Connection of ICP monitor and first static ICP and waveform check 107

Figure 2-5: Minute-by-minute ICP and pulse amplitude data after ICM+ analysis..... 112

Figure 2-6: Example of 24-hour ICP monitoring report. A. Summary results stratified by 24-hour, day and night; B. Pressure/Time graph with Mean ICP (green) and mean systolic/diastolic ICP (blue); C: frequency distribution graph; D: pulse amplitude/ICP scatter plot and linear regression stratified by day (orange, d) and night (blue, n). 115

Figure 3-1: Flowchart of the articles selection process..... 131

Figure 3-2: Age meta-analysis (mean years)..... 134

Figure 3-3: Sex meta-analysis (proportion of female patients) 135

Figure 3-4: Signs and symptoms of spontaneous intracranial hypotension 140

Figure 3-5: Symptoms duration meta-analysis (mean days) 141

Figure 3-6: Meta-analysis of proportions of patients with headache 142

Figure 3-7: Meta-analysis of proportions of patients without headache 143

Figure 3-8: Meta-analysis of proportions of patients with orthostatic headache 144

Figure 3-9: Meta-analysis of proportions of patients with non-orthostatic headache 145

Figure 3-10: Meta-analysis of proportions of headache location (diffuse) .. 146

Figure 3-11: Meta-analysis of proportions of headache location (occipital) 146

Figure 3-12: Meta-analysis of proportions of headache location (frontal)... 147

Figure 3-13: Meta-analysis of proportions of headache location (fronto-occipital) 147

Figure 3-14: Meta-analysis of proportions of headache location (temporal) 148

Figure 3-15: Meta-analysis of proportions of patients with nausea/vomiting 149

Figure 3-16: Meta-analysis of proportions of patients with neck pain/stiffness 150

Figure 3-17: Meta-analysis of proportions of patients with tinnitus..... 151

Figure 3-18: Meta-analysis of proportions of patients with dizziness 151

Figure 3-19: Meta-analysis of proportions of patients with hearing disturbances 152

Figure 3-20: Meta-analysis of proportions of patients with photophobia 153

Figure 3-21: Meta-analysis of proportions of patients with cognitive symptoms 153

Figure 3-22: Meta-analysis of proportions of patients with diplopia 154

Figure 3-23: Meta-analysis of proportions of patients with other ear-related symptoms 154

Figure 3-24: Meta-analysis of proportions of patients with vertigo 155

Figure 3-25: Meta-analysis of proportions of patients with movement disorders 155

Figure 3-26: Meta-analysis of proportions of patients with back pain 156

Figure 3-27: Meta-analysis of proportions of patients with other visual symptoms 156

Figure 3-28: Meta-analysis of proportions of patients with reduced consciousness 157

Figure 3-29: Meta-analysis of proportions of diffuse pachymeningeal enhancement (DPE) in brain MRI 159

Figure 3-30: Meta-analysis of proportions of subdural collections (SDC) in brain MRI 160

Figure 3-31: Meta-analysis of proportions of brain sagging brain MRI 161

Figure 3-32: Meta-analysis of proportions of enlarged pituitary gland (EPG) in brain MRI 162

Figure 3-33: Meta-analysis of proportions of venous engorgement in brain MRI 163

Figure 3-34: Meta-analysis of proportions of normal brain MRI 163

Figure 3-35: Brain MRI findings of spontaneous intracranial hypotension . 164

Figure 3-36: Spinal imaging findings of Spontaneous Intracranial Hypotension (SIH). 166

Figure 3-37: Meta-analysis of proportions of positive findings in spinal MRI 167

Figure 3-38: Meta-analysis of proportions of positive findings in CT myelography (CTM) 167

Figure 3-39: Meta-analysis of proportions of positive findings in MR myelography 168

Figure 3-40: Meta-analysis of proportions of positive findings in MR myelography with intrathecal gadolinium 169

Figure 3-41: Meta-analysis of proportions of positive findings in radionuclide cisternography 170

Figure 3-42: Meta-analysis of proportions of positive findings in digital subtraction myelography 171

Figure 3-43: Meta-analysis of proportions of positive findings in digital subtraction myelography performed in lateral decubitus position 172

Figure 3-44: Meta-analysis of proportions of leak location (cervical) 174

Figure 3-45: Meta-analysis of proportions of leak location (cervico-thoracic) 175

Figure 3-46: Meta-analysis of proportions of leak location (thoracic) 176

Figure 3-47: Meta-analysis of proportions of leak location (thoraco-lumbar) 177

Figure 3-48: Meta-analysis of proportions of leak location (lumbar) 178

Figure 3-49: Meta-analysis of proportions of leak location (sacral) 179

Figure 3-50: Meta-analysis of proportions of leak location (multiple) 180

Figure 3-51: Meta-analysis of proportions of lumbar puncture opening pressure (low) 181

Figure 3-52: Meta-analysis of proportions of lumbar puncture opening pressure (normal) 182

Figure 3-53: Meta-analysis of proportions of lumbar puncture opening pressure (high) 183

Figure 3-54: Meta-analysis of proportions of successful conservative treatment 185

Figure 3-55: Meta-analysis of proportions of unsuccessful conservative treatment 186

Figure 3-56: Epidural Blood Patches (EBP) outcomes. Pooled estimates of proportions (95% CI) of successful EBP treatment stratified by EBP technique (non-targeted/targeted, small/large)..... 187

Figure 3-57: Meta-analysis of proportions of successful first epidural blood patch..... 188

Figure 3-58: Meta-analysis of proportions of successful non-targeted EBP189

Figure 3-59: Meta-analysis of proportions of successful targeted EBP 189

Figure 3-60: Meta-analysis of proportions of successful small EBP..... 190

Figure 3-61: Meta-analysis of proportions of successful large EBP 190

Figure 3-62: Flow-chart of proposed diagnostic pathway for spontaneous intracranial hypotension. Investigations are in blue, treatments in yellow. DSM: Digital Subtraction Myelography; MRM: MRI Myelogram; MDT: Multidisciplinary Team..... 199

Figure 4-1: Headache intensity in Verbal Reporting Scale (VRS). 212

Figure 4-2: Median 24-hour Intracranial Pressure (ICP) stratified by group (normal/borderline, high or low ICP). Means and standard deviations are displayed. 223

Figure 4-3: Median Day Intracranial Pressure (ICP) stratified by group (normal/borderline, high or low ICP). Means and standard deviations are displayed. 224

Figure 4-4: Median Night Intracranial Pressure (ICP) stratified by group (normal/borderline, high or low ICP). Means and standard deviations are displayed. 225

Figure 5-1: Example of intracranial pressure (ICP) monitoring recording during the short exercise battery.100 Hz raw ICP measurements are displayed. 247

Figure 5-2: Mean intracranial pressure (ICP) with standard deviations in different body positions stratified by shunt presence..... 252

Figure 5-3: Scatter plot and curve of best fit of pulse amplitude (PA) and intracranial pressure (ICP) measurements for 101 patients. 254

Figure 5-4: Mean pulse amplitude (PA) with standard deviations in different body positions stratified by shunt presence..... 255

Figure 5-5: Scatter plot of median day/night intracranial pressure (ICP) and pulse amplitude (PA) for Spiegelberg (A-B) and Raumedic sensors (C-D) in patients without shunt. Line of best fit and results of adjusted linear regression models are displayed. β is used to indicate the slope coefficient of the linear regression analysis. 258

Figure 6-1: Flow diagram of patients' selection process and reasons for exclusion..... 275

Figure 6-2: Summary of pre- and post-shunt adjustment night ICP (mean and SD) stratified by direction of valve setting adjustment (upwards/downwards) and effect of valve adjustment on ICP (Exp: expected effect, No: no effect, Par: paradoxical effect). 278

Figure 6-3: Scatter plot and line of best fit of night intracranial pressure change (mmHg) and magnitude of Medtronic Strata setting adjustment (post-adjustment setting minus baseline setting). 282

Figure 6-4: Scatter plot and line of best fit of night intracranial pressure change (mmHg) and magnitude of Miethke ProGAV setting adjustment (post-adjustment setting minus baseline setting). 283

Figure 7-1: Mean (SD) Simultaneous Intracranial Pressure (ICP) Measurements by Spontaneous Venous Pulsation Grade 300

Figure 7-2: Ranked simultaneous ICP stratified by presence or absence of SVP 301

Figure 7-3: Receiver Operating Characteristics Curve Plotting the Predictive Value of Spontaneous Venous Pulsation in Determining Intracranial Pressure 302

Figure 8-1: Example of the brain MRI biomarkers of intracranial hypertension. 315

Figure 8-2: Flowchart of patients' screening and inclusion 318

Figure 8-3: Mean (SD) intracranial pressure (ICP) stratified by normal (blue) and abnormal (red) biomarkers 323

Figure 8-4: Mean (SD) pulse amplitude (PA) stratified by normal (blue) and abnormal (red) biomarkers 324

Figure 8-5: Frequency distribution of minute-by-minute Intracranial Pressure (ICP) measurements in patients presenting with normal (blue) and abnormal (red) pituitary gland shape. 326

Figure 8-6: Frequency distribution of minute-by-minute Intracranial Pressure (ICP) measurements in patients without (blue) and with vertical tortuosity of the optic nerves (red) 327

Figure 8-7: Frequency distribution of minute-by-minute Intracranial Pressure (ICP) measurements in patients without (blue) and with optic nerve sheath distension (red). 328

Figure 8-8: Frequency distribution of minute-by-minute Intracranial Pressure (ICP) measurements in patients with presence (blue) and absence of spontaneous venous pulsations (red) 329

Figure 8-9: Frequency distribution of minute-by-minute Intracranial Pressure (ICP) measurements in patients without (blue) and with papilloedema (red). 330

Figure 8-10: Frequency distribution of minute-by-minute Intracranial Pressure (ICP) measurements in patients without (blue) and with protrusion of the optic disc on MRI imaging (red). 331

Figure 8-11: Frequency distribution of minute-by-minute Pulse Amplitude (PA) measurements in patients presenting with normal (blue) and abnormal (red) pituitary gland shape. 332

Figure 8-12: Frequency distribution of minute-by-minute Pulse Amplitude (PA) measurements in patients without (blue) and with vertical tortuosity of the optic nerves (red). 333

Figure 8-13: Frequency distribution of minute-by-minute Pulse Amplitude (PA) measurements in patients without (blue) and with optic nerve sheath distension (red). 334

Figure 8-14: Frequency distribution of minute-by-minute Pulse Amplitude (PA) measurements in patients with presence (blue) and absence of spontaneous venous pulsations (red). 335

Figure 8-15: Frequency distribution of minute-by-minute Pulse Amplitude (PA) measurements in patients without (blue) and with papilloedema (red). 336

Figure 8-16: Frequency distribution of minute-by-minute Pulse Amplitude (PA) measurements in patients without (blue) and with protrusion of the optic disc on MRI imaging (red). 337

Figure 8-17: Receiver Operating Characteristic (ROC) curves and Areas Under the Curves (AUC) representing the association of Intracranial Pressure (ICP) with the MRI biomarkers. 339

Figure 8-18: Receiver Operating Characteristic (ROC) curves and Areas Under the Curves (AUC) representing the association of Intracranial Pressure (ICP) with the ophthalmic biomarkers. 340

Figure 8-19: Frequency distribution of minute-by-minute Intracranial Pressure (ICP) measurements in patients presenting with normal (blue) and abnormal (red) biomarkers stratified by ophthalmic and MRI domains. LOWESS smoothing lines and median ICP are marked. 344

Figure 8-20: Receiver Operating Characteristic (ROC) curves representing the association of ICP with the biomarkers classified by domains (brain MRI and ophthalmic). 345

List of abbreviations

ANOVA	Analysis of Variance
AUC	Area Under the Curve
BS	Brain Sagging
CI	Confidence Interval
CBF	Cerebral Blood Flow
CDR	Cup-to-disc Diameter Ratio
CMI	Chiari Malformation type I
CPP	Cerebral Perfusion Pressure
CSF	Cerebrospinal Fluid
CT	Computed Tomography
CTM	Computed Tomography Myelogram
DESH	Disproportionately Enlarged Subarachnoid-space Hydrocephalus
DPE	Diffuse Pachymeningeal Enhancement

DSM	Digital Subtraction Myelography
EBP	Epidural Blood Patch
EPG	Enlarged Pituitary Gland
EVD	External Ventricular Drain
HIP	Hydrostatic Indifferent Point
HS	High Speed
ICHD	The International Classification of Headache Disorders
ICP	Intracranial Pressure
IIH	Idiopathic Intracranial Hypertension
IIHWOP	Idiopathic Intracranial Hypertension Without Papilloedema
IOP	Intraocular Pressure
IR	Infrared
LP	Lumbar Puncture
LPOP	Lumbar Puncture Opening Pressure
LOVA	Longstanding Overt Ventriculomegaly in Adults

MAP	Mean Arterial Pressure
MDT	Multidisciplinary Team
MRI	Magnetic Resonance Imaging
MRM	Magnetic Resonance Myelography
NHNN	National Hospital for Neurology and Neurosurgery
NIH	National Institute of Health
NIRS	Near Infrared Spectroscopy
NPH	Normal Pressure Hydrocephalus
NPV	Negative Predictive Value
OCT	Optical Coherence Tomography
ODP	Optic Disc Protrusion
ONSD	Optic Nerve Sheath Diameter
PA	Pulse Amplitude
PDPH	Post Dural Puncture Headache
PGS	Pituitary Gland Shape

PoTS	Postural Tachycardia Syndrome
PPV	Positive Predictive Value
PRISMA	Preferred Reporting Items for Systematic Reviews and Meta-Analyses
RAP	Correlation (R) between ICP pulse amplitude (A) and mean (P)
RNFL	Retinal Nerve Fiber Layer
ROC curve	Receiver Operating Characteristics curve
R_{OUT}	CSF outflow resistance
SD	Standard Deviation
SDC	Subdural Collection
SIH	Spontaneous Intracranial Hypotension
SVP	Spontaneous retinal Venous Pulsations
TBI	Traumatic Brain Injury
TCD	Transcranial Doppler ultrasonography
Time-SLIP	Time-Spatial Labelling Inversion Pulse

VE	Venous Engorgement
VRS	Verbal Reporting Scale
VT	Vertical Tortuosity of the optic nerves

Chapter 1. Introduction

The physiological mechanisms leading to cerebrospinal fluid (CSF) production, flow and absorption are current matters of debate. These gaps in knowledge affect our understanding of the pathophysiology of diseases in which the CSF dynamics are disrupted. Hydrocephalus and CSF dynamics disturbances can result from disruptions in the normal CSF production, flow/pulsation and reabsorption. This introduction chapter will describe the traditional model for CSF dynamics, the current debates around this model, intracranial pressure (ICP) monitoring and its use in disturbances of CSF dynamics.

1.1. Physiology of cerebrospinal fluid dynamics

The traditional hypothesis for CSF hydrodynamics has been followed for decades. According to this model, CSF is mainly secreted by the choroid plexus of the ventricles, it circulates unidirectionally through the ventricular system and the subarachnoid spaces and is finally absorbed into the dural venous sinuses through the arachnoid granulations (Cushing, 1914; Dandy, 1919; McComb, 1983). Several experiments have highlighted inconsistencies with the traditional model and have raised a number of questions on both the normal CSF dynamics and the pathophysiology of diseases in which these dynamics are disrupted. The following paragraphs will briefly summarise the current evidence on CSF dynamics.

1.1.1. Cerebrospinal fluid function

CSF is a clear, colourless fluid contained in the subarachnoid space surrounding the brain and spinal cord, in the brain ventricular system and in the ependymal canal. It has been estimated that the overall content of CSF in the central nervous system of an adult is approximately 150 ml: 100 ml in the cranial subarachnoid space, 25 ml in the spinal subarachnoid space and the remaining 25 ml in the ventricular system. CSF is believed to have several roles in the central nervous system including mechanical protection, metabolic homeostasis, removal of waste products, transport of nutrients and in the intracranial volume homeostasis (Tumani *et al.*, 2018; Bothwell *et al.*, 2019b).

The CSF provides mechanical protection to the brain with two mechanisms. It acts as a shock absorber between the brain and the skull preventing damage from fast and abrupt head movements and minor trauma (Tumani *et al.*, 2018; Bothwell *et al.*, 2019b). Additionally, CSF allows the brain and spinal cord to become buoyant, reducing the effective weight of the brain from about 1,500 grams to about 25-50 grams (Bothwell *et al.*, 2019b).

The rapid fluid exchanges occurring between the CSF and the brain extracellular spaces allow the clearance of waste products from the brain and the maintenance of the biochemical and immunological brain homeostasis (Spector *et al.*, 2015b). The CSF also has an important role for the transportation of nutrients to the central nervous system. Though most of the

nutrients reach the brain cells through the blood-brain barrier, there are a few substrates (e.g., vitamin C and folate) that are secreted in the CSF and then can reach the brain only through slow diffusion in the extracellular brain spaces (Spector, 2009; Spector *et al.*, 2015b). Moreover, CSF transports a number of peptides with poorly understood functions, suspected to be important for the preservation and longevity of the neural function as well as the ageing process (Spector *et al.*, 2015b).

1.1.2. Cerebrospinal fluid production and the role of the choroid plexus

Most of the CSF is produced in the choroid plexus of the lateral, third and fourth ventricles of the brain. This vascularised structure is made of ependymal cells that surround capillaries composing the blood-CSF barrier. The choroid plexus is able to regulate the passage of water and solute across this blood-CSF barrier and can therefore control the composition of the CSF (Spector *et al.*, 2015a).

In 1919, Walter E. Dandy conducted an experiment in which he removed the choroid plexus of a dog and caused blockage of the foramen of Monroe, he found that the ventricle became slit and concluded that "*this is absolute proof that the choroid plexus secretes cerebrospinal fluid and that ependyma takes no part in this formation*" (Dandy, 1919). Since then, the choroid plexus has been considered the main CSF forming structure. Keasley Welch provided additional evidence on the role of the choroid plexus in the CSF secretion by demonstrating that, in rabbits, the haematocrit of the venous blood from the

choroid plexus is 1.15 times greater that the systemic arterial blood and suggesting loss of fluid volume during the transit through the choroid plexus (Welch, 1963). Moreover, electron microscopy has demonstrated that the ultrastructure of the epithelial cells of the choroid plexus in rats is very similar to secretory cells, supporting their secretory role in the production of CSF (Brown *et al.*, 2004). The role of the choroid plexus as CSF-producing structure is also confirmed by the reported association between CSF production and choroid plexus hyperplasia (Hallaert *et al.*, 2012).

Traditionally, the anatomy of the choroid plexus has been studied in human brain autopsies, during which the CSF is completely drained. In these conditions, the choroid plexus appears like small stripes of tissue attached to the walls of the ventricles. According to Zheng *et al.*, these observations can be very misleading (Zheng and Chodobski, 2005). In fact, through new technologies using micro-video probes, Zheng *et al.* were able to observe the living anatomy of the choroid plexus and showed that “in the life situation where the brain ventricles are full of CSF, the choroid plexus expands to fill nearly all the cerebral ventricles” (Zheng and Chodobski, 2005). This configuration provides a large surface for exchange of water and solutes (Spector *et al.*, 2015a).

Many studies have tried to identify alternative structures responsible for the secretion of CSF. In particular, evidence suggests that the blood-brain barrier may contribute to the production of up to 20% of the CSF (Bothwell *et al.*,

2019a). The blood-brain barrier is an active producer of brain interstitial fluid and exchanges of extracellular fluid between interstitial spaces and CSF spaces may eventually lead to the net formation of CSF (Brinker *et al.*, 2014). However, the rate of production of the blood-brain barrier is much lower than the choroid plexus and further evidence will be required to confirm the role of this mechanism in the formation of CSF (Bradbury, 1976; Abbott, 2004).

Experiments using labelled water have demonstrated that rapid water absorption and filtration processes occur across the walls of the central nervous system microvessels. These processes allow the maintenance of constant CSF and extracellular interstitial fluid volumes. These volume exchanges are regulated by the osmotic pressure changes in the central nervous system microvessels (Bulat and Klarica, 2011). While these water exchanges may support the role of the blood-brain barrier in the formation of CSF, it is important to distinguish between water exchanges and CSF formation processes (Spector *et al.*, 2015a; Spector *et al.*, 2015b). Rapid water exchanges between blood, brain and CSF are well documented, however the CSF formation from the blood-brain barrier also requires a number of specific transporters on the brain capillary walls for the net unidirectional transport of ions across the blood-brain barrier (Spector *et al.*, 2015a). Good evidence for the presence of these transporters is still lacking (Spector *et al.*, 2015a).

1.1.3. Cerebrospinal fluid movement: bulk flow versus pulsatile flow

The traditional 'bulk flow' model describes a unidirectional flow of CSF from the brain ventricles to the subarachnoid spaces and reabsorption in the dural venous sinuses through the arachnoid granulations. According to this model, the movement of CSF is generated by the hydrostatic pressure gradient among CSF compartments. Growing evidence demonstrates that the CSF flow is not unidirectional but pulsatile and is the result of the pulsatile activity of the cardiac cycle on the cerebral arteries.

Recent imaging advances have demonstrated the pulsatile nature of the CSF movements. The recent time-spatial labelling inversion pulse (time-SLIP) MRI has introduced a new non-invasive method for the observation of CSF movement. This method allows the use of CSF as an endogenous tracer, resolving the limitations of previous methods employing exogenous tracers (Yamada, 2021). With time-SLIP MRI, it is now possible to observe the movement of CSF with high-speed imaging (48 msec/frame) (Yamada, 2021). This technology has clearly demonstrated the bi-directional character of the CSF flow at the level of the aqueduct of Sylvius and the third ventricle (Yamada *et al.*, 2008; Yamada *et al.*, 2015). Alperin *et al.* and Enzmann *et al.* have demonstrated the bi-directional CSF flow between the cranial and spinal compartments through the use of cine phase-contrast MRI techniques (Enzmann and Pelc, 1991; Alperin *et al.*, 2005a). Additionally, the pulsatile nature of the CSF flow was already observed in 1987 by Feinberg *et al.*, who

described the vascular-driven movement of the brain and speculated on its role for the circulation of the CSF (Feinberg and Mark, 1987).

Experiments observing the distribution of substances across the CSF spaces have been used to test the traditional bulk flow theory. The distribution of tracers depends on their rate of removal from the microvessels. For example, labelled water, has a rapid turnover though the central nervous system microvessels, therefore it will have very limited distribution across the CSF spaces. Macromolecular tracers are not rapidly removed by the central nervous system microvessels and reside in the CSF for long enough to be distributed across the CSF spaces over time (Bulat and Klarica, 2011). When the experiments involve the application of a macromolecular tracer in the lateral ventricle, through the brain pulsatility, the tracer will be distributed across the CSF spaces creating the illusion of unidirectional bulk flow. However, experiments that have applied the tracer to other parts of the CSF system have demonstrated that the distribution of the tracer also occurs in the opposite direction, refuting the traditional bulk flow theory (Hindmarsh, 1977; Vladić *et al.*, 2000; Vladić *et al.*, 2009; Bulat and Klarica, 2011).

Another interesting observation has been made in regards to the microscopic movement of CSF on the surface of the ventricular ependyma. The ependymal cells lining the ventricular walls are in fact characterised by the presence of motile cilia. A study on mice by Ibanez-Tallon *et al.* demonstrated that the movement of these cilia generates laminar flow of

CSF through the cerebral aqueduct (Ibañez-Tallon *et al.*, 2004). In addition, they demonstrated that when the gene responsible for the ependymal flow is damaged in mutant mice (Mdnah5 gene), they develop triventricular hydrocephalus (Ibañez-Tallon *et al.*, 2004). These observations are not only contributing to our knowledge of CSF dynamics physiology, but they also open a discussion on the role of CSF ependymal flow in the pathogenesis of some forms of hydrocephalus.

1.1.3.1. Continuous fluid exchange theory

Some of the most recent findings regarding CSF dynamics physiology pertain to the continuous fluid exchange theory. According to this theory, there are continuous fluid exchanges between the interstitial fluid and the CSF and these exchanges are bidirectional (Brinker *et al.*, 2014; Matsumae *et al.*, 2016). In this model, there is no net bulk flow of CSF from the ventricular system to the absorption sites, but rather a pulsatile movement of the CSF across these spaces; this idea is supported by the results of research employing time-SLIP MRI (Yamada *et al.*, 2008). The ventricular system and the subarachnoid spaces would therefore act as mere reservoir systems (Matsumae *et al.*, 2016).

1.1.4. Cerebrospinal fluid absorption

The arachnoid granulations have been considered for many years the structures that are responsible for the absorption of CSF from the subarachnoid space into the venous sinuses. Most of the evidence supporting this theory is anatomical, rather than physiological. The arachnoid granulations are structures composed by villi embedded in the dura mater of the superior sagittal sinus. The arachnoid villi are believed to work as one-way valve systems that allow the passage of CSF into the venous sinus only when a certain hydrostatic pressure gradient is achieved. New evidence suggests that the arachnoid granulation may be a complementary site of CSF drainage that is mainly active when the CSF pressure is high and may have an important role in the context of CSF dynamics disturbances more than the normal physiology (Zakharov *et al.*, 2004; Johanson *et al.*, 2008; Bothwell *et al.*, 2019a).

Osaka *et al.* studied the development of the CSF pathways in human embryos and found that subarachnoid spaces form earlier than arachnoid granulations (not seen in embryos), therefore they concluded that embryonic pathways of CSF absorption must exist and it is possible that they would persist in adult humans (Osaka *et al.*, 1980).

At normal CSF pressure levels, the cribriform plate and the cervical lymphatic drainage may have a main role in the absorption of the CSF (Johanson *et al.*, 2008; Bothwell *et al.*, 2019b). Mollanji *et al.* demonstrated that at low ICPs

the olfactory pathway represents a major site for CSF drainage and an obstruction of the cribriform plate causes significant increases in the ICP in sheep (Mollanji *et al.*, 2002). Other animal experiments provided further evidence of a rapid drainage of CSF into the cervical lymphatic system via the olfactory, optic and cranial nerves (Brinker *et al.*, 1997).

Additionally, CSF absorption also occurs along the spinal nerves (Edsbagge *et al.*, 2004; Johanson *et al.*, 2008). Due to the increases in the hydrostatic pressure, this spinal CSF clearance mechanism may be enhanced during activity and in the upright posture (Voelz *et al.*, 2007; Johanson *et al.*, 2008).

1.1.5. The glymphatic system

The central nervous system lacks conventional lymphatic vessels. The glymphatic system is considered as the central nervous system analogue of the lymphatic system. According to the glymphatic theory first described by Illif *et al.*, the CSF passes from the subarachnoid space through the periarteriolar spaces and through the astrocytes end feet membranes to the brain parenchyma (Iliff *et al.*, 2012). In the brain parenchyma it mixes with the interstitial fluid and then exits the parenchyma through perivenous spaces (Iliff *et al.*, 2012). The fluids transport has also been found to be dependent on the expression of the channel aquaporin-4 in the astrocyte end feet (Iliff *et al.*, 2012), but the role of these channels in the elimination of solutes is still a matter of debate (Bakker *et al.*, 2019).

This mechanism seems to have an important role in the homeostasis of the brain interstitial fluid, in particular for the elimination of waste products that cannot be removed through the blood-brain barrier with simple diffusion or transporters. Amongst these waste products, amyloid-β has been identified as one of the products eliminated through the glymphatic system (Iliff *et al.*, 2012), highlighting the possible role of this system in the pathophysiology of Alzheimer's disease and other neurodegenerative disorders. Since its first description, the glymphatic system has also been associated with other conditions such as ageing, traumatic brain injuries and small infarcts (Kress *et al.*, 2014; Petraglia *et al.*, 2014; Wang *et al.*, 2017). Another interesting characteristic of the glymphatic system is its increased level of activity during sleep and general anaesthesia, suggesting the importance of sleep in the clearance of waste products from the brain (Xie *et al.*, 2013).

Further research by Iliff et al. demonstrated that the slowing of the arterial pulsatility in mice (through ligation of the internal carotid artery), significantly slowed the rate of paravascular exchanges between CSF and interstitial fluid (Iliff *et al.*, 2013). These results suggest that cerebral arterial pulsatility could be a driver of the glymphatics paravascular flow.

There are many aspects of the glymphatic system that remain unexplained, for example the forces driving the paravascular flow as well as the exact role of pressure pulsations and aquaporin 4. The glymphatic system theory is an

actively growing area of research and future studies will hopefully shed further light on its role in the various aspects of CSF physiology.

1.2. Intracranial pressure monitoring

1.2.1. Intracranial pressure physiology: importance of the intracranial compliance

The skull is a rigid structure, and its content has a fixed volume. The three main intracranial components are: brain parenchyma, blood and CSF. According to the Monro-Kellie doctrine, the sum of volumes of brain, CSF, and intracranial blood is constant. An increase in the volume of any of these components (or the presence of a space occupying lesion) could result in an increase of the ICP. However, physiological compensatory mechanisms are in place to avoid pathological ICP swings. These mechanisms are mainly related to the ability of the CSF and blood to buffer intracranial volume changes through a modulation of the arterial blood inflow, venous blood outflow, and CSF movement through the foramen of magnum.

In addition to these mechanisms, cerebrovascular autoregulation has the objective of maintaining a physiological cerebral blood flow (CBF) despite fluctuations in cerebral perfusion pressure (CPP) and ICP, through the modulation of the cerebral arterioles' resistance. Cerebral autoregulation is only effective when the CPP is between 50 and 150 mmHg, below and above these thresholds hypoperfusion and cerebral oedema can occur respectively (Figure 1-1).

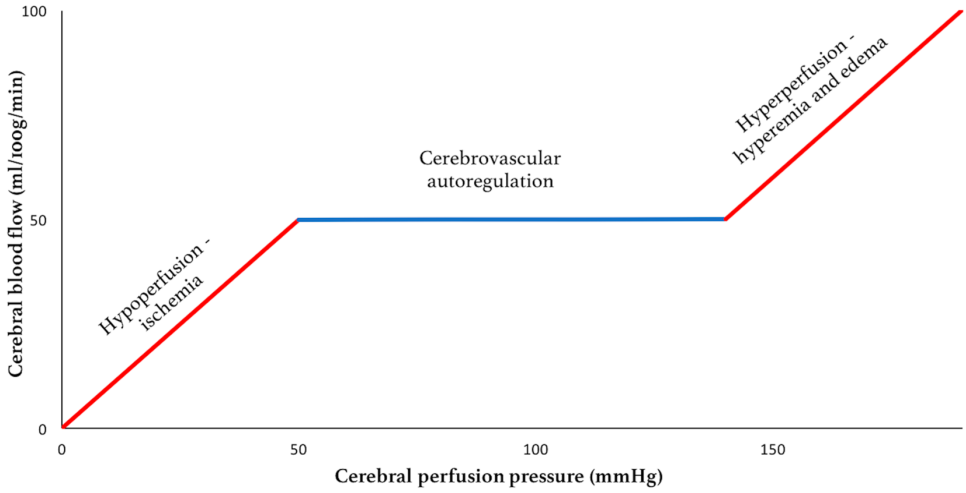


Figure 1-1: Cerebral autoregulation

Figure from Harary *et al.* (Harary et al., 2018)

Intracranial volume and pressure have an exponential relationship (Figure 1-2) and a volume increase will have a very minimal effect on ICP in the compensated phase (left part of the curve). However, at increasing levels of baseline volume (right part of the curve) the compensatory reserve will become more and more depleted, and a minimal change of volume will produce a significant increase in ICP. This could, if left untreated, result in brain herniation and coning.

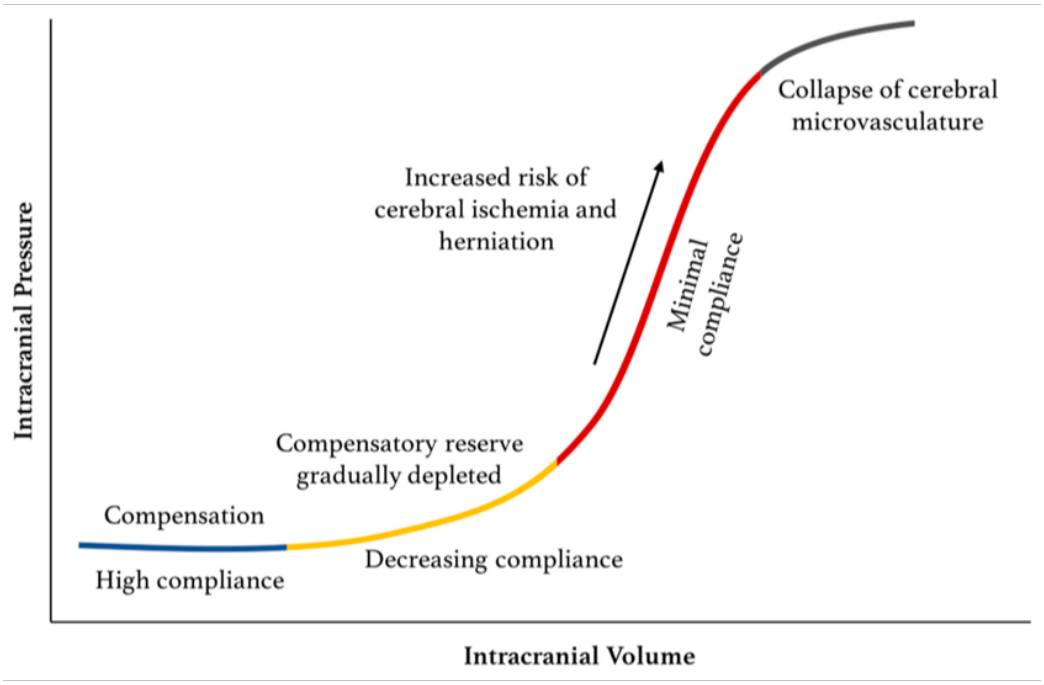


Figure 1-2: Intracranial pressure-volume curve.

Figure from Harary *et al.* (Harary et al., 2018).

Intracranial compliance is the ratio of volume change (ΔV) to pressure change (ΔP) and it is an index of the residual compensatory reserve:

$C=\Delta V/\Delta P$.

A degree of intracranial compliance (within certain limits) is essential as it allows for physiological volume (and pressure) changes related to the cardiac and respiratory cycles, posture, adrenergic tone and brain activity.

The dissipation of arterial pulsations is essential to protect the capillary bed and parenchyma, this is obtained through the Windkessel effect. In organs

outside the brain, the dissipation of the arterial pulsations occurs through the surrounding soft tissues that are characterised by a high compliance. The cerebral Windkessel model differs from the other organs because the brain is enclosed in a rigid container (the skull). In the brain, the dissipation of the arterial pulsations occurs through the overall cranial compliance (Wagshul *et al.*, 2011). This dissipation makes the capillary flow smooth, whereas the blood flow of the intracranial arteries and veins is quite pulsatile (Egnor, 2019).

The overall intracranial compliance is determined by the following four factors:

- Brain tissue compliance (small)
- Arterial compliance
- Venous compliance
- Compliance of the spinal thecal sac (Wagshul *et al.*, 2011)

Therefore, a compliance issue can also arise from conditions affecting the transfer of the pulsations outside the brain (e. g. CSF outflow pathway blockage and venous hypertension).

1.2.2. Intracranial pressure waveform: mean ICP and markers of compliance

ICP presents periodical oscillations due to the effects of the cardiovascular and respiratory cycles, its waveform has three main components (Figure 1-3):

- Respiratory waveform (0.1 – 0.3 Hz): these oscillations of the ICP are related to the respiratory activity,
- Pulse pressure waveform (heart rate): this component depends on the cardiac cycle and therefore has the same frequency as the heart rate,
- Slow vasogenic waveforms (0.33 - 3 cycles per minute): this component is thought to reflect the vasogenic activity of the cerebral autoregulation. These include the B waves and there is still some uncertainty about their origin (see section 1.2.2.1).

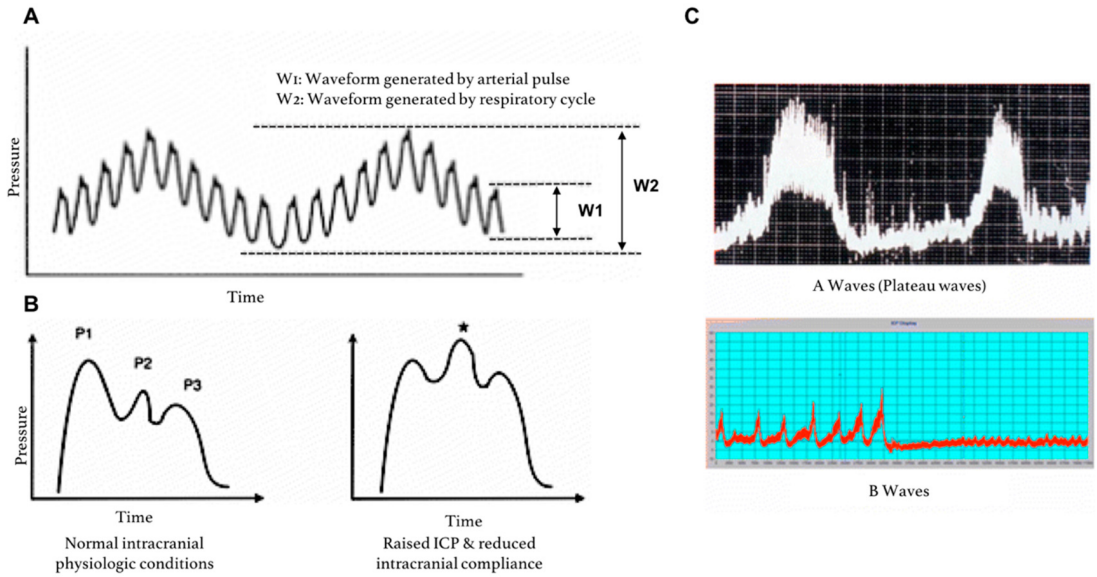


Figure 1-3: Intracranial pressure waveform components

A. Respiratory and pulse pressure waveforms (W1 and W2); B. Example of normal and abnormal pulse pressure waveform; C. Slow vasogenic waveforms. Figure from Harary *et al.* (Harary *et al.*, 2018)

The pulse pressure waveform offers a graphical representation of the ICP changes during one cardiac cycle. These changes reflect the cardiac pressure pulses propagating through the brain at the speed of sound. The pulse pressure waveform is typically characterised by three pressure peaks (Figure 1-3 B):

- P1 is the percussion wave and it is generated by the arterial pulsation,
- P2 is the tidal wave and it is a proxy for intracranial compliance,
- P3 is the dicrotic wave and is believed to be generated by the aortic valve closure.

An analysis of the ICP pulse pressure allows the quantification of the mean ICP as well as the pulse amplitude, which is the difference between the systolic and diastolic ICP.

The pulse amplitude offers important information about the intracranial compliance: when the compliance is low a small volume change (e.g., from diastole to systole) can cause a significant increase in the ICP, therefore a raised pulse amplitude is a sign of reduced compliance (Figure 1-4).

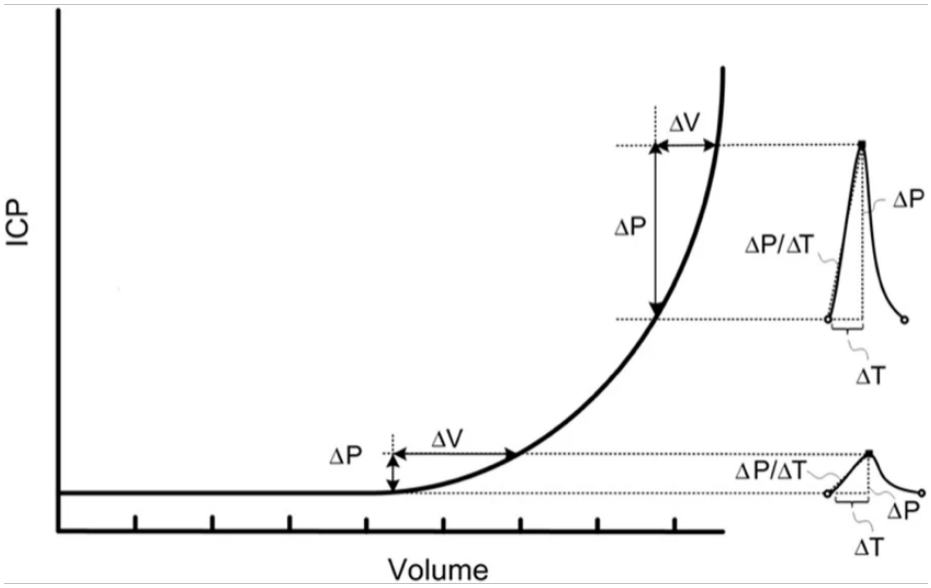


Figure 1-4: Intracranial pressure-volume curve and pulse amplitude changes

Figure from Wagshul *et al.* (Wagshul *et al.*, 2011)

Moreover, also the shape of the pulse pressure waveform can be affected by high pressure. In fact, in cases of high ICP, the P2 component tends to become more prominent (Figure 1-3 B).

A marker of brain homeostasis that could anticipate brain function deterioration, especially in the context of traumatic brain injury, has been desired for decades. For this reason, many efforts have been made to identify the best index to predict outcomes and guide clinical management (e.g., pulse amplitude, RAP index, “true ICP”, RAC index) (Czosnyka *et al.*, 2005; Kim *et al.*, 2009; Budohoski *et al.*, 2012; Eide *et al.*, 2014; Zeiler *et al.*, 2018). A consensus regarding which would be the best marker for guiding the clinical management of patients has not been achieved yet (Hall and O'Kane, 2016). At present, the mean ICP remains the most commonly used ICP marker to guide the treatment of patients affected by severe traumatic brain injuries (TBI) (Steiner and Andrews, 2006; Nourallah *et al.*, 2018).

1.2.2.1. B waves

In 1962, Lundberg described three types of slow spontaneous fluctuations of the ICP trace and named them the A, B and C waves (Lundberg, 1962). The A waves are large plateau waves of 50-100 mmHg, lasting 5-10 minutes and associated with intracranial hypertension. The B waves are rhythmic oscillations up to 50 mmHg (one every minute, lasting half to two minutes) of possible vasogenic origin. The C waves were described as six oscillations per minute, up to 20 mmHg (Lundberg, 1962).

B waves, also called ‘slow waves’ and ‘vasogenic waves’, have attracted clinical interest for years. They have been considered as pathological oscillations of ICP, signs of intracranial hypertension and their presence was associated with shunt responsiveness by some authors (Lemaire *et al.*, 2002). However, over the years, it has emerged that B waves are not necessarily a pathological phenomenon and can be observed in healthy individuals (Lemaire *et al.*, 2002).

Despite the evident clinical interest, B waves are heterogeneous and difficult to define. This also results in considerable difficulties in measuring and quantifying them (Evensen and Eide, 2020). Figure 1-5 shows different morphological characteristics that B waves can display (Martinez-Tejada *et al.*, 2019).

A recent systematic review on B waves highlighted the clear lack of consensus on definition, amplitude, frequency and origin of B waves (Martinez-Tejada *et al.*, 2019). The clinical significance and utility of B waves will remain unclear until these aspects are better understood.

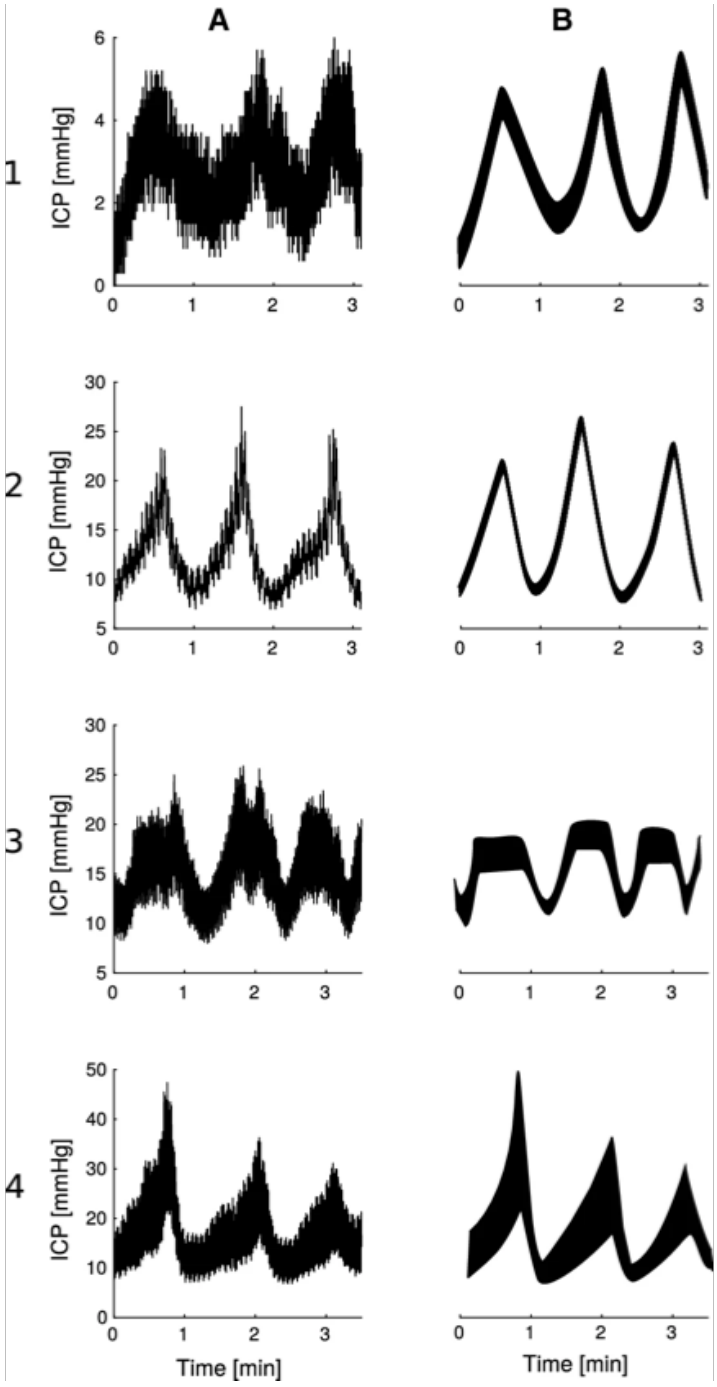


Figure 1-5: Presentation of different B waves sub-classification patterns. Each is illustrated by two computer-generated examples: column A simulating ICP recordings and column B showing an artistic rendering.

Figure from Martinez-Tejada et al. (Martinez-Tejada et al., 2019)

1.2.3. Effect of posture on CSF dynamics: hydrostatic indifferent point and jugular vein collapse

In addition to cardiac cycles, respiratory cycles and vasogenic activities, body posture has an important influence on CSF dynamics. Historically, most ICP monitoring studies have been performed in the supine position; this is counter-intuitive since humans spend most of their time in upright posture.

The first to extensively describe the effect of posture on CSF dynamics, was Bjorn Magnaes in 1976 (Magnaes, 1976a, b). He observed that when humans move from lateral decubitus to sitting posture, the CSF pressure rises in the lower part of the body and decreases in the upper part of the body. He therefore hypothesised the existence of a hydrostatic indifferent point (HIP), a transition point in which both lateral decubitus and sitting pressures are equal (Magnaes, 1976b). His experiments described the HIP, identifying its position between the vertebral bodies of C6 and T5 in healthy subjects (Magnaes, 1976b). This work also highlighted how diseases and treatments can affect the position of the HIP. For example, an increase in the compliance of the caudal spinal dura would result in a caudal displacement of the HIP, while treatment with ventriculoperitoneal shunts or large skull defects would result in a cranial displacement of the HIP (Magnaes, 1976b). When performing CSF pressure monitoring it is therefore of vital importance to understand that pressures measured at different distances from the HIP will have very different results in upright posture.

Another important observation is that, while humans move from supine to upright posture the ICP decrease occurs with a biphasic pattern. This is characterised by a fast initial decrease proportional to the degree of tilt, followed by a stabilization period (above 30 degrees) (Magnaes, 1976a; Gergelé and Manet, 2021). According to a review by Gergelé and Manet, this biphasic pattern can be explained by two factors. The first factor is the rapid shift of CSF from the cranial to the spinal compartment (initial fast ICP drop phase) and the exhaustion of this spinal buffer (stabilization phase). The second factor is the occurrence of the jugular vein collapse. In supine position, the internal jugular vein is the main cerebral venous outflow system, a collapse of the internal jugular vein has been observed in upright posture (Holmlund *et al.*, 2017; Holmlund *et al.*, 2018). The collapse of the internal jugular vein may occur in the second phase (stabilisation) of the biphasic ICP decrease when moving from supine to upright posture (Gergelé and Manet, 2021).

1.2.4. Methods of intracranial pressure monitoring

There are fundamental differences in measuring ICP with continuous or snapshot methods. Snapshot methods, such as lumbar punctures, take only one CSF pressure measurement, without taking into account the dynamic nature of the ICP waveform. Whereas, when ICP is continuously monitored, multiple ICP measurements can be recorded at a high frequency (e.g., 100Hz for Raumedic Neurovent-P); this data can then be summarised in different ways, also allowing morphological analysis of the ICP waveform and

the analysis of brain compliance. Considering the dynamic nature of ICP and its physiological changes (for example with posture), snapshot methods offer very limited information. Many methods of non-invasive ICP measurements have been attempted, however invasive methods remain the gold standard to date.

1.2.4.1. Invasive methods of ICP measurements

ICP monitors have been placed at epidural, subdural, intraparenchymal, and intraventricular sites (Figure 1-6), but the intraparenchymal and intraventricular sites remain the most used at present. Intraparenchymal measurements are commonly performed using implantable micro-transducers, while intraventricular measurements use fluid-based systems.

Several studies have investigated the potential differences in measuring ICP inside the ventricles versus the parenchyma and found good agreement (Chambers *et al.*, 2001; Brean *et al.*, 2006; Vender *et al.*, 2011). ICP measurements performed with intraparenchymal and intraventricular monitors are therefore considered equivalent, however there are differences that will be highlighted in the following paragraphs.

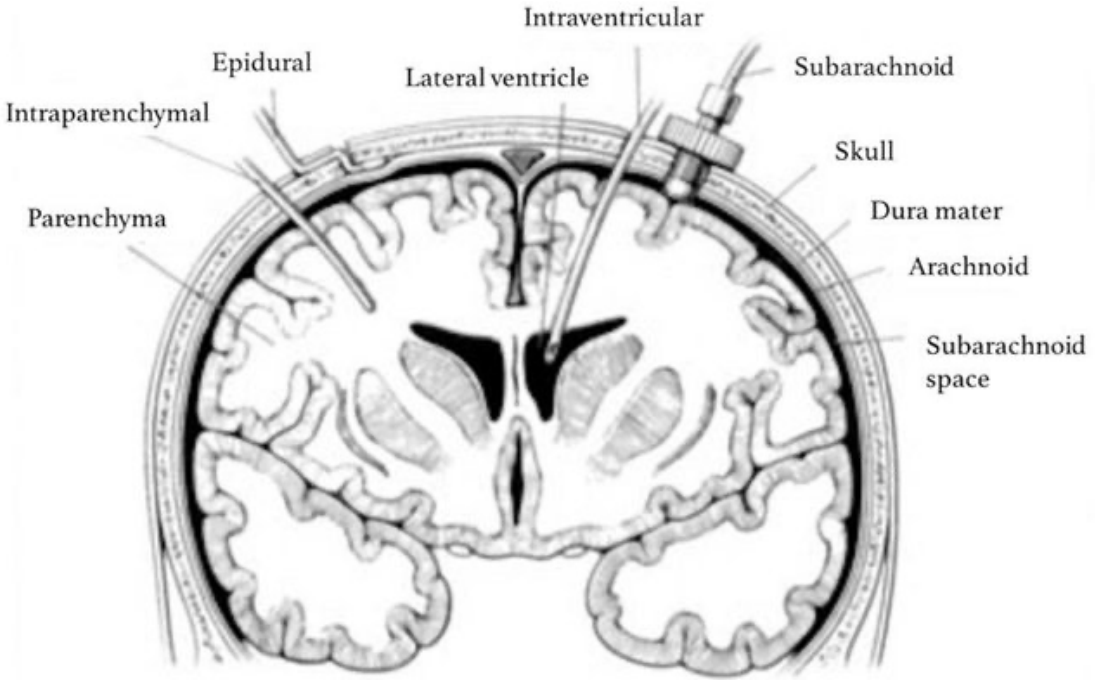


Figure 1-6: Sites of cranial invasive intracranial pressure monitoring

Figure from Lyons and Meyer (Lyons and Meyer, 1990)

Fluid-based systems

External Ventricular Drains (EVD) are still considered the gold standard for ICP measurement by many, they involve the insertion of an intraventricular drain connected to an external pressure transducer. The main advantage of EVDs is the possibility of draining the CSF when the ICP is raised, therefore they are able to monitor the ICP but also to treat intracranial hypertension and monitor the effects of such treatment. However, CSF drainage needs to be interrupted to obtain reliable ICP readings. EVDs are also relatively cheap, widely available and allow recalibration (zeroing). On the other hand, the risks of infection of an EVD system are considerable (5-8%) and significantly increase when the EVD is in place for more than 8 days

(Jamjoom *et al.*, 2018). For this reason, EVDs can only be used to perform ICP monitoring for a short period of time.

Moreover, their insertion can become difficult in cases of small ventricles or brain oedema, and they can fail due to blockage (especially if used to drain blood) or to inadvertent displacement. Another fluid-based system of ICP measurement are bolts inserted in the subarachnoid space, which are not as useful as EVDs as they do not allow CSF drainage.

Implantable microtransducers

Implantable microtransducers are more commonly used in the elective setting when a need for immediate CSF drainage is not anticipated. They can be implanted in various locations of the brain: in the brain parenchyma (most common), in the lateral ventricles, in the subarachnoid, epidural or subdural spaces. They are associated with lower risks of infection (1-2%), bleeding (0.15-0.47%) and technical failure (1.4-3.1%) when compared to EVDs (Zhang *et al.*, 2017). One of the drawbacks of microtransducers is the fact that the majority of them cannot be recalibrated once implanted and a considerable zero drift can occur (Piper *et al.*, 2001), however this issue seems to have been solved with newer transducers (Czosnyka and Pickard, 2004). Despite their higher cost, they are minimally invasive, safer than EVDs, easier to insert in patients with small ventricles and easier to manage. Therefore, microtransducers are generally preferred in cases where immediate CSF drainage is not needed.

CSF pressure measurements at lumbar level

CSF pressure can be assessed at the lumbar level through the use of lumbar punctures (LP) and lumbar drains. These techniques measure the CSF pressure through the lumbar spine and are not reliable in predicting the brain pressure when an obstruction between intracranial and spinal CSF spaces exists. Moreover, they are not recommended in patients with brain lesions or obstructions due to the theoretical risk of inducing cerebral herniation.

LP opening pressure is a snapshot measurement method which has been demonstrated to be misleading in some cases (Czosnyka and Pickard, 2004; Xu *et al.*, 2017b; Lalgudi Srinivasan *et al.*, 2020). Another aspect to consider is the effect that posture has on CSF pressure especially at the lumbar level: a lumbar puncture or lumbar drain will give a much higher CSF pressure if performed in a sitting position due to the hydrostatic effect of the above column of CSF. The great advantage of lumbar punctures and lumbar drains is the fact that they do not involve direct access to the brain, can often be performed at the patient's bedside (especially true for lumbar punctures) and can allow therapeutic CSF drainage. These are the reasons why they are still very commonly used in clinical practice. Due to their popularity, LPs have been studied extensively in the past leading to a degree of agreement on normal LP opening pressures ranges; in contrast, normal ICP ranges are still uncertain for cranial measurements.

1.2.4.2. Non-invasive methods of ICP measurement

Attempts to identify high ICP through the characteristics of intracranial imaging (CT and MRI) are made in routine clinical practice. Positive imaging findings associated with the relevant clinical picture can suggest the need for further investigations (e.g., ICP monitoring). They are widely available and non-invasive; however, they only offer snapshot information on ICP and heavily rely on the observers' interpretation.

Transcranial doppler ultrasonography (TCD) is also very commonly used to noninvasively assess ICP and CPP. This technique is safe and repeatable but requires training and has been found to have significant intra- and interobserver variations (Robba *et al.*, 2016).

The anatomical connection between the subarachnoid space and the eyeball through optic nerve sheath has supported the use of papilledema as a clinical sign for raised ICP. Despite its undoubted utility in clinical practice, it should be kept in mind that papilledema takes time to develop (and disappear), and that different people may have different thresholds for its development (Bridges and Raslan, 2018; Funnell *et al.*, 2018).

Measurements of the Optic Nerve Sheath Diameter (ONSD) with ultrasound have demonstrated a good correlation with ICP>20mmHg (Jeon *et al.*, 2017). This is one of the most popular non-invasive methods of assessment of ICP and has demonstrated promising results as bedside tool in a variety of diseases (Lochner *et al.*, 2019). A study by Cipriani *et al.* demonstrated that

ONSD measurements can also be useful in low CSF pressure/volume states, in particular they found that ONSD dynamically decreases during orthostatic stress in spontaneous intracranial hypotension (SIH) (Cipriani *et al.*, 2019). Other studies have supported the measurement of ONSD with MR or CT imaging (Robba *et al.*, 2016). Despite its popularity, at present ONSD measurements with ultrasound have not substituted invasive measurements. One of the main limitations is the heterogeneity of assessment methods reported in the literature (Hirzallah *et al.*, 2022). In addition, there may be anatomical variations in the compliance of the optic nerve sheath affecting the way it distends in response to a rise in ICP (Lochner *et al.*, 2019). Another concern is that the optic nerve sheath may not be able to shrink back once a high ICP state has been treated, limiting its use as a follow-up monitoring tool (Lochner *et al.*, 2019).

Many other methods of non-invasive ICP measurements have been investigated: tympanic membrane displacement, near infrared spectroscopy (NIRS) and multiple neurophysiology tests. A study by Kolecki *et al.* supports the correlation between reversible eye tracking changes and raised ICP (Kolecki *et al.*, 2018). More recently, studies employing Optical Coherence Tomography (OCT) have demonstrated the associations of optic nerve head volumes and peripapillary Bruch's membrane angle with ICP (Vijay *et al.*, 2020; Jacobsen *et al.*, 2022).

The spontaneous pulsation of retinal veins (SVP), which can be seen during a fundoscopy exam, is believed to disappear when ICP is high. However, a previous study has raised concerns regarding the usefulness of this sign to non-invasively identify patients with raised ICP (Wong and White, 2013). Further details on the use of SVP as non-invasive marker of ICP are discussed in Chapter 7 and Chapter 8.

1.3. Cerebrospinal fluid dynamics disturbances and applications of elective continuous intracranial pressure monitoring

CSF dynamics disturbances can occur at any point between CSF production, flow and absorption. The gaps in our knowledge on the normal CSF dynamics physiology inevitably limits our ability to understand the pathophysiological mechanisms leading to the clinical picture in CSF dynamics disturbances. While it is generally recognised that the choroid plexus is the main producer of CSF, there is no certainty on potential extra-choroidal areas of production. Moreover, lots of debate is still occurring regarding the structures and mechanisms leading to CSF absorption. The more recent proposition of a cerebral glymphatic system has raised additional questions and has opened the way to a new research field. Normal ranges for ICP in healthy individuals are still a matter of debate.

ICP monitoring has the potential of offering new information useful for the understanding of CSF dynamics in both healthy and ill subjects. Due to obvious ethical concerns, invasive ICP monitoring cannot be performed in

healthy volunteers. The use of continuous ICP monitoring in patients with CSF dynamics disturbances has provided insights in some aspects of the pathophysiology of these diseases.

1.3.1. Hydrocephalus

The term hydrocephalus is often used to identify a spectrum of conditions characterised by CSF dynamics disturbances. The diseases considered under the umbrella term 'hydrocephalus' are heterogeneous. Ventriculomegaly is a characteristic that is often associated with the term hydrocephalus, however there are diseases that are part of this spectrum in which ventricles are normal (or slit), as for example in Idiopathic Intracranial Hypertension (IIH). Intracranial hypertension is also often associated with hydrocephalus, however there are cases in which ICP is within normal parameters (e.g. Normal Pressure Hydrocephalus, NPH). There is still no international consensus on the classification for hydrocephalus disorders and different classification schemes have been used. A simple classification system based on CSF dynamics distinguishes hydrocephalus in obstructive (non-communicating) and non-obstructive (communicating). Another simple classification takes into account the possible aetiology of hydrocephalus classifying it into three different groups: idiopathic, acquired or congenital. Congenital forms of hydrocephalus include Chiari Malformation, aqueductal stenosis and Dandy-Walker complex. Acquired forms of hydrocephalus include hydrocephalus secondary to tumours, haemorrhages, and infections.

Some of the most common idiopathic forms of hydrocephalus will be described below (e.g., NPH, IIH) (sections 1.3.2 and 1.3.4).

It is outside the scope of this thesis to describe all CSF dynamics disturbances that are part of the hydrocephalus spectrum. The following paragraphs describe the experience with ICP monitoring with the most common CSF dynamics disturbances managed in the elective setting: IIH, NPH, Chiari Malformation type I (CMI) and low CSF pressure/volume syndromes.

1.3.2. Idiopathic Intracranial Hypertension (IIH)

IIH, also known as pseudotumor cerebri and benign intracranial hypertension, is a CSF dynamics disorder characterised by raised ICP without a detectable cause. IIH was clearly described by Walter E. Dandy who described 22 cases of 'intracranial pressure without brain tumor' (Dandy, 1937). The 'modified Dandy criteria' adapted by Smith in 1985 have been used to make diagnosis of IIH for many years (Smith, 1985).

The revised diagnostic criteria proposed by Friedman *et al.* for a definite diagnosis of IIH are shown in Table 1-1 (Friedman *et al.*, 2013). If only criteria A-D are met and the lumbar puncture opening pressure does not reach the thresholds indicated in criterion E, the diagnosis of IIH is considered probable (Friedman *et al.*, 2013). In the absence of papilloedema, a diagnosis of IIH without papilloedema (IIHWOP) can be made if the criteria B-E are met and a sixth nerve palsy is present (Markey *et al.*, 2016).

Table 1-1: Diagnostic criteria for a definite diagnosis of idiopathic intracranial hypertension by Friedman *et al.* (2013).

A	Papilloedema
B	Normal neurological examination except for cranial nerve abnormalities
C	Neuroimaging: Normal brain parenchyma without evidence of hydrocephalus, mass, or structural lesion and no abnormal meningeal enhancement on MRI, with and without gadolinium, for typical patients (female and obese), and MRI, with and without gadolinium, and magnetic resonance venography for others; if MRI is unavailable or contraindicated, contrast-enhanced CT may be used
D	Normal CSF composition
E	Elevated lumbar puncture opening pressure (≥250 mm CSF in adults and ≥280 mm CSF in children [250 mm CSF if the child is not sedated and not obese]) in a properly performed lumbar puncture

1.3.2.1. Epidemiology

IIH is most commonly seen in obese women of childbearing age (Markey *et al.*, 2016). The mean age at diagnosis is commonly between 25 and 36 years old (Markey *et al.*, 2016). According to a large retrospective study only 9% of IIH patients are male (Bruce *et al.*, 2009).

A recent systematic review and meta-analysis by McCluskey *et al.* reported that the incidence of IIH is 1.2 per 100 000 per year (95% CI 0.82 to 1.57) (McCluskey *et al.*, 2018). A population-based study by Kilgore *et al.* reported a slightly higher age- and sex-adjusted annual incidence of 1.8/100 000 (Kilgore *et al.*, 2017). Data on the prevalence of IIH are less commonly

reported and this was estimated to be between 5.1 and 14.3 per 100 000 population (McCluskey *et al.*, 2018). The systematic review by McCluskey *et al.* also found an association between the national prevalence of obesity and the incidence of IIH highlighting the issue of IIH as a public health concern (McCluskey *et al.*, 2018).

1.3.2.2. Clinical and imaging features

Headache is the most common symptom of IIH (Markey *et al.*, 2016). According to the International Classification of Headache Disorders (ICHD-III), these are the diagnostic criteria for headache secondary to IIH:

A. New headache, or a significant worsening of a pre-existing headache, fulfilling criterion C
B. Both of the following:
    - IIH has been diagnosed
    - cerebrospinal fluid (CSF) pressure exceeds 250 mm CSF (or 280 mm CSF in obese children)
C. Either or both of the following:
    - headache has developed or significantly worsened in temporal relation to the IIH, or led to its discovery
    - headache is accompanied by either or both of the following: a. pulsatile tinnitus, b. papilloedema
D. Not better accounted for by another ICHD-III diagnosis (ICHD-III, 2018).

IIH patients have a non-specific headache that can commonly resemble migraine or tension-type headache. Moreover, IIH patients frequently present with non-pressure related headaches (Friedman and Rausch, 2002). A study by Yri and Jensen found that the headache attributed to IIH is most commonly daily, fronto-temporal and aggravated by coughing and straining (Yri and Jensen, 2015). It is worse in the morning only for a small percentage of patients (20%) (Yri and Jensen, 2015).

Other common symptoms of IIH are transient visual obscurations (68-72%), pulsatile tinnitus (52-60%), back pain (53%), dizziness (52%), neck pain (42%) and visual loss or blurring (32%) (Markey *et al.*, 2016). The association of headache with retrobulbar pain, transient visual obscurations and/or pulsatile tinnitus are more frequent in IIH patients than controls and can be a useful indicator of IIH (Yri and Jensen, 2015).

Brain MRI signs suggestive of IIH are an empty sella, distension of the optic nerve sheaths, vertical tortuosity of the optic nerves, flattening of the globe, protrusion of the optic nerve and stenosis of the transverse venous sinus (Agid *et al.*, 2006; Holbrook and Saindane, 2017; Morris *et al.*, 2017). Further description of these imaging findings is provided in Chapter 8 (section 8.3.3).

1.3.2.3. Pathophysiology

The mechanisms leading to raised ICP in IIH remain unknown. Increased CSF production and/or reduced CSF absorption have been hypothesised to be potential mechanisms leading to IIH, however to this date none of the

proposed theories has been confirmed (Markey *et al.*, 2016). Increased venous sinus pressures (especially in the transverse sinuses) are often seen in IIH, but their role in the pathogenesis of the disease is unclear and they may be epiphenomenal to, rather than cause of, intracranial hypertension (King *et al.*, 2002; Markey *et al.*, 2016).

Weight gain and obesity may have a role in the pathogenesis of IIH. This theory is based on the observations of a strong association between weight and IIH and the reports of clinical improvement with weight reduction (Markey *et al.*, 2016). Additionally, hormonal factors may have an important role since women of childbearing age are most commonly affected by this disease (Markey *et al.*, 2016).

1.3.2.4. Treatment

According to the recent UK consensus guidelines on IIH, the main principles in the management of IIH are:

1. to treat the underlying disease
2. to protect the vision
3. to minimise the headache morbidity (Mollan *et al.*, 2018).

The only treatment with a proven disease-modifying effect on IIH is weight loss (Mollan *et al.*, 2018). For this reason, independent of other medical or surgical management approaches, support to achieve weight loss should be provided to all (overweight) IIH patients. This could be in the form of a

community or hospital-based weight management programme (Mollan *et al.*, 2018). Bariatric surgery could also be offered, in fact there is evidence demonstrating its success in the management of obese IIH patients (Fridley *et al.*, 2011; Mollan *et al.*, 2021).

Patients at risk of visual loss should be offered treatments to lower their ICP and protect the vision. These treatments may consist of CSF diversion shunts or optic nerve sheath fenestration procedures. Additionally, lumbar drainage could be performed as a temporising measure if delays in surgical treatments are expected. Mollan *et al.* clearly discourage clinicians from performing serial lumbar punctures as they are associated with anxiety and can lead to chronic back pain (Mollan *et al.*, 2018).

Medical treatment with acetazolamide is also commonly offered to IIH patients. Acetazolamide is believed to work in IIH by reducing the CSF production at the choroid plexus. However, further evidence will be needed to officially recommend or reject this treatment in IIH (Piper *et al.*, 2015; Mollan *et al.*, 2018). Other proposed medical treatments are topiramate, furosemide and octreotide but there is limited evidence supporting their use in IIH.

Neurovascular stenting of venous sinuses is another option in patients with IIH, a venous sinus stenosis and a significant pressure gradient across the stenosis. The IIH consensus guidelines state that the role of neurovascular stenting in IIH is not yet established (Mollan *et al.*, 2018).

CSF diversion shunts and neurovascular stenting are not currently recommended for the treatment of IIH patients affected by headache when vision is not threatened (Mollan *et al.*, 2018).

Finally, it should be noted that the management of IIH is multidisciplinary, and the patient should routinely be followed up by neurologists, neurosurgeons, ophthalmologists and weight-loss specialists.

1.3.2.5. Intracranial pressure monitoring in idiopathic intracranial hypertension

Lumbar puncture opening pressures are considered the gold standard for the diagnosis of high ICP in IIH patients (Mollan *et al.*, 2018) therefore the employment of ICP monitoring is not very common.

There are limitations in the use of snapshot ICP measurements in IIH. Their results can be affected by the patient's posture during the lumbar puncture, the level of experience of the person performing the lumbar puncture can also influence the result (traumatic lumbar punctures causing excessive pain may give falsely high CSF pressure readings) and they do not offer any type of information on the ICP waveform or pulse amplitude/compliance. For these reasons some centres have started performing ICP monitoring in appropriately selected IIH patients.

The typical findings of ICP monitoring in IIH patients are a high mean ICP and high amplitude of the ICP waveform. These findings were confirmed by

two studies comparing the results of ICP monitoring of IIH patients with reference to pseudo normal subjects (Chari *et al.*, 2017; Fric and Eide, 2017).

Two studies comparing ICP monitoring and lumbar punctures in patients with suspected IIH found that ICP monitoring (even for short period) can be more useful than lumbar punctures when the diagnosis of IIH is in doubt (Warden *et al.*, 2011; Lalgudi Srinivasan *et al.*, 2020). Similarly, Bridges and Raslan suggest that ICP monitoring may have an important role for the investigation of patients with suspected IIHWOP (Bridges and Raslan, 2018). Xu *et al.* report that ICP monitoring can reduce the occurrence of misdiagnosis of IIH due to false positive results of lumbar punctures (Xu *et al.*, 2017a). Moreover, Matloob *et al.* provided evidence that ICP monitoring can be used to confirm the success of treatment with neurovascular stenting in IIH (Matloob *et al.*, 2017).

1.3.3. Chiari Malformation type I

Chiari Malformation type I (CMI) is a cranio-cervical junction disorder characterised by the herniation of elongated cerebellar tonsils through the foramen magnum. A descent of more than 5 mm is the conventional cut-off for making this diagnosis. CMI is also associated with the development of fluid-filled cavities in the spinal cord, known as syrinxes. The incidence if syringomyelia in CMI has been variably reported between 30 and 70% (Arnautovic *et al.*, 2015).

1.3.3.1. Epidemiology

Tonsillar ectopia is a common incidental finding in the general population. Meadows *et al.* analysed 22,591 MRI images of asymptomatic patients and found that 175 individuals (0.8%) met the diagnostic criteria for CMI (tonsillar ectopia >5 mm below the foramen magnum) (Meadows *et al.*, 2000). Vernooij *et al.* found similar results from the analysis of 2,000 brain MRIs performed in asymptomatic patients and demonstrated that 0.8% of patients met the diagnostic criteria for CMI (Vernooij *et al.*, 2007). Strahle *et al.* reported a 3.6% incidence of CMI in children and adolescents (<18 years old) (Strahle *et al.*, 2011).

1.3.3.2. Clinical features

In most cases patients present to the attention of a clinician when symptomatic, however, there is an increasing number of diagnoses of CMI in asymptomatic patients with incidental tonsillar ectopia on MRI scans performed for unrelated reasons.

Symptomatic CMI patients can present with a variety of symptoms. The CSF dynamics abnormalities are believed to be responsible for the headache, which is one of the most common complaints. Additionally, the tonsillar pressure on the adjacent structures (brain stem, upper cervical cord and lower cranial nerves) can be responsible for somatic sensory disturbances, mild motor symptoms and dysfunctions of the bulbar and lower cranial

nerves functions (Pepper *et al.*, 2021). In patients with associated syringomyelia further manifestations of spinal cord disturbances can occur.

A large study by Milhorat *et al.* described the clinical presentation of CMI in 364 symptomatic patients (Milhorat *et al.*, 1999). According to this study, the most common symptoms of CMI is suboccipital headache that was reported by 81% of the patients. The distinctive feature of this headache is that it is accentuated by physical exertion, Valsalva manoeuvres, head dependency and sudden changes in posture (Milhorat *et al.*, 1999).

Ocular, otoneurological and lower cranial nerve disturbances were also very common and were reported by 78%, 74% and 52% of the patients respectively (Milhorat *et al.*, 1999). Most patients with syringomyelia (94%) reported some manifestation of spinal cord dysfunction (Milhorat *et al.*, 1999).

1.3.3.3. Pathophysiology

The aetiology and pathophysiology of CMI and syringomyelia are still unknown.

The aetiology of CMI has been attributed to numerous causes and the role of tonsillar descent is not completely understood. Recently, the use of the term ‘malformation’ has been debated as CMI does not comply with the concept of malformation and the term ‘syndrome’ has been proposed (Frič and Eide, 2020).

Some theories attribute CMI to an underdevelopment of the posterior cranial fossa and overcrowding of the hind brain (Stovner *et al.*, 1993; Nishikawa *et al.*, 1997; Milhorat *et al.*, 2010). However, this is not seen in all cased of CMI. Additionally, CMI has been associated with a variety of clinical conditions including hydrocephalus, low pressure/volume states, tethered cord syndrome and connective tissue disorders (Milhorat *et al.*, 2009; Milhorat *et al.*, 2010). This observation supports the idea that CMI could represent a clinical syndrome resulting from a variety of different aetiologies.

Also, the origin and progression of syringomyelia are still poorly understood. According to the 'piston hypothesis' proposed by Oldfield *et al.*, the progression of syringomyelia would be associated with the transmission of the systolic pressure pulses to the spinal cord (Oldfield *et al.*, 1994). In particular, at each heartbeat the systolic pressure pulse would cause a compression of the spinal cord wall and a longitudinal progression of the syrinx (Oldfield *et al.*, 1994). This model however does not explain the initial mechanism of formation of the syrinx.

The 'intramedullary pulse pressure theory' by Greitz hypothesises that the fluid contained in the syrinx is not CSF but extracellular fluid (Greitz, 2006). According to this theory, the event leading to the formation of the syrinx would be a spinal cord distension triggered by increases in pulse pressure (Greitz, 2006).

There is still uncertainty on the origin of CMI as well as the formation of syringomyelia and further research will be required to understand the mechanisms leading to the typical clinical presentation of CMI patients. The 'decoupling' of the cranial and spinal CSF compartments due to the tonsillar ectopia is likely to play an important role.

1.3.3.4. Treatment

Patients affected by CMI can be managed conservatively with observations or surgically. Evidence suggests that the natural history of CMI in asymptomatic patients is benign, therefore surgery is not routinely offered in these cases (Langridge *et al.*, 2017; Chatrath *et al.*, 2019; Carey *et al.*, 2020). While the fact that asymptomatic patients should be managed conservatively is widely accepted, there is no general consensus on specific criteria to offer surgical treatment. Most commonly, patients with MRI and clinical findings typical of CMI would be offered surgical treatment, especially when this is causing a significant effect on the quality of life.

Foramen magnum decompression surgery is the most common surgical treatment for CMI. There is great variability in the way different surgeons perform this surgery. As described by Oró et al. this procedure ranges from a minimally invasive extradural approach to durotomy, duraplasty, internal decompression, and cranioplasty (Oró and Mueller, 2011).

Other treatment options proposed for the treatment of CMI are CSF diversion shunts, craniocervical stabilization procedures and section of the filum terminale.

1.3.3.5. Intracranial pressure monitoring in Chiari Malformation type I

There are only few reports on the use of ICP monitoring to investigate the CSF dynamics of patients with CMI (Frič and Eide, 2015; Chari *et al.*, 2017; Fric and Eide, 2017; Dyson *et al.*, 2020). Different authors have demonstrated that one of the characteristics of CMI is an increased pulse amplitude of the ICP waveform which indicates a reduced intracranial compliance. Chari et al. found that the median pulse amplitude of patients with CMI was significantly higher compared to a group of pseudo normal patients, while there was no statistically significant difference in the median ICP values (Chari *et al.*, 2017). These findings were supported by the results of a larger study by Frič and Eide (Fric and Eide, 2017). The authors also compared the results of ICP monitoring in CMI patients with a group of IIH patients finding that while both groups have elevated pulsatile ICP (indicating abnormal brain compliance), only the IIH patients had elevated static ICP values (Fric and Eide, 2017). More recently, Dyson et al. employed ICP monitoring to investigate the CSF dynamics of CMI patients who failed to improve after foramen magnum decompression and found that these patients had persistently high pulse amplitudes (similar to untreated CMI patients) (Dyson *et al.*, 2020). Based on these results, it could be speculated that

surgical treatment of CMI fails if normal pulse amplitude (and therefore compliance) is not restored.

1.3.4. Normal Pressure Hydrocephalus

NPH is a form of communicating hydrocephalus affecting elderly people that is characterised by ventriculomegaly, normal ICP and the Hakim's triad of symptoms that includes gait/balance deterioration, urinary disturbances and cognitive decline (Adams *et al.*, 1965).

1.3.4.1. Epidemiology

A systematic review of population-based studies demonstrated that the prevalence of NPH in people above 65 years of age is 1.3% (Martín-Láez *et al.*, 2015). More recently, a large Swedish population-based study, found a higher prevalence in a population within the same age group (3.7%) (Andersson *et al.*, 2019). Despite being common, NPH is hugely underdiagnosed (Martín-Láez *et al.*, 2015). The diagnosis of NPH can be challenging as numerous conditions can present similarly to NPH or can be concurrent comorbidities of NPH (Relkin *et al.*, 2005). Additionally, enlargement of the ventricles is a common incidental finding in the elderly (Barron *et al.*, 1976).

1.3.4.2. Clinical and imaging features

The complete clinical triad is not necessary to make diagnosis of NPH. Symmetrical gait impairment is the most common sign of NPH. NPH patients

can typically present with difficulties with transitional movements, gait initiation, poor foot clearance and shuffling (Williams and Malm, 2016). They are often at high risk of falling. Cognitive and urinary disturbances may occur at later stages. Cognitive dysfunction reflects involvement of the prefrontal brain cortex with memory dysfunction and memory deficits (Williams and Malm, 2016). Urinary dysfunction is most commonly represented by urinary frequency and urgency. Frank urinary incontinence is considered a late sign of NPH (Meier *et al.*, 1999). It should be noted that the gait disturbances add a functional element to the urinary incontinence.

Brain imaging consisting of either CT or MRI scan is essential to diagnose NPH. Ventriculomegaly in the absence of an obstructive cause is the most typical feature of NPH and can be assessed through the calculation of the Evan's index. The Evan's index is the ratio between the width of the frontal horns and the widest diameter of the brain in the same axial slice, an Evan's index of more than 0.3 is indicative of ventriculomegaly. This sign is sensitive for NPH but not specific and should be considered as an indicator of ventriculomegaly that can be present in different types of hydrocephalus. Another important limitation is the fact that the Evan's index is highly plane-dependent and significant variations on the Evan's index calculation can occur depending on the level of the brain selected for the measurements (Toma *et al.*, 2011). Other important imaging signs that can support the diagnosis of NPH are the callosal angle and the 'DESH' sign. The callosal angle measured on coronal MR brain images is significantly smaller in NPH

patients than controls (Ishii *et al.*, 2008). In particular a callosal angle of less than 90 degrees allows to discriminate NPH from Alzheimer's disease and normally aged subjects (Ishii *et al.*, 2008). Another typical feature of NPH is the Disproportionately Enlarged Subarachnoid-space Hydrocephalus (DESH). This sign is visible on coronal MRI sequences and consists in tight subarachnoid spaces in the brain convexity and concomitant enlargement of the Sylvian fissures (Hashimoto *et al.*, 2010). Despite its utility, absence of the DESH sign does not exclude NPH and does not exclude responsiveness to shunt insertion (Craven *et al.*, 2016b).

1.3.4.3. Pathophysiology

NPH can be primary/idiopathic or secondary. Secondary NPH can occur following various types of brain insult (e.g., subarachnoid haemorrhage, meningitis, trauma, tumours). The pathophysiology of idiopathic NPH is still a matter of debate and multiple hypotheses have been proposed.

One of the most popular theories is that NPH may be a 'pulse wave encephalopathy' due to the breakdown of the Windkessel phenomenon. Patients with NPH have poor vascular compliance (probably as a result of the vascular risk factors) and higher arterial pulsatility (Bateman, 2003). The energy transmitted with each arterial pulsation needs to be dissipated, this normally occurs through the Windkessel effect. The Windkessel effect is the dampening of the arterial pulsatility resulting in a nearly pulseless capillary blood flow. In order for this effect to work the energy needs to be dissipated

through the CSF pulsatile movements (craniospinal compliance) and through the compliance of the venous outflow system (Bateman, 2004). NPH patients have been demonstrated to have poor CSF craniospinal compliance and poor vessel compliance therefore they are unable to dissipate the energy coming from the high arterial pulsatility. This results in a 'water hammer' effect on the brain parenchyma that causes compression of the outflow vessels, increase their pressure and reduced CSF absorption (Bateman, 2003).

This theory is in keeping with the significant association between NPH and vascular risk factors (Jaraj *et al.*, 2016), in fact vascular factors are believed to be involved in the pathogenesis of idiopathic NPH (Bateman, 2004).

Several aspects of the 'pulse wave encephalopathy' theory are not understood and further research will be needed to confirm the pathophysiology of NPH, however the available evidence points towards a key role of the abnormal brain compliance for the development of NPH.

1.3.4.4. Treatment

NPH can be successfully treated with CSF diversion shunts. High proportions of NPH patients treated with CSF diversion shunt report significant clinical improvement and enhanced quality of life (Toma *et al.*, 2013; Petersen *et al.*, 2014). A health economics analysis performed by Kameda *et al.* also demonstrates that shunt insertions are cost-effective in NPH with ventriculoperitoneal shunts showing a positive return on investment after only

18 months (Kameda *et al.*, 2017). Despite the age, the frailty and the comorbidities often affecting NPH patients, shunt surgery is safe when performed in specialised centres (Thompson *et al.*, 2017b; D'Antona *et al.*, 2019a; D'Antona *et al.*, 2020).

However, it should be taken into account, that not all NPH patients are shunt-responsive and it is therefore important to select patients appropriately and avoid performing unnecessary surgery in patients who are unlikely to benefit from a shunt insertion. The optimal identification of shunt-responsive patients is still a matter of debate, the current idiopathic NPH guidelines suggest that prolonged external lumbar drainage has high sensitivity and positive predictive value (PPV) and is the most effective test for the identification of shunt responsive patients (Marmarou *et al.*, 2005). Evidence also demonstrates that the natural history of NPH is progression and that treatment delays can result in worse outcomes (Andrén *et al.*, 2014). Additionally, longer symptoms duration before surgery is associated with delays in clinical improvement after treatment (Vakili *et al.*, 2016). It is therefore important to treat NPH in a timely manner.

1.3.4.5. Intracranial pressure monitoring in normal pressure hydrocephalus

Different centres have adopted different techniques to investigate the CSF dynamics of NPH. The role of invasive CSF pressure monitoring techniques in the diagnosis and management of NPH is still uncertain. The main issue in

the interpretation of the available evidence is the variability of the techniques employed by different centres which makes the results very centre-specific (Marmarou *et al.*, 2005). The CSF dynamics findings described in NPH are normal ICP, increased pulse amplitude, increased CSF outflow resistance (R_{OUT}) and pathological B waves (Eide and Sorteberg, 2008; Chari *et al.*, 2017; Lalou *et al.*, 2018; Spiegelberg *et al.*, 2018; Lalou *et al.*, 2021). Reports on the use of lumbar punctures, lumbar infusion studies and intraparenchymal ICP monitoring in NPH are available in the literature.

Lumbar punctures have led to the observation that CSF pressure is normal in NPH. According to a consensus achieved by European and American experts, the lumbar puncture opening pressure in NPH is between 60-240 mmH_2O (4.4-17.6 mmHg) (Marmarou *et al.*, 2005). Not allowing continuous CSF pressure measurements and analysis of CSF dynamics, lumbar punctures are not useful for the diagnosis and management of NPH and are not routinely performed.

Lumbar infusion studies have been reported to be useful in diagnosing NPH as well as identifying shunt-responsive patients (Boon *et al.*, 1997; Brean and Eide, 2008). In a large case-control study, Jacobsson *et al.* compared the results of lumbar infusion studies between NPH patients and healthy controls confirming no significant differences in CSF pressures between the two groups, but a significantly higher R_{OUT} in NPH patients compared to controls (Jacobsson *et al.*, 2018). While they found a trend for a higher pulse

amplitude in NPH patients, the difference in pulse amplitudes between the two groups was not statistically significant (Jacobsson *et al.*, 2018). The role of R_{OUT} for the identification of shunt responsive patients is still uncertain. For example Delwel *et al.* found no predictive value in R_{OUT} (Delwel *et al.*, 2005), in addition a study by Brean and Eide reported that CSF pressure pulse amplitude is a better predictor of shunt-responsiveness than R_{OUT} (Brean and Eide, 2008). Another study, by Eide and Brean, compared lumbar infusion studies and intraparenchymal ICP monitoring in NPH patients and confirmed that CSF pressure pulse amplitude measured through lumbar infusion studies correlated well to both the clinical response to shunt treatment and the pulse amplitude measured through ICP monitoring (Eide and Brean, 2010).

The dampening of CSF pulsations from the cervical to the spinal compartments can probably affect the assessment of CSF pressure pulse amplitude through lumbar infusion studies and may make the interpretation of these results more difficult. For this reason, the interpretation of CSF pulse pressures through direct intraparenchymal ICP monitoring techniques may be more reliable. In a study by Chari *et al.*, the use of continuous intraparenchymal ICP monitoring confirmed higher pulse amplitude levels in NPH patients compared to control subjects (Chari *et al.*, 2017). A large study employing intraparenchymal ICP monitoring on 214 NPH patients provided further evidence that an abnormal pulse amplitude (mean >4 mmHg and > 5 mmHg for 10% of the time of monitoring) predicts response to shunt surgery

in 9 out of 10 NPH patients (Eide and Sorteberg, 2010). Another study by Eide and Sorteberg described the effect of shunt treatment on ICP monitoring parameters of 13 patients with NPH, demonstrating a significant reduction in ICP waves amplitude after shunt implantation (Eide and Sorteberg, 2008). These results suggest that shunt may be effective in NPH because of their ability to normalise pulse amplitude.

B waves (see section 1.2.2.1) have also been reported as good predictors of shunt-responsiveness in hydrocephalus, but their utility in the context of NPH is still a matter of debate (Pickard *et al.*, 1980; Stephensen *et al.*, 2005; Evensen and Eide, 2020).

1.3.5. Low CSF pressure/volume syndromes

Low CSF pressure/volume syndromes include conditions typically characterised by the sudden onset of orthostatic headache and believed to be related to a spontaneous or secondary spinal CSF leak.

Low CSF pressure/volume syndromes can be divided into 3 groups:

- Post-Dural Puncture Headache (PDPH)
- Secondary CSF leaks
- Spontaneous Intracranial Hypotension (SIH)

In PDPH and secondary CSF leaks the low CSF pressure/volume syndromes are secondary to dural punctures, spinal surgery or spinal trauma.

In SIH, the sudden onset of orthostatic headache is believed to be secondary to a spontaneous spinal CSF leak. According to the most recent ICHD-III classification (ICHD-III, 2018) a diagnosis of SIH can be made if the following diagnostic criteria are satisfied:

A. Any headache fulfilling criterion C
B. Low CSF pressure (<60 mm CSF) and/or evidence of CSF leakage on imaging
C. Headache has developed in temporal relation to the low CSF pressure or the CSF leakage, or has led to its discovery
D. Not better accounted for by another ICHD-III diagnosis.

Table 10-1 describes the evolution of the ICHD diagnostic criteria for SIH.

It is important to specify that the term low CSF pressure/volume syndrome does not include patients with cranial CSF leaks. Skull base CSF leaks do not cause orthostatic headache, are not associated with a low CSF pressure state and there is evidence suggesting their association with high pressure (Kranz *et al.*, 2018). Despite the similarity of being characterised by CSF leaks, the fact that these leaks occur cranially to the hydrostatic indifferent point makes skull CSF leaks a completely different pathology to the low CSF pressure/volume syndromes (see 1.2.3 for a description of the hydrostatic indifferent point). In fact, in upright posture (when the patients with low CSF pressure/volume syndromes are typically symptomatic) the pressure cranial to the hydrostatic indifferent point would be lower than supine posture.

Therefore, a cranial CSF leak would be much more likely to leak when the patient is in supine position than upright.

1.3.5.1. Intracranial pressure monitoring in low CSF pressure/volume syndromes

Despite the increasing applications of ICP monitoring for investigation of various CSF dynamic disorders, its use in the context of low CSF pressure/volume syndromes is limited and only a few authors have reported any experience in this field (Zada *et al.*, 2007; Eide *et al.*, 2012; Sass *et al.*, 2013; Craven *et al.*, 2016a; Beck *et al.*, 2017; Häni *et al.*, 2020).

The most common among the low CSF pressure/volume syndromes is the post-dural (post-lumbar) puncture headache syndrome that can arise in 7.5% of the patients undergoing a lumbar puncture (Amorim *et al.*, 2012). The temporal correlation between the causing event and the onset of the orthostatic headache is a clear indicator for the diagnosis of this condition, and CSF pressure measurements do not offer many advantages for these patients.

Inadvertent dural tears during spinal surgery and severe trauma can also generate spinal CSF leaks. There are reports of intracranial hypotension resulting from a secondary CSF leak (Albayram *et al.*, 2008b). Craven *et al.* described the ICP monitoring results of a groups of 5 patients with persistent and treatment-refractory CSF leak post spinal surgery. Interestingly, they these patients had raised ICP and pulse amplitude and their CSF leaks

resolved only when these abnormalities were addressed (with shunt surgery, venous sinus stenting or acetazolamide treatment). They concluded that abnormal CSF dynamics could be the underlying factor in patients with a persistent and treatment-refractory CSF leaks post spinal surgery (Craven *et al.*, 2016a). The results of this study suggest that there might be justification for the application of ICP monitoring when patients fail to recover after a CSF leak as raised ICP might need to be excluded.

The SIH diagnostic criteria proposed for SIH by the ICHD have included a 'low CSF pressure' since 2004 (ICHD-II, 2004). For this reason, lumbar puncture opening pressures are routinely checked in patients with suspected SIH. Both Mokri *et al.* and Kranz *et al.* highlighted how low lumbar puncture opening pressure is often not present in SIH, these observations raise concerns on the validity of the use of 'low CSF pressure' as a diagnostic criterion as well as the utility of performing lumbar punctures in these patients (Mokri *et al.*, 1998; Kranz *et al.*, 2016b). Chapter 3 of this thesis provides a comprehensive systematic review on SIH clinical presentation, investigation findings and treatment outcomes. The results of lumbar punctures in SIH patients will be described in the context of chapter 3 (section 3.4.4.5).

ICP monitoring has rarely been reported in low CSF pressure/volume syndromes. Sass *et al.* report the case of a patient with severe clinical manifestations of SIH with low ICP who responded to lumbar intrathecal infusion (Sass *et al.*, 2013). Eide *et al.* described the morphology of the

cardiac induced ICP waveform in patients with low ICP of various aetiologies, their group included 4 patients with SIH and they concluded that pulse amplitude seems to be increased when ICP is extremely negative (<-15 mmHg) (Eide *et al.*, 2012). In another case, ICP monitoring was reported to be useful for the diagnosis of SIH and allowed the tracking of ICP changes after epidural blood patch treatment (Zada *et al.*, 2007).

Beck *et al.* reported their experience with the use of lumbar infusion studies in 31 patients with suspected SIH. They showed that patients with a proven CSF leak had lower CSF opening pressure, plateau pressures and R_{out} compared to patients with suspected SIH without evidence of a spinal CSF leak on spinal imaging. They suggested that R_{out} could be included in the SIH diagnostic criteria (Beck *et al.*, 2017). A larger study by the same group reported the results of lumbar infusion testing in 137 patients with suspected SIH (Häni *et al.*, 2020). They found lower CSF baseline pressures, lower R_{OUT}, higher compliance and pressure volume index in patients with confirmed CSF leaks. Additionally, they highlighted that these features were most common in patients in the acute disease phase and that patients with a longer disease duration were less likely to present these CSF abnormalities (Häni *et al.*, 2020).

The value of lumbar infusion studies in SIH is still to be determined as it has the important limitation of assessing the patients in lateral decubitus position and not in upright posture. Results obtained with this technique may not be

reliable as infusion studies do not take into account the fact that SIH patients' signs and symptoms mainly occur in the upright posture.

Chapter 4 of this thesis describes the use of continuous intraparenchymal ICP monitoring in low CSF pressure/volume syndromes.

1.4. Aims of this thesis

As highlighted throughout this introduction chapter, there are many aspects of CSF physiology and CSF dynamics disturbances pathophysiology that are still unknown and controversial. Over the past decades, the use of clinically indicated invasive ICP monitoring in disease states has provided a unique opportunity to improve our knowledge about many aspects of CSF dynamics. Despite the utility of invasive ICP monitoring, non-invasive ICP monitoring techniques remain an important objective for the research in this field. In addition, the creation of a truly programmable shunt system, a 'smart shunt', is still sought-after, but the uncertainties on many aspects of CSF dynamics make this difficult to achieve. This PhD thesis focuses on the use of continuous intraparenchymal ICP monitoring in patients with CSF dynamics disorders, trying to answer the following questions:

1. Is there a role for ICP monitoring in the diagnosis and management of SIH?
2. What is the effect of posture on CSF dynamics and on pulse amplitude?
3. What is the effect of valve setting changes on ICP *in vivo*?

4. Is the absence of SVPs a useful non-invasive marker of raised ICP?
5. Can we use imaging and ophthalmic biomarkers of raised ICP to reliably predict intracranial hypertension?

Chapter 2 describes in detail the methods used to measure, collect, analyse and interpret ICP monitoring data.

Chapters 3 and 4 investigate the utility of ICP monitoring for the diagnosis and management of low CSF pressure/volume syndromes. While the role of ICP monitoring is relatively more established for high pressure syndromes (e.g., idiopathic intracranial hypertension) and hydrocephalus, its use in low CSF pressure/volume syndromes is rare. In particular, chapter 3 is a comprehensive systematic review on the clinical presentation, investigation findings and treatment outcomes of spontaneous intracranial hypotension (SIH). Chapter 4 describes the utility of continuous ICP monitoring in patients with orthostatic headache and unidentifiable CSF leaks on spinal imaging.

Chapter 5 and 6 investigate the effect of position on intracranial pulse amplitude and the effect of shunt valve settings adjustments on ICP. Both aspects are important for a better understanding of CSF dynamics and to provide information useful for patient and disease-tailored shunt treatments.

Finally, chapter 7 and 8 describe non-invasive methods of identification of raised ICP based on ophthalmic and imaging markers of intracranial

hypertension. Chapter 7 describes the association between ICP and spontaneous retinal venous pulsations (SVP) identified through infrared video recordings of the retina. Chapter 8 describes the utility of combining ophthalmic and imaging markers of raised ICP (on brain MRI) for the identification of patients with intracranial hypertension.

Chapter 2. Methods: Elective 24-hour Intracranial Pressure Monitoring at the National Hospital for Neurology and Neurosurgery

Intracranial Pressure (ICP) monitoring is commonly performed in the acute care setting, especially for patients affected by traumatic brain injuries and/or intracranial bleeding. The use of ICP monitoring in the elective non-acute setting is less common but has demonstrated its utility in the management of patients with cerebrospinal fluid (CSF) dynamics disorders including Idiopathic Intracranial Hypertension (IIH), Normal Pressure Hydrocephalus (NPH), Chiari malformation type I and hydrocephalus (Eide and Kerty, 2011; Andresen *et al.*, 2015; Chari *et al.*, 2017; Czosnyka and Czosnyka, 2017; Fric and Eide, 2017; Bridges and Raslan, 2018; Eide, 2018; Dyson *et al.*, 2020; Evensen and Eide, 2020; Lalgudi Srinivasan *et al.*, 2020). There is no international consensus on the way that elective ICP monitoring should be performed resulting in a lack of methodology standardization. Methods and types of equipment can affect ICP monitoring results, especially the static ICP readings, making results obtained with different techniques not directly comparable (Evensen and Eide, 2020). The National Hospital for Neurology and Neurosurgery (NHNN) is one of the few centres with a long history (about 20 years) of performing elective ICP monitoring. This chapter describes the method for elective ICP monitoring adopted at this centre, discussing the implications of each step. The methods described in this chapter apply to all the experimental chapters of this thesis.

2.1. Indications for elective ICP monitoring

Elective 24-hour ICP monitoring is performed as a diagnostic investigation for patients with suspected CSF dynamics disorders when patients are affected by intractable symptoms and other non-invasive investigations are inconclusive. The other indication for elective 24-hour ICP monitoring is for patients with confirmed CSF dynamics disturbances, possibly with CSF drainage shunts in situ, who have complex symptom management and require ICP-guided treatment.

Figure 2-1 describes the sequence of events occurring for each patient who undergoes ICP monitoring at the NHNN. When ICP monitoring is being considered, patients with suspected intracranial hypertension or abnormal brain compliance will first undergo brain imaging and an ophthalmology assessment performed by an experienced neuro-ophthalmologist. Patients with suspected spontaneous intracranial hypotension or CSF leaks not responding to conservative treatment undergo brain and spinal imaging (most commonly MRI with contrast), a neurology review and an autonomic assessment for the exclusion of Postural Tachycardia Syndrome (PoTS).

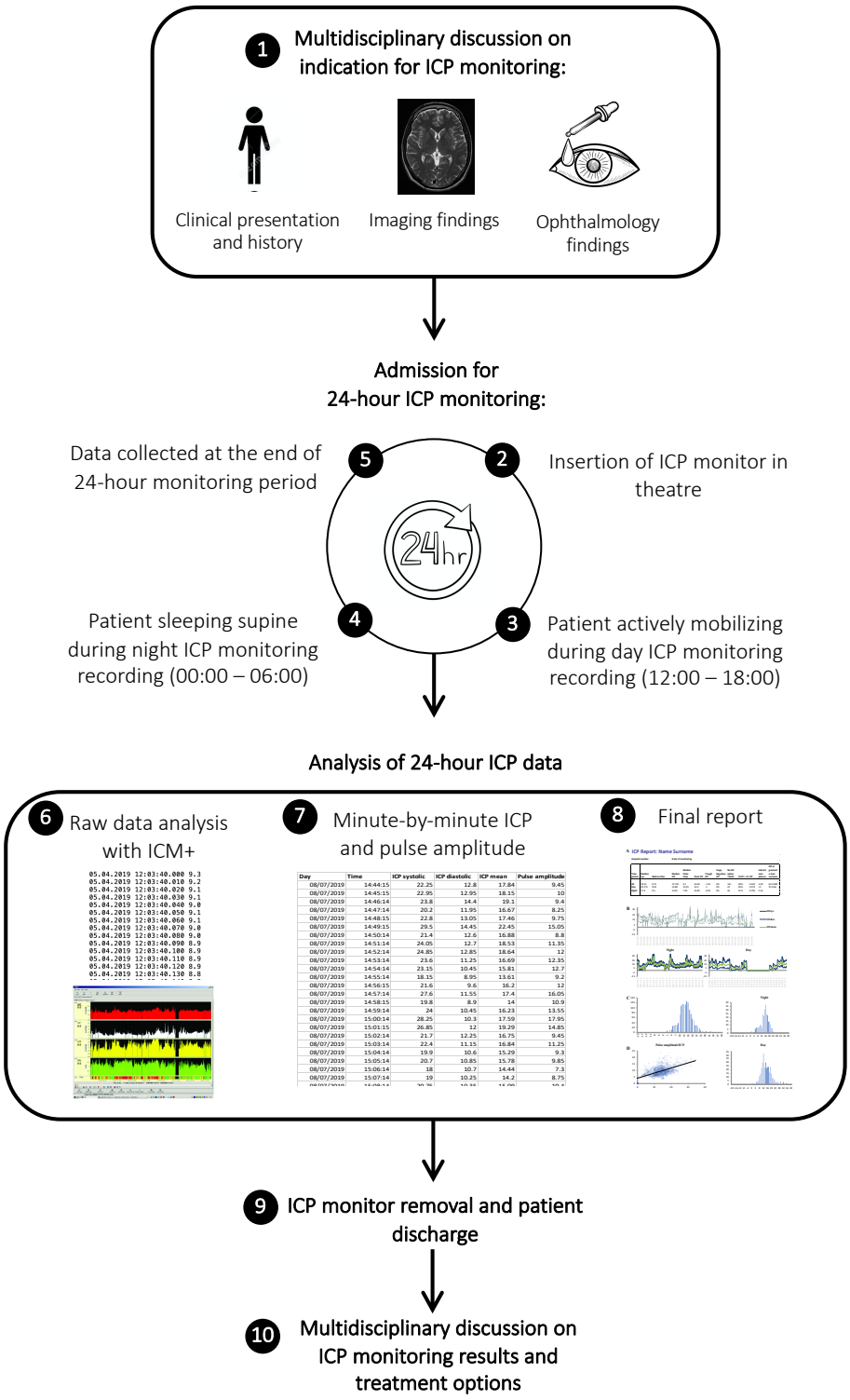


Figure 2-1: Flowchart of 10 steps ICP monitoring at NHNN

Candidates considered for ICP monitoring have commonly undergone previous lumbar punctures with results that were inconclusive. While the available results of these investigations are taken into account, further lumbar punctures are not repeated in our centre before ICP monitoring. The main reasons for avoiding further lumbar punctures are:

- lumbar punctures are a snapshot assessment of ICP and do not provide information about brain compliance which is essential for the patients' management;
- lumbar punctures do not provide information about CSF dynamics including changes in ICP with different postures and day/night cycles;
- considering that lumbar punctures were previously inconclusive, repeating the same investigation is unlikely to obtain better results and would only cause patient's discomfort.

Additionally, patients with suspected spontaneous intracranial hypotension or CSF leaks may be at higher risk of post-lumbar puncture headaches and lumbar punctures may actually worsen their symptoms or create new CSF leaks, especially if the patient is affected by connective tissue disorders (e.g., Ehlers-Danlos Syndrome).

Previous invasive CSF measurements (e.g., lumbar punctures, lumbar infusion studies) could potentially have an impact on CSF dynamics and therefore alter ICP monitoring results. There are no standardised protocols setting out how long the time interval between these investigations should

be. At NHNN, patients who had prior inconclusive invasive CSF measurements, would typically wait several weeks (2 or more) before elective ICP monitoring is performed.

All the available clinical information and investigation findings are taken into account and the indication for 24-hour ICP monitoring is confirmed in the context of a multidisciplinary discussion including neurosurgeons, neurologists, ophthalmologists, radiologists and nurse specialists.

2.2. ICP monitoring equipment

The ICP monitoring equipment includes: the ICP measuring sensor (Figure 2-2), the ICP monitor (Figure 2-3) and the ICP recording/analysis laptop.

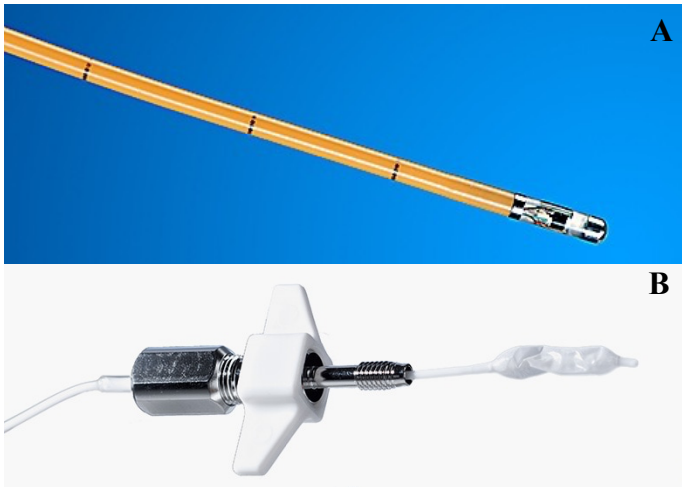


Figure 2-2: Raumedic NEUROVENT-P (A) and Spiegelberg (B) ICP monitoring sensors



Figure 2-3: MPR 1 Raumedic (A) and Spiegelberg (B) ICP monitors

There are multiple commercially available ICP sensors. Although all provide continuous ICP recordings, few allow direct exporting of the data for mathematical analysis, Two types of ICP sensors are currently used at the NHNN: the NEUROVENT-P (Raumedic AG, Münchberg, Germany) and the Spiegelberg parenchymal probe (Spiegelberg GmbH & Co. KG, Hamburg, Germany) (Figure 2-2). They are both intraparenchymal sensors but present a different structure and method of ICP measurement. While the Spiegelberg probe is a pneumatic system (air-pouch), the Raumedic NEUROVENT-P probe has a strain-gauge sensor. Both systems are calibration-free and have demonstrated acceptable results in terms of accuracy and zero-drift (Lang *et al.*, 2003; Citerio *et al.*, 2004; Citerio *et al.*, 2008). It has been suggested that the use of a pneumatic system (like Spiegelberg) could affect the ability of the sensor to reliably estimate the ICP pulse amplitude and to perform ICP waveform analysis (Evensen and Eide, 2020). For this reason, pulse amplitude analyses performed in the following chapters have been stratified by type of ICP sensor.

Another important difference between the Raumedic NEUROVENT-P and Spiegelberg ICP monitoring systems is purely logistic. The Spiegelberg ICP monitor requires continuous connection to a separate laptop for the data recording and live analysis. The Raumedic NEUROVENT-P monitor is more modern and has the ability to store data, therefore, it does not require continuous connection to a laptop. This inevitably affects the level of mobility achieved by the patients assessed with the two different types of monitors.

2.3. Description of the surgical procedure

Patients undergoing insertion of ICP monitors are admitted on the day of surgery. The procedure is performed in the operating theatre with local anaesthesia (Bupivacaine 0.25%) and the patient is positioned supine. Sedation (or more rarely general anaesthesia) is employed in selected patients depending on individual needs.

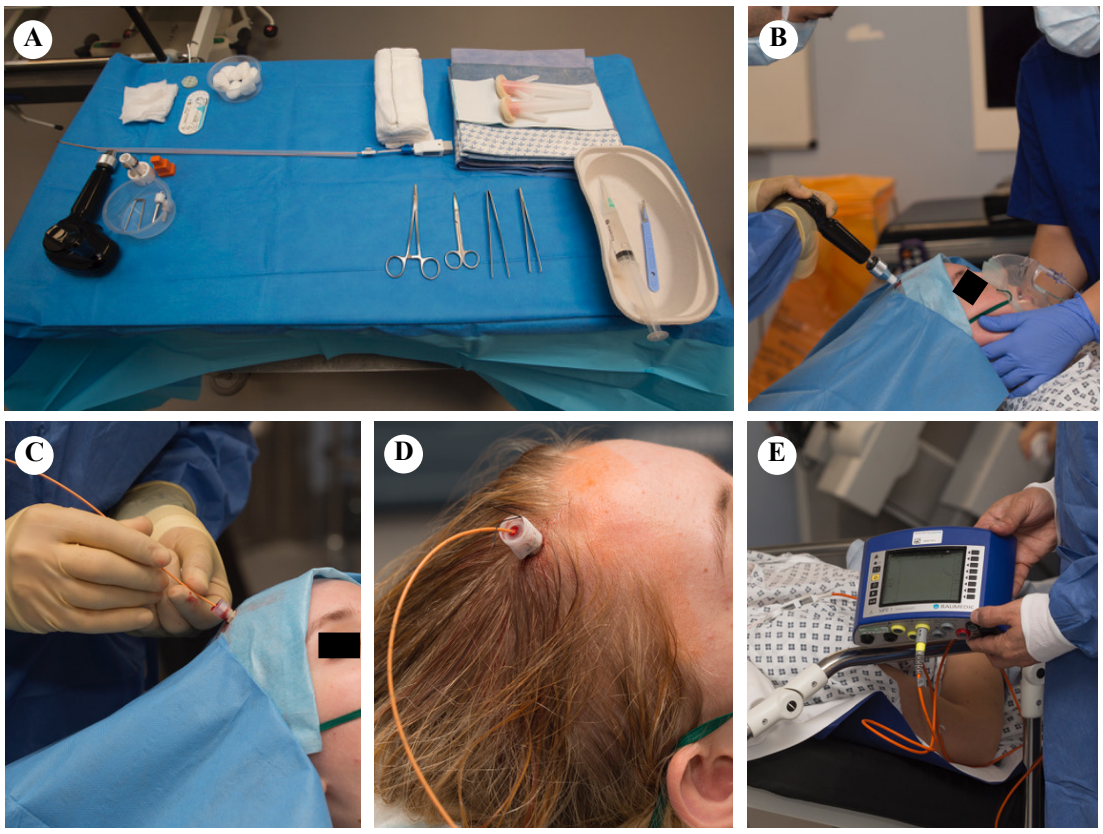


Figure 2-4: Procedure of ICP monitor insertion at NHNN. A: equipment; B: Burr hole with hand drill in the right frontal area; C: Insertion of ICP monitoring sensor; D: Final result; E: Connection of ICP monitor and first static ICP and waveform check

The site of insertion of the intraparenchymal ICP sensor is right frontal. The area is cleaned and draped. After infiltration of the local anaesthetic, a 2 cm linear incision is performed. The twist-drill hole is created through the use of a hand drill (Figure 2-4B). Bone fragments are removed from the area of incision and a dura perforator is used to pass the dura. The ICP monitor bolt is then fixed on the skull and the ICP measuring sensor passed and secured in the bolt (Figure 2-4C). The ICP monitoring sensor is inserted until the 6 cm mark meets the top edge of the bolt; this positions the sensor at about 1-3 cm depth in the brain parenchyma. A purse string 2-0 silk suture is secured across the linear incision around the bolt. The ICP monitoring sensor cable is then connected to the monitor at the theatre bedside (Figure 2-4E). The initial ICP readings are checked on the monitor and recorded, this step allows the early identification of an eventual sensor misplacement. The patient is transferred to the postoperative recovery area and once ready, transferred to the neurosurgical ward.

2.4. Duration of 24-hour ICP monitoring

In the initial stages of the NHNN ICP monitoring practice, ICP monitoring was performed for 48 continuous hours. The clinical practice shifted towards 24-hour ICP monitoring after an observational study demonstrated no significant difference between monitoring for 24 or 48 hours (Thompson *et al.*, 2015). The duration of ICP monitoring is usually longer for patients with a shunt in place who require ICP-guided valve setting adjustments. In these cases, the patient is monitored for the first 24 hours, the valve is adjusted and then the

patient is monitored for further 24 hours following the valve setting adjustment. If optimal ICP and symptoms control is not achieved, another valve setting adjustment and another 24-hour of ICP monitoring may be required.

Occasionally, ICP monitoring is prolonged for longer periods of time for patients without a shunt in place. This usually occurs if further investigations/treatments are performed and continuous ICP monitoring data are required.

2.5. Patients' activities during ICP monitoring

Posture has known effects on ICP, in fact ICP is higher in supine position compared to upright position (Farahmand *et al.*, 2014; Andresen *et al.*, 2015). This is relevant for 24-hour ICP monitoring as the level of activity that patients maintain during the monitoring period can significantly affect the final results. For example, more active patients are expected to have lower median 24-hour ICP compared to bedbound patients.

At the NHNN, patients receiving 24-hour ICP monitoring are asked to mobilise in the daytime and sleep in the supine position at night. This is different compared to other neurosurgical centres where elective CSF pressure measurements are usually performed in the supine position. This protocol permits the close simulation of the patients' daily activities and thereby allows observation of the ICP in conditions similar to the

circumstances in which they experience their symptoms. Additionally, night ICP monitoring readings can provide useful information on static supine ICP.

For the interpretation of the ICP monitoring results, it is assumed that patients were upright for most part of the day and supine for most part of the night. The obvious risk of this assumption is that if patients do not comply with these instructions the final ICP monitoring results could be skewed by an unexpected level of activity (upright during the night and/or supine during the day). For this reason, patients and bedside nurses are asked about the patients' level of activity during the ICP monitoring at the end of the 24-hour period. Other information collected at the end of the monitoring period are about the patients' symptoms; if any headache has occurred, patients are asked about the approximate time of the day and the position (or activity) in which they experienced it.

2.6. Data analysis and ICP monitoring report

Both the NEUROVENT-P Raumedic and Spiegelberg ICP monitors allow high frequency sampling of ICP readings (>100 Hz). The raw data is analysed with the software ICM+© (University of Cambridge, UK) that performs a frequency-domain ICP analysis resulting in mean ICP and pulse amplitude values for each minute of recording (Figure 2-5).

The frequency domain analysis has been the most common method for the analysis of the ICP waveform since the 1980s (Holm and Eide, 2008). In the frequency domain analysis, the signals are converted from the time domain

to the frequency domain by a fast Fourier Transform. Whereas, in the time domain analysis the ICP waveform is analysed identifying the average peak-peak value (systolic minus diastolic peak) (Holm and Eide, 2008). Although there are concerns that frequency domain analysis could underestimate pulse amplitudes in certain conditions (Holm and Eide, 2008), this is unlikely to translate into clinically relevant issues as long as the same analysis tool is used consistently and the reference values are based on studies using the same analysis tool. While time-domain analysis represents a valid alternative, the frequency domain analysis method was employed for this thesis due to the large previous experience of this centre and its availability.

Day	Time	ICP systolic	ICP diastolic	ICP mean	Pulse amplitude
08/07/2019	14:44:15	22.25	12.8	17.84	9.45
08/07/2019	14:45:15	22.95	12.95	18.15	10
08/07/2019	14:46:14	23.8	14.4	19.1	9.4
08/07/2019	14:47:14	20.2	11.95	16.67	8.25
08/07/2019	14:48:15	22.8	13.05	17.46	9.75
08/07/2019	14:49:15	29.5	14.45	22.45	15.05
08/07/2019	14:50:14	21.4	12.6	16.88	8.8
08/07/2019	14:51:14	24.05	12.7	18.53	11.35
08/07/2019	14:52:14	24.85	12.85	18.64	12
08/07/2019	14:53:14	23.6	11.25	16.69	12.35
08/07/2019	14:54:14	23.15	10.45	15.81	12.7
08/07/2019	14:55:14	18.15	8.95	13.61	9.2
08/07/2019	14:56:15	21.6	9.6	16.2	12
08/07/2019	14:57:14	27.6	11.55	17.4	16.05
08/07/2019	14:58:15	19.8	8.9	14	10.9
08/07/2019	14:59:14	24	10.45	16.23	13.55
08/07/2019	15:00:14	28.25	10.3	17.59	17.95
08/07/2019	15:01:15	26.85	12	19.29	14.85
08/07/2019	15:02:14	21.7	12.25	16.75	9.45
08/07/2019	15:03:14	22.4	11.15	16.84	11.25
08/07/2019	15:04:14	19.9	10.6	15.29	9.3
08/07/2019	15:05:14	20.7	10.85	15.78	9.85
08/07/2019	15:06:14	18	10.7	14.44	7.3
08/07/2019	15:07:14	19	10.25	14.2	8.75
08/07/2019	15:08:14	20.75	10.35	15.09	10.4
08/07/2019	15:09:14	21.2	9.2	15.26	12
08/07/2019	15:10:14	21.2	10	15.37	11.2
08/07/2019	15:11:14	20.25	9.85	14.42	10.4
08/07/2019	15:12:14	21.8	10	15.43	11.8
08/07/2019	15:13:14	19.25	8.7	14.14	10.55

Figure 2-5: Minute-by-minute ICP and pulse amplitude data after ICM+ analysis

The minute-by-minute ICP and pulse amplitude data is then imported into a standardised in-house analysis tool that summarises the results in terms of median ICP and median pulse amplitude over 24 hours, during the day

(12:00 - 18:00 hours) and during the night (00:00 to 06:00 hours). An example of ICP monitoring results report is showed in Figure 2-6.

The ICP monitoring summary table (Figure 2-6A) also reports the peak and trough ICPs, these are the highest and lowest ICP readings recorded in the monitoring period. These results, especially the peak ICP, can be significantly affected by artefacts, therefore they should be looked at in the context of the whole ICP monitoring report. The percentage of time the ICP is negative ('%age negative ICP' in Figure 2-6A) is expected to be high during the day and low during the night, as the upright ICP should be negative and the supine ICP positive (Norager *et al.*, 2021). In this example, the percentage of negative ICP is 0% throughout the recording; in fact, this patient was diagnosed with intracranial hypertension (Figure 2-6). The percentage of time that ICP is above 15 mmHg ('% ICP>15' in Figure 2-6A) and the number of episodes that ICP raised above 25 mmHg ('No ICP>25' in Figure 2-6A) allow further quantification of intracranial hypertension, both these parameters should be close to zero in normal ICP recordings.

The ICP monitoring report also provides information on the pressure-volume compensation through the calculation of the Pearson coefficient between mean ICP and mean pulse amplitude ('PIP" in Figure 2-6). This is also known as the pressure-volume compensation index (RAP) and has been used for the assessment of the compensatory reserve in trauma and chronic CSF dynamics disturbances (Czosnyka *et al.*, 1996; Schuhmann *et al.*, 2008; Kim

et al., 2009). This coefficient can range from -1 to +1, with upper normal threshold of +0.6 (Kim *et al.*, 2009; Eide *et al.*, 2014). The indirect compliance (calculated as 1/slope of ICP and pulse amplitude) is also useful to identify patients with abnormal brain compliance and loss of compensatory reserve.

The pressure/time graphs (Figure 2-6B) display the pressure systolic and diastolic parameters in blue and the mean ICP in green. The wider the gap between systole and diastole, the higher the pulse amplitude. The frequency distribution graphs show the frequency distribution of the minute-by-minute ICP means highlighting the median ICP as a peak (Figure 2-6C). Finally, Figure 2-6D is a scatter plot of pulse amplitude (y axis) and ICP (x axis), the linear regression line has a slope close to zero in patients with normal ICP.

Once the report is generated the ICP monitoring results are screened for technical issues.

ICP Report: Name Surname

Hospital Number Date of Monitoring

A

Time period	Median Sys	Median Dias	Median ICP	Median Pulse Amp	Peak ICP	Trough ICP	%age Negative ICP	No ICP spikes >25/hr	%ICP > 15	PIP	Indirect compliance	PIP at greatest x hour variance
All	14.01	7.1915	10.555	5.479	49.36	-0.2116	0%	85	39%	0.118	>4	6h 0.648
Day	10.245	4.273	7.2155	5.574	22.7	-0.1063	0%	0	13%	0.207	>4	3h 0.648
Night	20.1	15.715	17.495	4.668	49.36	2.154	0%	64	97%	0.792	3.02	

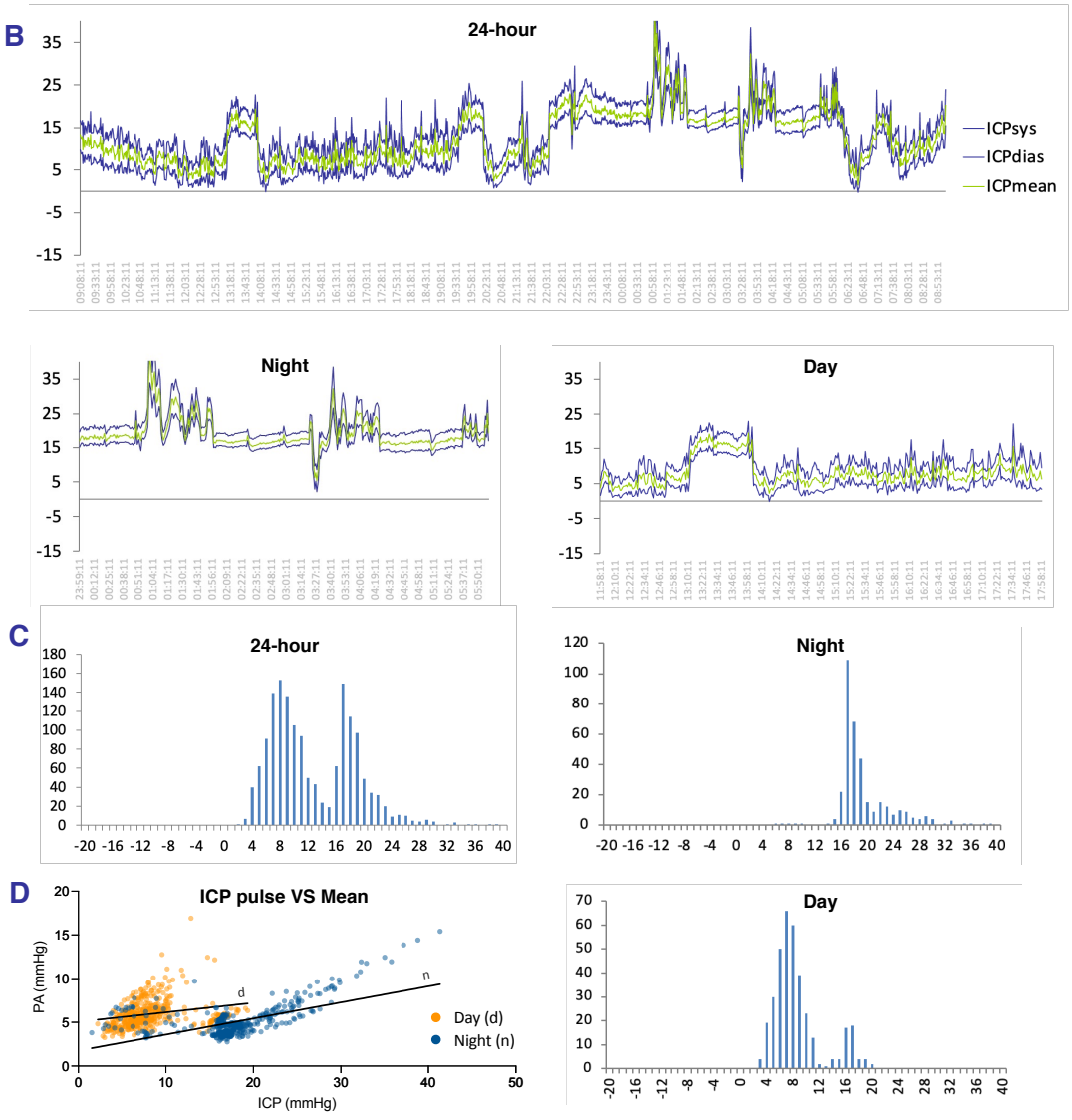


Figure 2-6: Example of 24-hour ICP monitoring report. A. Summary results stratified by 24-hour, day and night; B. Pressure/Time graph with Mean ICP (green) and mean systolic/diastolic ICP (blue); C: frequency distribution graph; D: pulse amplitude/ICP scatter plot and linear regression stratified by day (orange, d) and night (blue, n).

2.7. ICP monitoring results

When the monitoring period is complete and sufficient data is collected, the ICP monitoring device is removed and the patient is discharged home. The ICP monitoring report and raw data are prospectively stored in the clinical ICP monitoring database. Patients with obvious CSF dynamics abnormalities may undergo additional investigations during the same admission before discharge. The final results are discussed in the following multidisciplinary team (MDT) meeting and best patients' management options are decided. The results of the MDT are discussed with the patient at their follow-up appointment.

2.8. Limitations

This method for ICP monitoring is invasive and requires a surgical procedure performed in the operating theatre. Various non-invasive ICP monitoring methods have been proposed, however, none of them has been considered reliable enough to replace invasive methods in clinical practice (Evensen and Eide, 2020). While non-invasive ICP monitoring would be preferable, the method adopted at the NHNN has demonstrated to be safe with very low complication rates. A retrospective study including 338 patients undergoing this procedure reported the following complication rates: 1.2% superficial infections, 0.3% symptomatic intracerebral haematoma, 0.9% misplacements and no cases of deep intracranial infection (Chari *et al.*, 2015).

As discussed by Evensen and Eide, different ICP measuring devices and analysis tools produce different estimates of the static ICP (Evensen and Eide, 2020). As a result, there is limited generalisability of the ICP monitoring results, making the comparison of results obtained with different ICP measuring methods challenging. This issue is less likely to affect individual patients but is very relevant when ICP monitoring results are reported for research purposes.

Another limitation for ICP monitoring is the lack of standards for the analysis of the ICP waveform. At NHNN, the ICP monitoring protocol incorporates a frequency-domain analysis through the software ICM+© (University of Cambridge, UK), however time-domain analyses are another alternative that can be considered. Holm and Eide found that compared to time-domain analysis, the frequency-domain analysis performed through ICM+ can underestimate pulse amplitude (Holm and Eide, 2008). The same study also found that pulse amplitude values were significantly abnormal in head injury patients with both types of analysis (frequency and time domain) and larger comparative studies will be needed to confirm the superiority of one of these two different analysis methods.

Despite the fact that different analysis tools could produce different results, these differences are not thought to be significant enough to affect clinical decisions. These differences however explain why different units make

different estimates of what can be considered normal ICP (Norager *et al.*, 2021).

Further considerations need to be made about the use of conscious sedation in ICP monitoring. The sedation employed at NHNN includes propofol and fentanyl used during the insertion of the ICP probe. These agents have clinical manifestations of short duration, but their effects on CSF dynamics are not entirely known. One of the concerns on the use of sedative agents in non-ventilated patients with CSF dynamics disturbances is their effect on the respiratory function and the potential for CO_2 retention that could lead to an increase in ICP. Girad *et al.* studied the effect of propofol and remifentanil on ICP in patients undergoing stereotactic brain tumour biopsy under regional anaesthesia (Girard *et al.*, 2004; Girard *et al.*, 2009). The results of these studies showed that the use of these sedative agents in non-ventilated patients did not significantly increase ICP (Girard *et al.*, 2004; Girard *et al.*, 2009). However, studies on patients with traumatic brain injuries and mechanical ventilation have demonstrated a reduction in ICP secondary to the use of propofol (McKeage and Perry, 2003). At our centre, sedative agents are only used when strictly necessary and in the smallest effective doses, but further specifically designed studies are needed to prospectively investigate the effect that different sedative agents have on the ICP monitoring results of patients with CSF dynamics disturbances.

Finally, as previously discussed (section 2.5), levels of activity can affect 24-hour static ICP monitoring results. In our experience, patients' reports of their activities and mobility during the ICP monitoring period are useful. Night ICP monitoring results are less likely to be affected by this issue. Future solutions would be represented by technologies able to perform continuous monitoring of patients' posture paired with the continuous ICP measurements.

Chapter 3. Spontaneous Intracranial Hypotension Syndrome: A Systematic Review and Meta-analysis

3.1. Abstract

3.1.1. Background

Spontaneous Intracranial Hypotension (SIH) is a highly misdiagnosed and underdiagnosed disease. The best management course for SIH patients is still uncertain. While scientific publications on SIH have progressively grown in number in the past decade, no large randomised controlled trials or systematic reviews of the literature are available. This is a comprehensive systematic review of the literature on SIH. The aim is to provide a summary of the available evidence on the clinical presentation, investigations findings and treatment outcomes for SIH.

3.1.2. Methods

Systematic review and meta-analysis of the literature on SIH including papers published until the 30th of April 2020 (no start date limit). Three databases were searched: Pubmed/MEDLINE, Embase and Cochrane. Only original studies in English language reporting 10 or more patients with SIH (or spontaneous CSF leaks) were included. Both summary data and patient-level data were extracted from published reports. Data on clinical presentation, investigations findings and treatment outcomes were collected and summarised. Random effect meta-analyses were used to calculate pooled estimates of proportions [95% CI]. The variability within studies and

between studies was assessed with the I^2 estimate of heterogeneity. PROSPERO registration number CRD42019147300.

3.1.3. Results

The initial search identified 68788 articles. Among these, 144 articles reporting on average 53 SIH patients each (range 10-568) met the inclusion criteria and were eligible for analysis. The most common symptoms of SIH were headache in 97% of the patients (95% CI 94-99), nausea in 54% (95% CI 46-62) and neck pain/stiffness in 43% (95% CI 32-53). Brain MRI was the most sensitive investigation for SIH, with diffuse pachymeningeal enhancement present in 73% of the patients (95% CI 67 to 80). Brain MRIs were normal in 19% of the patients (95% CI 13-24). Spinal investigations identified the presence of extradural CSF in 48-76% of the cases. Lumbar puncture opening pressures were low (<6 mmH_2O) in 67% of the patients (95% CI 54-80), normal in 32% (95% CI 20-44) and high (>200 mmH_2O) in 3% (95% CI 0-6). Conservative treatment was effective (resolution of symptoms with no further intervention needed) in 28% of the patients (95% CI 18-37), while the first epidural blood patch (EBP) was successful in 64% (95% CI 56-72). Large EBPs (>20 ml) had better success rates than small EBPs (77% and 66% respectively).

3.1.4. Conclusion

The limitations of this systematic review are the heterogeneous nature of the SIH studies available in the literature, the lack of randomised controlled trials

and the lack of continuity in the diagnostic criteria used over the past decades. Despite its limitations this study offers a comprehensive summary of the evidence on SIH that could be useful in guiding clinical practice and future research.

3.2. Introduction

The term spontaneous intracranial hypotension (SIH) defines a clinical condition characterised by debilitating postural headaches secondary to spontaneous spinal cerebrospinal fluid (CSF) leak and/or CSF hypotension. According to the 3rd International Classification of Headache Disorders (ICHD-III), SIH is diagnosed when headache has developed spontaneously and in temporal relation to a CSF leak (evident on imaging) and/or CSF hypotension (lumbar puncture opening pressure <60mmCSF) (ICHD-III, 2018).

SIH is a highly misdiagnosed and underdiagnosed disorder (Schievink, 2003). SIH is also relatively common. A recent population based incidence study conducted between 2006 and 2020 in California (USA) demonstrated that SIH has an incidence of 3.7/100000/year (Schievink *et al.*, 2022). In addition, a recent patients' survey conducted by Cheema *et al.* demonstrated that SIH is a highly disabling disorder with significant impact on patients' quality of life as well as economical health (Cheema *et al.*, 2022). The exact pathogenetic mechanism of SIH is unknown and this lack of knowledge has

led to a series of misconceptions (Kranz *et al.*, 2018). Moreover, the ICHD diagnostic criteria for SIH have changed significantly over the last few decades and alternative diagnostic criteria have been proposed (Schievink *et al.*, 2008; Schievink *et al.*, 2011). These factors have probably contributed to the current uncertainty on how to reliably diagnose SIH and effectively treat these patients.

Despite the increasing number of publications on SIH over the last two decades, this is the first comprehensive systematic review on this condition. The aim of this study is to summarise the available evidence on clinical presentation, diagnostic investigations and treatment outcomes for SIH. Specific questions addressed in this systematic review are:

- What are the signs and symptoms of SIH and how frequently do they occur?
- What is the sensitivity of brain MRI, spinal imaging and lumbar puncture opening pressures in detecting signs of SIH?
- What is the most sensitive spinal imaging technique to detect CSF leaks? What are the outcomes of conservative treatment and epidural blood patches (EBP) in SIH patients?
- What is the most efficient EBP technique in SIH (non-targeted versus targeted, small versus large volume patches)?

3.3. Methods

This is a systematic review and meta-analysis of the clinical presentation, investigations findings and treatment outcomes of SIH. This study is compliant with the Preferred Reporting Items for Systematic Reviews and Meta-Analyses (PRISMA) checklist and registered on PROSPERO (CRD42019147300) (Liberati *et al.*, 2009).

3.3.1. Search strategy

Three electronic databases were searched for studies on SIH or spontaneous CSF leaks (Pubmed/MEDLINE, Embase and Cochrane). The search did not have a start date limit and was last updated on 30 April 2020. The following search terms were used in each database: 'Spontaneous intracranial hypotension', 'Low CSF syndrome', 'Low CSF pressure syndrome', 'Low CSF volume syndrome', 'Intracranial hypotension' 'Low CSF pressure', 'Low CSF volume', 'CSF hypovolemia', 'CSF hypovolaemia', 'Spontaneous spinal CSF leak', 'Spinal CSF leak', 'CSF leak syndrome'.

3.3.2. Selection criteria

The inclusion criteria were:

- topic SIH or spontaneous CSF leaks,
- English language,
- original study ,
- reporting at least 10 patients.

Manuscripts reporting intracranial hypotension or CSF leaks secondary to other causes (traumatic or iatrogenic) were excluded. Articles reporting a mixed population of patients affected by spontaneous and secondary leaks were included if they were compliant with the inclusion criteria and it was possible to clearly distinguish the characteristics of the spontaneous CSF leak group. Due to the comprehensive nature of the systematic review and the large volume of papers obtained from the search, it was not possible to include articles written in languages other than English. Manuscripts published ahead of print and any study design were considered. Reference lists of the selected papers were screened. Case reports and small case series (reporting less than 10 patients) were screened for unusual findings before exclusion. Search and screening were performed by the PhD thesis author (L. D'Antona) and revised by one of the supervisors (M. S. Matharu); conflicts on inclusion of data were resolved by consensus with a third author (A. K. Toma or I. Davagnanam).

3.3.3. Risk of bias

The risk of bias of the selected studies was assessed through the NIH Quality Assessment Tool for Case Series Studies (National Institute of Health, 2021). Papers were rated as good, fair or poor by two independent assessors (A. Jaime Merchan and A. Vassiliou). Disagreements were settled through discussion between the two assessors. In order to prevent bias due to duplicated information, only the biggest case series per author/research group (highest number of patients) was included in each analysis.

3.3.4. Data extraction

The selected articles were assessed to identify the presence of information on each of the following domains: study design, demographic characteristics, risk factors, clinical presentation, brain MRI, spinal imaging, CSF leak location, CSF pressure, treatments and outcomes (see

Table 3-1 for detailed list of variables).

A two-stage data extraction process was performed: an initial screening of publications allowed the identification of all the possible items and variables reported in the literature for each domain, followed by reassessment of the papers to extract the data in deeper detail. Both summary data and patient-level data were extracted from published reports. The data extraction was performed by L. D'Antona and revised by A. Jaime Merchan, A. Vassiliou, M. S. Matharu and I. Davagnanam (imaging findings only).

Table 3-1: Variables included in the systematic review

Domain	**Variables**
Study characteristics	Authors, affiliations, SIH diagnostic criteria, study design (prospective/retrospective, observational/interventional), number of patients.
Demographics	Age (mean, SD, range), sex (male/female).
Risk factors	Patients with connective tissue disorders, spinal pathologies, other risk factors.

Clinical presentation	Symptoms duration (mean, SD, range), headache (n. patients and characteristics), nausea/vomiting, neck pain/stiffness, hearing impairment, tinnitus, other ear signs/symptoms, dizziness, vertigo, photophobia, diplopia, other visual signs/symptoms, reduced level of consciousness, cognitive disturbances, back pain, movement disturbances, other signs/symptoms.
Brain MRI	N. of investigations performed, diffuse pachymeningeal enhancement, subdural collections, brain sagging, pituitary gland enlargement, venous engorgement, slit ventricles, tonsillar descent, normal brain MRI appearances, other findings.
Spinal imaging	For each type of spinal investigation: n. of investigations performed, n. of extradural CSF detection, type of leak detection (specific leak site, broad area, unspecified). Type of investigations: spine MRI, CT myelogram, radionuclide cisternography, MR myelography (with and without intrathecal gadolinium), other spinal investigations.
CSF leak location	N. of leaks identified, leaks location (cervical, cervico-thoracic, thoracic, thoraco-lumbar, lumbar, lumbo-sacral, sacral, multiple leaks).
CSF pressure	N. of lumbar punctures (or CSF pressure measurements), pressure findings: low (<60 mmH_20), normal (60-200 mmH_20), high (>200 mmH_20).
Treatments and outcomes	Conservative treatment: n. of patients treated, duration of treatment, outcomes, type (bed rest, hydration, caffeine, analgesia, steroids); EBP: n. of patients treated, duration of treatment, outcomes, n. of EBPs, type (targeted, non-targeted, large(>20ml), small); Other treatments.
CSF: Cerebrospinal Fluid; EBP: Epidural Blood Patch; SD: Standard Deviation.	

3.3.5. Statistical analysis

Meta-analyses with the commands *metaprop* and *metan* of the software Stata were used to calculate pooled estimates of proportions [95% CI] and pooled estimates of means [95% CI] of demographic characteristics (age and sex), clinical presentation, investigations findings and treatment outcomes (Nyaga *et al.*, 2014). All summary means and proportions included in the results are pooled estimates obtained with meta-analyses. Specific inclusion criteria for each meta-analysis are detailed in

Table 3-2. The variability within studies and between studies was assessed with the I^2 estimate of heterogeneity. Given the heterogeneity of the selected studies, a random effects analysis was chosen for all meta-analyses.

Microsoft® Excel (version 16.25 for macOS) and Stata© (version 15.0) were used for the data collection and statistical analysis.

Table 3-2: Inclusion criteria for meta-analyses

Meta-analyses	Inclusion criteria for metanalyses
Age	Mean age and SD specified.
Sex	N. of males/females specified.
Symptoms duration	Mean duration and SD specified.
Sign/Symptoms	For each sign/symptom: n. of patients with the sign/symptom specified.
Brain MRI	N. of investigations, type of positive findings and proportion of positive findings specified.
Spinal imaging	N. of investigations, type of investigations and proportion of positive findings (extradural CSF) specified.
CSF pressure	N. of investigations and findings (n. low pressure, normal pressure and high pressure) specified. Studies in which all patients had low CSF opening pressure were excluded.
Outcomes of conservative treatment	N. of patients who received treatment and n. good outcomes specified. Studies in which all (or none) of the patients had good outcomes were excluded.
Outcomes of first EBP	N. of patients who received treatment and n. good outcomes after 1st EBP specified. Studies in which all (or none) of the patients had good outcomes were excluded.
Outcomes of non-targeted/targeted EBP	N. of patients who received treatment, type of EBP (non-targeted or targeted) and n. good outcomes after 1st EBP specified. Studies in which all (or none) of the patients had good outcomes were excluded.

Outcomes of small/large EBP	N. of patients who received treatment, type of EBP (small or large) and n. good outcomes after 1st EBP specified. Studies in which all (or none) of the patients had good outcomes were excluded.
All	Studies with 0% or 100% proportion of findings were excluded. For each meta-analysis, if more than one study from the same author met the inclusion criteria, only the study reporting the largest number of patients was included.
CSF: Cerebrospinal Fluid; EBP: Epidural Blood Patch; SD: Standard Deviation.	

3.4. Results

The screening and selection of articles is described in

Figure 3-1. One hundred forty-four papers reporting on average 53 SIH patients each (range 10-568) met the selection criteria. Table 10-2 provides a complete list of the selected studies and information on their inclusion/exclusion from the meta-analyses.

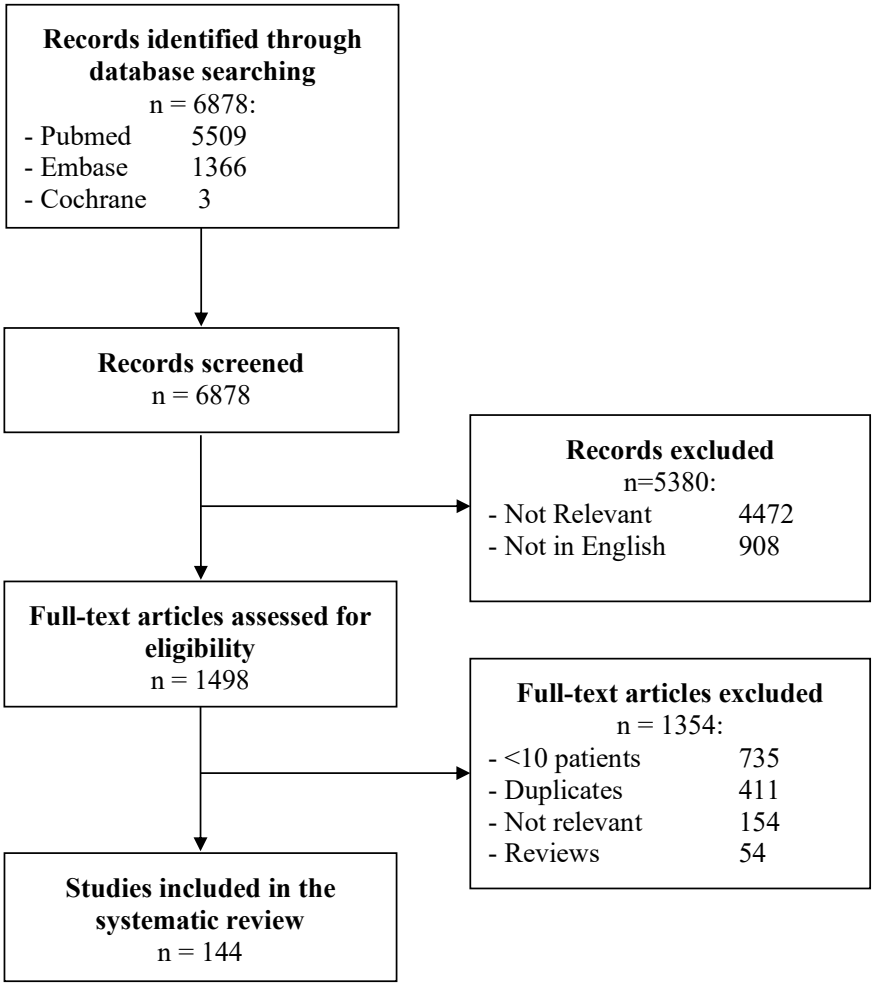


Figure 3-1: Flowchart of the articles selection process

There were no controlled interventional studies, 90 were retrospective (62.5%), 21 were prospective (14.6%) and the remaining articles did not clearly specify the type of data collection (n=33, 22.9%). The ICHD diagnostic criteria were used to diagnose SIH in 49 (34%) articles [ICHD-II, n=33 papers (22.9%); ICHD-III beta, n=7 papers (4.9%); ICHD-III, n=9 papers (6.3%)] (ICHD-II, 2004; ICHD-III beta, 2013; ICHD-III, 2018). The

2008 and 2011 Schievink diagnostic criteria were used in 17 (11.8%) articles, other criteria were used in 31 (21.5%) articles and the diagnostic criteria were not clearly specified in the remaining 47 (32.6%) (Schievink *et al.*, 2008; Schievink *et al.*, 2011). Table 3-3 shows the number of papers and patients diagnosed with each of the diagnostic criteria. Table 10-1 reports the ICHD and Schievink diagnostic criteria in detail. The selected articles were rated as 'fair' (64.6%) or 'good' quality (35.4%) according to two independent assessors using the NIH Quality Assessment Tool for Case Series Studies (2021)(2021)(National Institute of Health, 2021).

Table 3-3: Diagnostic criteria used to make diagnosis of spontaneous intracranial hypotension in the selected articles

Definition of SIH	Number of articles	% of articles	Number of patients	% of patients
ICHD-III (2018)	9	6.3 %	416	5.5 %
ICHD-III beta (2013)	7	4.9 %	290	3.8 %
ICHD-II (2004)	33	22.9 %	1702	22.4 %
Schievink 2011 (Schievink *et al.*, 2011)	8	5.5 %	567	7.5 %
Schievink 2008 (Schievink *et al.*, 2008)	9	6.3 %	701	9.2 %
Other	31	21.5 %	2144	28.3 %
Not clearly specified	47	32.6 %	1764	23.3 %
ICHD: International Classification of Headache Disorders SIH: Spontaneous Intracranial Hypotension				

3.4.1. Demographic characteristics

The patients' mean age was 42.5 years (95% CI 41.1 to 43.9, I^2=79.3%, see Figure 3-2) with a range of 2 to 88 years (Schievink *et al.*, 2016a). The proportion of females was 63% (95% CI 60 to 66, I^2=52.4, see

Figure 3-3).

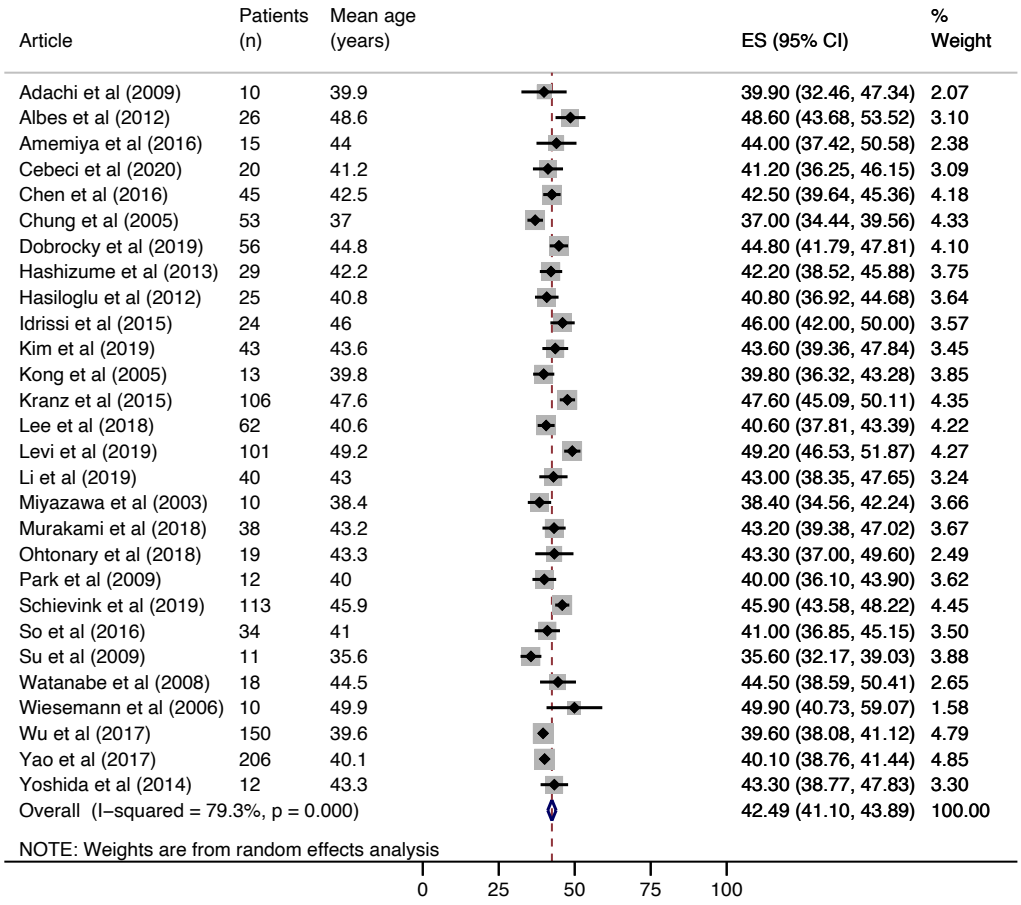


Figure 3-2: Age meta-analysis (mean years)

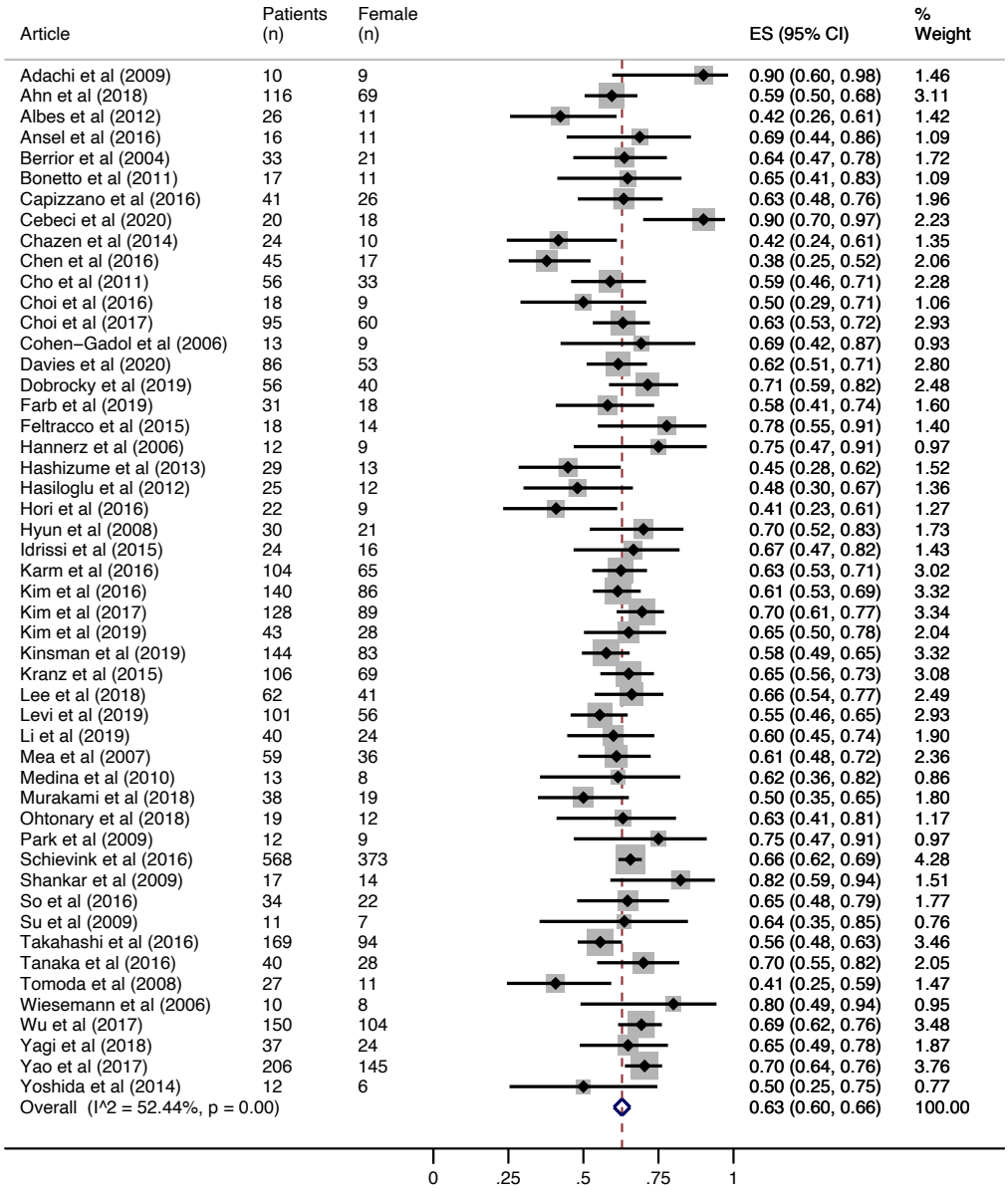


Figure 3-3: Sex meta-analysis (proportion of female patients)

3.4.2. Risk factors and associated factors

Connective tissue disorders, spinal pathologies (i.e., osteophytes, disc prolapse and discogenic micro spurs) and bariatric surgery were identified as

risk factors for SIH and reported by several authors (Schrijver *et al.*, 2002; Schievink *et al.*, 2004a; Liu *et al.*, 2011; Reinstein *et al.*, 2013; Schievink *et al.*, 2013b; Chazen *et al.*, 2014; Schievink *et al.*, 2014a; Yoshida *et al.*, 2014; Thielen *et al.*, 2015; Ansel *et al.*, 2016; Beck *et al.*, 2016b). Table 3-4 shows the percentage of patients in which these factors were reported, however, due to the design of these studies, these percentages are likely to be overestimates. Other factors commonly associated with SIH were abnormal echocardiogram findings (Pimienta *et al.*, 2014).

Table 3-4: Risk factors associated with spontaneous intracranial hypotension

Risk factor	Number of articles	Total number of patients	Number of patients with the risk factor	% of patients with the risk factor
Connective tissue disorders (Liu *et al.*, 2011; Reinstein *et al.*, 2013; Chazen *et al.*, 2014; Ansel *et al.*, 2016)	4	145	57	39.3 %
Lumbar disc prolapse, osteophytes or discogenic micro spurs (Chazen *et al.*, 2014; Yoshida *et al.*, 2014; Thielen *et al.*, 2015; Ansel *et al.*, 2016; Beck *et al.*, 2016b)	5	80	35	43.8 %
Bariatric surgery (Schievink *et al.*, 2014a)	1	338	11	3%

3.4.3. Clinical presentation

Table 3-5 and Figure 3-4 show a summary of the clinical characteristics of 1694 SIH patients (33 articles).

Table 3-5: Clinical presentation of spontaneous intracranial hypotension patients

	Number of patients (simple %)	Pooled estimates of proportions (95% confidence intervals)
Headache (33 articles, 1694 patients)		
Headache	1671 (98.6)	97 (95% CI 94-99)
No Headache	23 (1.4)	3 (95% CI 1-6)
Orthostatic headache (among patients with headache)	1632 (97.7)	92 (95% CI 87-96)
Non-orthostatic headache (among patients with headache)	39 (2.3)	8 (95% CI 4-13)
Headache location (5 articles, 234 patients)		
Diffuse/holocranial	72 (30.8)	30 (95% CI 13-46)
Occipital	65 (27.8)	33 (95% CI 19-46)
Frontal	54 (23.1)	21 (95% CI 10-32)
Fronto-occipital	9 (3.8)	11 (95% CI 4-18)
Temporal	6 (2.6)	8 (95% CI 2-13)
Undefined	28 (12.0)	-
Other signs/symptoms (32 articles, 1531 patients)		
Nausea/vomiting	775 (50.6)	54 (95% CI 46-62)
Neck pain/stiffness	507 (33.1)	43 (95% CI 32-53)
Tinnitus	295 (19.3)	20 (95% CI 14-26)
Dizziness	216 (14.1)	27 (95% CI 13-42)

	Number of patients (simple %)	Pooled estimates of proportions (95% confidence intervals)
Hearing disturbances	163 (10.7)	28 (95% CI 18-38)
Photophobia	70 (4.6)	11 (95% CI 5-16)
Other visual signs/symptoms [a]	63 (4.1)	14 (95% CI 7-21)
Diplopia	60 (3.9)	6 (95% CI 3-10)
Vertigo	58 (3.8)	17 (95% CI 2-32)
Back pain	49 (3.2)	14 (95% CI 7-21)
Cognitive symptoms [b]	40 (2.6)	6 (95% CI 2-11)
Other ear-related symptoms [c]	38 (2.5)	33 (95% CI 10-57)
Reduced level of consciousness	27 (1.8)	15 (95% CI 8-22)
Movement disorders [d]	18 (1.2)	10 (95% CI 2-40)
Less commonly reported: dysgeusia, sleepiness, cranial nerve palsy (unspecified), fever, radicular symptoms, galactorrhoea, incontinence, fatigue, vocal tics, convulsions, facial spasms/numbness/pain and dysphagia.		
[a] blurred vision, oscillopsia, nystagmus and/or visual loss [b] cognitive impairment, behavioural changes, memory and/or slow thinking [c] aural fullness, hyperacusis or unspecified [d] gait disorder, ataxia, dysarthria, tremor, bradykinesia and/or poor balance CI: Confidence Intervals		

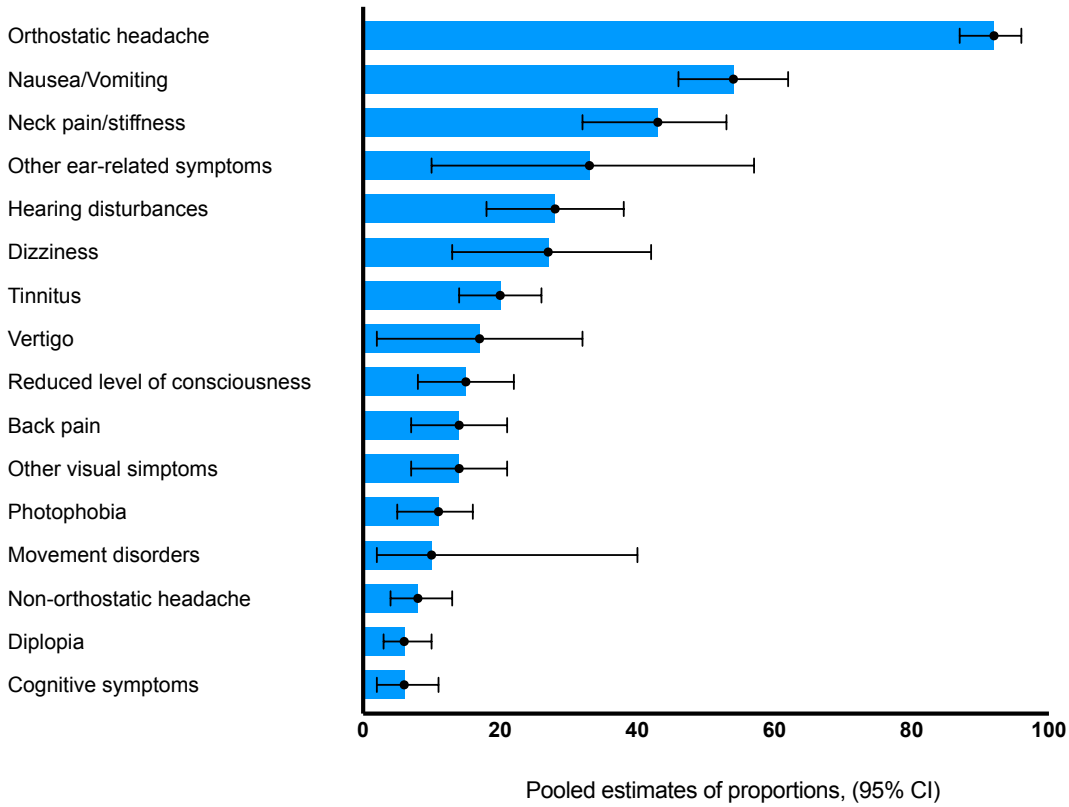


Figure 3-4: Signs and symptoms of spontaneous intracranial hypotension

Percentages indicate the pooled estimates of proportions. Other ear-related symptoms: aural fullness, hyperacusis or unspecified. Other visual signs/symptoms: blurred vision, oscillopsia, nystagmus and/or visual loss.

The duration of symptoms at the time of diagnosis and/or treatment was variable ranging from 1 day to 19.7 years (Kranz *et al.*, 2016a; Wu *et al.*, 2017), with a pooled estimated average of 31.7 days (95% CI 24.8 to 38.5, I^2=97.4%,

Figure 3-5).

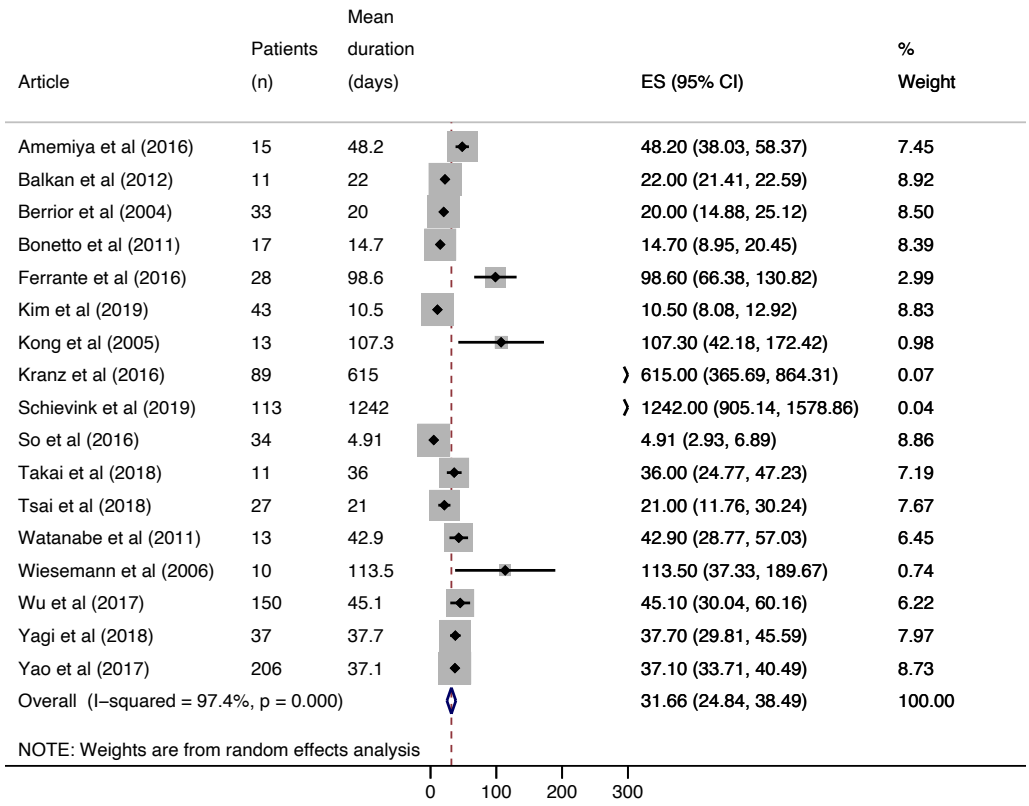


Figure 3-5: Symptoms duration meta-analysis (mean days)

Headache was the most frequent symptom, being present in 97% of the patients (95% CI 94 to 99, I^2=52.2%,

Figure 3-6) and was most commonly orthostatic (92%, 95% CI 87 to 96, I^2=80.9,

Figure 3-8); however, 3% of the patients did not report any headache (95% CI 1 to 6, I^2= 52.2%,

Figure 3-7).

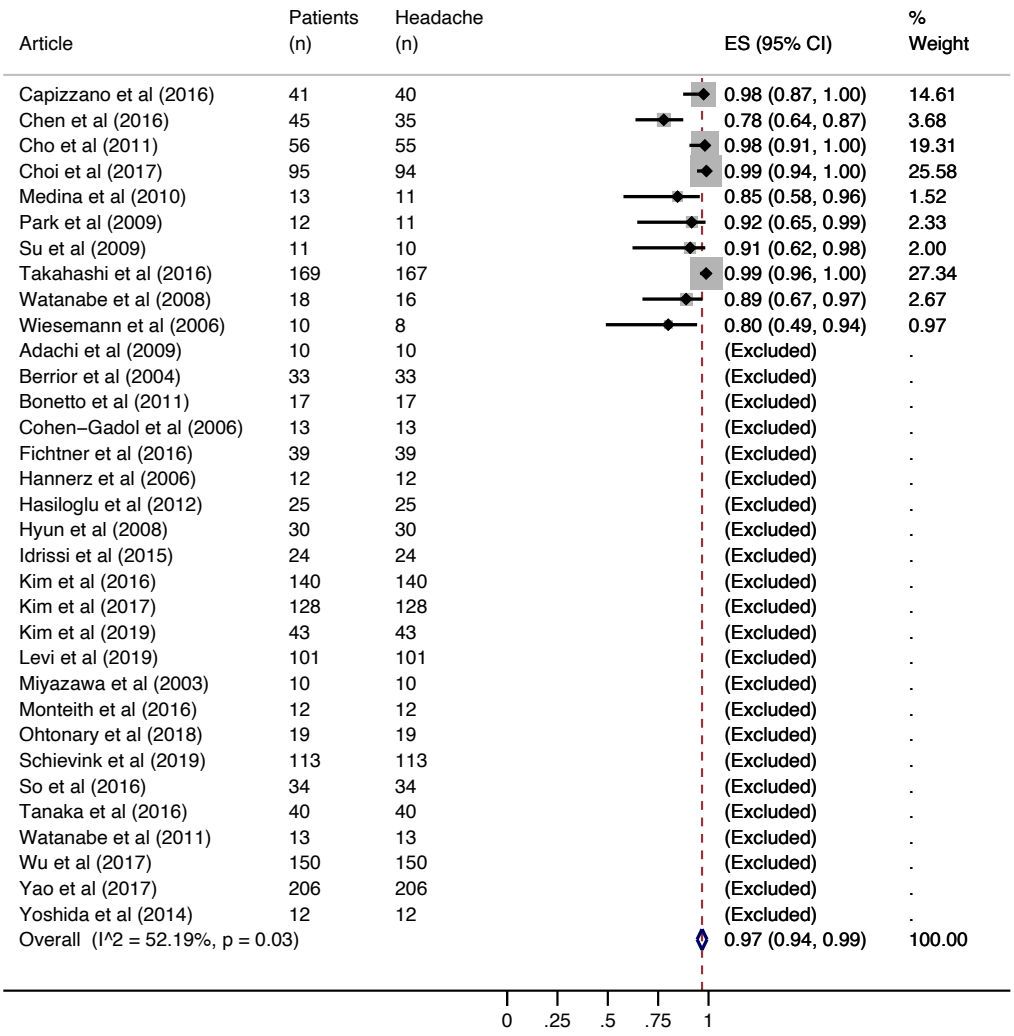


Figure 3-6: Meta-analysis of proportions of patients with headache

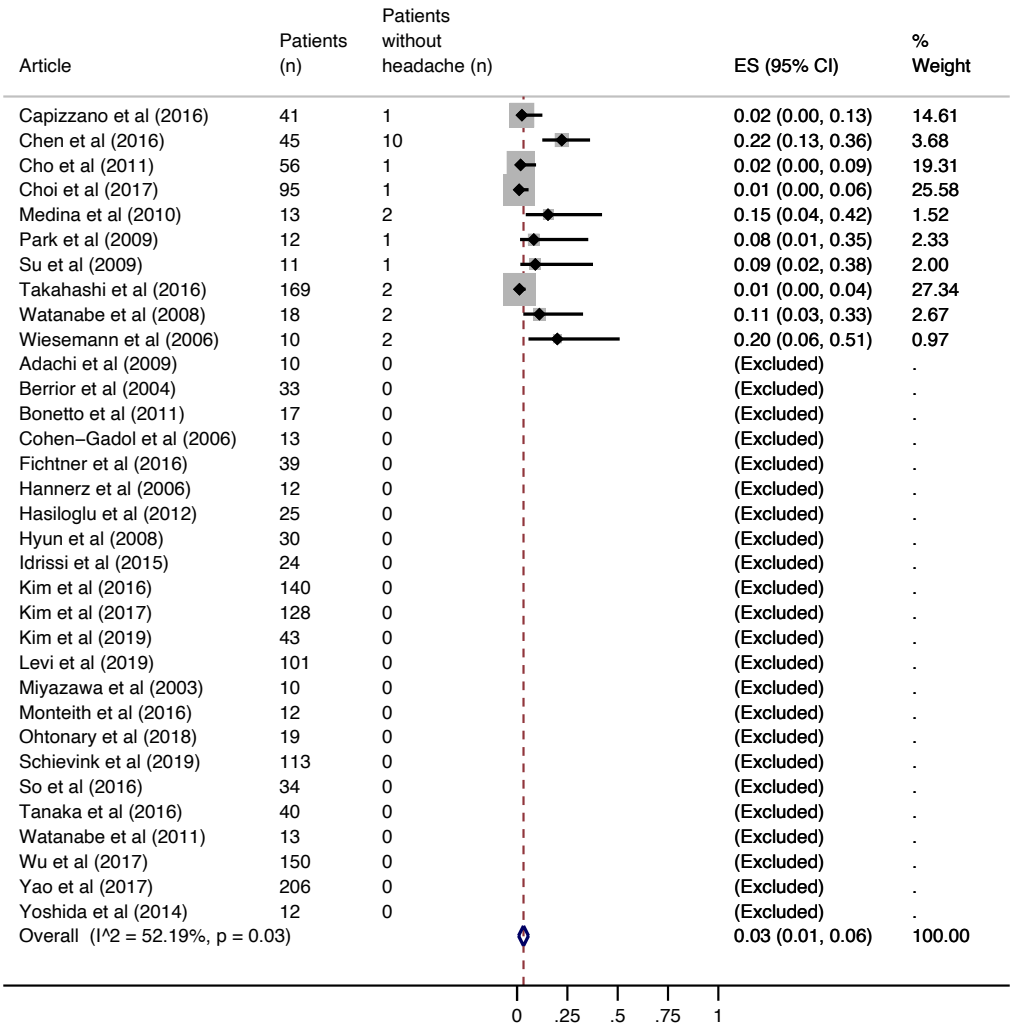


Figure 3-7: Meta-analysis of proportions of patients without headache

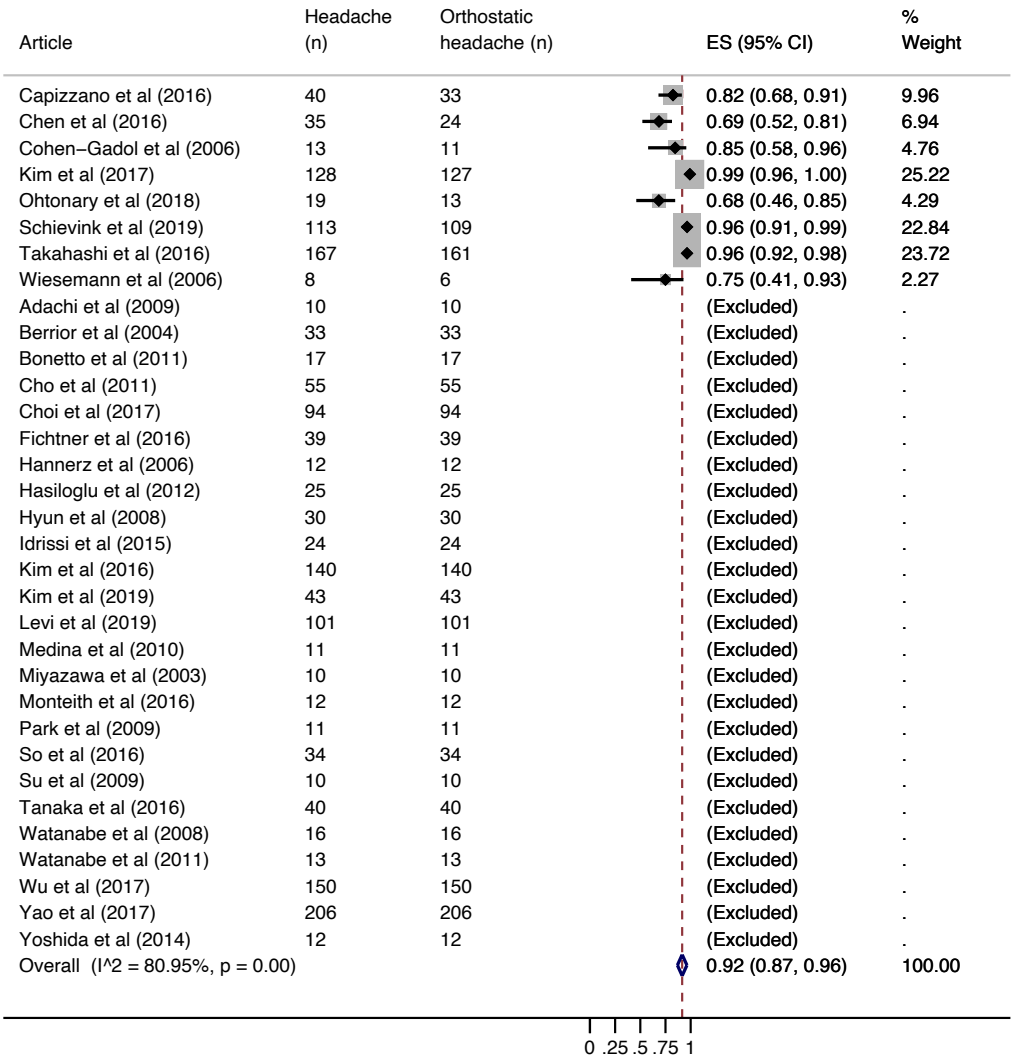


Figure 3-8: Meta-analysis of proportions of patients with orthostatic headache

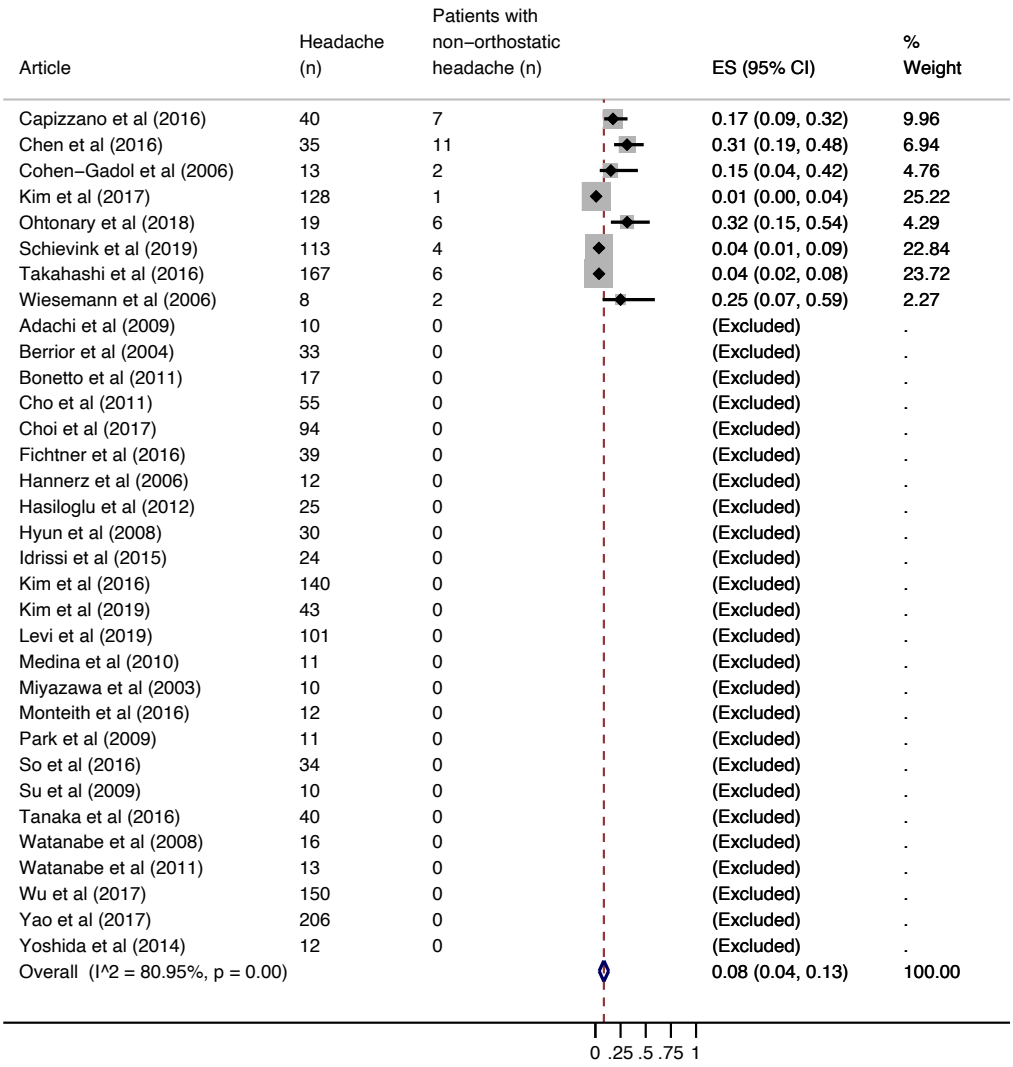


Figure 3-9: Meta-analysis of proportions of patients with non-orthostatic headache

The headache location was most commonly diffuse, occipital or frontal (

Figure 3-10 to

Figure 3-14) (Chung *et al.*, 2000; Schievink *et al.*, 2013b; Idrissi *et al.*, 2015; Ferrante *et al.*, 2016a; Kim *et al.*, 2017).

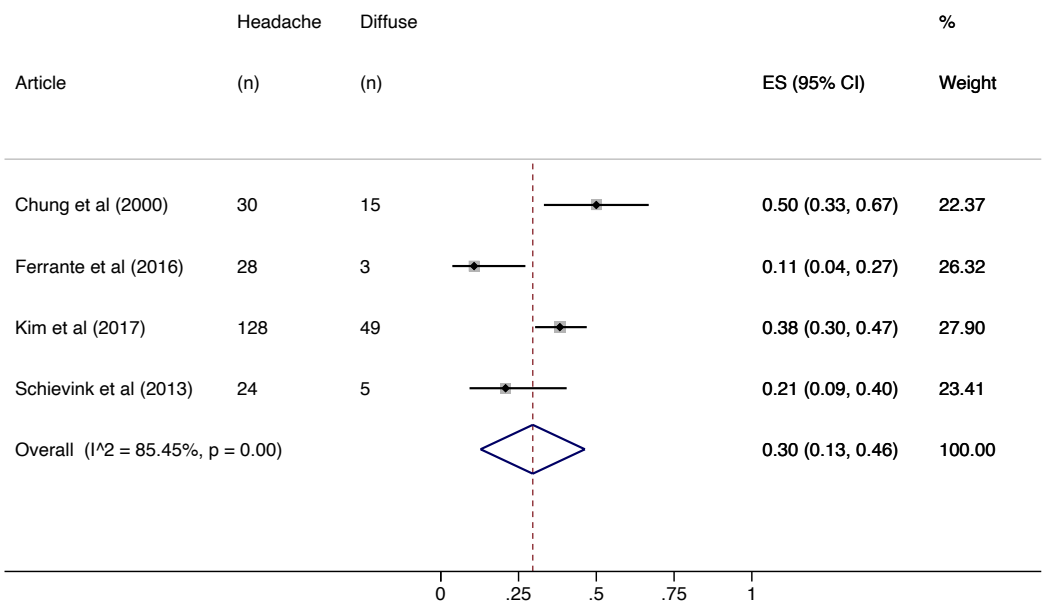


Figure 3-10: Meta-analysis of proportions of headache location (diffuse)

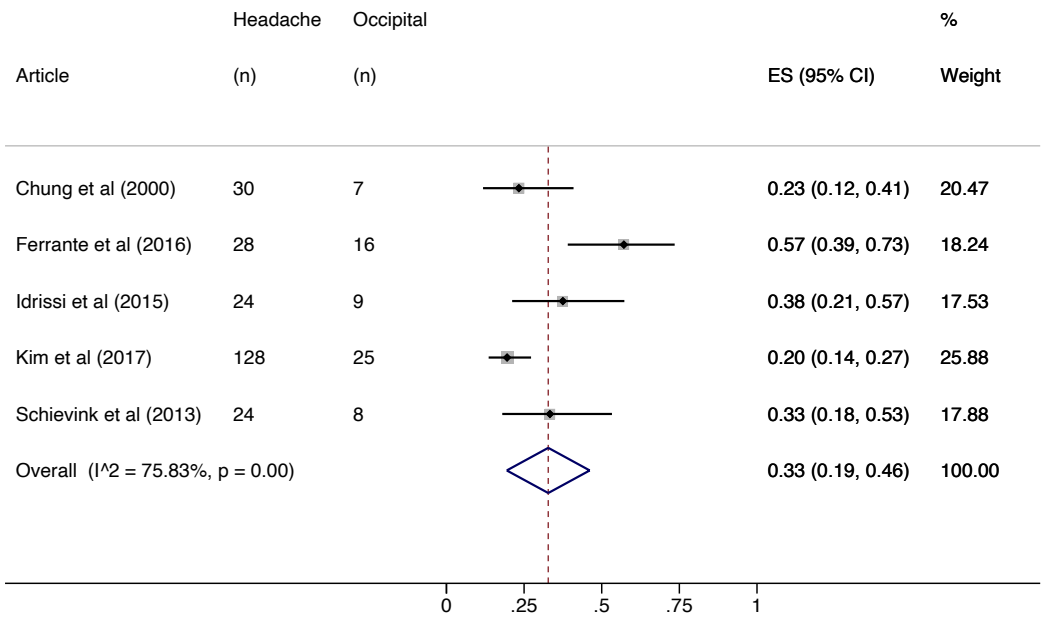


Figure 3-11: Meta-analysis of proportions of headache location (occipital)

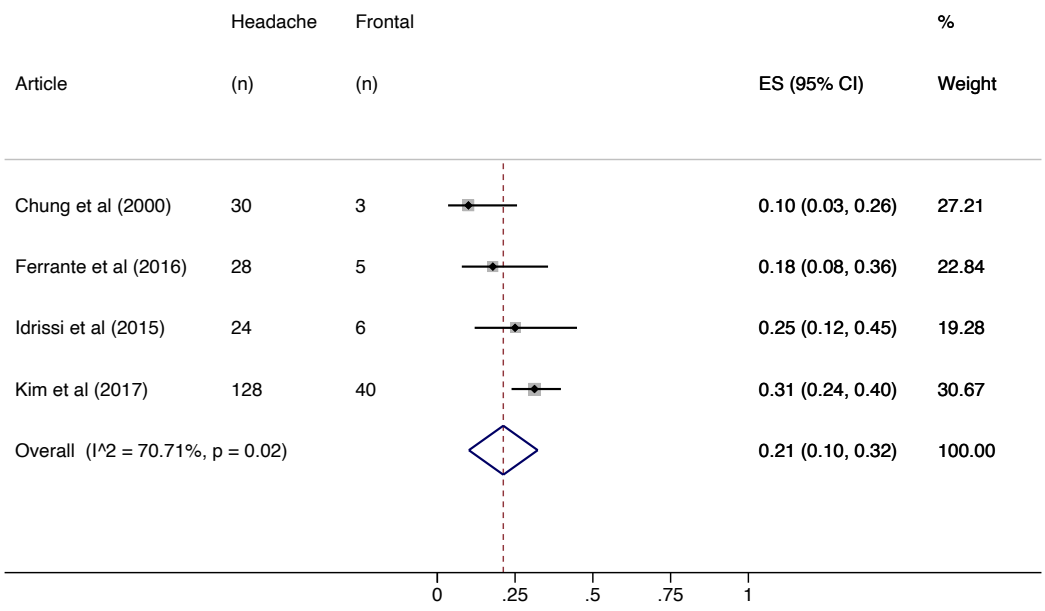


Figure 3-12: Meta-analysis of proportions of headache location (frontal)

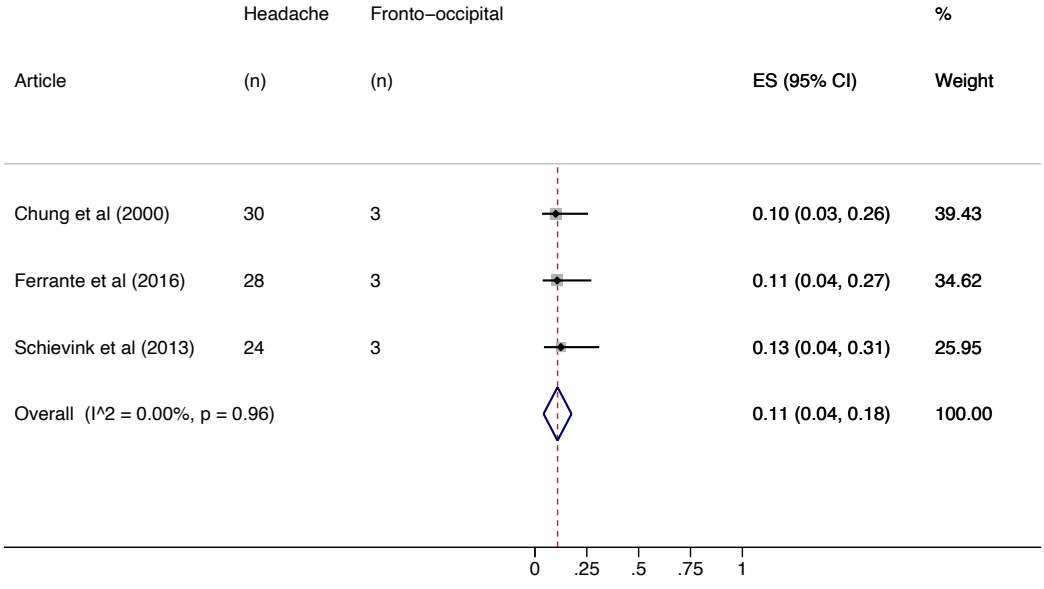


Figure 3-13: Meta-analysis of proportions of headache location (fronto-occipital)

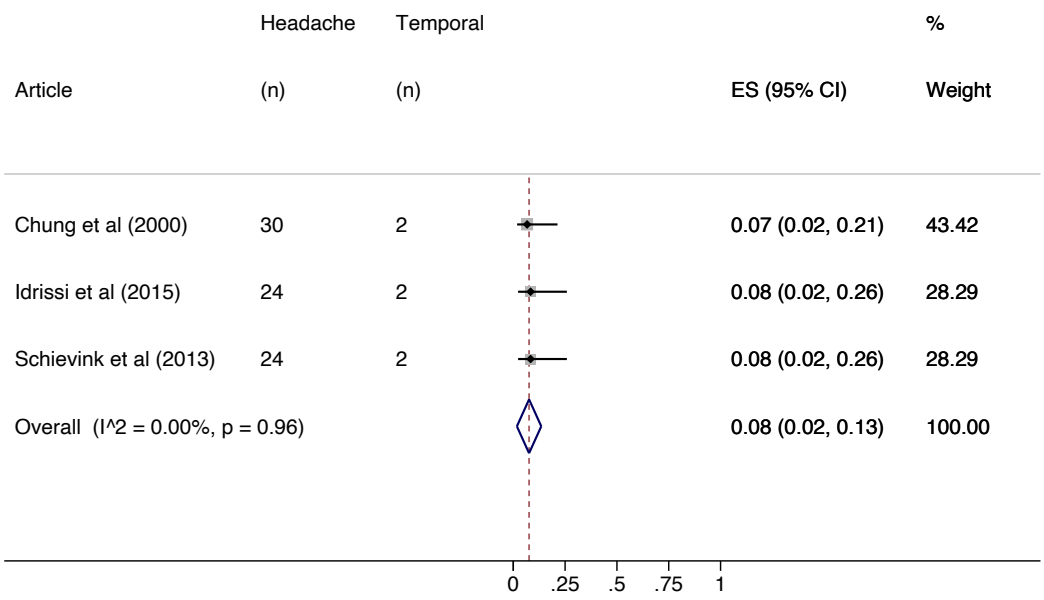


Figure 3-14: Meta-analysis of proportions of headache location (temporal)

Figure 3-15 to

Figure 3-28 show the meta-analyses for all the other signs and symptoms reported and their pooled estimates of proportions.

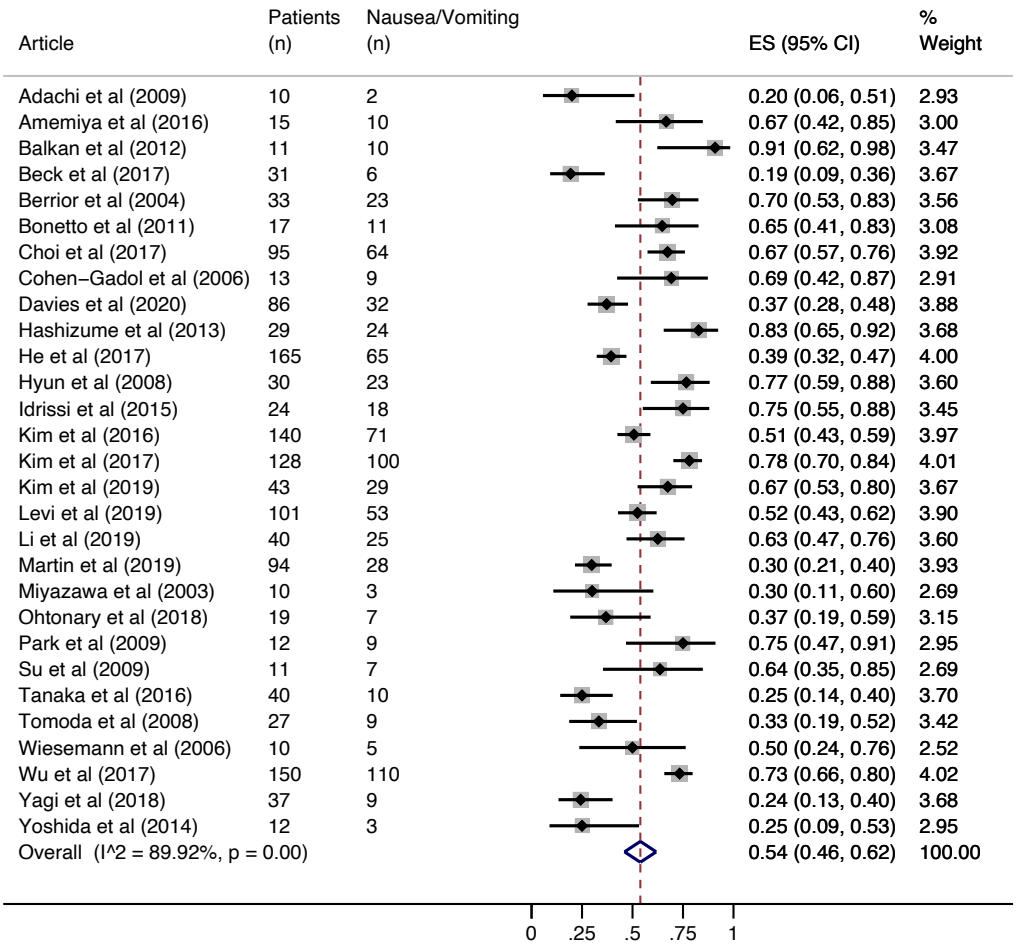


Figure 3-15: Meta-analysis of proportions of patients with nausea/vomiting

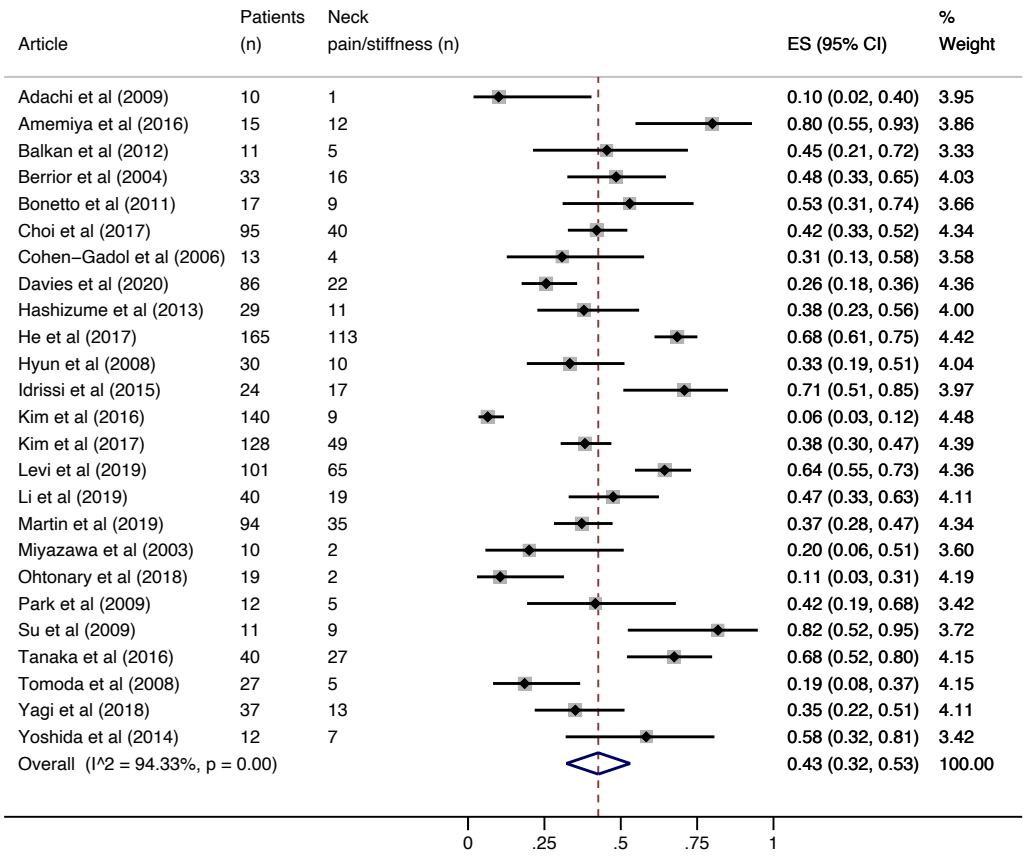


Figure 3-16: Meta-analysis of proportions of patients with neck pain/stiffness

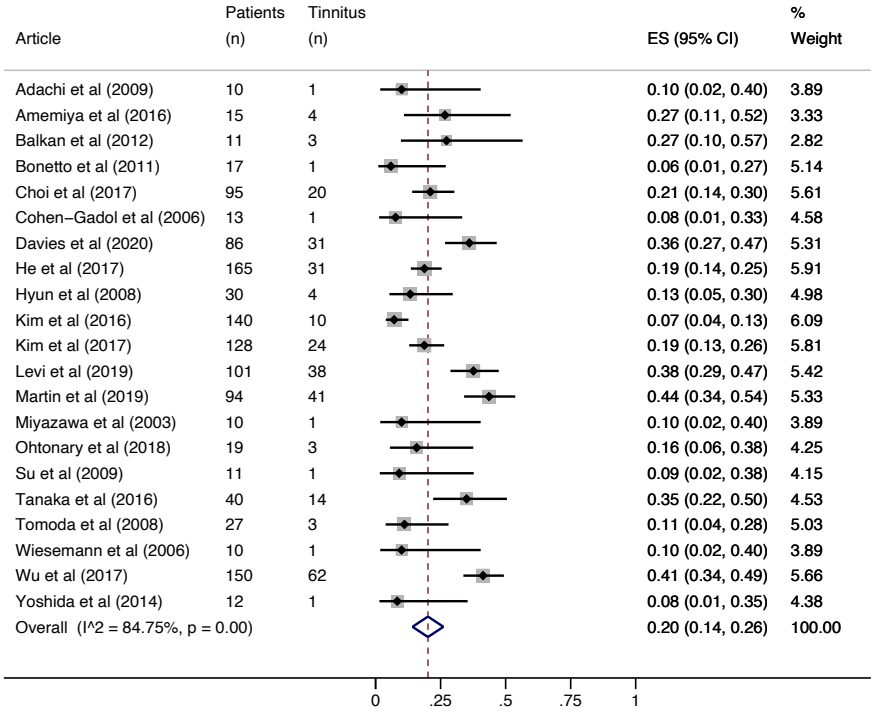


Figure 3-17: Meta-analysis of proportions of patients with tinnitus

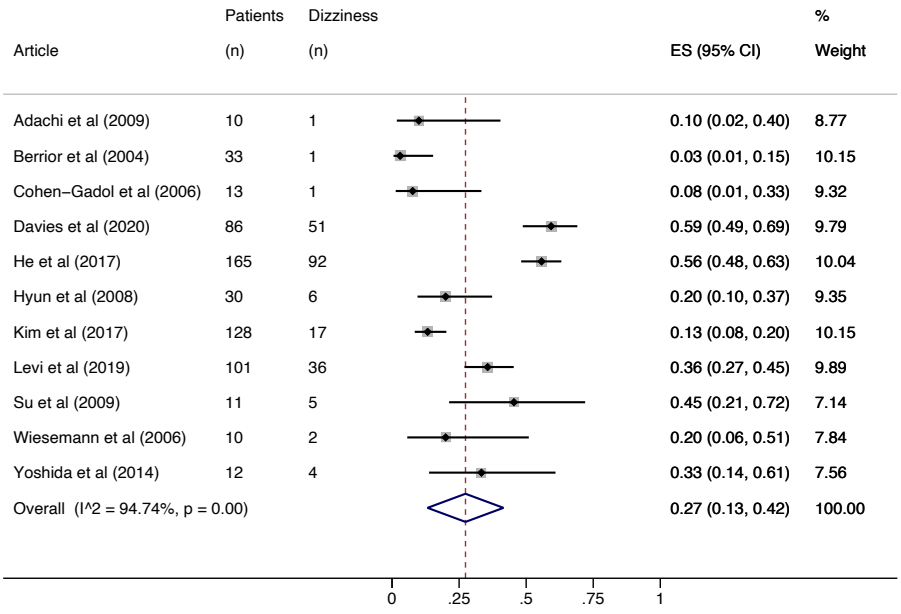


Figure 3-18: Meta-analysis of proportions of patients with dizziness

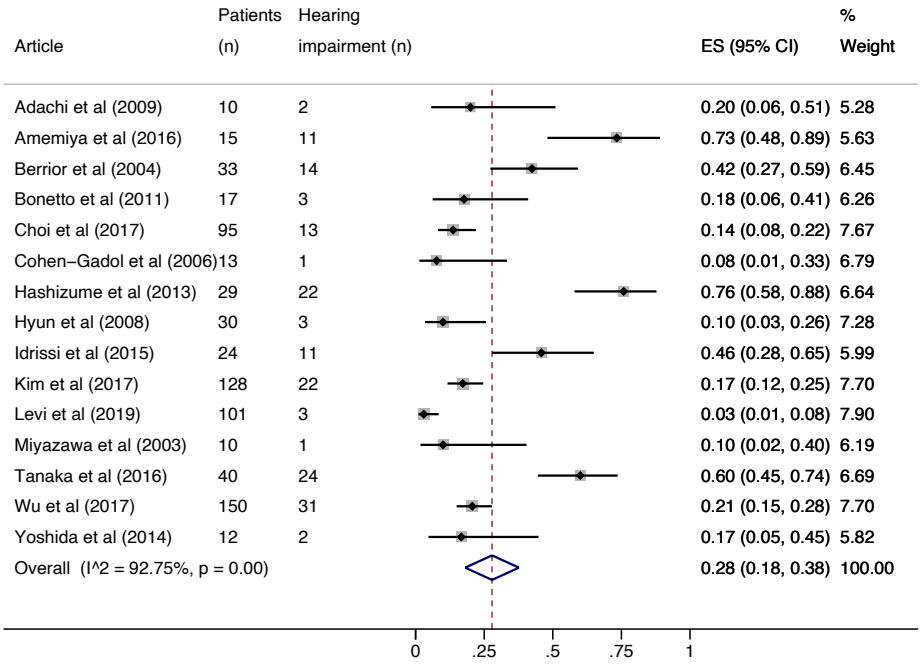


Figure 3-19: Meta-analysis of proportions of patients with hearing disturbances

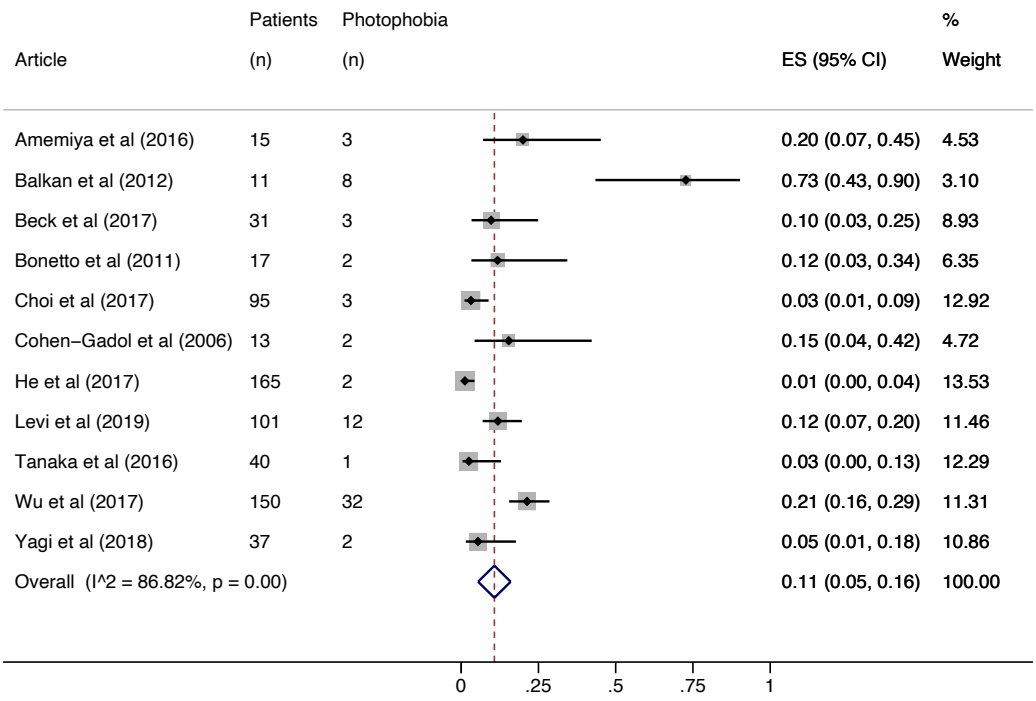


Figure 3-20: Meta-analysis of proportions of patients with photophobia

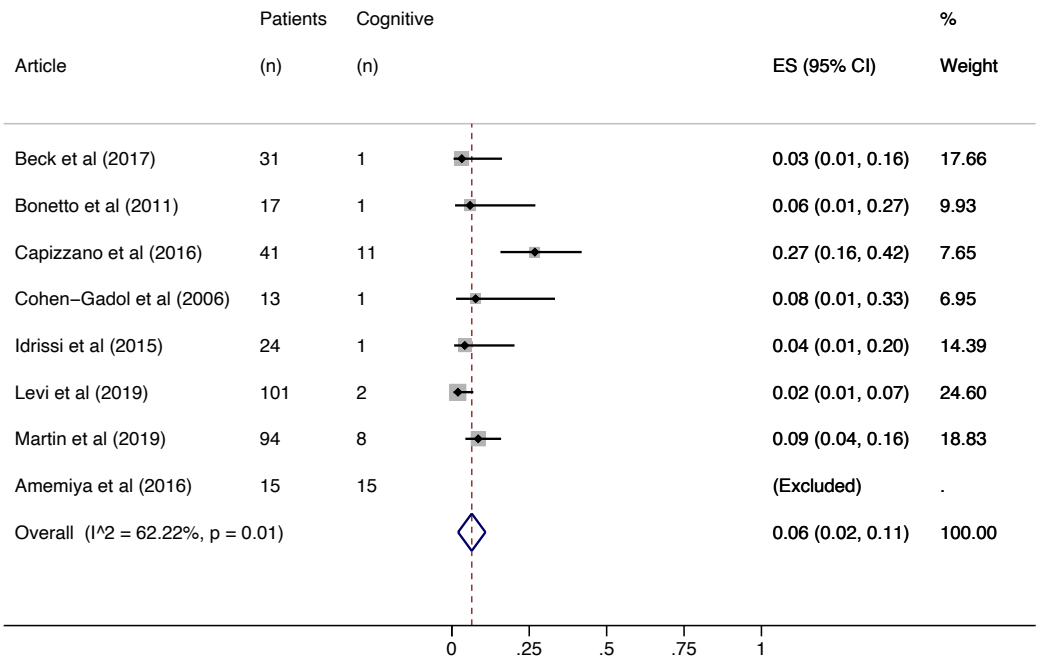


Figure 3-21: Meta-analysis of proportions of patients with cognitive symptoms

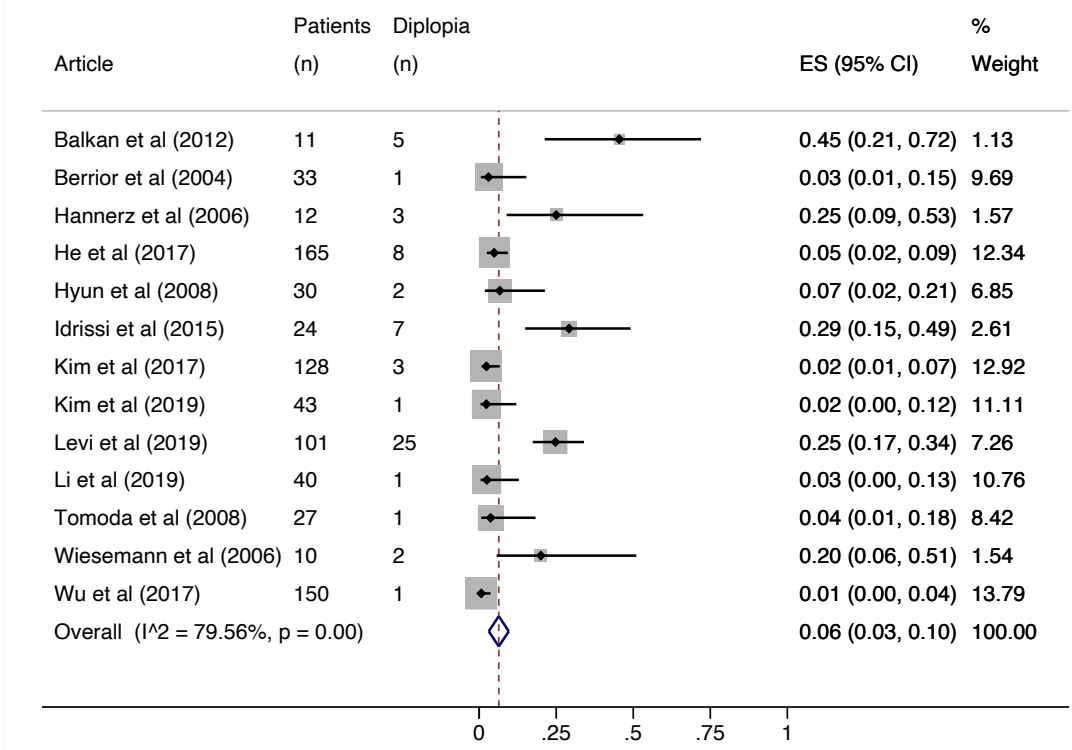


Figure 3-22: Meta-analysis of proportions of patients with diplopia

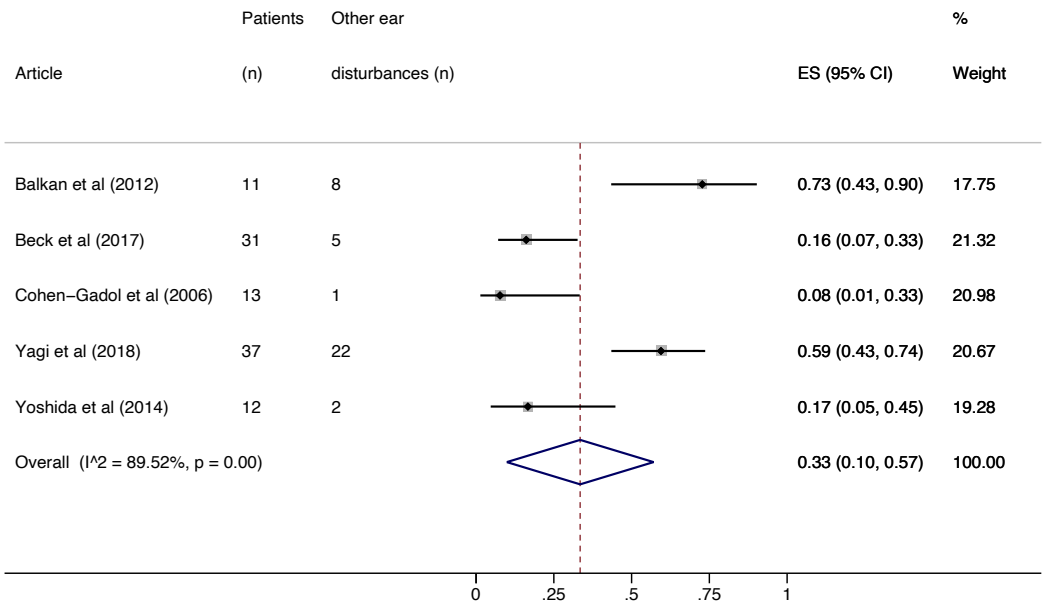


Figure 3-23: Meta-analysis of proportions of patients with other ear-related symptoms

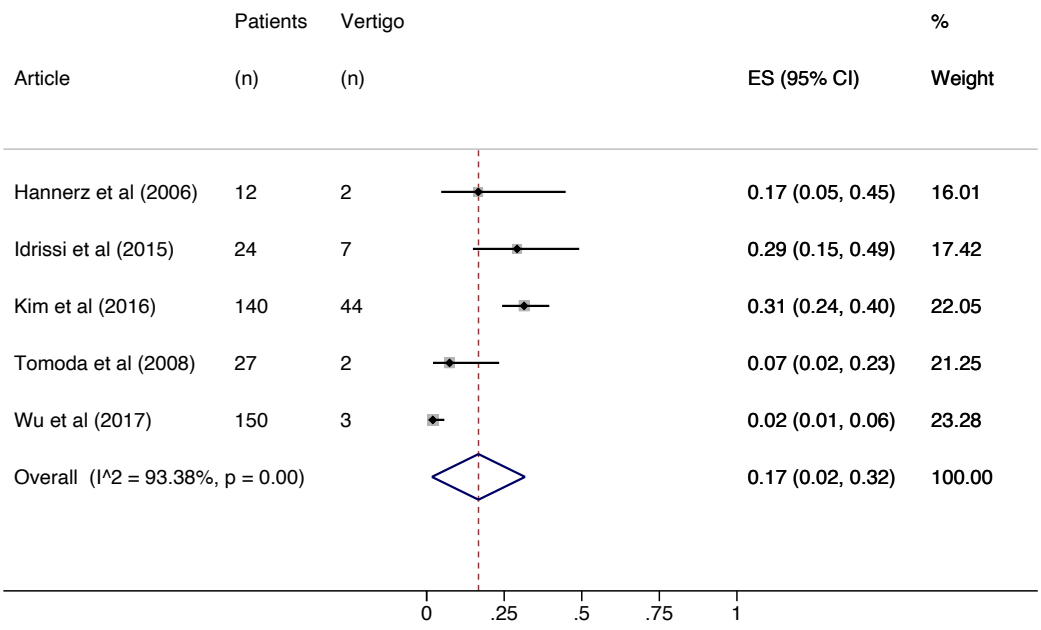


Figure 3-24: Meta-analysis of proportions of patients with vertigo

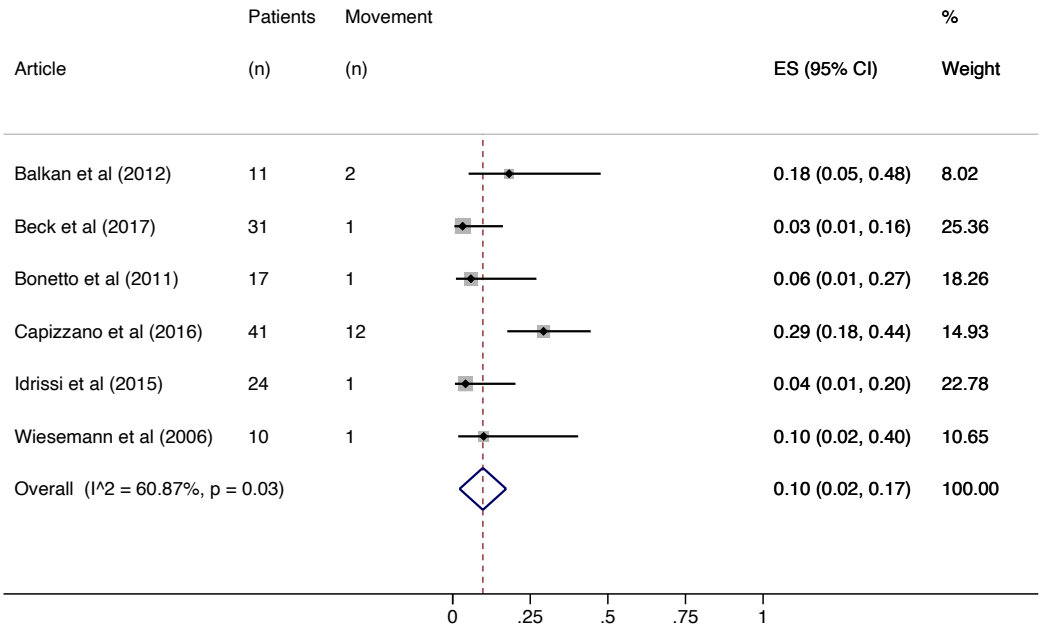


Figure 3-25: Meta-analysis of proportions of patients with movement disorders

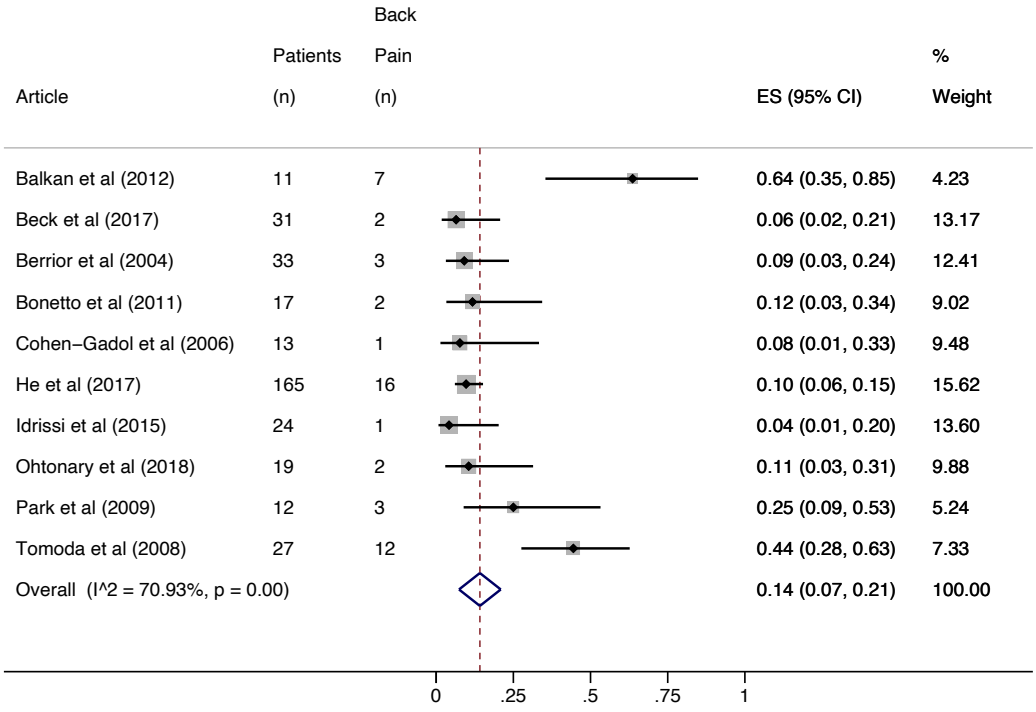


Figure 3-26: Meta-analysis of proportions of patients with back pain

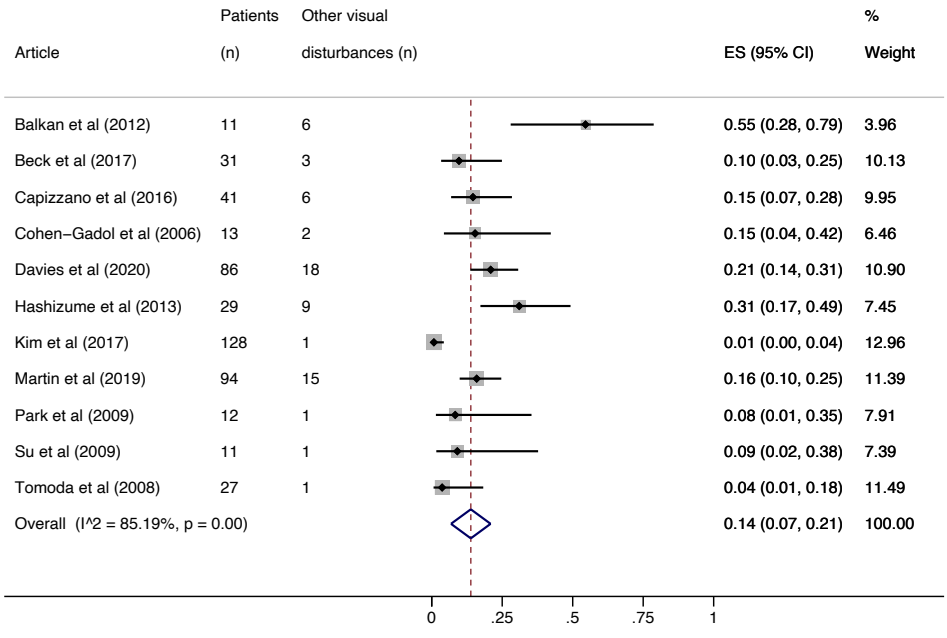


Figure 3-27: Meta-analysis of proportions of patients with other visual symptoms

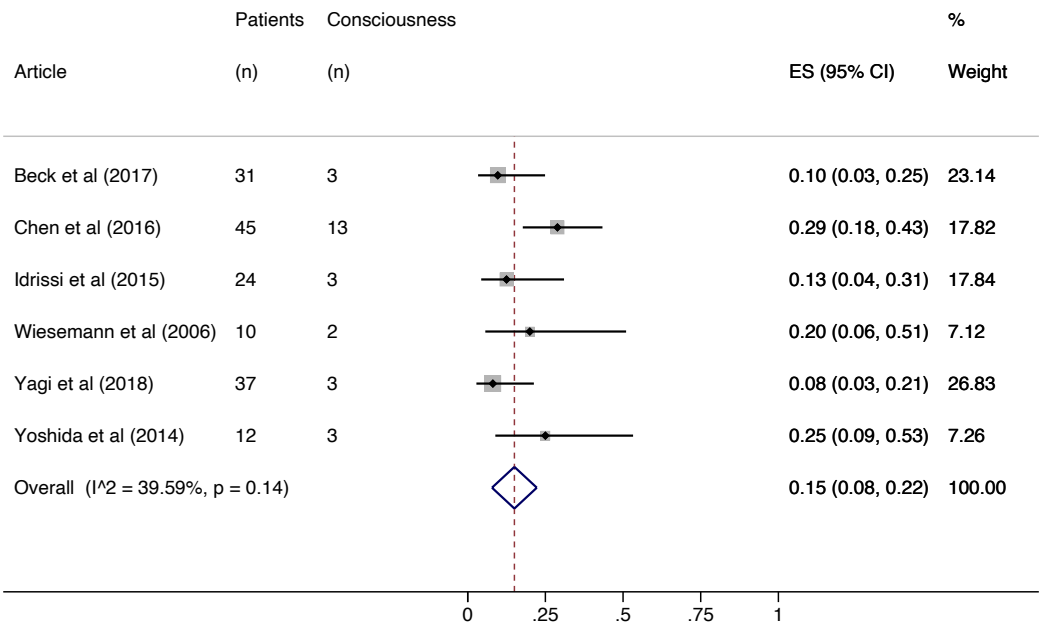


Figure 3-28: Meta-analysis of proportions of patients with reduced consciousness

3.4.4. Assessment and Diagnosis

3.4.4.1. Brain MRI

Thirty-eight articles were selected for the description of the brain MRI findings of 2078 patients diagnosed with SIH: 73% showed diffuse gadolinium pachymeningeal enhancement (95% CI 67 to 80, I^2=90.9%,

Figure 3-29), 35% subdural collections (95% CI 28 to 42, I^2=88.5%,

Figure 3-30), 43% brain sagging (95% CI 32 to 54, I^2=95.8%,

Figure 3-31), 38% pituitary gland enlargement (95% CI 15 to 60, I^2=99.2%,

Figure 3-32) and 57% signs of venous engorgement (95% CI 40 to 74, I^2=94.8%,

Figure 3-33). Brain MRIs were normal in 19% of the patients (95% CI 13 to 24, I^2=59.3,

Figure 3-34). Figure 3-35 shows a summary of the main brain MRI findings.

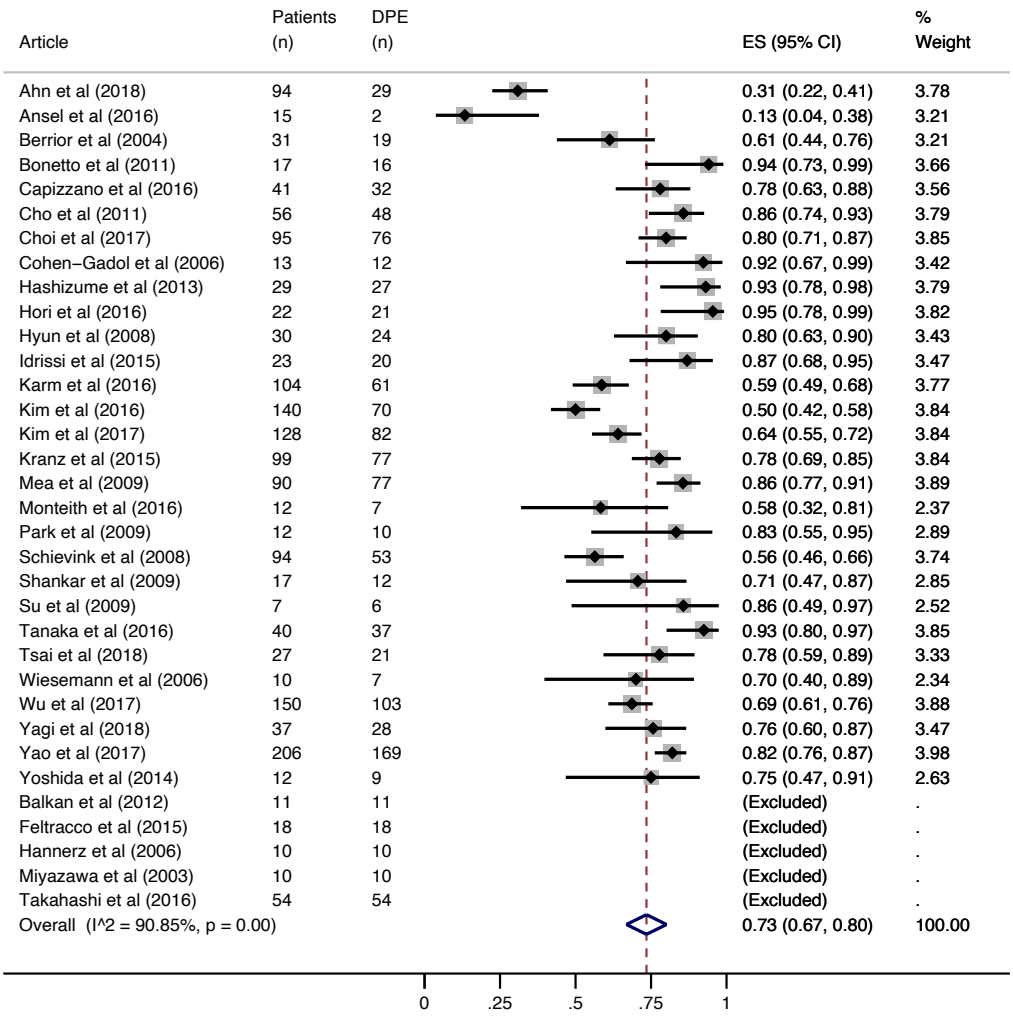


Figure 3-29: Meta-analysis of proportions of diffuse pachymeningeal enhancement (DPE) in brain MRI

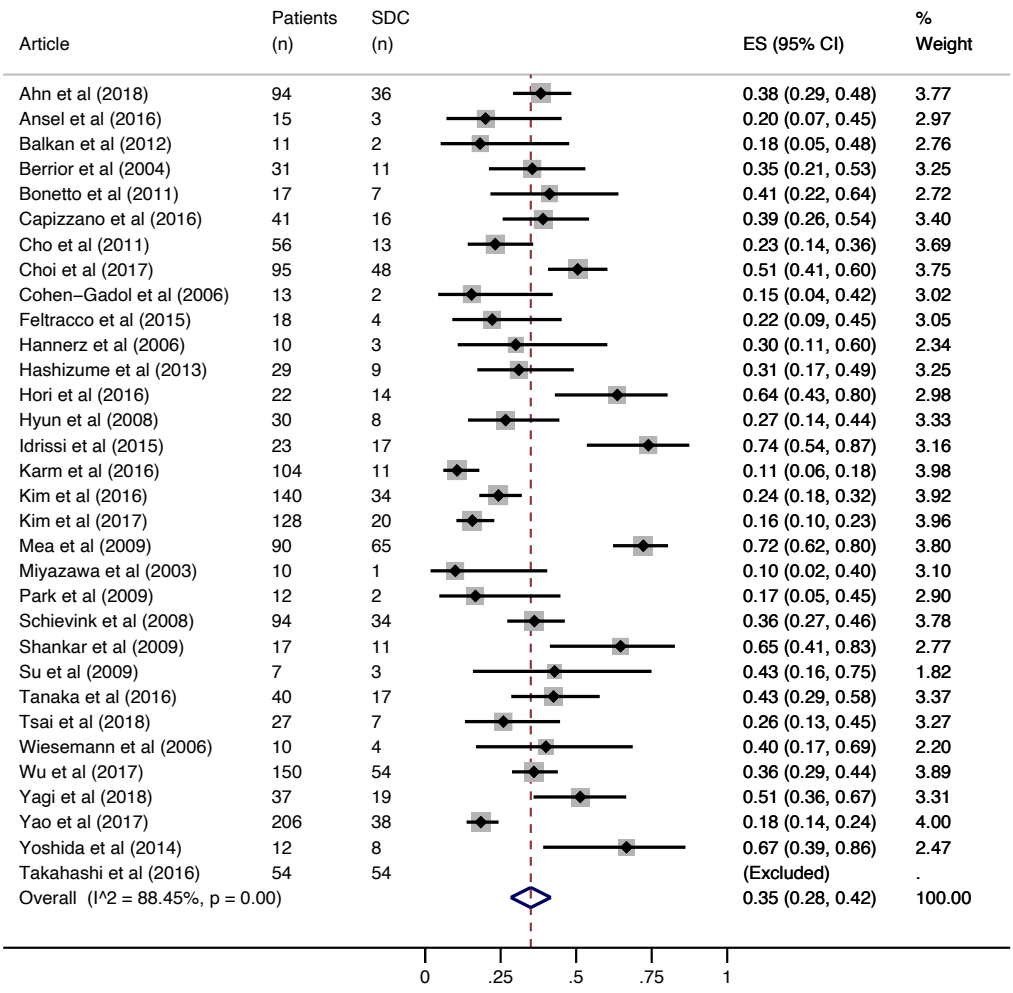


Figure 3-30: Meta-analysis of proportions of subdural collections (SDC) in brain MRI

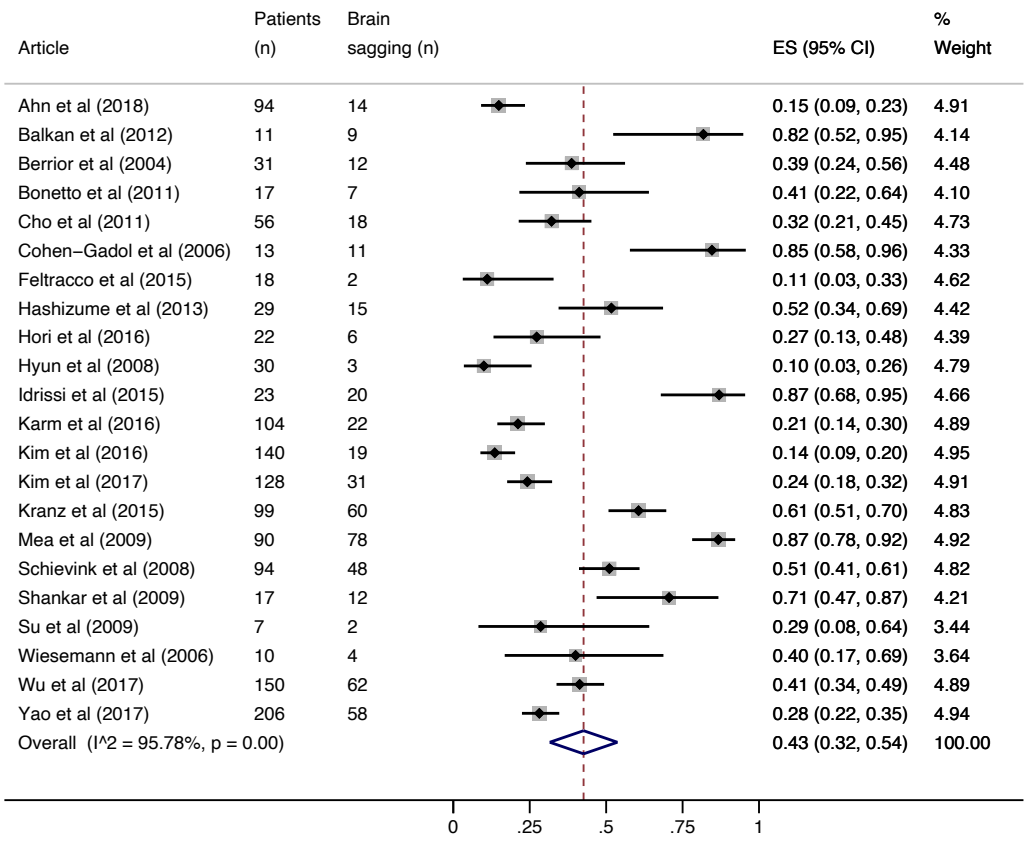


Figure 3-31: Meta-analysis of proportions of brain sagging brain MRI

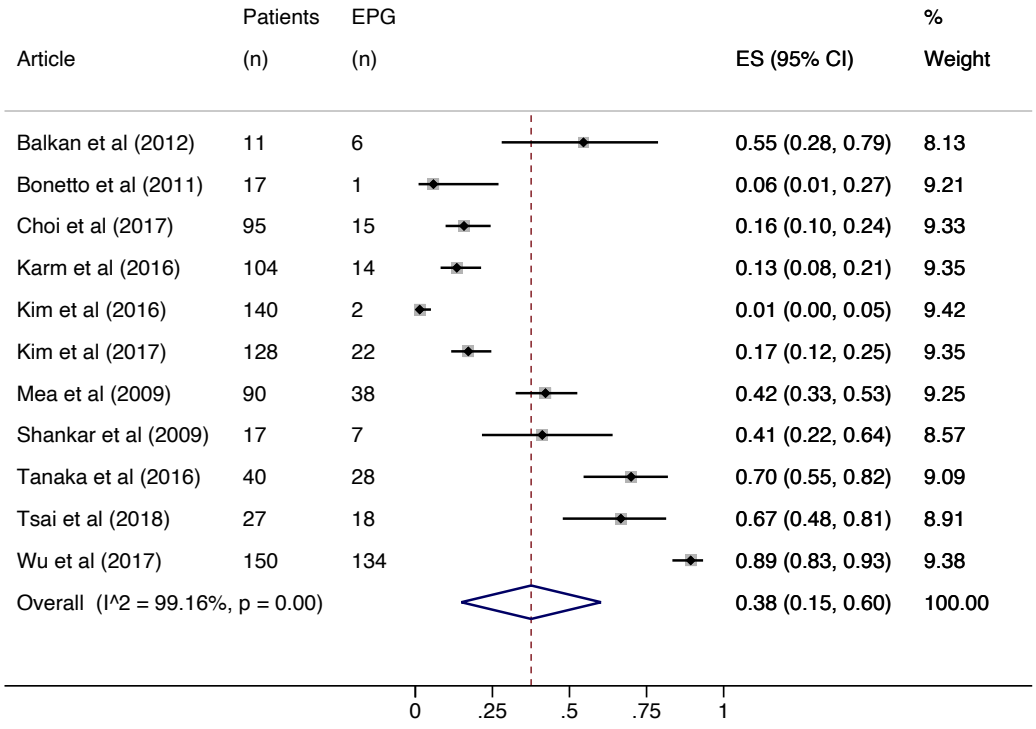


Figure 3-32: Meta-analysis of proportions of enlarged pituitary gland (EPG) in brain MRI

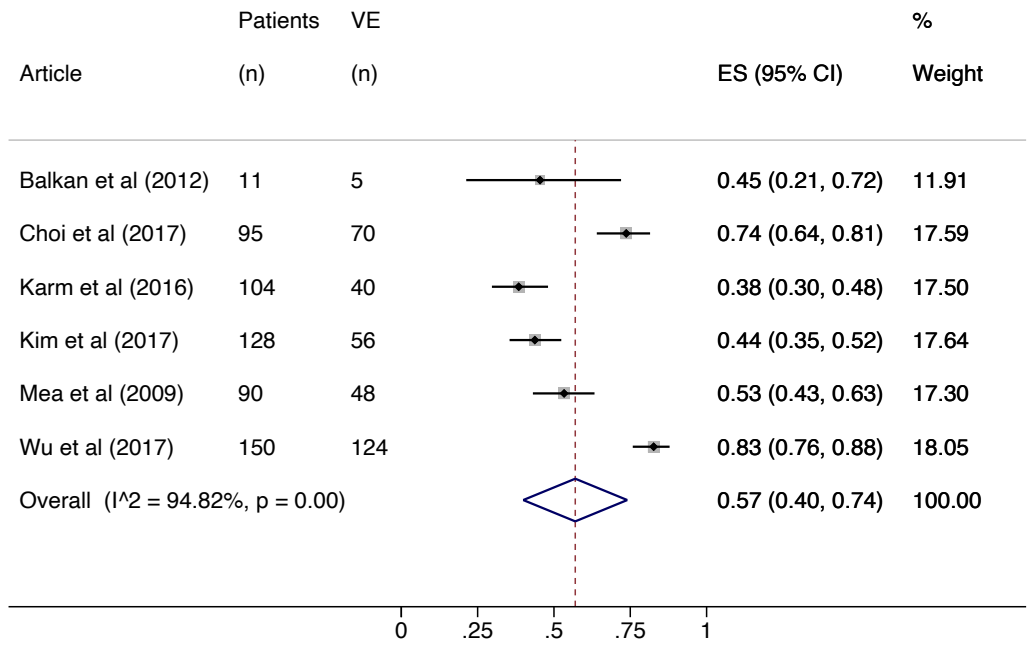


Figure 3-33: Meta-analysis of proportions of venous engorgement in brain MRI

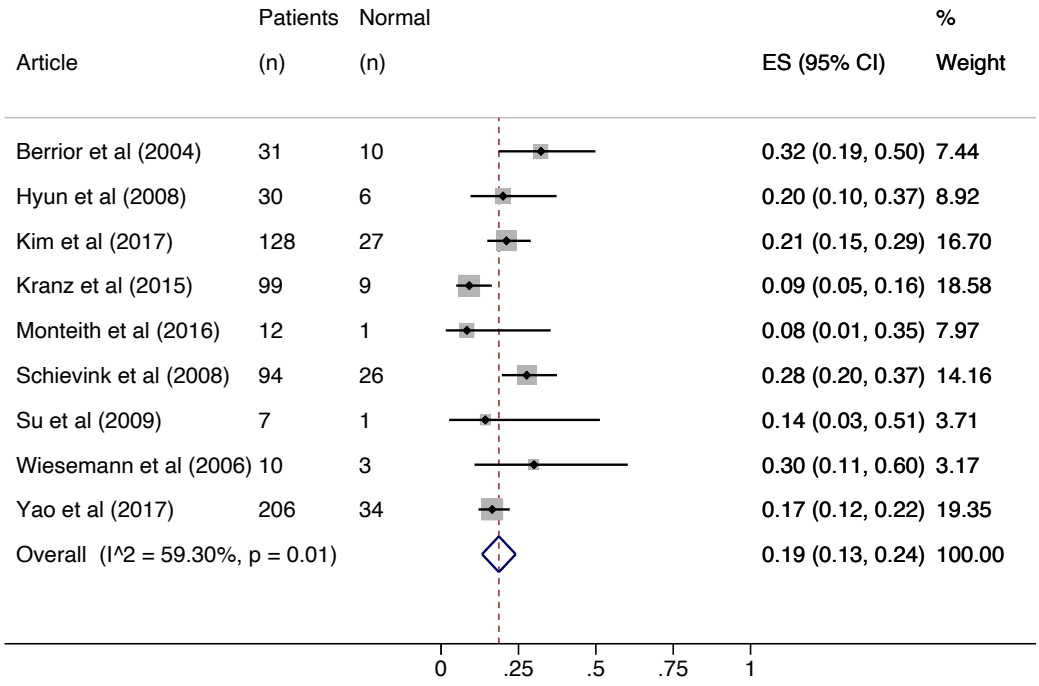


Figure 3-34: Meta-analysis of proportions of normal brain MRI

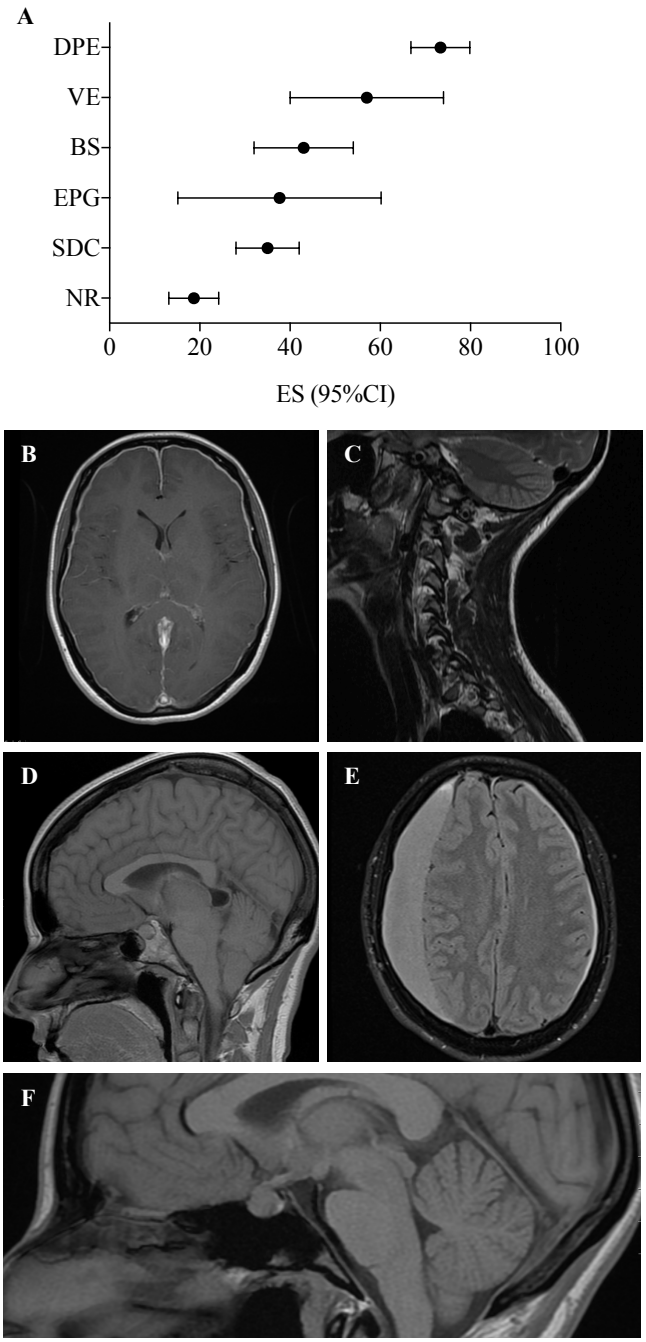


Figure 3-35: Brain MRI findings of spontaneous intracranial hypotension

(A) Pooled estimates of proportions (ES, 95% CI) of positive findings in SIH. (B) Example of diffuse pachymeningeal enhancement (DPE) in T1W axial MRI sequence. (C) Example of venous engorgement (VE, transverse sinus venous distension sign) in T2W sagittal MRI sequence. (D) Example of brain sagging (BS) and enlarged pituitary gland (EPG) in T1W sagittal MRI sequence. (E) Example of subdural

collection (SDC) in T2W axial MRI sequence. (F) Example of enlarged pituitary gland (EPG) in T1W sagittal MRI sequence.

3.4.4.2. Spinal imaging

The sensitivity of spinal investigations for identifying CSF leaks (defined as detection of extradural CSF) was analysed for spinal MRI, CT myelography, radionuclide cisternography, MR myelography (with and without intrathecal gadolinium) and digital subtraction myelography (DSM). Presence of extradural CSF was detected in 48-76% of the cases (Figure 3-36 to Figure 3-43). The techniques able to identify the specific leak site most frequently were the MR myelography with intrathecal gadolinium and the DSM, however only 87 and 133 patients respectively underwent these types of spinal investigation. Among the other spinal investigations described, dynamic CT myelography was reported to be useful for the detection the exact leak site in fast CSF leaks but none of these studies met the inclusion criteria for meta-analysis (Luetmer *et al.*, 2012; Thielen *et al.*, 2015; Dobrocky *et al.*, 2018).

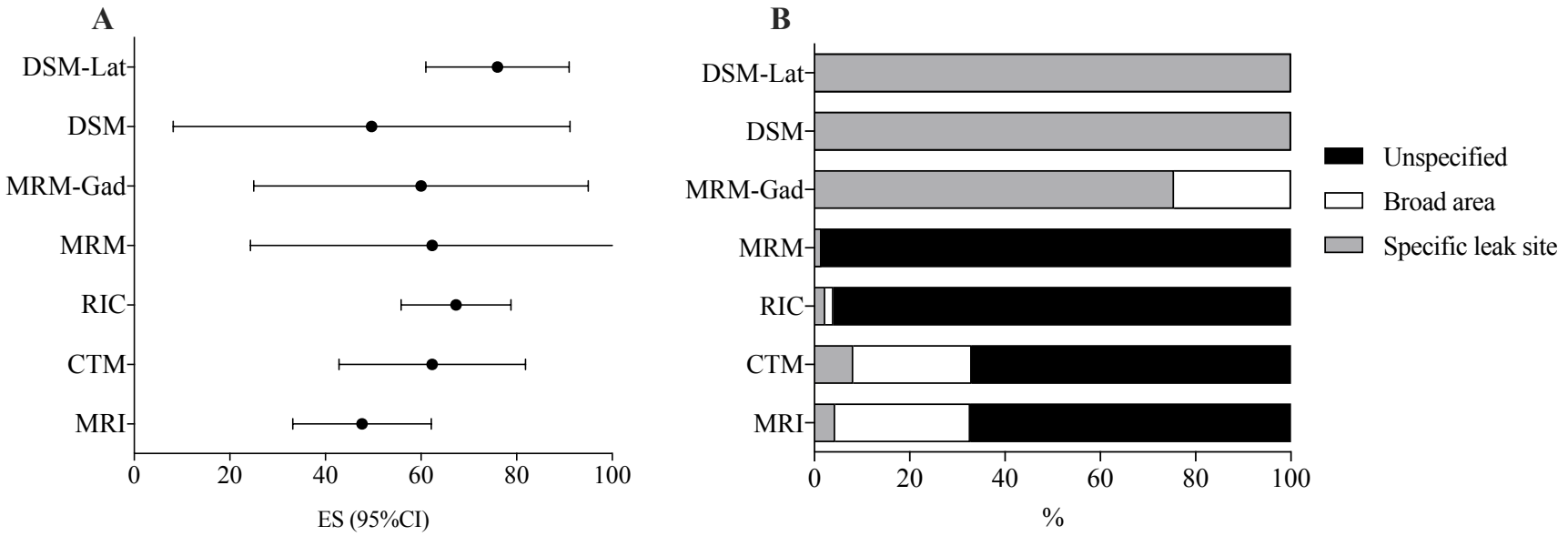


Figure 3-36: Spinal imaging findings of Spontaneous Intracranial Hypotension (SIH).

(A) Pooled estimates of proportions (95% CI) of cerebrospinal fluid (CSF) leakage found in spinal imaging investigations. (B) Positive imaging findings stratified by type of CSF leak localisation: specific leak site, broad area and unspecified. DSM: Digital Subtraction Myelography, DSM-Lat: Digital Subtraction Myelography in lateral decubitus position, RIC: radionuclide cisternography, MRM: MRI Myelography, CTM: CT Myelography, MRM-Gad: MRI Myelography with intrathecal Gadolinium.

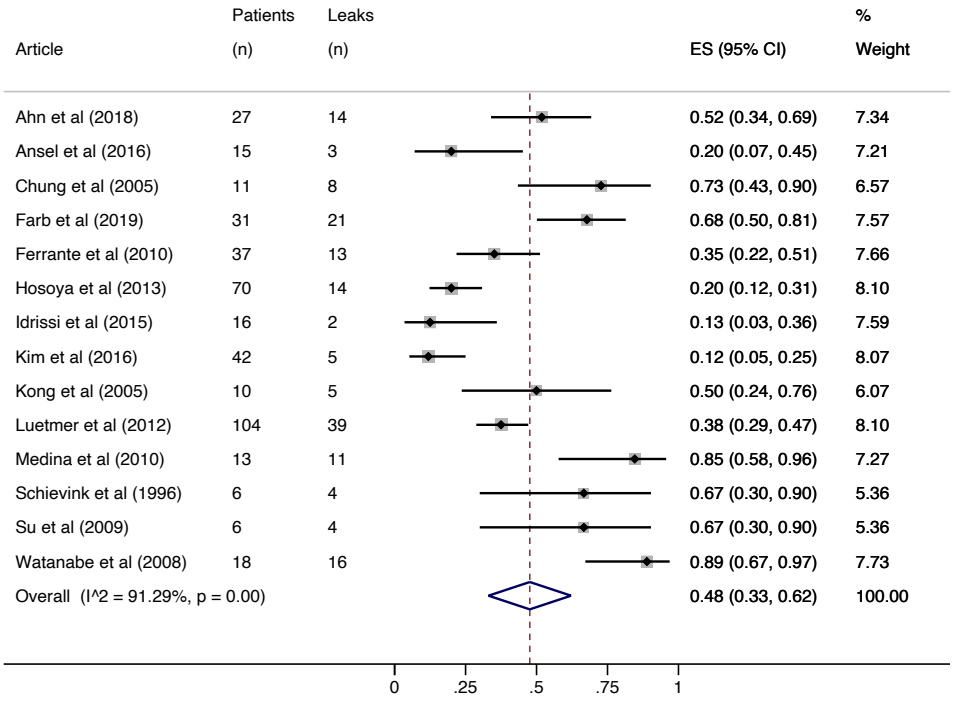


Figure 3-37: Meta-analysis of proportions of positive findings in spinal MRI

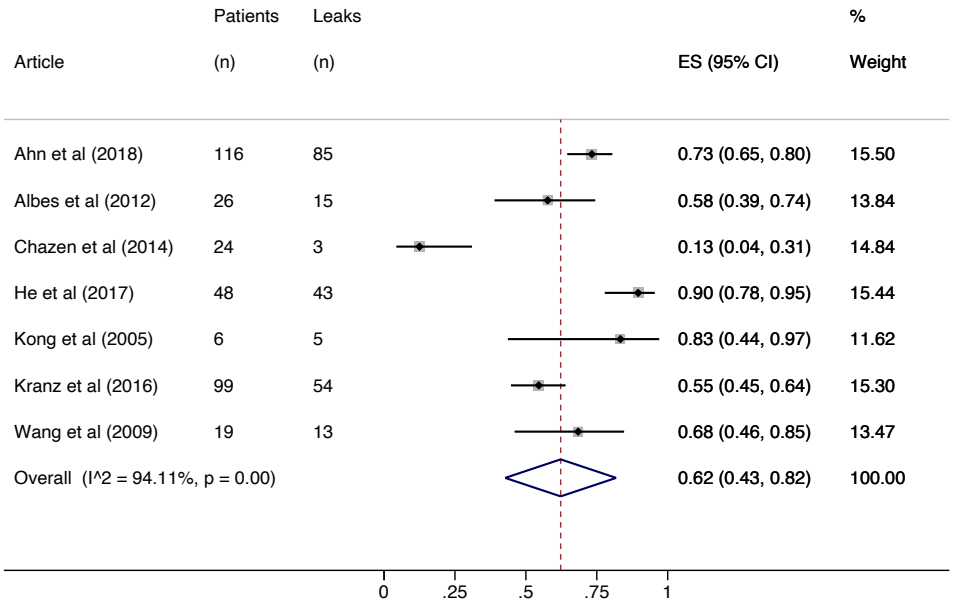


Figure 3-38: Meta-analysis of proportions of positive findings in CT myelography (CTM)

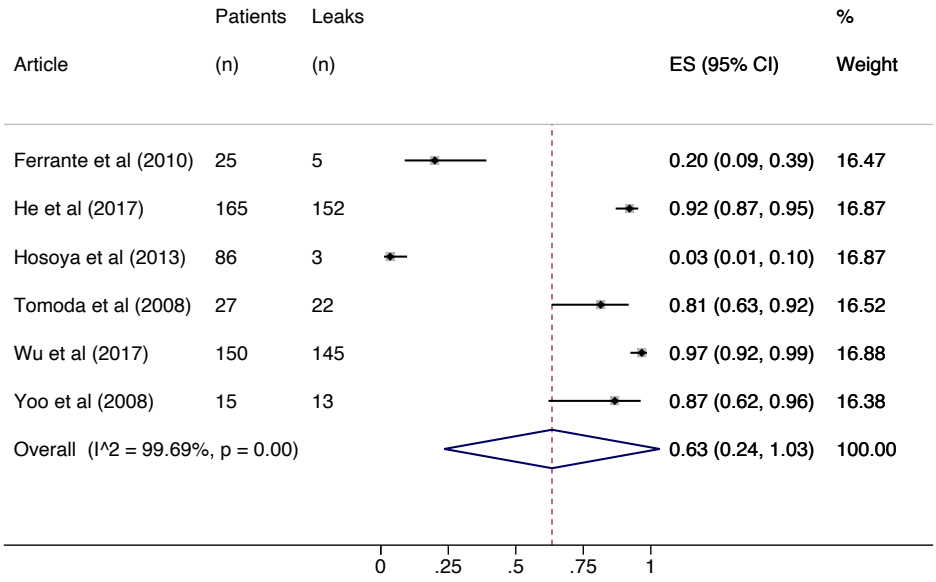


Figure 3-39: Meta-analysis of proportions of positive findings in MR myelography

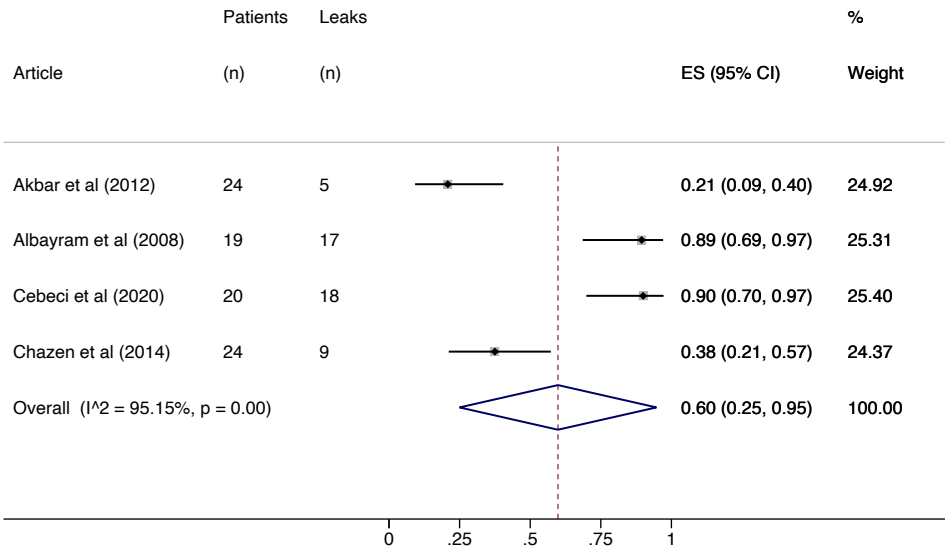


Figure 3-40: Meta-analysis of proportions of positive findings in MR myelography with intrathecal gadolinium

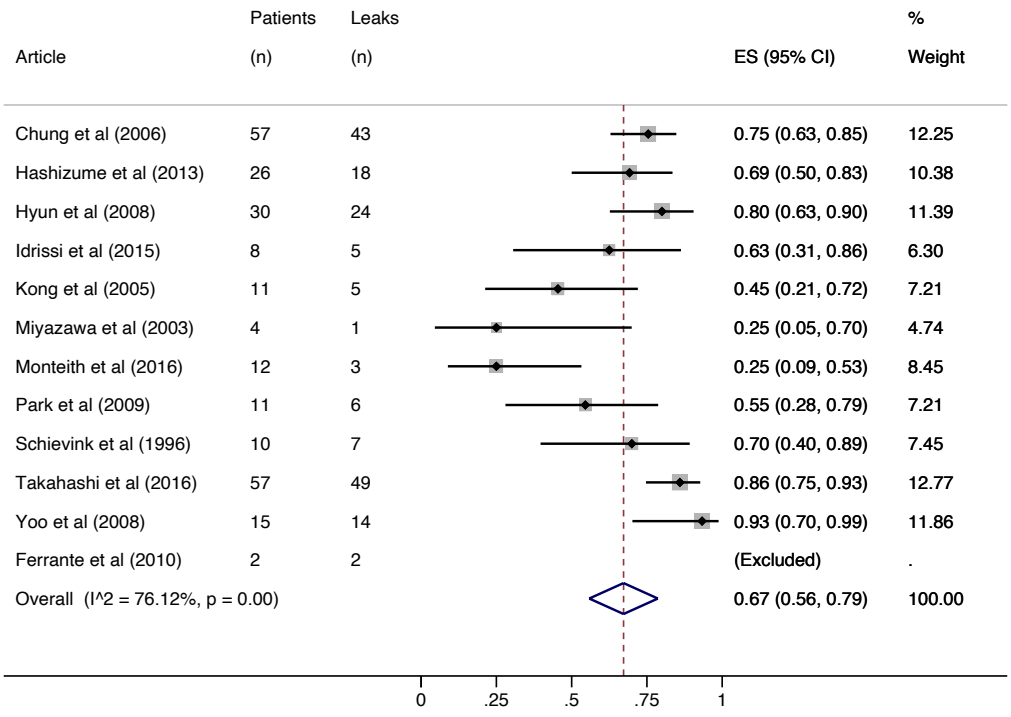


Figure 3-41: Meta-analysis of proportions of positive findings in radionuclide cisternography

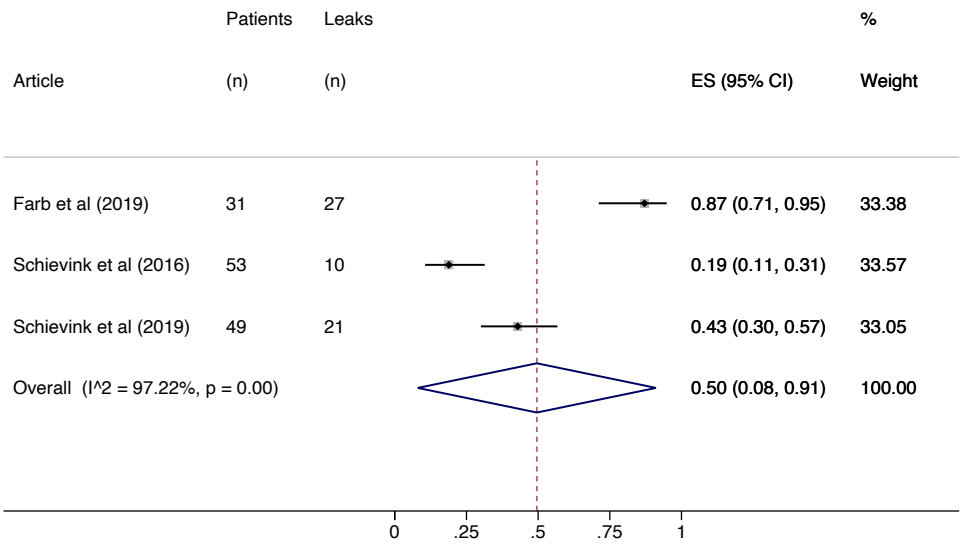


Figure 3-42: Meta-analysis of proportions of positive findings in digital subtraction myelography

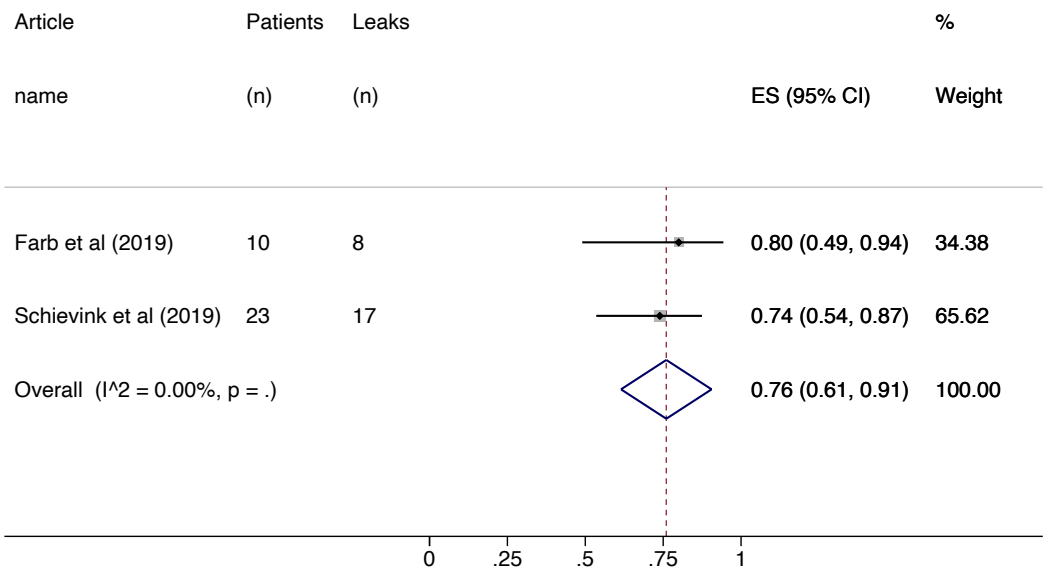


Figure 3-43: Meta-analysis of proportions of positive findings in digital subtraction myelography performed in lateral decubitus position

3.4.4.3. Ophthalmic findings

Several authors attempted identification of novel signs of SIH by investigating the optic nerve sheath diameter and the superior ophthalmic vein diameter (Chen *et al.*, 1999; Chen *et al.*, 2003a; Dubost *et al.*, 2011; Takeuchi *et al.*, 2012; Fichtner *et al.*, 2016; Holbrook *et al.*, 2017; Fichtner *et al.*, 2019). Despite the different methodologies (ultrasound scan and contrast MRI), various studies demonstrated that the diameter of the optic nerve sheath is reduced in patients with SIH (Dubost *et al.*, 2011; Takeuchi *et al.*, 2012; Fichtner *et al.*, 2016; Holbrook *et al.*, 2017; Fichtner *et al.*, 2019). Conversely, the two studies on superior ophthalmic vein diameter found opposite results,

therefore the utility of this parameter in the context of SIH is still uncertain (Chen *et al.*, 1999; Chen *et al.*, 2003a).

3.4.4.4. CSF leak location

Twenty-eight articles describing 1523 leaks were selected to summarise the location of spinal CSF leaks. The most common leak location was the thoracic spine (41%, 95% CI 29 to 52, I^2=97.3%, Figure 3-46) followed by the cervicothoracic junction (25%, 95% CI 17 to 32, I^2=88.0%, Figure 3-45), the cervical spine (14%, 95% CI 10 to 17, I^2=70.7%, Figure 3-44) and the lumbar spine (12%, 95% CI 8 to 16, I^2=82.5%, Figure 3-48). Leaks were reported to be multiple in 24% of the cases (95% CI 15 to 33, I^2=88.7%, Figure 3-50).

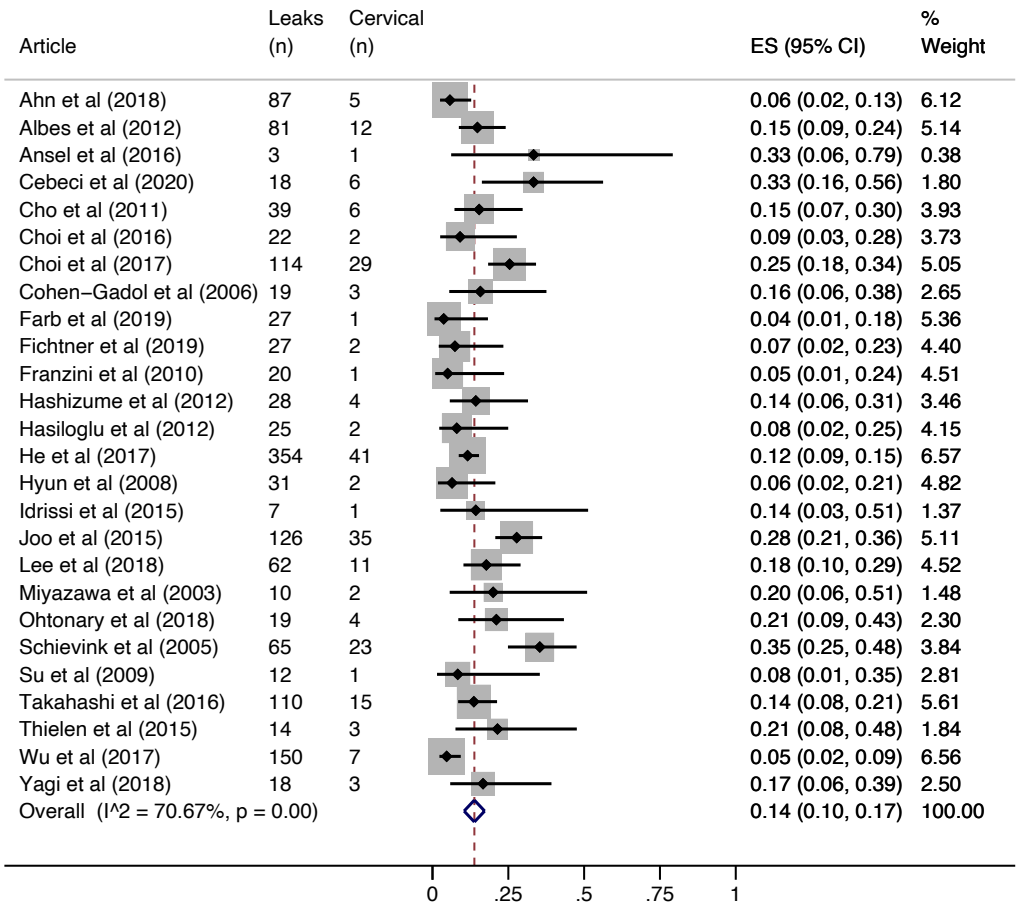


Figure 3-44: Meta-analysis of proportions of leak location (cervical)

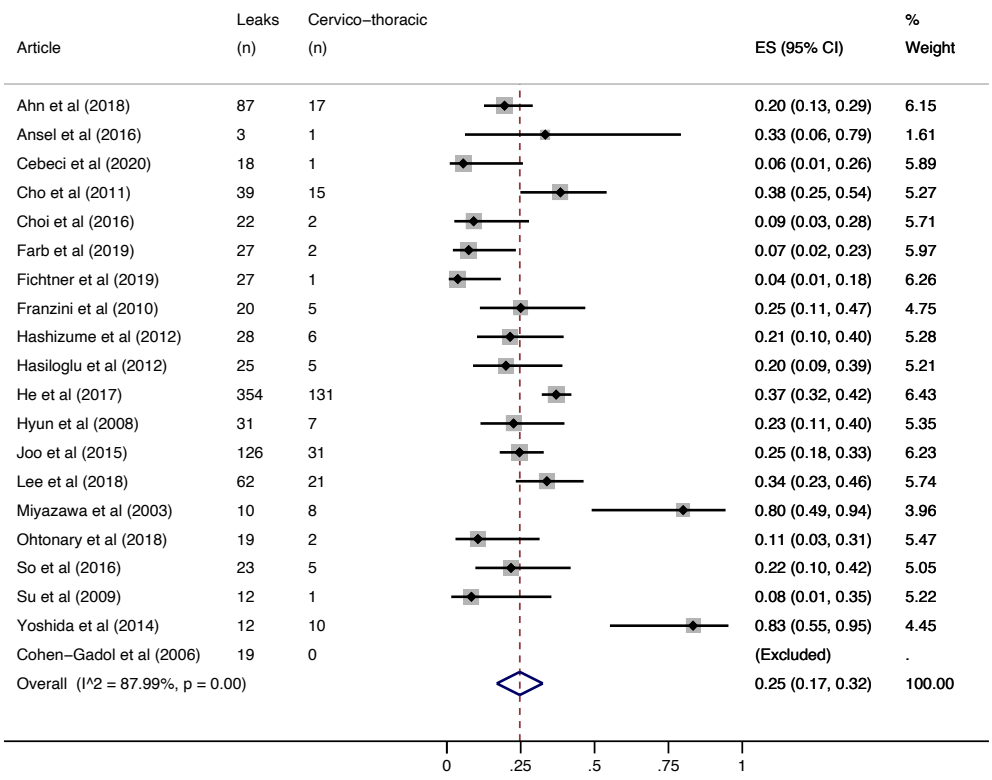


Figure 3-45: Meta-analysis of proportions of leak location (cervico-thoracic)

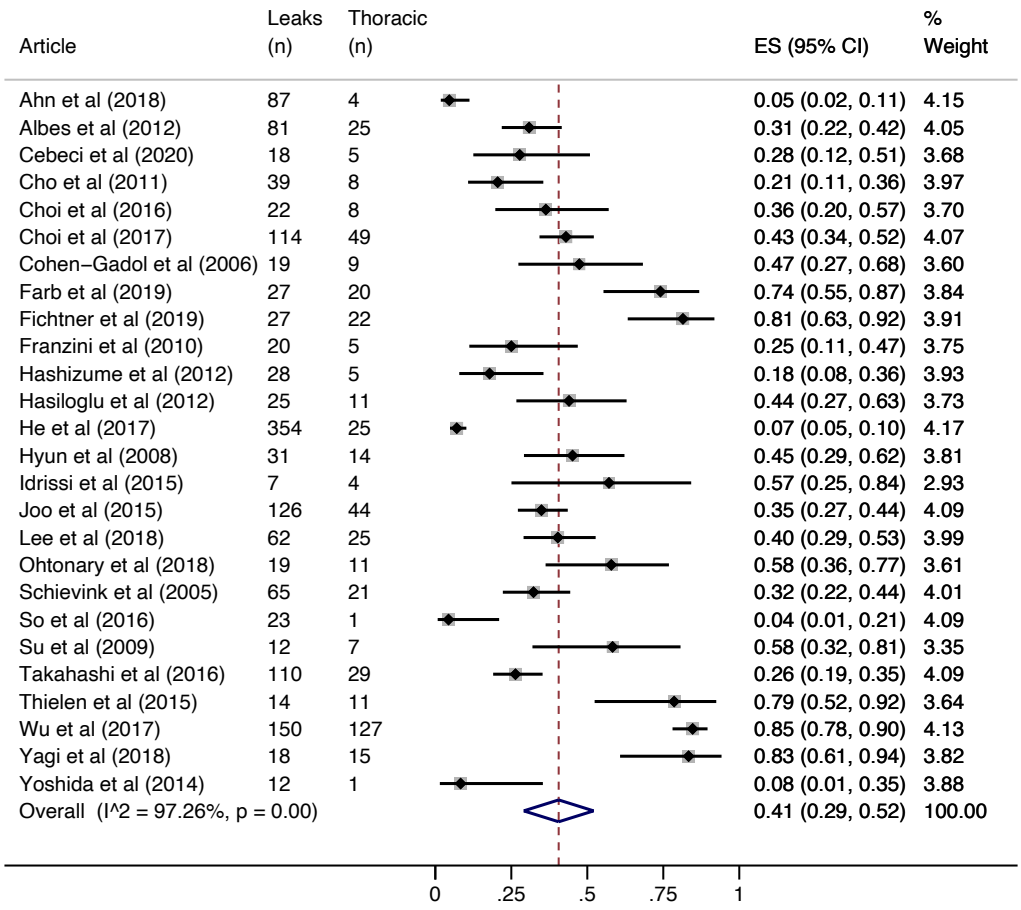


Figure 3-46: Meta-analysis of proportions of leak location (thoracic)

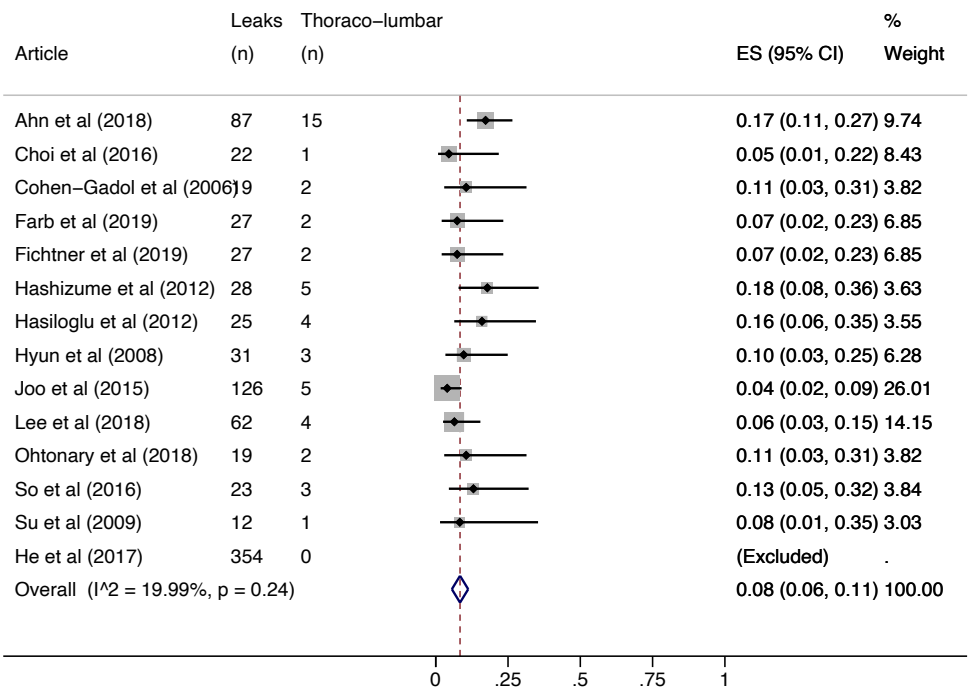


Figure 3-47: Meta-analysis of proportions of leak location (thoraco-lumbar)

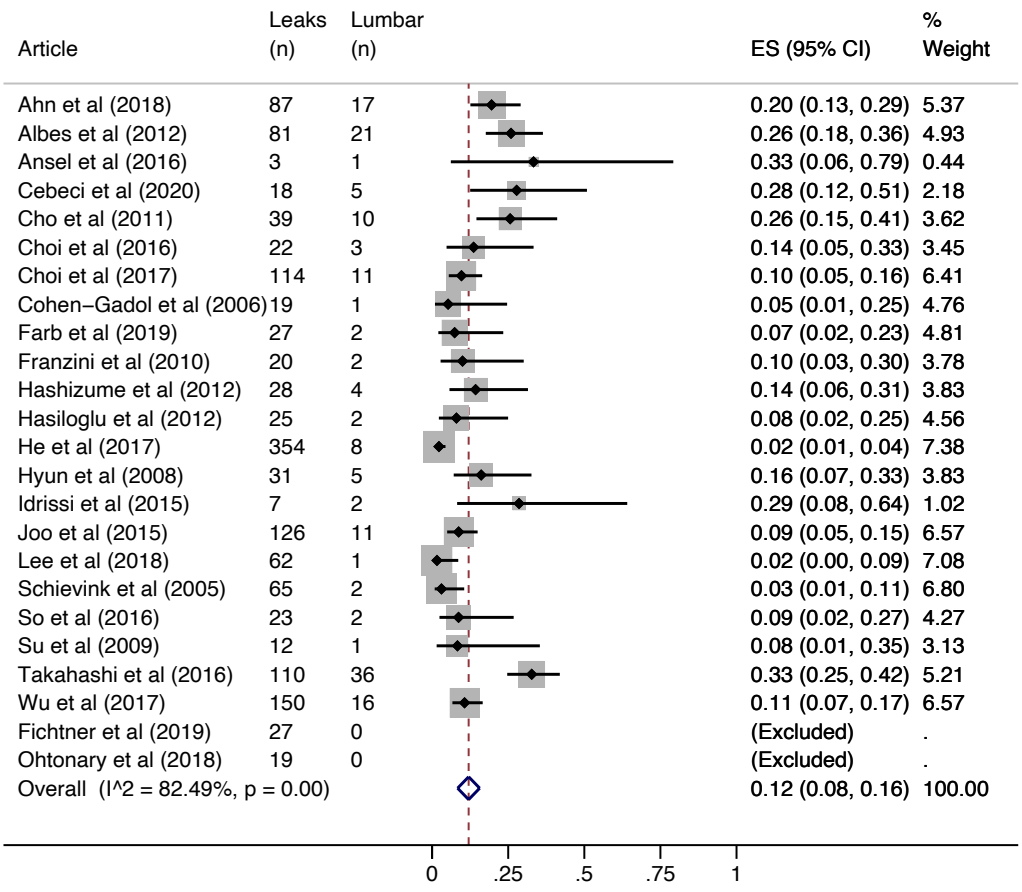


Figure 3-48: Meta-analysis of proportions of leak location (lumbar)

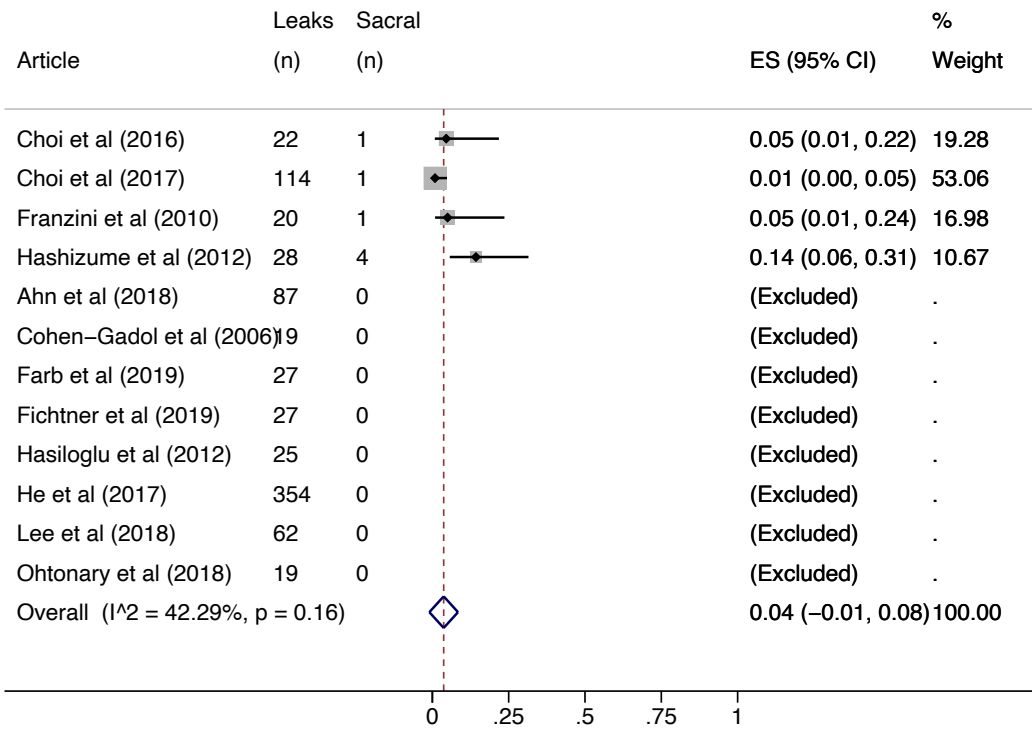


Figure 3-49: Meta-analysis of proportions of leak location (sacral)

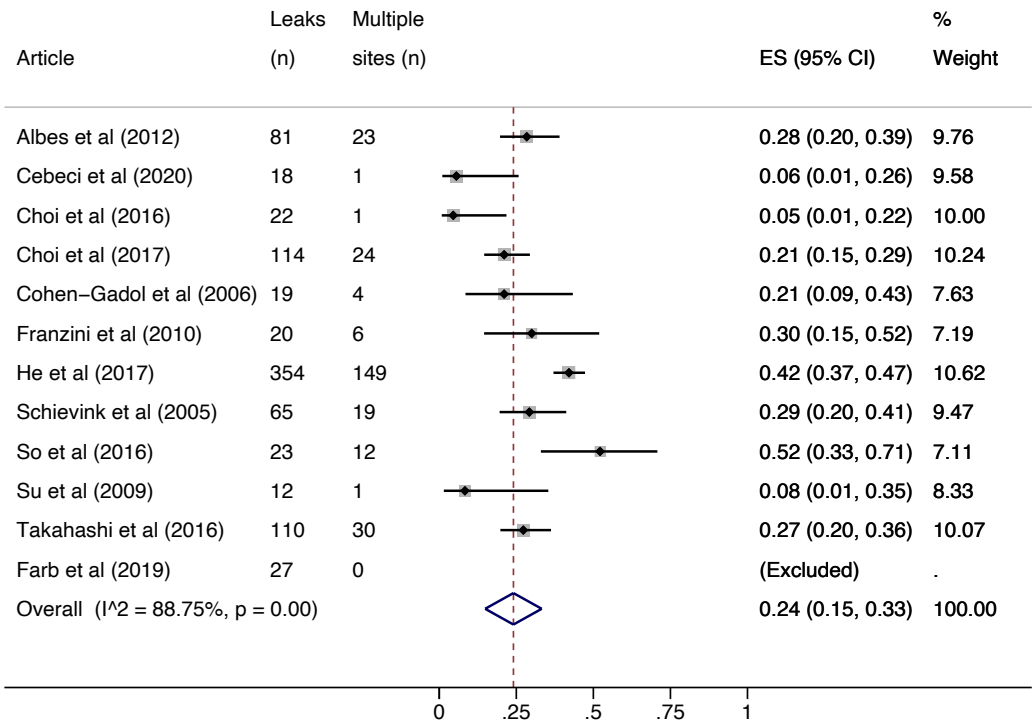


Figure 3-50: Meta-analysis of proportions of leak location (multiple)

3.4.4.5. Lumbar puncture opening pressure

Twenty-one articles, including 738 patients, were selected to analyse the findings of lumbar puncture opening pressure: 67% of the patients had low pressure (<60 mmH_2O, 95% CI 54 to 80, I^2=94.7%, Figure 3-51), 32% normal pressure (60-200 mmH_2O, 95% CI 20 to 44, I^2=94.3%, Figure 3-52) and 3% high pressure (>200 mmH_2O, 95% CI 0 to 6, I^2=43.4%, Figure 3-53). The highest reported opening pressure was 228 mmH_2O (Kranz *et al.*, 2016b).

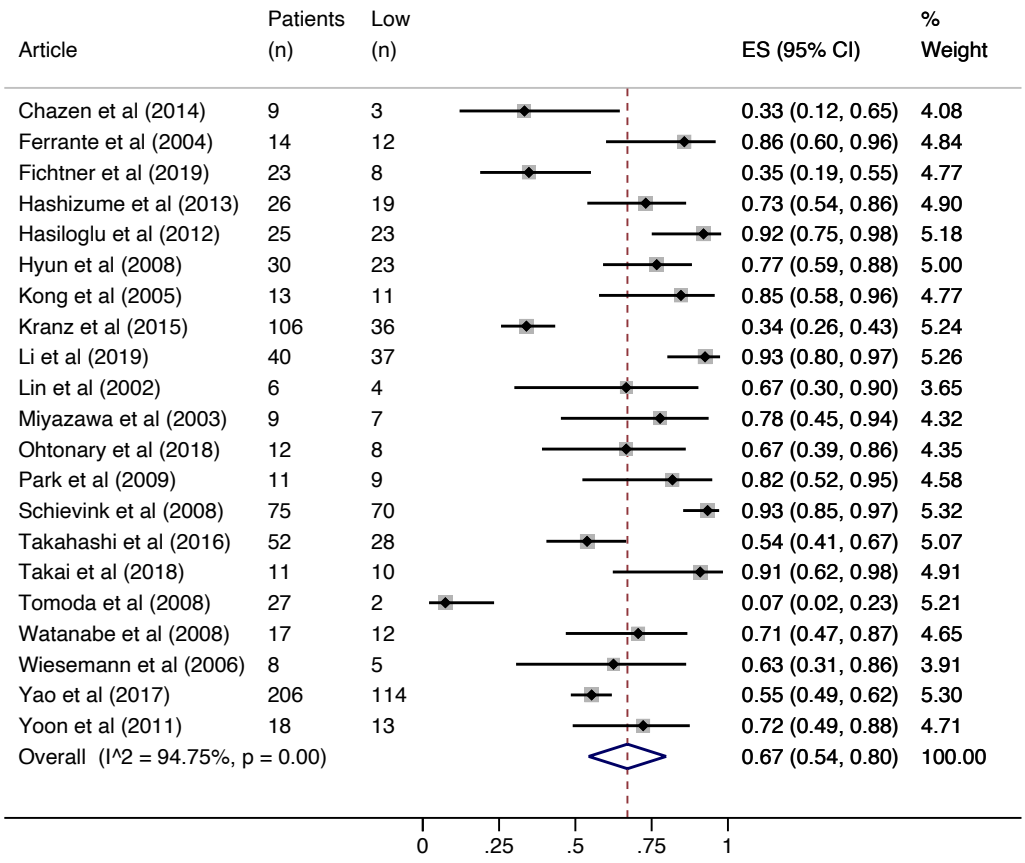


Figure 3-51: Meta-analysis of proportions of lumbar puncture opening pressure (low)

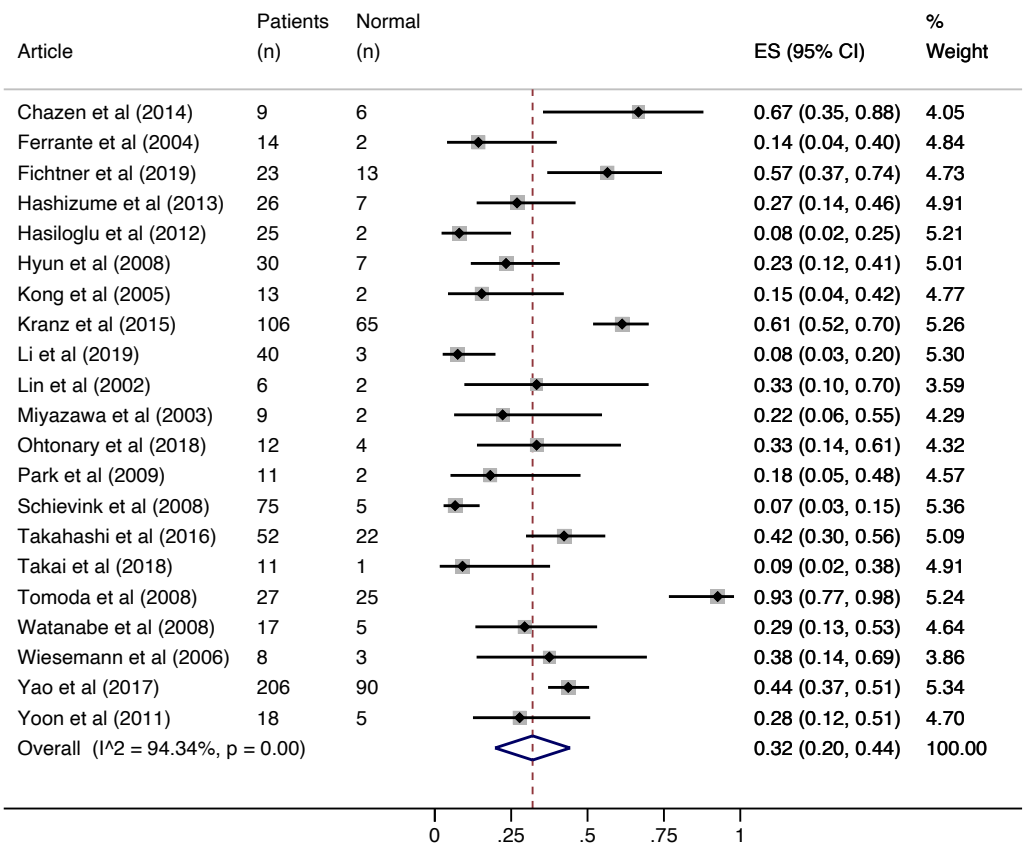


Figure 3-52: Meta-analysis of proportions of lumbar puncture opening pressure (normal)

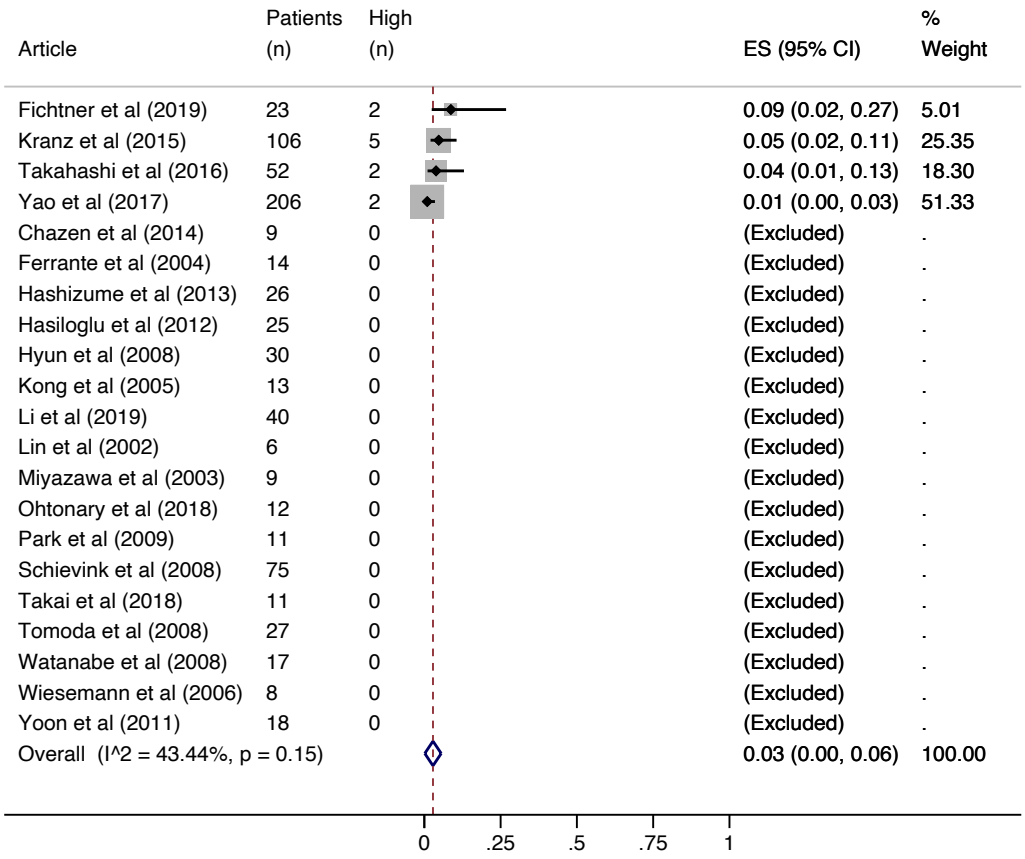


Figure 3-53: Meta-analysis of proportions of lumbar puncture opening pressure (high)

3.4.5. Treatments and outcomes

3.4.5.1. Conservative treatment

Conservative treatment was attempted in 881 patients for a period ranging from 7 days to 9 weeks. This most commonly consisted of bed rest and hydration (Table 3-6). Authors reported a successful conservative treatment (resolution of symptoms with no further intervention needed) in 28% of the patients (95% CI 18 to 37, I^2=91.4%, Table 3-6 and Figure 3-54).

Table 3-6: Treatment of spontaneous intracranial hypotension and outcomes

	Number of patients (simple %)	Pooled estimates of proportions (95% confidence intervals)
Conservative treatment (17 articles, 748 patients)		
Conservative treatment effective	183 (24.5)	28 (95% CI 18-37, I^2=91.5)
Conservative treatment ineffective	565 (75.5)	72 (95% CI 63-82, I^2=91.5)
Type of conservative treatment:		
Bed rest	658 (88.0)	-
Hydration	621 (83.0)	-
Analgesia	205 (27.4)	-
Steroids	30 (4.0)	-
Caffeine	2 (0.3)	-
Epidural Blood Patch (EBP)		
Success rate of first EBP, (33 articles, 1758 patients)	1062 (60.4)	64 (95% CI 56-72, I^2=93.0)
Success rate of non-targeted EBP, (10 articles, 264 patients)	177 (67.1)	69 (95% CI 61-76, I^2=34.9)
Success rate of targeted EBP, (14 articles, 816 patients)	544 (66.7)	70 (95% CI 59-80, I^2=90.5)
Success rate of small EBP (<20ml), (12 articles, 680 patients)	466 (68.5)	66 (95% CI 55-77, I^2=90.3)
Success rate of large EBP (≥20 ml), (4 articles, 169 patients)	139 (82.3)	77 (95% CI 63-91, I^2=69.2)

Other less common treatments: surgical repair of CSF defects, surgical repair of meningeal diverticula, surgical repair of CSF venous fistulas, evacuation of subdural collections, dural reduction surgery.

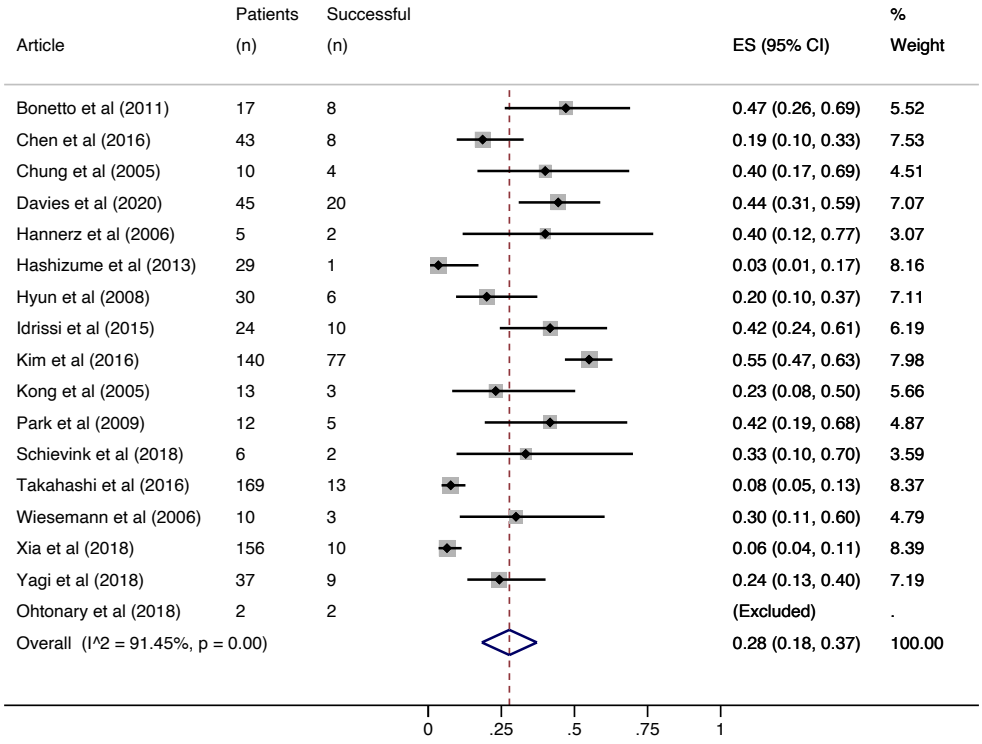


Figure 3-54: Meta-analysis of proportions of successful conservative treatment

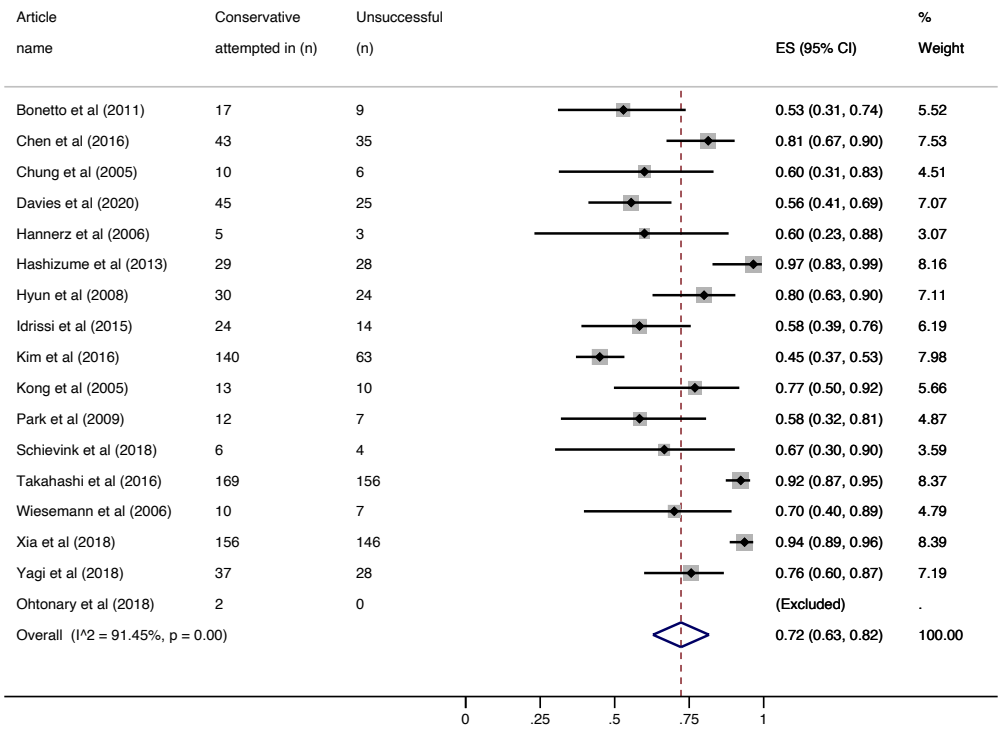


Figure 3-55: Meta-analysis of proportions of unsuccessful conservative treatment

3.4.5.2. Epidural blood patches

EBP was the treatment most commonly offered to patients failing conservative treatment and the first EBP was reported to be successful (clinical improvement without need for further intervention) in 64% of the patients (95% CI 56-72, I^2=93.0, Table 3-6 and Figure 3-57). An analysis of the outcomes of EBPs stratified by targeted/non-targeted EBPs, demonstrates similar proportions of successful results for the targeted and non-targeted techniques (Figure 3-56, Figure 3-58 and Figure 3-59). Large

EBPs (>20ml) had a higher success rate than small EBPs (Figure 3-56, Figure 3-60 and Figure 3-61).

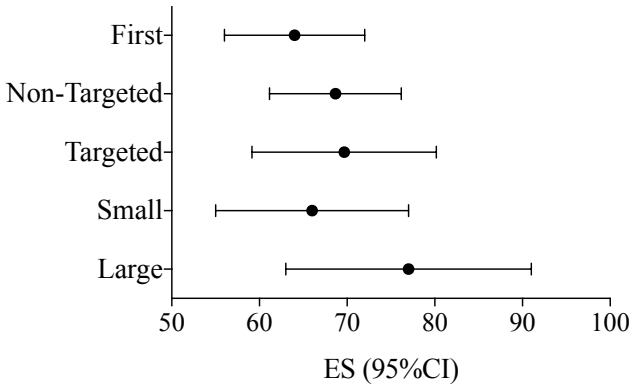


Figure 3-56: Epidural Blood Patches (EBP) outcomes. Pooled estimates of proportions (95% CI) of successful EBP treatment stratified by EBP technique (non-targeted/targeted, small/large).

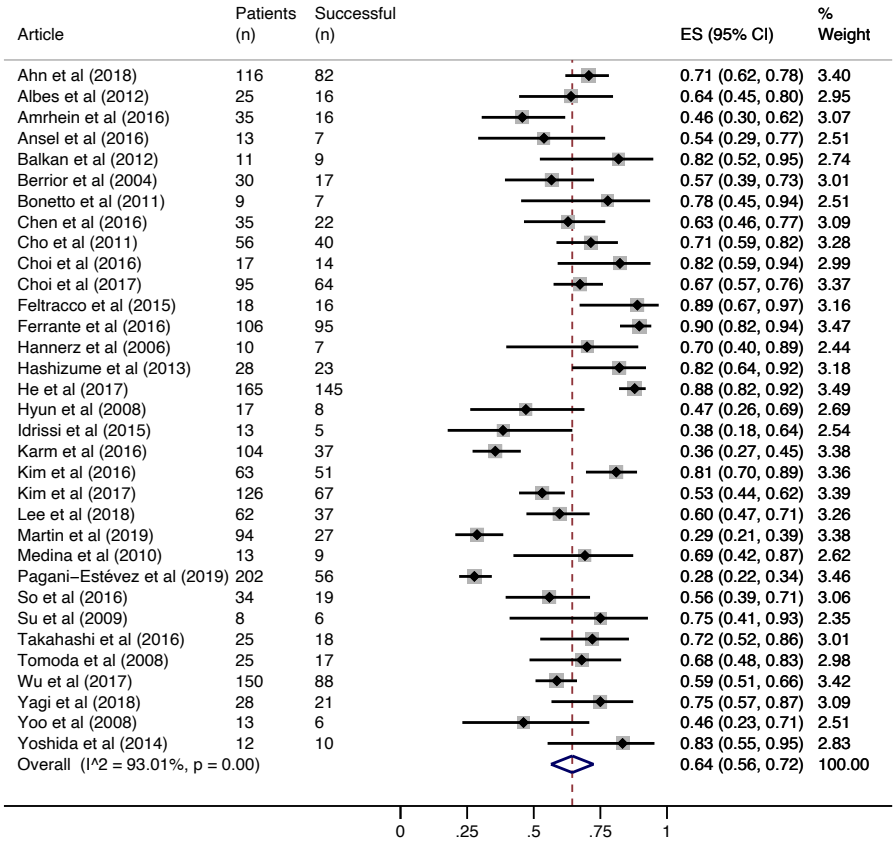


Figure 3-57: Meta-analysis of proportions of successful first epidural blood patch

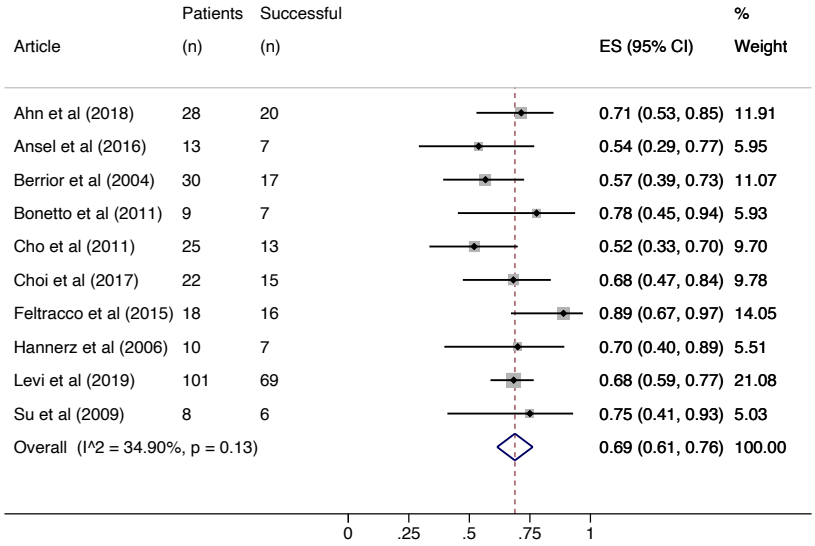


Figure 3-58: Meta-analysis of proportions of successful non-targeted EBP

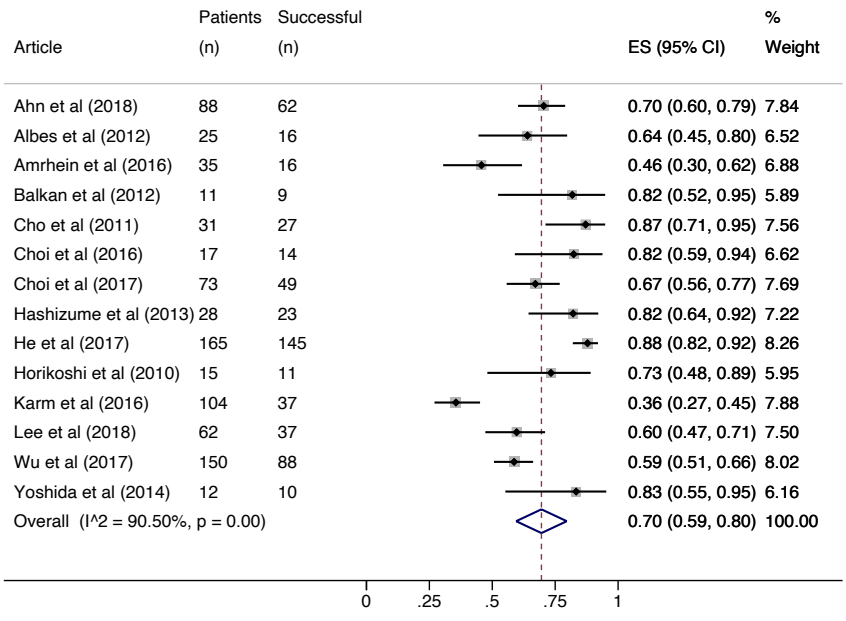


Figure 3-59: Meta-analysis of proportions of successful targeted EBP

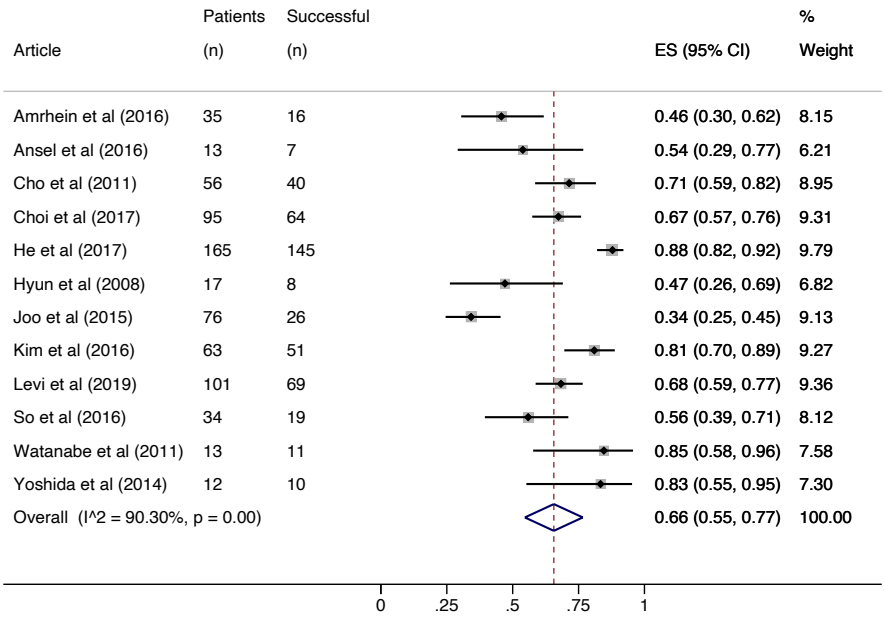


Figure 3-60: Meta-analysis of proportions of successful small EBP

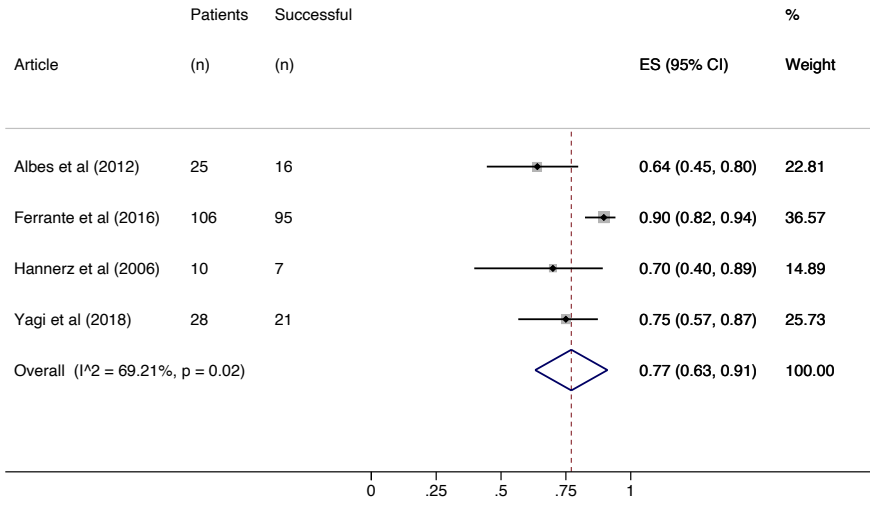


Figure 3-61: Meta-analysis of proportions of successful large EBP

No serious adverse events were reported after EBP treatments. The minor transient adverse events included: back pain, radicular pain, tinnitus, paraesthesia, numbness, bradycardia and dizziness (Wang *et al.*, 2009; Watanabe *et al.*, 2011; He *et al.*, 2018). Spread of autologous blood in the subarachnoid space has been reported as a complication of EBP occurring in 8.5% of procedures (Ferrante *et al.*, 2016b). This event has not been associated with any neurological sequela and has been reported to cause the following transient (mostly intraprocedural) symptoms: palpitation, nausea and headache (Watanabe *et al.*, 2011; Ferrante *et al.*, 2016b).

3.4.5.3. Surgical treatment

Surgical repair of dural defects, meningeal diverticula or CSF-venous fistulas was less frequently performed (Schievink *et al.*, 1998; Kranz *et al.*, 2017; Beck *et al.*, 2019; Wang *et al.*, 2020). Wang et al. recently reported objective headache severity improvement in a group of 20 patients treated with surgical ligation of CSF-venous fistulas (Wang *et al.*, 2020). Dural reduction surgery was not performed in any of the selected papers but was proposed as a potential surgical treatment for SIH by Schievink et al. in 2009 (Schievink, 2009). The incidence of rebound intracranial hypertension after treatment of SIH (EBP, percutaneous or microsurgical treatment) has been reported to be between 7% and 27.4% (Pagani-Estevez *et al.*, 2019b; Schievink *et al.*, 2019a).

3.5. Discussion

This systematic review and meta-analysis provides a comprehensive summary of the available evidence on demographics, clinical presentation, investigation findings and treatment outcomes in SIH patients.

3.5.1. Demographics and phenotype of spontaneous intracranial hypotension

This review highlighted a certain variability in the clinical presentation of SIH. Starting with the demographic characteristics, SIH can occur at any age (range 2-88 years) and in both sexes with a predilection for females (63%). The variability of SIH is also demonstrated by the great diversity of signs and symptoms at presentation (Figure 3-4). As expected, headache is the most common symptom. However, the orthostatic headache, once believed to be an essential characteristic of SIH, is not invariably present. In this review, 8% of patients had a non-orthostatic headache and 3% did not suffer headaches. These percentages are likely to be underestimations as most authors used the ICHD-II diagnostic criteria that include the presence of orthostatic headache as an essential criterion (ICHD-II, 2004). Therefore, a diagnosis of SIH should not be excluded based on the absence of orthostatic headache. The most recent versions of the SIH diagnostic criteria (ICHD-III beta and ICHD-III) do not use this criterion, therefore future studies could clarify what is the true frequency of non-orthostatic headache in SIH (ICHD-III beta, 2013; ICHD-III, 2018). The more detailed headache description offered by some of the authors demonstrated a common pattern in the SIH headache

phenotype: it is frequently occipital, frontal or diffuse (Table 3-5). The occipital location may be one possible pointer towards this condition.

3.5.2. The role of imaging in the diagnosis of spontaneous intracranial hypotension

Among all investigations examined in this review, brain MRI was the most sensitive in detecting signs of SIH. In particular, diffuse pachymeningeal enhancement was detected in 73% of SIH patients. Brain MRI has also the advantage of being readily available, non-invasive and easy to perform. Brain MRI can be particularly useful in confirming diagnosis of SIH in patients with normal CSF pressure and CSF leaks that are difficult to identify with spinal imaging. However, it should be borne in mind that 19% of SIH patients have normal brain MRIs, therefore a normal brain MRI does not exclude SIH. While useful for confirming a diagnosis of SIH, brain MRIs do not give any information regarding the CSF leak location and need to be followed by spinal investigations if targeted treatment is planned. Considering the general availability, the lack of radiation, the sensitivity and the experience built over the last few decades, brain MRI with intravenous contrast should be offered as initial imaging test for the investigation of SIH.

One of the challenges in the management of SIH patients, comes from the inability to clearly identify a CSF leak with the currently available spinal investigation methods. In a significant proportion of patients who have a convincing clinical history for SIH, a CSF leak cannot be demonstrated radiologically. According to the results of this systematic review, spinal

imaging techniques (spinal MRI, CT myelograms, radionuclide cisternography, MR myelogram and DSM) can identify evidence of extradural CSF leak in only 48-67% of the patients (Figure 3-36). Moreover, when a leak is identified with these techniques, its exact location can often remain unknown (Figure 3-36). DSM and MR myelography with the unconventional use of intrathecal gadolinium had the highest sensitivity for identifying the exact leak site (100% and 75.5% respectively). However, the number of cases investigated with these techniques and reported in the literature is very small (133 and 87 patients respectively). Most importantly, MR myelography with intrathecal gadolinium is not commonly available, intrathecal gadolinium has been reported to induce neurotoxicity (especially at higher doses) and more recent evidence (published after the systematic review period) suggest non-superiority of this technique compared to MRM without intrathecal gadolinium (Li *et al.*, 2008; Dobrocky *et al.*, 2020). Dynamic CT myelography has been reported to facilitate the localisation of fast CSF leak; however, further studies will be needed to confirm its role in the diagnosis of SIH (Luetmer *et al.*, 2012; Thielen *et al.*, 2015; Dobrocky *et al.*, 2018). In view of the availability, safety and the sensitivity (comparable to other spinal investigations), spinal MRI with contrast should probably be preferred as first step spinal imaging to other more invasive spinal investigations involving the need for spinal punctures and/or the exposure to high doses of radiation. DSM could instead play an important role in the identification of the exact leak site and guide targeted treatment, however larger studies confirming the utility of this investigation are required.

3.5.3. The role of lumbar punctures in the diagnosis of spontaneous intracranial hypotension

Low lumbar puncture CSF pressure (<60 mmH_20) was initially considered an essential feature of SIH (giving the name to this condition) and has been part of the ICHD diagnostic criteria since 2004. As initially reported by Mokri *et al* and later confirmed by Kranz *et al*, this systematic review also confirms that this finding is inconsistent and that many patients with SIH have normal (and occasionally high) lumbar puncture opening pressure (Mokri *et al.*, 1998; Kranz *et al.*, 2016b). Our results show that CSF pressure is normal in 32% of patients with SIH (Figure 3-52). It should be noted that the presence of low CSF opening pressure in many diagnostic criteria for SIH could have led clinicians to exclude this diagnosis in patients with normal pressure. Therefore, the number of patients with normal or high pressure may actually be much higher than currently reported. The reasons why 32% of the patients with SIH have normal CSF opening pressure on lumbar puncture might be related to the inadequate methods of measurement or to the actual absence of a low CSF pressure state. Lumbar puncture opening pressure is a snapshot method of measurement, is not reflective of the intracranial pressure in the upright position and does not offer any information regarding the CSF dynamics during a postural change. The correlation between SIH and connective tissue disorders supports the hypothesis of a dural compliance disorder as the main cause for this syndrome (Schievink *et al.*, 2004a; Liu *et al.*, 2011; Reinstein *et al.*, 2013). The finding of intracranial hypertension in 3% of the patients also raises the possibility that some of

these patients might actually be affected by a high CSF pressure disorder with a paradoxical presentation, though the only mildly elevated CSF pressures and the lack of papilloedema would point away from this notion. Alternatively, the presence of an initially raised CSF pressure could predispose the patient to the onset of a spontaneous CSF leak at a weak point of the dura. Lumbar punctures have modest sensitivity (67%) and can support the diagnosis of SIH, however a normal opening pressure does not exclude this disorder.

3.5.4. Treatment outcomes

SIH is a disabling disorder with a severe impact on quality of life and financial health (Cheema *et al.*, 2022). While most patients with SIH can be managed in an outpatient setting, there are instances in which patients with SIH become critically unwell with reduced consciousness, mainly secondary to brain herniations or subdural collections (Schievink *et al.*, 2005c; Lai *et al.*, 2007; Xia *et al.*, 2015; Takahashi *et al.*, 2016; Takai *et al.*, 2019). Effective treatment of SIH patients aims to alleviate symptoms, improve patients' quality of life, prevent deterioration and improve outcomes of SIH patients who are critically unwell. A significant proportion of patients (28%) successfully respond to conservative treatment measures (Figure 3-54). Based on this finding, it would be beneficial to attempt conservative treatment before EBP in every patient with SIH, but further studies will need to clarify the best type and duration of conservative treatment. One EBP was effective in 64% of the patients (Figure 3-57). "Improvement after EBP" was

one of the diagnostic criteria included in the ICHD-II classification, therefore the proportion of successful outcomes reported in this systematic review could be an overestimate. According to the literature EBPs also have a very safe profile, with only transient minor complications. When comparing different EBP techniques, large EBPs (>20 ml) gave successful outcomes in a higher proportion of patients than small EBPs (Figure 3-56). This finding is in line with the results of a previous study by Wu et al (Wu *et al.*, 2017). On the other hand, the use of targeted EBPs gave similar success rates compared to non-targeted EBPs. It is difficult to objectively compare the success rates of targeted and non-targeted EBPs because the patients in the two groups are different: patients who had targeted treatment had a known leak site, while this was not true for patients having non-targeted treatment either because EBP was attempted before any second line spinal investigation, or because these investigations were inconclusive. Indeed, many patients who have a targeted EBP have done so after they have failed to respond to non-targeted EBPs further emphasising the superiority of efficacy of targeted EBPs, albeit that invasive investigations are required before they can be administered. Randomised controlled trials will be required to confirm the superiority of large EBPs and investigate the potential difference between targeted and non-targeted EBPs. Based on the results of this review, large non-targeted epidural blood patches could be attempted in SIH patients who fail to improve with conservative treatment.

3.5.5. Proposed algorithm for the diagnosis and management of spontaneous intracranial hypotension

The results of this study suggest that the absence of orthostatic headache, normal imaging or normal lumbar puncture opening pressures can occur in SIH, therefore this diagnosis cannot be excluded in patients who do not present with all the typical features of this disorder. We propose that brain MRI and spine MRI with contrast could be performed as first line investigations in patients with clinical suspicion of SIH. While a lumbar puncture could be offered to patients with a clinical picture suggestive of SIH but inconclusive first line imaging, it needs to be undertaken with caution bearing in mind that the sensitivity of this investigation is modest (67%) and there is a risk of worsening SIH. Treatment with EBPs could be attempted early, even if the exact leak location is unknown. Second line spinal imaging (e.g., DSM or MR myelography with intrathecal Gadolinium) could be offered to patients who do not respond to EBP and require targeted treatment (EBP or surgical surgical). Figure 3-62 displays the proposed diagnostic pathway for SIH.

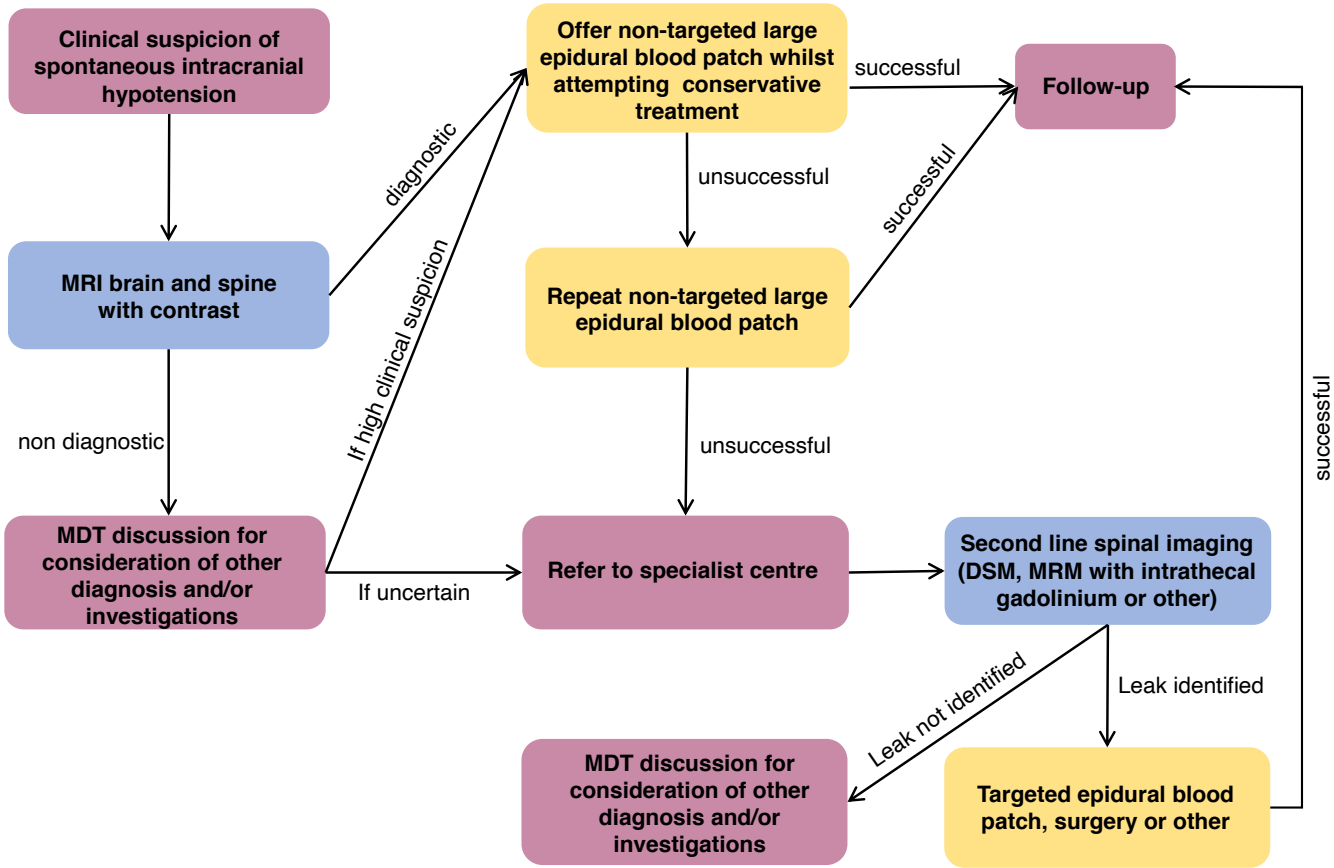


Figure 3-62: Flow-chart of proposed diagnostic pathway for spontaneous intracranial hypotension. Investigations are in blue, treatments in yellow. DSM: Digital Subtraction Myelography; MRM: MRI Myelogram; MDT: Multidisciplinary Team

3.5.6. Limitations

The limitations of this systematic review are related to the heterogeneous nature of the SIH studies available in the literature, the lack of randomised controlled trials and the lack of continuity in the diagnostic criteria used over the past decades. This heterogeneity is clearly reflected in the results of the various meta-analyses often showing a I^2>75% and was addressed through the use of random effect analyses. Future research should aim at investigating the exact aetiology of this condition, as well as improving the diagnostic and treatment techniques for SIH through large randomised controlled studies. Despite its limitations, this study offers a comprehensive and objective summary of the evidence on SIH that could be useful in guiding clinical practice and future research.

3.6. Conclusions

This systematic review and meta-analysis summarises the clinical presentation, investigation findings and treatment outcomes of SIH based on the reports of 144 articles. Absence of orthostatic headache, normal imaging or normal lumbar puncture opening pressure should not exclude a diagnosis of SIH. A single EBP was successful in 64% of the patients. While this meta-analysis suggests that large EBPs have successful outcomes in a higher proportion of patients compared to small EBPs, this requires further validation. Large randomised controlled trials will be required to define the best management for SIH.

Chapter 4. Intracranial pressure monitoring in patients with spontaneous onset of orthostatic headache

4.1. Abstract

4.1.1. Introduction

Spontaneous intracranial hypotension (SIH) is a common and debilitating disorder. Patients affected by this disorder can often present with normal investigation findings posing a difficult diagnostic challenge for the clinicians. Intracranial pressure (ICP) monitoring has been suggested as a useful investigation in patients with orthostatic headaches highly suggestive of SIH but with inconclusive investigations.

4.1.2. Methods

This is a single centre retrospective observational study conducted at a tertiary/quaternary referral centre specialising in SIH and CSF dynamics disorders. Consecutive patients affected by spontaneous orthostatic headache with inconclusive investigation findings who underwent diagnostic 24-hour ICP monitoring were considered eligible. Patients were identified through the standardised screening of two clinical databases.

Patients underwent 24-hour ICP monitoring according to an established standardised protocol. ICP data was collected for 24 hours, and the results derived for median ICP and pulse amplitude (marker of brain compliance)

during the daytime, night-time and over the 24-hour period. The main objective of the study was to identify the proportion of patients with abnormal ICP monitoring results. Specific cut-offs for low and high ICP states were predetermined based on the current best available evidence.

4.1.3. Results

Thirty-eight patients (23 females, mean age 41±14 years) were identified. All patients had orthostatic headaches with spontaneous onset. The mean duration of symptoms was 46±36 months. ICP monitoring identified 3 patients with low ICP (8%, mean 24-hour ICP -2±2 mmHg) and 6 patients with high ICP (16%, mean 24-hour ICP 9±3 mmHg). Obvious CSF dynamics disturbances were excluded in the remaining 29 patients (76%, mean 24-hour ICP 3±3 mmHg). None of the clinical features were reliable predictors of low ICP state, but aural fullness or muffled hearing were more common in patients with abnormal ICP results. There were no complications from the ICP monitoring procedure for any of the patients.

4.1.4. Conclusions

When appropriately selected, patients with a clinical picture highly suggestive of SIH and uncertain or equivocal investigation findings can benefit from the use of invasive ICP monitoring. Additionally, a significant minority of patients with orthostatic headache can have a high CSF pressure state that can be identified with ICP monitoring.

4.2. Introduction

Spontaneous intracranial hypotension (SIH) is a disorder characterised by orthostatic headache secondary to the spontaneous occurrence of a spinal cerebrospinal fluid (CSF) leak. According to current International Classification of Headache Disorders, SIH can be diagnosed when the headache has developed spontaneously and in temporal relation to a low CSF pressure state, CSF leakage, or has led to its discovery (ICHD-III, 2018). To meet the ICHD-III diagnostic criteria patients also have to show evidence of either CSF leak on imaging or low CSF opening pressure (<60 mm CSF) (ICHD-III, 2018). Diffuse pachymeningeal enhancement, brain sagging, cerebral tonsillar descent, subdural collections, venous engorgement and pituitary enlargement are typical signs of SIH on brain MRI (Figure 3-35) (Schievink, 2021). A variety of spinal imaging techniques can be used to identify the spinal CSF leak and to guide targeted treatment (Figure 3-36) (Schievink, 2021). Epidural blood patches are often successful in the treatment of SIH (64% success rate for the first patch) especially if large patches are employed (Figure 3-56) (Wu *et al.*, 2017).

SIH can pose an arduous diagnostic challenge. According to a recent patients' survey by Cheema *et al.*, the median time between symptoms onset and diagnosis of SIH was 2 months (Cheema *et al.*, 2022). In addition, 45% of SIH patients had to see more than one specialist to receive a correct diagnosis (Cheema *et al.*, 2022). This is not surprising considering that MRI brain can be normal in up to 19% of the patients, spinal imaging is able to

identify extradural CSF in only 48-76 % of the patients and a significant proportion of SIH patients (32-61%) do not have low CSF opening pressure when undergoing lumbar punctures (Figure 3-36, 3.4.4.5) (Kranz *et al.*, 2016b). Moreover, there are patients who meet the SIH diagnostic criteria who do not respond to treatment with epidural blood patches. The findings described above are considered atypical, however they are not rare and atypical forms of SIH have potentially been underestimated for a long time due to the previously used diagnostic criteria. According to the second edition of the international classification of headache disorders, SIH could only be diagnosed in patients who improved with epidural blood patches (ICHD-II, 2004). While these diagnostic criteria have now been revised, their use for almost a decade has probably contributed to the underestimation of atypical forms of SIH.

There are currently no national or international guidelines to support patients and clinicians in the investigation and treatment of SIH. The study of CSF dynamics in patients with SIH has the potential to help delineate the pathophysiology of this disease and identify patients who present with atypical features. The current experience of CSF pressure measurements in low CSF pressure syndromes is almost entirely based on snapshot measurements with lumbar puncture opening pressures. Lumbar punctures are of limited use due to the dynamic nature of CSF pressure and the measurement of CSF pressure in a position (lateral decubitus) that does not trigger the patient's main symptom. Previous studies have highlighted the

utility of lumbar infusion studies and isolated case reports have documented the utility of intracranial pressure (ICP) monitoring in patients with SIH (Zada *et al.*, 2007; Eide *et al.*, 2012; Fichtner *et al.*, 2012; Beck *et al.*, 2017; Häni *et al.*, 2020; Jensen *et al.*, 2021).

This study reports the use of ICP monitoring in a series of patients with longstanding orthostatic headache, strong clinical suspicion of SIH, equivocal investigation findings and/or lack of response to epidural blood patches. The aim of the study was to identify the proportion of patients with orthostatic headache and diagnostic uncertainty for SIH who have confirmed CSF dynamics abnormalities identified with ICP monitoring.

4.3. Methods

4.3.1. Ethics

This is a single-centre retrospective observational study conducted at the National Hospital for Neurology and Neurosurgery (London, UK). This study has been approved by the North-East Newcastle and North Tyneside 2 Research Ethics Committee and the Health Research Authority (20/NE/0127). Due to its retrospective nature, written consent to take part in this study was waived. All patients provided written consent to undergo the ICP monitoring procedure as part of their standard clinical care.

4.3.2. Patients' selection

Patients meeting all the following inclusion criteria were selected:

(a) orthostatic headache,

(b) negative or equivocal results of brain MRI with contrast,

(c) negative or equivocal results of spinal investigations (CT myelogram or MRI with contrast) and lumbar puncture opening pressures if performed,

(d) failure to respond to epidural blood patches if performed,

(e) Postural Tachycardia Syndrome (PoTS) was excluded with tilt-table/active stand test; when PoTS was present then cardiovascular parameters were optimally treated,

(f) cervicogenic headache excluded clinically and with neuroimaging,

(g) investigated with 24-hour ICP monitoring.

Patients were excluded if their orthostatic headache was secondary to significant trauma, surgery, shunt placement/overdrainage and/or lumbar puncture. Eligible patients were identified through the screening of two sources: the clinical letters database and the ICP monitoring clinical database. The clinical letters database is prospectively built; every letter is written in a standardised and systematic fashion that allows access to a complete clinical summary of the patients' management history. Clinical letters including the terms "ICP", "leak" or "orthostatic headache" were identified using the Microsoft Word search within the document function. Each patient was then tested for eligibility against the predetermined eligibility criteria. The ICP monitoring results clinical database was also

screened to identify patients who met the inclusion criteria but were not identified with the previous screening method.

4.3.3. Intracranial pressure monitoring methods

The National Hospital for Neurology and Neurosurgery (London, UK) is a tertiary/quaternary referral centre for patients with CSF dynamics disturbances. Patients with ongoing orthostatic headaches who are referred to our centre would only undergo ICP monitoring for diagnostic purposes when there is a strong clinical suspicion for SIH (orthostatic headache not better explained by any other diagnosis), but diagnostic uncertainty, either due to the inability to identify obvious signs of SIH on imaging or due to the lack of response to empirical treatment with epidural blood patches. Each patient's case is discussed in a multidisciplinary meeting during which potential benefits and risks of ICP monitoring are discussed. The multidisciplinary meeting is composed of neurologists, neurosurgeons, neuroradiologists and ophthalmologists with an interest in CSF dynamics disturbances. The decision to perform ICP monitoring is based on the consensus of this multidisciplinary team.

Details on the standardised protocol for ICP monitoring have been described above (Chapter 2). An intraparenchymal ICP probe is inserted in the operating theatre under local anaesthetic (with/without sedation). The probe is connected to a recording ICP monitor and continuous data on ICP (approximately 100 Hz) is recorded for a period of 24 hours. The patients are

encouraged to mobilise, sit up and stand as much as possible during the daytime and to lie supine in bed during the night-time. This protocol permits the recreation of conditions similar to the patients' daily life and increases the possibility of capturing their ICP when they are symptomatic (in this case most commonly in the upright position). The continuous ICP monitoring data are then analysed through a specialised software (ICM+©, University of Cambridge, UK). The ICP monitoring results are summarised in terms of 24-hour, daytime and night-time median ICP and pulse amplitude (PA). The PA is considered a marker of brain compliance, with the pulse amplitude being inversely correlated with brain compliance (Evensen and Eide, 2020). The percentage of time spent in negative ICP territories was also calculated.

4.3.4. Data extraction

Information on the following variables was collected: age, sex, duration of orthostatic headache, intensity of orthostatic headache (verbal reporting scale for both supine and upright position), comorbidities, headache phenotype (location, quality, radiation), associated symptoms, precipitants, features on MRI head/spine and outcomes of epidural blood patch (if performed). All patients' clinic letters and electronic records were reviewed.

4.3.5. Interpretation of ICP monitoring results

A recent systematic review and meta-analysis has provided reference values for normal ICP, the 95% confidence interval for normal daytime ICP is between -2.27 and 2.05 mmHg, while the 95% confidence interval for normal

night-time ICP is between 2.85 and 9.78 mmHg (Norager *et al.*, 2021). The present study used the above reference values to classify the patients' ICP monitoring results as 'low', 'high' or 'normal/borderline' ICP:

(i) patients with 'low' ICP had daytime ICP < -2.27 mmHg and night-time ICP < 2.85 mmHg,

(ii) patients with 'high' ICP had daytime ICP > 2.05 mmHg and night-time ICP > 9.78 mmHg,

(iii) patients with 'normal/borderline' ICP did not meet the criteria for high or low ICP.

4.3.6. Statistical analysis

Continuous variables were summarised as means (standard deviation) and categorical variables as percentages. The clinical characteristics of the patients in the 3 groups were compared through Kruskal-Wallis H Test (for continuous variables) and Fisher's exact test (for categorical variables). A significance level 0.05 was used. Microsoft® Excel for Mac (version 16.25), Stata© (version 15.0) and GraphPad Prism for macOS (version 8.4.1) were used for the data collection and statistical analysis.

4.4. Results

The clinic letters database identified 4,397 clinic letters (out of a total of 38,240 letters) in which the terms "ICP", "Leak" or "Orthostatic Headache" were used. The letters belonged to a total of 828 patients. Only 37 of these

patients met the inclusion criteria for the study. The screening of the ICP monitoring database (including a total of 799 records) identified one extra patient meeting the inclusion criteria for the study.

Thirty-eight patients were included in the study, 23 were female (61%) and the average age was 41 years (SD ±14 years). All patients had orthostatic headaches with spontaneous onset. Twenty-seven patients (71%) had at least another headache diagnosis: 18 patients had chronic/episodic migraine, 7 patients had medication overuse headache and 6 patients had another type of headache. Other common comorbidities were Ehlers Danlos syndrome or hypermobility spectrum disorder (14 patients, 37%), anxiety and depression (9 patients, 24%), PoTS (9 patients, 24%) and asthma (4 patients, 11%).

4.4.1. Clinical presentation

The mean duration of orthostatic headache at the time of ICP monitoring was 46 months (SD ±36 months). The headache was most commonly bilateral (32 patients, 84%) and centred over the occipital (21 patient, 55%), frontal (12 patients, 32%) or cervical regions (9 patients, 24%) (Table 4-1).

Table 4-1: Central location of orthostatic headache

Central location of orthostatic headache	N (%)
Occipital	21 (55)
Frontal	12 (32)
Cervical and/or neck	9 (24)
Vertex	7 (18)
Temples	5 (13)
Retro-orbital	5 (11)
Parietal	4 (11)
Holocranial	3 (8)
Peri-auricular	2 (5)
Temporal	1 (3)

The pain quality was most commonly described as throbbing (18 patients, 47%), pressing (18 patients, 47%), aching (9 patients, 24%) or sharp (8 patients, 21%). In addition to the upright posture, 20 patients (53%) reported that Valsalva manoeuvres were triggers or exacerbating factors for the headaches. The headache intensity in supine and upright posture are displayed in Figure 4-1.

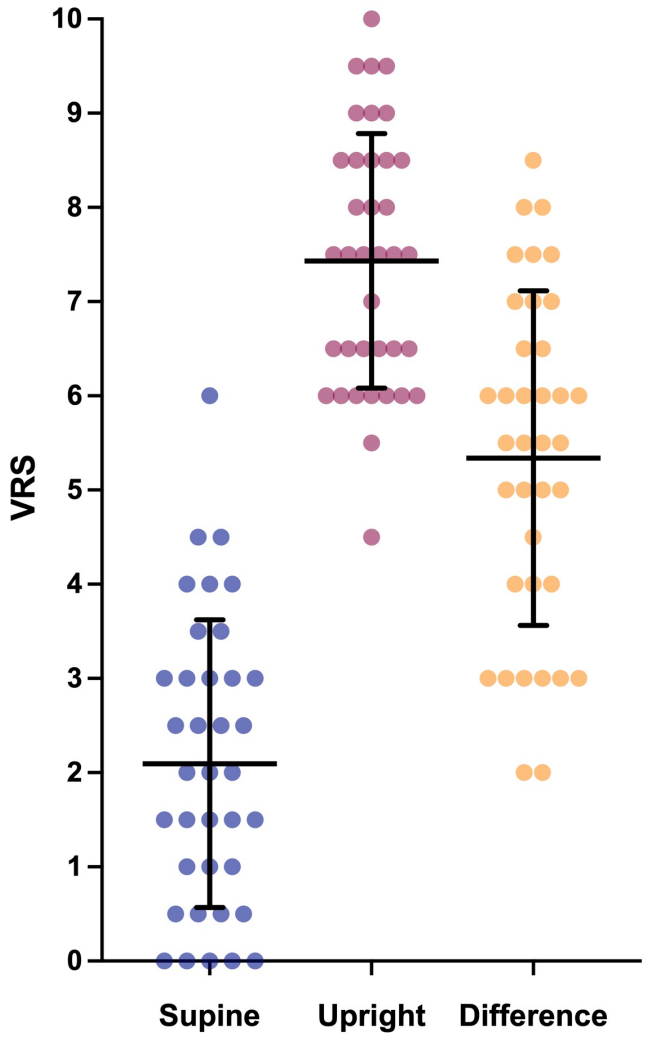


Figure 4-1: Headache intensity in Verbal Reporting Scale (VRS).

The intensity in supine, upright position, and the difference (upright VRS minus supine VRS) are reported.

The most frequently reported associated symptoms were motion sensitivity (24 patients, 63%), phonophobia (24 patients, 63%) nausea/vomiting (23 patients 61%), photophobia (23 patients, 61%), difficulties concentrating (13 patients, 34%), aural fullness (11 patients, 29%), osmophobia (9 patients, 24%) and tinnitus (9 patients, 24%).

4.4.2. Investigations and treatments prior to ICP monitoring

Before consideration of ICP monitoring, all patients were investigated with imaging. Additionally, some patients received empirical treatment with non-targeted lumbar epidural blood patches and/or intravenous caffeine infusions. Table 4-2 provides a summary of the investigations and treatments for each patient, as well as the rationale for performing ICP monitoring.

All patients had brain MRI imaging with contrast that did not demonstrate any sign of low CSF pressure/volume state (Table 4-2). Thirty-three patients underwent spinal MRI with contrast and 18 patients had CT myelograms; none of these investigations showed evidence of a CSF leak. Fourteen patients had a lumbar puncture performed elsewhere and the results were either normal or inconclusive (one patient who had 3 dry lumbar puncture attempts) (Table 4-2). Five patients underwent lumbar infusion studies elsewhere; the results were negative in 4 patients and equivocal in one (Table 4-2). Twenty-six patients were treated with non-targeted lumbar epidural blood patches (1-6 patches per patient) and 16 patients received intravenous caffeine infusion, these treatments were either ineffective or provided only a partial or temporary improvement of the symptoms (Table 4-2).

Table 4-2: Summary of patients' investigation findings, treatment outcomes and intracranial pressure monitoring results

Pt	Sex	Age[1] (years)	Brain MRI + c	Spine MRI + c	CTM	LPOP	PoTS testing	EBP (n)	EBP outcome	Caff. inf. (n)	Caff. inf. outcome	ICPM results[2]	ICPM indication
1	M	35	-ve	-ve	equiv.	n.d.	-ve a.s.t.	1	Partial improvement	n.d.	n/a	Normal/ Borderline	Inconclusive imaging + partial response to EBP
2	F	44	-ve	equiv.	n.d.	n.d.	-ve a.s.t.	n.d.	n/a	n.d.	n/a	Normal/ Borderline	Inconclusive imaging
3	F	34	-ve	-ve	n.d.	n.d.	+ve tilt table	n.d.	n/a	n.d.	n/a	High	Inconclusive imaging
4	F	16	-ve	-ve	n.d.	equiv.	-ve a.s.t.	n.d.	n/a	n.d.	n/a	Normal/ Borderline	Inconclusive imaging
5	M	32	-ve	-ve	equiv.	normal	-ve a.s.t.	4	Ineffective	2	Ineffective	Normal/ Borderlin	Inconclusive imaging +

Pt	Sex	Age[1] (years)	Brain MRI + c	Spine MRI + c	CTM	LPOP	PoTS testing	EBP (n)	EBP outcome	Caff. inf. (n)	Caff. inf. outcome	ICPM results[2]	ICPM indication
												e	ineffective EBP
6	M	37	-ve	n.d.	n.d.	normal	-ve tilt table	1	Transient improvement	n.d.	n/a	Normal/ Borderline	Inconclusive imaging + partial response to EBP
7	F	57	-ve	-ve	-ve	equiv. infusion study	-ve tilt table	2	Ineffective	1	Ineffective	Normal/ Borderline	Inconclusive imaging + ineffective EBP
8	F	43	-ve	equiv.	n.d.	normal	-ve a.s.t.	2	Ineffective	3	Ineffective	Normal/ Borderline	Inconclusive imaging + ineffective EBP
9	F	54	-ve	equiv.	equiv.	normal	-ve a.s.t.	1	Ineffective	n.d.	n/a	Normal/ Borderline	Inconclusive imaging + ineffective EBP
10	F	42	-ve	n.d.	-ve	normal	-ve a.s.t.	4	Transient improvemen	2	Ineffective	Low	Inconclusive imaging +

Pt	Sex	Age[1] (years)	Brain MRI + c	Spine MRI + c	CTM	LPOP	PoTS testing	EBP (n)	EBP outcome	Caff. inf. (n)	Caff. inf. outcome	ICPM results[2]	ICPM indication
									t				ineffective EBP
11	F	41	-ve	-ve	equiv.	normal infusion study	-ve a.s.t.	4	Ineffective	2	Ineffective	High	Inconclusive imaging + ineffective EBP
12	M	28	-ve	-ve	equiv.	normal infusion study	+ve tilt table	3	Ineffective	3	Ineffective	Normal/ Borderline	Inconclusive imaging + ineffective EBP
13	F	35	-ve	-ve	equiv.	normal	-ve a.s.t.	2	Ineffective	n.d.	n/a	Normal/ Borderline	Inconclusive imaging + ineffective EBP
14	M	40	-ve	-ve	-ve	normal	-ve a.s.t.	6	Ineffective	4	Ineffective	Normal/ Borderline	Inconclusive imaging + ineffective EBP
15	M	32	-ve	-ve	n.d.	n.d.	+ve tilt table	n.d.	n/a	n.d.	n/a	Normal/ Borderline	Inconclusive imaging

Pt	Sex	Age[1] (years)	Brain MRI + c	Spine MRI + c	CTM	LPOP	PoTS testing	EBP (n)	EBP outcome	Caff. inf. (n)	Caff. inf. outcome	ICPM results[2]	ICPM indication
16	F	50	-ve	-ve	n.d.	n.d.	-ve a.s.t.	2	Ineffective	2	Ineffective	Normal/ Borderline	Inconclusive imaging + ineffective EBP
17	F	44	-ve	-ve	equiv.	normal	-ve a.s.t.	3	Ineffective	3	Ineffective	Normal/ Borderline	Inconclusive imaging + ineffective EBP
18	F	79	-ve	-ve	n.d.	normal	-ve tilt table	1	Ineffective	3	Ineffective	Normal/ Borderline	Inconclusive imaging + ineffective EBP
19	F	43	-ve	-ve	n.d.	n.d.	-ve tilt table	1	Ineffective	n.d.	n/a	Normal/ Borderline	Inconclusive imaging + ineffective EBP
20	M	60	-ve	-ve	n.d.	normal	-ve a.s.t.	n.d.	n/a	n.d.	n/a	High	Inconclusive imaging + normal LPOP
21	F	58	-ve	-ve	equiv.	n.d.	+ve tilt	6	Ineffective	n.d.	n/a	Normal/ Borderlin	Inconclusive imaging +

Pt	Sex	Age[1] (years)	Brain MRI + c	Spine MRI + c	CTM	LPOP	PoTS testing	EBP (n)	EBP outcome	Caff. inf. (n)	Caff. inf. outcome	ICPM results[2]	ICPM indication
							table					e	ineffective EBP
22	M	26	-ve	-ve	-ve	normal infusion study	-ve a.s.t.	3	Partial improvement	2	Ineffective	Normal/ Borderline	Inconclusive imaging + ineffective EBP
23	M	17	-ve	-ve	n.d.	n.d.	+ve tilt table	n.d.	n/a	n.d.	n/a	Normal/ Borderline	Inconclusive imaging
24	F	33	-ve	equiv.	n.d.	n.d.	+ve tilt table	3	Ineffective	n.d.	n/a	Normal/ Borderline	Inconclusive imaging + ineffective EBP
25	M	47	-ve	n.d.	n.d.	n.d.	-ve a.s.t.	2	Transient improvement	n.d.	n/a	Normal/ Borderline	Inconclusive imaging + ineffective EBP
26	F	59	-ve	n.d.	-ve	normal	+ve tilt table	n.d.	n/a	2	Ineffective	Low	Inconclusive imaging + normal LPOP

Pt	Sex	Age[1] (years)	Brain MRI + c	Spine MRI + c	CTM	LPOP	PoTS testing	EBP (n)	EBP outcome	Caff. inf. (n)	Caff. inf. outcome	ICPM results[2]	ICPM indication
27	F	58	-ve	-ve	equiv.	n.d.	-ve a.s.t.	3	Ineffective	3	Ineffective	High	Inconclusive imaging + ineffective EBP
28	M	39	-ve	-ve	equiv.	normal	-ve a.s.t.	2	Ineffective	4	Ineffective	Normal/ Borderline	Inconclusive imaging + ineffective EBP
29	F	49	-ve	-ve	n.d.	n.d.	-ve a.s.t.	n.d.	n/a	n.d.	n/a	Normal/ Borderline	Inconclusive imaging
30	M	50	-ve	-ve	n.d.	normal	-ve a.s.t.	n.d.	n/a	n.d.	n/a	Normal/ Borderline	Inconclusive imaging + normal LPOP
31	F	26	-ve	-ve	n.d.	n.d.	-ve a.s.t.	3	Transient improvement	n.d.	n/a	Normal/ Borderline	Inconclusive imaging + ineffective EBP
32	M	58	-ve	-ve	n.d.	n.d.	-ve a.s.t.	2	Transient improvemen	n.d.	n/a	High	Inconclusive imaging +

Pt	Sex	Age[1] (years)	Brain MRI + c	Spine MRI + c	CTM	LPOP	PoTS testing	EBP (n)	EBP outcome	Caff. inf. (n)	Caff. inf. outcome	ICPM results[2]	ICPM indication
									t				ineffective EBP
33	F	17	-ve	-ve	n.d.	n.d.	-ve a.s.t.	5	Partial improvement	n.d.	n/a	Low	Inconclusive imaging + ineffective EBP
34	F	42	-ve	-ve	-ve	normal infusion study	-ve tilt table	3	Ineffective	3	Ineffective	High	Inconclusive imaging + ineffective EBP
35	F	39	-ve	-ve	n.d.	n.d.	-ve a.s.t.	n.d.	n/a	n.d.	n/a	Normal/ Borderline	Inconclusive imaging
36	F	54	-ve	equiv.	-ve	n.d.	+ve tilt table	n.d.	n/a	n.d.	n/a	Normal/ Borderline	Inconclusive imaging
37	F	27	-ve	n.d.	n.d.	n.d.	+ve tilt table	n.d.	n/a	n.d.	n/a	Normal/ Borderline	Inconclusive imaging

Pt	Sex	Age[1] (years)	Brain MRI + c	Spine MRI + c	CTM	LPOP	PoTS testing	EBP (n)	EBP outcome	Caff. inf. (n)	Caff. inf. outcome	ICPM results[2]	ICPM indication
38	F	29	-ve	-ve	-ve	n.d.	-ve a.s.t.	6	Transient improvement	5	Ineffective	Normal/ Borderline	Inconclusive imaging + ineffective EBP

[1]Age at the time of onset of orthostatic headache

[2]Low: daytime ICP < -2.27 mmHg and night-time ICP < 2.85 mmHg; High: daytime ICP > 2.05 mmHg and night-time ICP > 9.78 mmHg.

-ve: negative; +ve: positive, a.s.t.: Active Stand Test; Caff. Inf.: Caffeine Infusion; CTM: CT Myelogram, EBP: Epidural Blood Patch; ICPM: Intracranial Pressure monitoring; LPOP: Lumbar Puncture Opening Pressure; n/a: Not Applicable; n.d.: Not Done; PoTS: Postural Tachycardia Syndrome.

4.4.3. ICP monitoring results

The median 24-hour ICP monitoring results ranged from -4.1 mmHg to +12.5 mmHg. According to the prespecified criteria for low and high ICP monitoring results (see 4.3.5), 3 patients had low ICP (8%) and 6 patients had high ICP (16%). The remaining 29 patients did not meet the prespecified criteria for low or high pressure (76%). Figure 4-2**,** Figure 4-3 and Figure 4-4 display the 24-hour, daytime and night-time median ICP results of the patients stratified by ICP monitoring results (low, high and normal/borderline ICP groups).

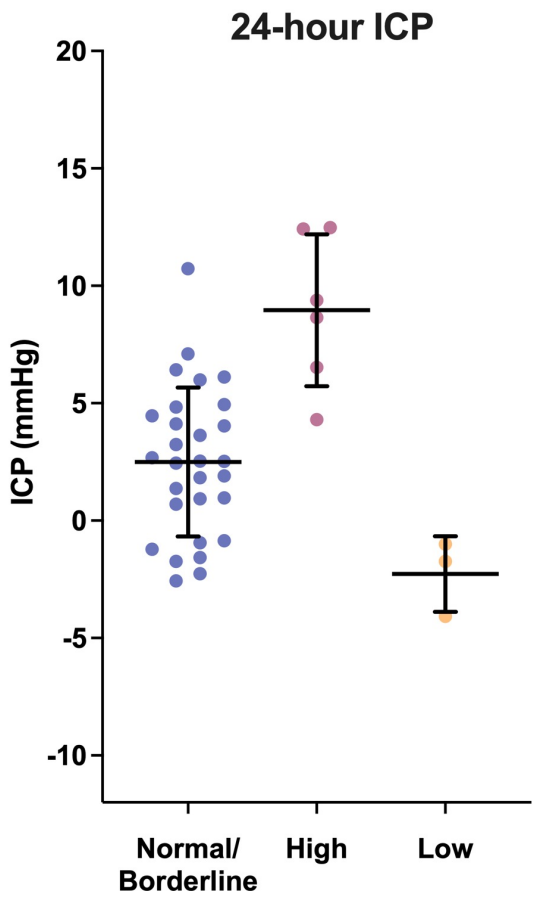


Figure 4-2: Median 24-hour Intracranial Pressure (ICP) stratified by group (normal/borderline, high or low ICP). Means and standard deviations are displayed.

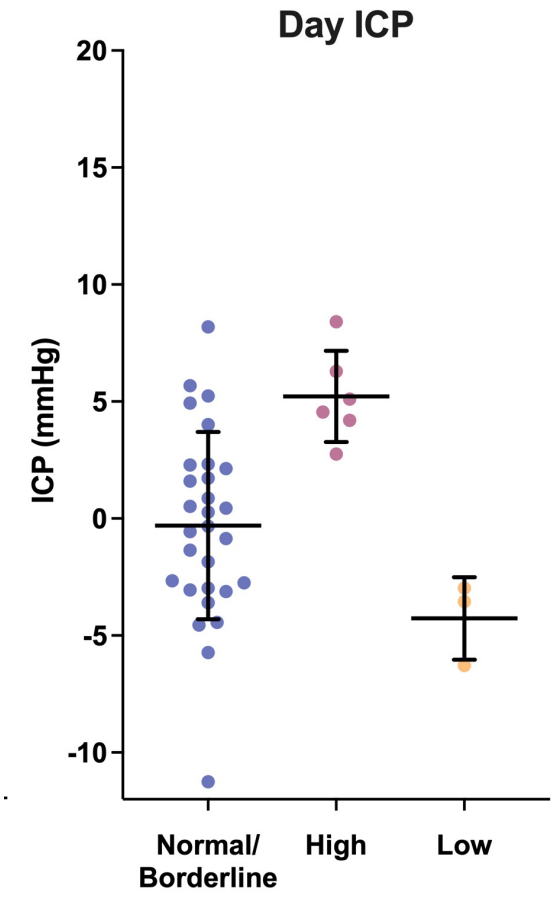


Figure 4-3: Median Day Intracranial Pressure (ICP) stratified by group (normal/borderline, high or low ICP). Means and standard deviations are displayed.

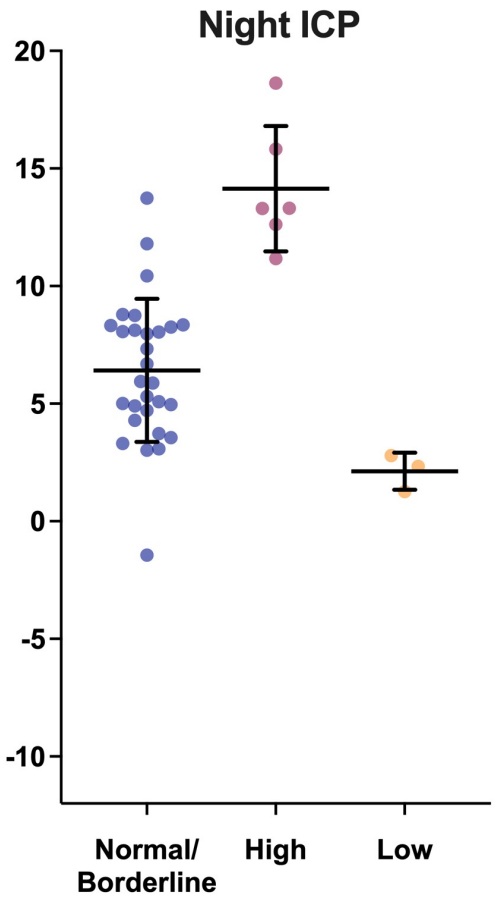


Figure 4-4: Median Night Intracranial Pressure (ICP) stratified by group (normal/borderline, high or low ICP). Means and standard deviations are displayed.

The clinical presentation and headache phenotype did not differ across the 3 groups, except for the presence of aural fullness or muffled hearing that were more common in patients with abnormal ICP results rather than normal/borderline ICP results (67% and 17% respectively, Fisher's exact test p=0.015, Table 4-3).

As expected, 24-hour, daytime and night-time mean ICPs were significantly higher in patients with high ICP and significantly lower in patients with low ICP (Kruskal-Wallis H Test $p<0.01$ in all analyses, Table 4-3). In addition, the proportion of time spent in negative ICP territories was significantly lower for patients with high ICP and significantly higher in patients with low ICP (Kruskal-Wallis H Test $p<0.01$ in all analyses, Table 4-3). The mean pulse amplitude of the patients in the three groups did not significantly differ (Table 4-3).

The six patients with high ICP did not have any ophthalmic sign of intracranial hypertension on clinical examination. Of these six patients with high ICP results, five were treated with insertion of a CSF diversion shunt and one was managed medically with acetazolamide. Two of the patients treated with CSF diversion shunts benefited from surgery and their headaches are currently well controlled. One patient treated with CSF diversion shunt reported ongoing headaches with improved intensity. The remaining three patients, who had high ICP results, have persistent headaches despite treatment. Of the three patients with low ICP results, one died of unrelated causes and two have ongoing orthostatic headache and are waiting for further specialist opinion.

There were no complications from the ICP monitoring procedure for any of the patients.

Table 4-3: Clinical presentation and investigation findings of patients with orthostatic headache stratified by intracranial pressure monitoring results

Variables	Normal/ Borderline ICP (N=29)	High ICP (N=6)	Low ICP (N=3)	P values
Age in years, mean (SD)	40 (13)	49 (11)	40 (21)	0.31
Female, n (%)	18 (62%)	4 (67%)	3 (100%)	0.61
Ehler Danlos and/or hypermobile, n (%)	10 (35%)	2 (33%)	2 (67%)	0.62
PoTS, n (%)	7 (24%)	1 (17%)	1 (33%)	1
Other headache diagnosis, n (%)	20 (69%)	4 (67%)	3 (100%)	0.69
Duration of symptoms in months, mean (SD)	46 (35)	25 (16)	88 (53)	0.08
Occipital pain, n (%)	17 (59%)	3 (50%)	1 (33%)	0.74
Associated with tinnitus, n (%)	7 (24%)	1 (17%)	1 (33%)	1
Associated with aural fullness/muffled hearing, n (%)	5 (17%)	4 (67%)	2 (67%)	**0.015***
Triggered by Valsalva, n (%)	14 (48%)	3 (50%)	3 (100%)	0.37
VRS in upright posture, mean (SD)	7 (1)	8 (1)	8 (1)	0.61
VRS difference (upright minus supine), mean (SD)	5 (2)	6 (2)	6 (2)	0.94
24-hour ICP in mmHg, mean (SD)	3 (3)	9 (3)	-2 (2)	**< 0.01***

Variables	Normal/ Borderline ICP (N=29)	High ICP (N=6)	Low ICP (N=3)	P values
Day ICP in mmHg, mean (SD)	0 (4)	5 (2)	-4 (2)	**<0.01***
Night ICP in mmHg, mean (SD)	6 (3)	14 (3)	2 (1)	**< 0.01***
ICP difference (night minus day) in mmHg, mean (SD)	7 (5)	9 (2)	6 (3)	0.41
24-hour PA in mmHg, mean (SD)	4 (1)	5 (1)	4 (1)	0.22
Day PA in mmHg, mean (SD)	5 (1)	5 (2)	4 (1)	0.12
Night PA in mmHg, mean SD	3 (1)	5 (2)	3 (1)	0.10
Proportion of time spent in negative ICP territories, mean of time % (SD)	34 (18)	9 (9)	59 (3)	**< 0.01***
Proportion of daytime spent in negative ICP territories, mean of time % (SD)	53 (28)	12 (10)	84 (5)	**< 0.01***
Proportion of night-time spent in negative ICP territories, mean of time % (SD)	3 (10)	0 (0)	15 (16)	**< 0.01***

P values: Kruskal-Wallis H Test for continuous variables and Fisher's exact test for categorical variables.

ICP: Intracranial Pressure; PA: Pulse Amplitude; PoTS: Postural Tachycardia Syndrome; SD: Standard Deviations; VRS: Verbal Reporting Scale

4.5. Discussion

In this single-centre observational study ICP monitoring of patients with clinically suspected SIH identified 8% of patients with low ICP and 16% of patients with pathologically high ICP. These results demonstrate that some patients with orthostatic headache, equivocal investigation findings and not responsive to epidural blood patches have a CSF dynamics disorder that can be identified through ICP monitoring. As suggested in previously published case reports, this study provides evidence on the potential utility of ICP monitoring in well selected cases of suspected SIH (Zada *et al.*, 2007; Jensen *et al.*, 2021). Interestingly, these results also demonstrate that orthostatic headache can be misleading and represent the paradoxical presentation for a high ICP state. The presence of aural fullness or muffled hearing was significantly more common in patients with abnormal CSF dynamics (high or low ICP) than patients with normal/borderline ICP results (Fisher's exact test p=0.015, Table 4-3). There were no reliable clinical predictors of low ICP results (Table 4-3).

There are limited reports on the use of ICP monitoring in patients with low CSF pressure/volume syndrome. Two previous case reports discussed the utility of ICP monitoring to confirm the diagnosis of SIH and to monitor the efficacy of epidural blood patch treatment (Zada *et al.*, 2007; Jensen *et al.*, 2021). On the other hand, Fichtner *et al.* could not detect any ICP increase after epidural blood patch using a subdural ICP monitor and hypothesised that a rise in ICP may not be the therapeutic mechanism of epidural blood

patches (Fichtner *et al.*, 2012). Eide *et al.* performed ICP monitoring in patients with low CSF pressure/volume syndrome (only 4 were SIH patients) and found that morphological changes of the ICP pulse waveform only occur when ICP falls below -15 mmHg (Eide *et al.*, 2012). The patients with low ICP in our study had mean ICPs above this threshold and this may be the reason why we did not identify significant differences in pulse amplitude among the 3 ICP groups (Table 4-3). Lumbar infusion studies have provided useful insights in the CSF dynamics of patients with confirmed CSF leaks, it is interesting to note how the abnormalities in CSF dynamics tend to become less evident in the chronic stages of the disease (Beck *et al.*, 2017; Häni *et al.*, 2020).

Similarly to our study, Kranz *et al.* found high CSF pressures in some patients with a diagnosis of SIH (Kranz *et al.*, 2016b). The study by Kranz *et al.* investigated the lumbar puncture opening pressures of 106 patients with a diagnosis of SIH and reported that 5% of them had a CSF opening pressure above 20 cm H_2O (Kranz *et al.*, 2016b). Our results are also in keeping with a study by Craven *et al.*, demonstrating that high ICP state can be the cause of persistent CSF leaks after spinal surgery (Craven *et al.*, 2016a). Of course, the different populations included in these studies have to be taken into account, but we also found that patients with spontaneous onset of orthostatic headache can sometimes have an underlying high ICP state (Craven *et al.*, 2016a; Kranz *et al.*, 2016b).

The main limitations of this study are the relatively small cohort and the retrospective design. ICP monitoring is an invasive procedure and should only be offered to selected patients for whom all other less invasive investigations have been inconclusive. While small, this case series is the largest study describing ICP monitoring results in patients with suspected SIH to date. Despite the retrospective design, the standardised screening process and the systematic structure of both clinical letters and ICP monitoring protocol, reduced the risk of selection, detection and reporting biases. Another important limitation is the scarce knowledge on normal ICP ranges, it would be unethical to perform ICP monitoring in healthy volunteers and in this context the systematic review and meta-analysis by Norager *et al.* currently provides the best evidence on normal ICP ranges (Norager *et al.*, 2021). We have used this evidence to classify the ICP monitoring results in this study objectively, but we are unable to exclude that some patients classified as having normal ICP should actually be considered having borderline high or low ICP results.

In more recent years, a better understanding of SIH has led to the discovery of CSF-venous fistulas as the cause of some cases of SIH (Schievink *et al.*, 2014b; Kranz *et al.*, 2021). CSF-venous fistulas do not cause obvious collection of CSF in the epidural space and their identification with traditional spinal imaging techniques can be challenging. Dynamic CT myelography or digital subtraction myelography (DSM) with lateral decubitus views can be useful in the identification of CSF-venous fistulas, though these techniques

are not widely available. The patients included in this study have been investigated for SIH prior to the availability of these specialised spinal imaging techniques at our centre. A limitation of this work is the poor diagnostic yield for the identification of CSF-venous fistulas of the spinal imaging used in the study (spinal MRI with intravenous contrast and CTM). Future studies should investigate for the presence of CSF-venous fistulas with dedicated spinal imaging before ICP monitoring is employed.

We found 3 patients in the normal ICP group who had signs of SIH on brain imaging. It is possible, as previously described by Beck *et al.*, that the CSF dynamics abnormalities of these patients may have become less apparent due to the long duration of the disease (Beck *et al.*, 2017).

Lumbar puncture opening pressure is often tested when SIH is suspected, but this investigation can be misleading. Whilst low CSF opening pressures are suggestive of SIH, normal or high CSF opening pressures do not allow to exclude this diagnosis (see 3.4.4.5 and 3.5.3). A retrospective study by *Kranz et al.*, demonstrated that there is poor correlation between CSF opening pressures and individual imaging signs of SIH (Kranz *et al.*, 2016c). Mokri *et al.* also described the cases of patients with confirmed CSF leaks and consistently normal lumbar puncture opening pressures (Mokri *et al.*, 1998). These studies emphasise the fact that a diagnosis of SIH cannot be based solely on the results of a lumbar puncture (Mokri *et al.*, 1998; Kranz *et al.*, 2016c). This is also supported by the results of our study in which three

of the patients who had normal CSF opening pressures, had abnormal ICP monitoring results (2 low ICP and 1 high ICP) (see Table 4-2). As previously discussed, lumbar punctures should be undertaken with caution bearing in mind that the sensitivity of this investigation is modest and there is a risk of worsening SIH (see 3.5.3 and 3.5.5). However, if a lumbar puncture is performed at the time of a myelogram, a low opening pressure would be highly suggestive of SIH, in these cases ICP monitoring would be unnecessarily risky.

On the basis of this study, ICP can be useful for the investigation of some patients with orthostatic headache, however these patients should be carefully selected. In all cases, the potential benefits of performing ICP monitoring should outweigh the possible risks. In addition, the following criteria for the employment of ICP monitoring are suggested:

(i) strong clinical suspicion for SIH,

(ii) inconclusive or normal brain imaging (brain MRI with contrast),

(iii) inconclusive or normal spinal imaging dedicated to the identification of possible epidural fluid collections (e.g., whole spine MRI with contrast, and dynamic CTM or DSM),

(iv) inconclusive or normal spinal imaging dedicated to the identification of CSF-venous fistulas (e.g., dynamic CTM or DSM with lateral decubitus views),

(v) inconclusive or normal lumbar puncture opening pressures, if this investigation is performed in the context of myelography (or for other diagnostic reasons),

(vi) exclusion of other potential causes of orthostatic headaches including PoTS, cervicogenic headaches, primary new daily persistent headaches and craniocervical instability.

4.6. Conclusions

Patients with a clinical picture strongly suggestive of SIH and uncertain or equivocal investigation findings can benefit from the use of invasive ICP monitoring provided the patients are carefully selected.

In this study we provide evidence that ICP monitoring in this group of patients can allow confirmation of a low CSF pressure state in 8% of the patients and exclude an obvious CSF dynamics abnormality in 76% of the patients. Importantly, this study also demonstrates that 16% of patients with suspected SIH, elusive CSF leaks and uncertain investigation findings actually suffer a high CSF pressure state and should be treated accordingly. Finally, ICP monitoring was a safe procedure with no complications in this cohort.

Chapter 5. Effect of position on intracranial pressure and brain compliance

5.1. Abstract

5.1.1. Background

A better understanding of the effect of position on ICP and compliance is important for the development of treatment strategies that can restore the normal CSF dynamics. There is limited knowledge of the effect of position on intracranial compliance. In this cross-sectional study we tested the association of pulse amplitude with position and day/night cycle. Additionally, we describe the postural ICP and pulse amplitude changes of patients with 'normal' ICP dynamics.

5.1.2. Methods

This single-centre retrospective study included patients with suspected/confirmed CSF dynamics abnormalities who were investigated with elective 24-hour ICP monitoring between October 2017 and September 2019. Patients were enrolled in a short exercise battery including four positions: supine, lumbar puncture position in left lateral decubitus, sitting and standing. Each position was maintained for two minutes. The mean ICP and pulse amplitude were calculated for each position. Twenty-four-hour, day and night median ICP and pulse amplitude data were also collected. Linear regression models were used to test the correlation of pulse amplitude with position and day/night cycle. All linear regressions were corrected for

confounders. The postural ICP monitoring results of patients without obvious ICP dynamic abnormality were summarised.

5.1.3. Results

One hundred and one patients (24 males and 77 females) with a mean age of 39 years (SD ±13), were included in the study. The adjusted linear regression models demonstrated a significant association of ICP with position and day/night cycle, resulting in upright (sitting and standing) and day ICP being lower than supine/night ICP values. The adjusted linear regression model was also significant for the association of pulse amplitude with position and day/night cycle, resulting in upright and day pulse amplitude being higher than supine/night pulse amplitude results. These associations were confirmed for patients with and without shunts. There was a tendency for patients without any clear ICP dynamics abnormality to have tighter control of these postural ICP changes compared to the other patients, however, the difference between groups was not statistically significant.

5.1.4. Conclusions

This is the largest study investigating the effect of postural changes on intracranial compliance. The results of this study suggest that pulse amplitude (as well as ICP) is significantly associated with posture, increasing in upright positions compared to supine. Further studies will be needed to investigate the mechanism behind this association.

5.2. Introduction

In recent years, ICP monitoring has gained an important role in the diagnosis and treatment of patients affected by chronic cerebrospinal fluid (CSF) dynamics disturbances as, for example, normal pressure hydrocephalus (NPH), idiopathic intracranial hypertension (IIH), Chiari malformation I and various forms of hydrocephalus (Evensen and Eide, 2020). Compared to patients in the acute setting, patients with chronic CSF dynamics disorders are most commonly mobile and provide the unique opportunity to study the changes of ICP and pulse amplitude in different body positions.

Most studies on ICP monitoring describe ICP in the supine position, even though humans spend most of their time in an upright posture. A better insight into the effect of position on ICP and compliance is important for several reasons. First of all, compared to other fields, the available knowledge on ICP physiology is limited and this is probably due to the invasive nature of the investigations needed to measure this important physiological parameter. More importantly, our treatments may not be able to restore the physiological CSF dynamics until we know how they work. Previous studies have demonstrated that ICP is lower in upright position compared to supine (Magnaes, 1976a; Qvarlander *et al.*, 2013; Farahmand *et al.*, 2014; Andresen *et al.*, 2015; Petersen *et al.*, 2016; Holmlund *et al.*, 2018). A better understanding of the effect of position on ICP dynamics could also allow the improvement of CSF shunt technologies towards the creation of the long-awaited ‘smart shunt system’ (Lutz *et al.*, 2013).

Intracranial compliance is the ability of the intracranial compartment to accommodate an increase in volume without a large increase in ICP. Pulse amplitude (the difference between systolic and diastolic ICP) is considered a reliable indirect marker of compliance: the higher the pulse amplitude, the lower the brain compliance. Intracranial compliance is recognised to be a very useful marker in clinical practice (Evensen and Eide, 2020), however, the effect of position on markers of intracranial compliance is not clear. For example, Farahmand *et al.* noticed slightly higher ICP waveform amplitude (indicating lower brain compliance) in the upright posture compared to supine posture (Farahmand *et al.*, 2014). In contrast, Raabe *et al.* analysed markers of intracranial compliance in 13 patients with intraventricular sensors and concluded that different levels of head-up tilts do not affect intracranial compliance (Raabe *et al.*, 1999). Non-invasive studies using MRI imaging or mathematical models have concluded that brain compliance is increased in the upright position compared to supine (Alperin *et al.*, 2005b; Gehlen *et al.*, 2017).

The intracranial compliance model proposed by Marmarou in 1975, demonstrates that higher ICP levels correspond to lower intracranial compliance (Marmarou *et al.*, 1975). Since supine position is associated with higher ICP levels, we hypothesised that intracranial compliance would be reduced in this position compared to upright posture. The specific aims of this cross-sectional study were:

1. to test the hypothesis that pulse amplitude (as a marker of intracranial compliance) is correlated to body position;

2. to test the hypothesis that pulse amplitude is correlated to the day/night cycle, since night ICP is recorded in supine position, while day ICP is mostly measured in an upright position;

3. to describe the mean ICP and pulse amplitude in different body positions for patients considered to have 'near-normal' ICP dynamics based on a post-hoc analysis.

5.3. Methods

This is a single centre cross-sectional study conducted at the National Hospital for Neurology and Neurosurgery (NHNN, London, UK) between October 2017 and September 2019. This study has been approved by the North East-Newcastle & North Tyneside 2 Research Ethics Committee and the Health Research Authority (20/NE/0127). Due to the study design (retrospective analysis) written consent was waived.

Patients with suspected or confirmed CSF dynamics disturbances (e.g., IIH, CSF leaks, hydrocephalus, Chiari malformation I) who underwent elective ICP monitoring were included if meeting the following eligibility criteria: (i) complete 24-hour ICP monitoring data available, (ii) ICP monitoring performed through intraparenchymal sensor (non-telemetric) and (iii) completion of short exercise battery during ICP monitoring period under the

supervision of one of the authors (L. D'Antona). Patients were identified through screening of the local clinical ICP monitoring database.

5.3.1. ICP monitoring method

In our institution, patients are considered for ICP monitoring only when affected by signs and symptoms consistent with altered CSF dynamics, in whom other less invasive or non-invasive investigation methods were inconclusive. The clinical indication for elective 24-hour ICP monitoring was agreed by a multidisciplinary team including neurosurgeons, neurologists and ophthalmologists. These multidisciplinary discussions occurred on a case-by-case basis. An intraparenchymal ICP probe was inserted in the operating theatre, under sedation or local anaesthesia, in the right frontal area. One of the following two types of ICP probes was chosen depending on the surgeon's preference: Spiegelberg parenchymal probe with cranial bolt (Spiegelberg GmbH & Co KG, Hamburg, Germany) or Raumedic Neurovent-P (Raumedic AG, Helmbrechts, Germany). The monitoring was performed for a period of 24 hours (Thompson *et al.*, 2017a). In order to match their usual level of activity, patients were encouraged to sit, stand and walk during the daytime and rest supine in bed overnight. Raw ICP data was collected through a bedside monitor at a sampling frequency of 100 Hz and then analysed through the ICM+ software (University of Cambridge Enterprise Ltd). The final ICP monitoring results are summarised as median ICP and median pulse amplitude over 24 hours, day (12:00 - 18:00) and night (00:00 - 06:00). The pulse amplitude is used as a marker of brain compliance

(Wagshul *et al.*, 2011). Further details of this ICP monitoring method have been described in Chapter 2.

5.3.2. Short exercise battery

During the 24-hour ICP monitoring period, the patients underwent a short exercise battery under clinical supervision. The patients were asked to assume the following 4 positions: (i) supine in bed (with one pillow under the head), (ii) lumbar puncture position in lateral decubitus (lying on the left side with flexed hips and knees and one pillow under the head), (iii) sitting at the edge of the bed, (iv) standing. Start and stop times for each position were marked using the ICP monitor time stamp (hh:mm:ss format). The data collection was performed in these positions in the described order and each of these positions was maintained for 2 minutes once the ICP steady state was confirmed. Stabilisation of the ICP in each position was sought and ascertained through the direct observation of the ICP trace on the bedside monitor. Recordings were discarded and repeated if the patient coughed, sneezed or talked during the exercise battery. Two-minute mean ICP and pulse amplitude for each of the positions was calculated.

5.3.3. Variables

Information on the patients' demographic characteristics, indications for ICP monitoring and previous treatments (e.g., presence and components of a CSF diversion shunt) was retrospectively retrieved. The following ICP monitoring results were recorded: median ICP and pulse amplitude (24-hour,

day and night), mean 2-minute ICP and pulse amplitude during each of the 4 exercise battery positions. All ICP and pulse amplitude values are expressed in mmHg.

5.3.4. Statistical analysis

Considering the structural differences between Spiegelberg and Raumedic ICP sensors, all results were stratified by type of sensor. Linear regression models were used to test the effect of position (independent variable) on mean pulse amplitude and ICP (dependent variables). Additionally, linear regression models were used to test the effect of the day/night cycle (independent variable) on median pulse amplitude and ICP (dependent variables). All analyses were stratified by type of sensor and also adjusted for the following confounding variables: age, sex, patient identification number, indication for ICP monitoring and ICP/pulse amplitude. Separate regression models were built for patients with pre-existing CSF diversion shunts at the time of ICP monitoring.

Patients were further categorised into one of three subgroups for further analysis: (a) ‘normal’ ICP monitoring results, (b) ‘abnormal’ ICP monitoring results, and (c) ‘shunted’ patients (grouped separately regardless of their ICP monitoring results). The ‘normal’ group included non-shunted patients complaining of intractable headaches who were suspected to have CSF dynamics abnormalities (e.g., IIH), but did not present any evident abnormality in their ICP monitoring results and did not proceed to further

neurosurgical input. The ‘abnormal’ group consisted of non-shunted patients considered to have abnormal ICP monitoring results requiring treatment or further neurosurgical investigations. The ‘shunt’ group consisted of patients with a CSF diversion shunt at the time of ICP monitoring. Interpretation of the ICP monitoring results and management decisions were conducted by the multidisciplinary team who were not aware of the results of the exercise battery. The parameters used to interpret the ICP monitoring results included median ICP (over 24 hours, during the day and night), median PA (over 24 hours, during the day and night), peak/trough ICP, number of ICP spikes above 25 mmHg, percentage of time the ICP was negative or above 15 mmHg, ICP frequency distribution histogram and Pearson coefficient of correlation between ICP/PA. These parameters were used to establish whether CSF dynamics abnormalities were present and make decisions on optimal management methods (e.g., surgical treatment, shunt setting adjustment).

Due to the exploratory nature of the study a formal sample size calculation was not performed, and all eligible patients were included in the study. Continuous variables were summarised as means (standard deviation) and categorical variables as percentages. A significance level 0.05 was used. Microsoft® Excel for Mac (version 16.25), Stata© (version 15.0) and GraphPad Prism for macOS (version 8.4.1) were used for the data collection and statistical analysis.

5.4. Results

Between October 2017 and September 2019, 264 patients underwent elective ICP monitoring at the NHNN. Of these, 101 met the eligibility criteria and were included in the study. Table 5-1 describes the patients' baseline characteristics and the clinical indications for ICP monitoring.

Table 5-1: Patients' characteristics and underlying diagnoses.

Sex	**N (%)**
- Male	24 (24)
- Female	77 (76)
Age (years)	**Mean (SD)**
	39 (13)
Underlying diagnosis at the time of ICP monitoring	**N (%)**
- Diagnosis not yet established	33 (32)
- Hydrocephalus	32 (32)
- Chiari malformation	19 (19)
- Idiopathic Intracranial Hypertension	17 (17)
CSF diversion shunt	**N (%)**
- No shunt	68 (67)
- Ventriculoperitoneal shunt	28 (28)
- Lumboperitoneal shunt	3 (3)
- Other type of shunt	2 (2)
Shunt valve	**N (%)**
- Miethke pro-GAV	12 (37)
- Fixed pressure valve	7 (21)
- Medtronic Strata	5 (15)
- Miethke pro-GAV and pro-SA	3 (9)
- Sophysa Polaris	2 (6)
- Valveless shunt	2 (6)

- Codman Certas	1 (3)
- Codman Hakim	1 (3)
Type of ICP monitor	**N (%)**
- Spiegelberg	61 (60)
- Raumedic Neurovent P	40 (40)
ICP: Intracranial Pressure	

5.4.1. Effect of position on ICP

An example of the ICP monitoring recording during the short exercise battery is displayed in Figure 5-1.

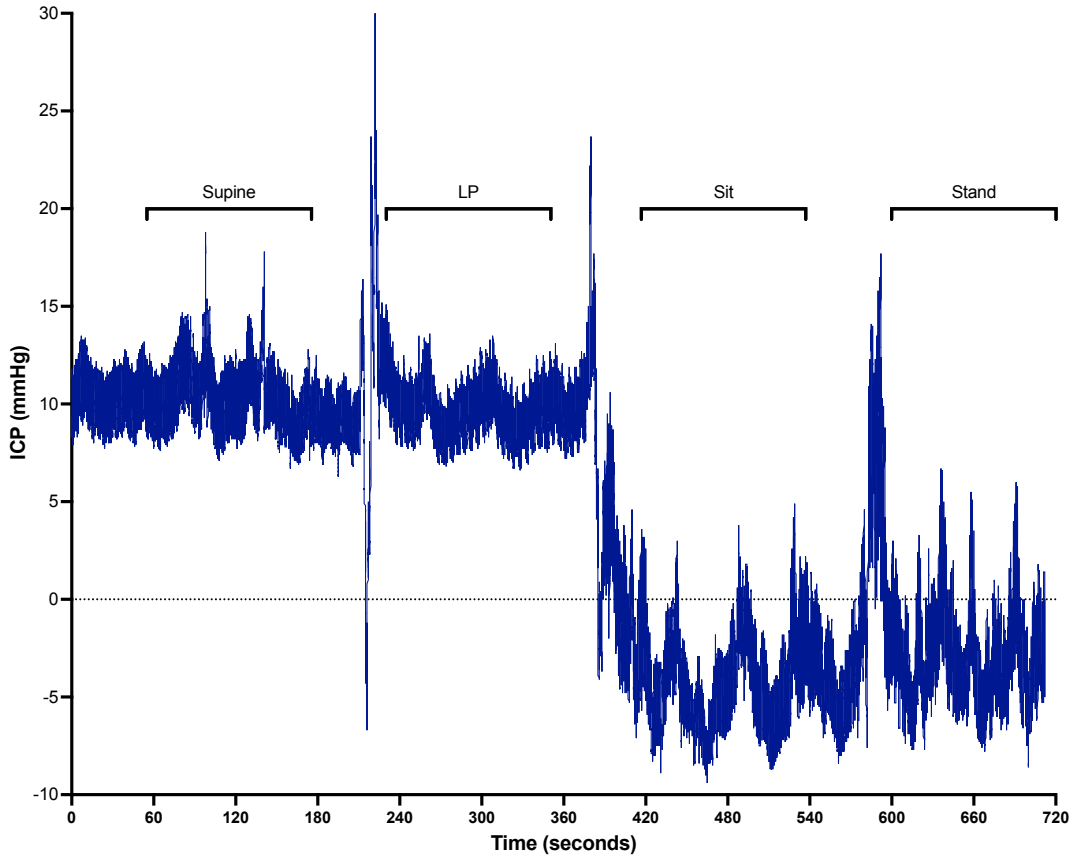


Figure 5-1: Example of intracranial pressure (ICP) monitoring recording during the short exercise battery.100 Hz raw ICP measurements are displayed.

Table 5-2 summarises the 24-hour and exercise battery ICP monitoring results for the 68 patients without shunts. Table 5-3 shows the ICP monitoring results for the 33 patients with CSF diversion shunts.

Table 5-2: Twenty-four-hour and exercise battery intracranial pressure (ICP) monitoring results stratified by type of monitor in patients without shunts

	All (n=68)	Spiegelberg (n=41)	Raumedic (n=27)
24-hour ICP monitoring results, mean (SD)			
24-hour ICP	6.9 (7.1)	4.6 (6.3)	10.4 (6.8)
24-hour PA	5.9 (2.7)	5.5 (2)	6.5 (3.4)
Day[1] ICP	4.3 (7.1)	2.1 (6.3)	7.7 (6.8)
Day PA	6.3 (2.6)	5.8 (2)	6.9 (3.1)
Night[2] ICP	10.4 (7.2)	7.7 (5.9)	14.5 (7.2)
Night PA	5.4 (2.9)	5.1 (2.1)	5.9 (3.7)
Exercise battery ICP monitoring results, mean (SD)			
Supine ICP	11.2 (6.9)	8.8 (5.7)	14.7 (7.2)
Supine PA	6.4 (3.1)	5.9 (2.8)	7.1 (3.6)
LP position ICP	14.9 (8.9)	12.5 (8.1)	18.5 (9)
LP position PA	7 (3.5)	6.9 (3.7)	7.3 (3.3)
Sitting ICP	2.6 (8.7)	-0.3 (8)	6.9 (8)
Sitting PA	7.5 (3.9)	7.5 (3.9)	7.6 (4)
Standing ICP	2 (7.3)	-0.9 (6.6)	6.3 (6.3)
Standing PA	7 (2.8)	6.8 (2.6)	7.2 (3.2)
ICP and PA differences, mean (SD)			
Night ICP minus day ICP	6.1 (4.6)	5.6 (4.7)	6.8 (4.2)

Night PA minus day PA	-0.8 (1.2)	-0.7 (1.2)	-1 (1.3)
LP position minus supine ICP	3.8 (4.2)	3.7 (4.7)	3.8 (3.5)
LP position minus supine PA	0.6 (3)	0.9 (3.6)	0.1 (1.7)
Sitting minus supine ICP	-8.6 (4.8)	-9.1 (4.9)	-7.8 (4.6)
Sitting minus supine PA	1.1 (2.6)	1.5 (2.9)	0.4 (2)
Standing minus supine ICP	-9.3 (4.6)	-10 (4.5)	-8.4 (4.7)
Standing minus supine PA	0.5 (2.1)	0.8 (2.2)	0.1 (2.0)

ICP: Intracranial Pressure, LP: Lumbar Puncture, PA: Pulse Amplitude, SD: Standard Deviation

[1]Day ICP/PA= median ICP/PA between 12:00 and 18:00 hours

[2]Night ICP/PA= median ICP/PA between 00:00 and 06:00 hours

Table 5-3: Twenty-four-hour and exercise battery intracranial pressure (ICP) monitoring results stratified by type of monitor in patients with CSF diversion shunts

	All (n=33)	Spiegelberg (n=20)	Raumedic (n=13)
24-hour ICP monitoring results, mean (SD)			
24-hour ICP	2.7 (4.6)	2.4 (3.0)	3.2 (6.3)
24-hour PA	4.3 (1.8)	3.9 (1.3)	4.8 (2.2)
Day[1] ICP	-0.3 (5.2)	-1.1 (4.1)	0.8 (6.5)
Day PA	4.9 (2.5)	4.2 (1.2)	6.0 (3.4)
Night[2] ICP	5.5 (5.6)	3.7 (3.5)	8.3 (7.0)
Night PA	4.1 (2.2)	3.6 (1.2)	4.7 (3.0)
Exercise battery ICP monitoring results, mean (SD)			
Supine ICP	7.4 (6.0)	7.6 (5.2)	7.0 (7.0)
Supine PA	5.1 (2.0)	5.1 (2.0)	5.1 (2.0)
LP position ICP	12.2 (7.6)	12.0 (7.0)	12.6 (8.5)
LP position PA	5.9 (2.7)	5.4 (1.9)	6.5 (3.5)
Sitting ICP	-3.3 (5.9)	-4.4 (5.0)	-1.5 (6.8)
Sitting PA	5.8 (2.1)	6.2 (1.8)	5.4 (2.3)
Standing ICP	-4.8 (6.0)	-6.3 (5.2)	-2.6 (6.4)
Standing PA	5.4 (1.9)	5.5 (2.0)	5.2 (1.6)
ICP and PA differences, mean (SD)			
Night ICP minus day ICP	5.8 (4.6)	4.8 (4.0)	7.5 (4.9)

Night PA minus day PA	-0.9 (2.3)	-0.6 (0.9)	-1.3 (3.4)
LP position minus supine ICP	4.9 (4.0)	4.4 (4.6)	5.6 (2.5)
LP position minus supine PA	0.7 (2.4)	0.3 (2.4)	1.4 (2.2)
Sitting minus supine ICP	-10.6 (4.9)	-12.0 (4.7)	-8.5 (4.4)
Sitting minus supine PA	0.7 (1.9)	1.0 (2.2)	0.2 (1.4)
Standing minus supine ICP	-12.2 (4.7)	-13.9 (3.6)	-9.6 (4.9)
Standing minus supine PA	0.2 (2.2)	0.4 (2.6)	0.1 (1.5)

ICP: Intracranial Pressure, LP: Lumbar Puncture, PA: Pulse Amplitude, SD: Standard Deviation

[1]Day ICP/PA= median ICP/PA between 12:00 and 18:00 hours

[2]Night ICP/PA= median ICP/PA between 00:00 and 06:00 hours

Compared to supine position, patients had a higher ICP in lumbar puncture position (average difference 3.8±4.2 mmHg for patients without shunts and 4.9±4 mmHg for patients with shunts), a lower ICP in sitting position (average difference -8.6±4.8 mmHg for patients without shunts and -3.3±5.9 for patients with shunts) and a lower ICP in standing position (average difference -9.3±4.6 mmHg for patients without shunts and -12.2±4.7 mmHg for patients with shunts) (Figure 5-2 A and B).

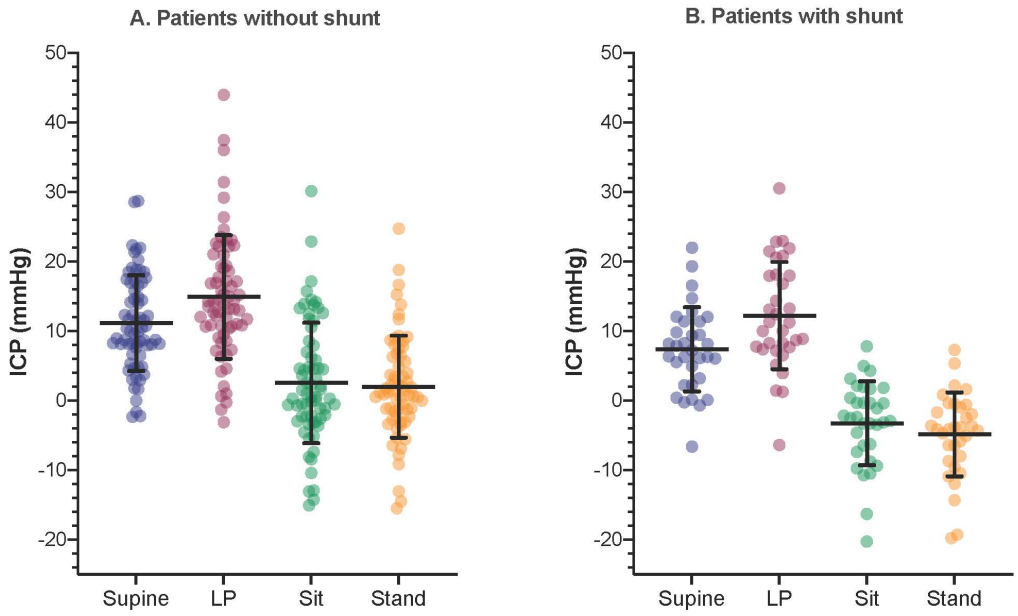


Figure 5-2: Mean intracranial pressure (ICP) with standard deviations in different body positions stratified by shunt presence.

In patients without shunts, the unadjusted linear regression models demonstrated a significant correlation between ICP (dependent variable) and all body positions (independent variable) with both Raumedic (adjusted R^2=0.3, F(3,104)=16.5, p<0.05) and Spiegelberg (adjusted R^2=0.39, F(3,159), p<0.05) ICP monitors. This correlation remained statistically significant in the adjusted multiple regression models (p<0.05 for all positions for both Raumedic and Spiegelberg ICP monitors).

Also for patients with shunts, the unadjusted linear regression models confirmed a significant association between ICP and all body positions with both Raumedic (adjusted R^2=0.4, F(3,48)=12.1, p<0.05) and Spiegelberg ICP monitors (adjusted R^2=0.6, F(3,76)=48.2, p<0.05). The adjusted linear

regression models for patients with shunts also confirmed a significant association between ICP and position ($p<0.05$ for all positions for both Raumedic and Spiegelberg ICP monitors).

A curve of best fit analysis suggests that at extremely low ICP levels (<-10 mmHg), pulse amplitude tends to slightly increase, a situation that most commonly occurs when the patient is in a sitting or standing posture (Figure 5-3).

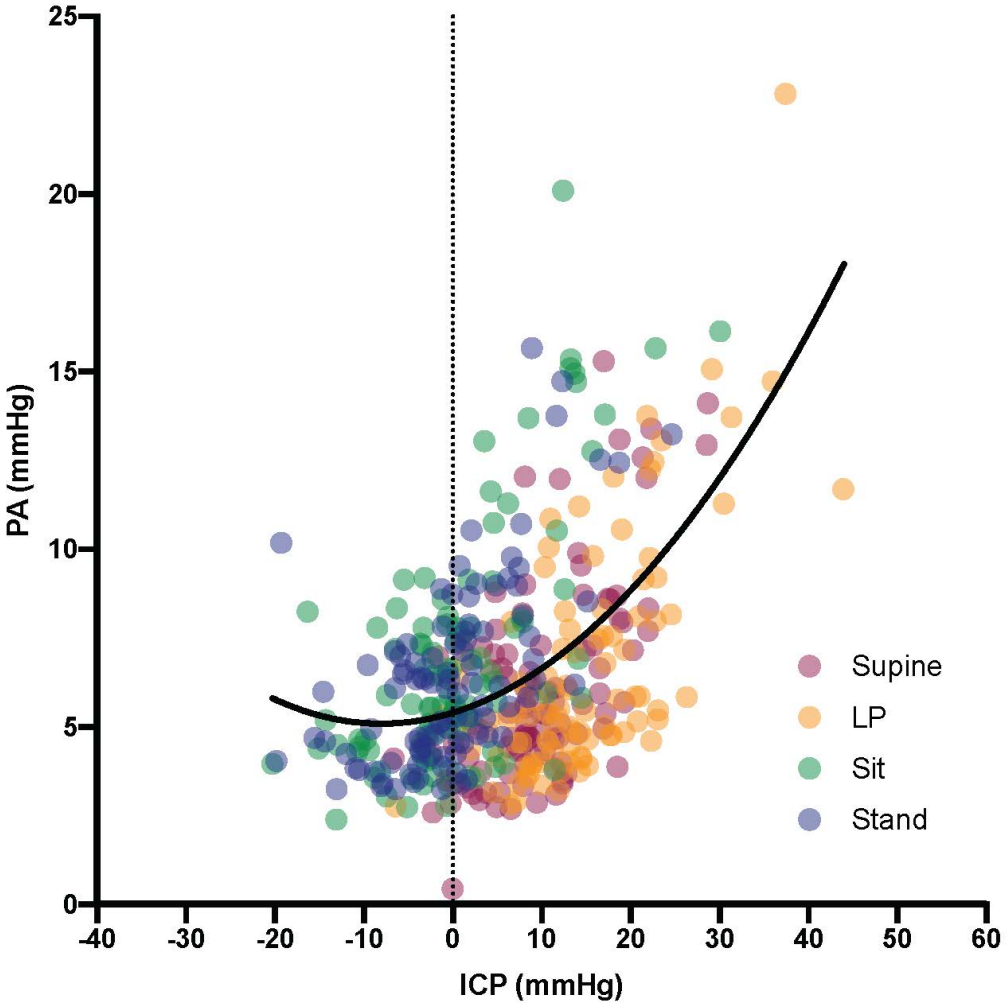


Figure 5-3: Scatter plot and curve of best fit of pulse amplitude (PA) and intracranial pressure (ICP) measurements for 101 patients.

5.4.2. Effect of position on PA

Table 5-2 and Table 5-3 summarise the PA results in patients without and with CSF diversion shunts respectively. Compared to supine position, pulse amplitude was slightly higher in lumbar puncture, sitting and standing

positions for both patients with and without shunts (Table 5-2, Table 5-3 and Figure 5-4).

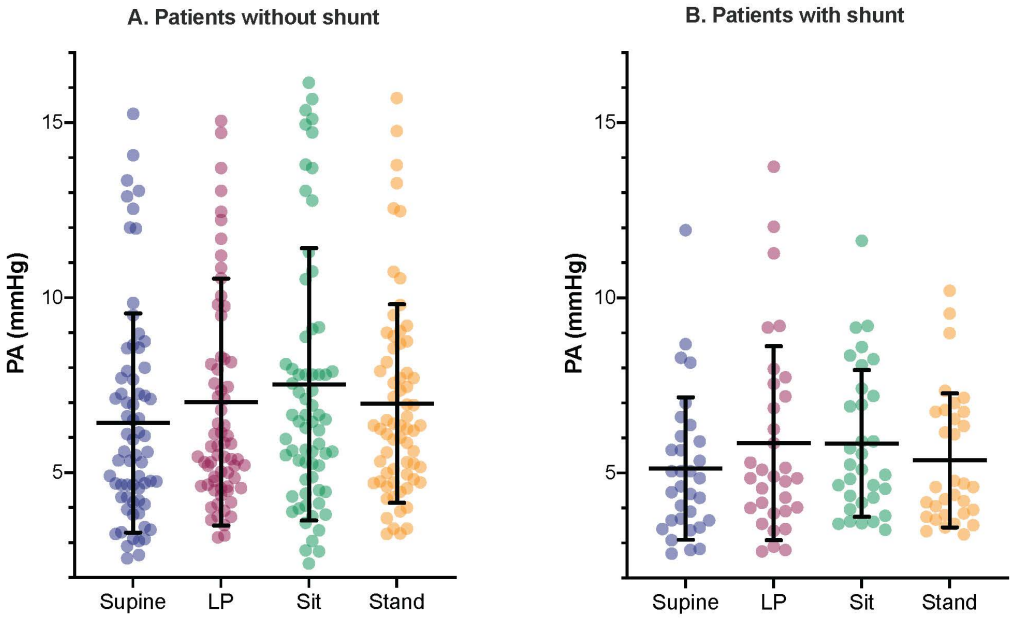


Figure 5-4: Mean pulse amplitude (PA) with standard deviations in different body positions stratified by shunt presence.

In the unadjusted linear regression models, no association between PA and position was found for patients with or without shunt (except for sitting position when Spiegelberg monitors were used in patients without shunts). However, when the models were corrected for confounders (outlined in the methods section 5.3.4) in the adjusted multiple regressions, pulse amplitude was significantly higher in sitting and standing positions independent of the type of monitor or presence of a shunt (Table 5-4).

Table 5-4: Adjusted multiple regression models testing the association between position and pulse amplitude (PA) stratified by monitor type.

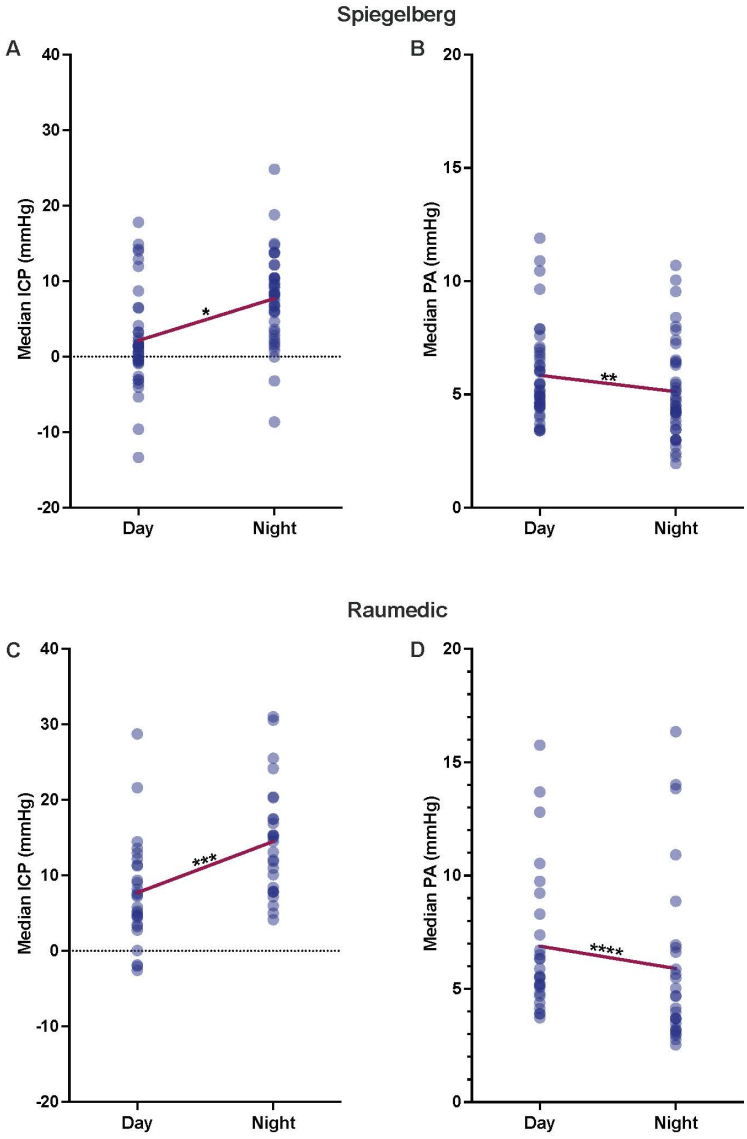
Adjusted multiple regression model testing the association between PA and position in patients without shunts						
PA	**Spiegelberg**			**Raumedic**		
Variables	**Beta**	**p**	**95% CI**	**Beta**	**p**	**95% CI**
LP*	-0.4	0.46	-1.5 to 0.7	-1.3	0.029	-2.5 to -0.1
Sitting*	4.7	<0.001	3.6 to 5.9	3.4	<0.001	2.2 to 4.7
Standing*	4.2	<0.001	3.1 to 5.4	3.3	<0.001	2 to 4.6
ICP	0.4	<0.001	0.3 to 0.4	0.4	<0.001	0.3 to 0.4
Sex	0.7	0.13	-	2.6	<0.001	-
Age	0.03	0.026	-	0.1	<0.001	-
Indication	0.04	0.84	-	0.5	0.007	-
	Adjusted R^2=0.47			Adjusted R^2=0.61		
Adjusted multiple regression model testing the association between PA and position in patients with shunts						
PA	**Spiegelberg**			**Raumedic**		
Variables	**Beta**	**p**	**95% CI**	**Beta**	**p**	**95% CI**
LP*	-0.3	0.650	-1.5 to 0.9	0.3	0.595	-0.9 to 1.6
Sitting*	2.7	0.001	1.2 to 4.2	1.8	0.012	0.4 to 3.2
Standing*	2.2	0.007	0.6 to 3.8	1.8	0.014	0.4 to 3.3
ICP	0.1	0.001	0.1 to 0.2	0.2	<0.001	0.1 to 0.3
Sex	-0.2	0.7	-	-0.5	0.4	-
Age	0.1	0.03	-	-0.1	0.028	-
Indication	0.3	0.23	-	-0.7	0.14	-

	Adjusted R^2=0.16	Adjusted R^2=0.63
CI: Confidence Intervals, ICP: Intracranial Pressure, LP: Lumbar Puncture position, PA: Pulse Amplitude *Compared to supine position ICP/PA		

5.4.3. Effect of day/night cycle on ICP and pulse amplitude in patients without shunts

Compared to daytime, the median night ICP was higher and the median night pulse amplitude was lower (Table 5-2). Adjusted multiple regression models, confirmed a significant association of ICP and pulse amplitude with the day/night cycle for both patients with and without shunts.

For patients without shunts, night ICP was higher than day ICP with both Spiegelberg (β=6.9, 95% CI 5.1 to 8.8, p< 0.001, adjusted R^2=0.64) and Raumedic monitors (β=8.3, 95% CI 6.2 to 10.5, p<0.001, adjusted R^2=0.75) (Figure 5-5 A and C).



* β=7, 95% CI 5.1 to 8.8, p< 0.001, adjusted R2=0.64;
** β=-2.1, 95% CI -2.9 to -1.4, p<0.001, adjusted R2=0.50;
*** β=8.3, 95% CI 6.2 to 10.5, p<0.001, adjusted R2=0.75;
**** β=-3.9, 95% CI -5.1 to -2.6, p<0.001, adjusted R2=0.65

Figure 5-5: Scatter plot of median day/night intracranial pressure (ICP) and pulse amplitude (PA) for Spiegelberg (A-B) and Raumedic sensors (C-D) in patients without shunt. Line of best fit and results of adjusted linear regression models are displayed. β is used to indicate the slope coefficient of the linear regression analysis.

Night pulse amplitude was lower than day pulse amplitude with both Spiegelberg (β=-2.1, 95% CI -2.9 to -1.4, p<0.001, adjusted R^2=0.50) and Raumedic monitors (β=-3.8, 95% CI -5.1 to -2.6, p<0.001, adjusted R^2=0.65) (Figure 5-5 B and D).

5.4.4. Effect of day/night cycle on ICP and pulse amplitude in patients with shunts

The adjusted regression models for the 33 patients with shunts in situ demonstrated a significant association between ICP with day/night cycle for both types of monitors, with night ICP being higher than day ICP (Spiegelberg β=5.3, 95% CI 3.2 to 7.5, p<0.001, adjusted R^2=0.48; Raumedic β=9.3, 95% CI 4.4 to 14.2, p=0.001, adjusted R^2=0.45). A significant association was also found between PA and day/night cycle, with day pulse amplitude being higher than night pulse amplitude (Spiegelberg β=-1.2, 95% CI -2.2 to -0.2, p=0.018, adjusted R^2=0.10; Raumedic β=-3.5, 95% CI -5.9 to -1, p=0.008, adjusted R^2=0.38).

5.4.5. Subgroup analysis of ICP monitoring results in 'normal', 'abnormal' and 'shunt' groups

The multidisciplinary team interpreted the ICP monitoring results as 'normal' in 20 patients, 'abnormal' in 44 patients and 37 patients had a shunt in situ at the time of ICPM monitoring (‘shunt’ group). During the exercise battery, patients considered to have ‘normal’ ICP monitoring results had the following mean ICP values: mean supine ICP of 7.2 (3.2 SD) mmHg, mean lumbar puncture position ICP of 10.5 (3.5 SD) mmHg, mean sitting ICP of -1.4 (4.1

SD) mmHg and mean standing ICP of -1.9 (3.2 SD) mmHg. The mean pulse amplitude results in the 'normal' group were: 5.3 (2.1 SD) mmHg in supine position, 5.9 (2.2 SD) mmHg in lumbar puncture position, 6.1 (1.6 SD) in sitting position and 6.2 (1.6 SD) in standing position. There was a tendency for patients in the 'normal' group to have smaller changes in ICP when changing body position compared to the 'abnormal' and 'shunt' groups; however, the amount of change in ICP was not statistically different among the three groups (Kruskal-Wallis H Test, $p>0.05$ for all positions). The ICP monitoring parameters of the patients in the 'normal' group were all normally distributed except for the ICP measured in lumbar puncture position and the ICP in sitting position (Skewness-Kurtosis normality test p values 0.03 and 0.01 respectively) (Table 5-5).

Table 5-5: ICP monitoring results of 20 patients in the 'normal' group

ICP monitoring parameter	Mean	Standard Deviation	95% confidence interval	Skewness-Kurtosis normality test
24-hour ICP	2.2	2.3	1.1 to 3.4	0.06
24-hour PA	4.5	0.6	4.2 to 4.8	0.23
Day ICP	-0.1	2.5	-1.3 to 1.1	0.14
Day PA	4.9	0.8	4.5 to 5.3	0.21
Night ICP	6.0	3.3	4.4 to 7.6	0.13
Night PA	4.0	0.8	3.6 to 4.4	0.19
Supine ICP	7.2	3.2	5.6 to 8.8	0.49
Supine PA	5.3	2.1	4.2 to 6.3	0.86
LP position ICP	10.5	3.5	8.7 to 12.2	**0.03**
LP position PA	5.9	2.2	4.8 to 6.9	0.08
Sitting ICP	-1.4	4.1	-3.4 to 0.7	**0.01**
Sitting PA	6.1	1.6	5.3 to 6.9	0.84
Standing ICP	-1.9	3.2	-3.5 to -0.3	0.78
Standing PA	6.2	1.6	5.4 to 7.0	0.42
ICP: Intracranial Pressure; PA: Pulse Amplitude All results are in mmHg				

5.5. Discussion

This cross-sectional study investigated the effect of position on ICP and pulse amplitude measurements in 101 patients with suspected CSF dynamics disorders. Our results confirmed previous findings suggesting a strong association between position and ICP (Magnaes, 1976a; Qvarlander *et al.*, 2013; Farahmand *et al.*, 2014; Andresen *et al.*, 2015; Petersen *et al.*, 2016; Holmlund *et al.*, 2018). In addition, we found that pulse amplitude (a marker of intracranial compliance) is also correlated to posture. Contrary to our initial hypothesis, pulse amplitude was higher in sitting and standing postures compared to supine position indicating a slight drop in intracranial compliance when the patients were upright. The investigation of the effect of the day/night cycle on ICP dynamics generated analogous results, with ICP significantly higher during the night (when patients are supine) and pulse amplitude significantly higher during the day (when patients spend most of their time upright). Additionally, the increase in pulse amplitude for upright postures and daytime was confirmed independently of the presence of a CSF diversion shunt.

The brain compliance model proposed by Marmarou in 1975 predicted that high ICP levels should correspond with lower compliance and therefore higher pulse amplitude of the ICP waveform (Marmarou *et al.*, 1975). ICP drops significantly when moving from supine to upright position, with an average decrease of 9.3 mmHg in this study (Table 5-2 and Table 5-3). However, this was not accompanied by a reduction in pulse amplitude,

indeed there was a slight increase of this marker (average increase of 1 mmHg, see Table 5-2 and Table 5-3). Similar findings were described by Farahmand *et al.* in 2014, who observed higher pulse amplitudes during sitting and walking compared to supine position in a group of 15 patients affected by communicating hydrocephalus (Farahmand *et al.*, 2014). They reported that the difference between sitting and supine pulse amplitude was not statistically significant and attributed the increase of pulse amplitude during walking to the irregular waveform recordings that can affect ICP monitoring quality during movement (Farahmand *et al.*, 2014). This interpretation is plausible, and we also observed that in some patients the upright ICP trace was 'noisier' even though the patients were sitting (or standing) completely still (Figure 5-1). This explanation might also apply to the finding that pulse amplitude is higher during the day compared to night ICP recordings.

A study by Raabe *et al.* investigated the effect of posture (more specifically head-tilt angles) on intracranial compliance using invasive techniques (intraventricular sensors) in 13 patients (Raabe *et al.*, 1999). The authors concluded that posture does not change intracranial compliance but rather creates a shift of the pressure-volume curve along the pressure axis, without changing its shape. For these reasons, they suggested that measurements of intracranial compliance should be conducted with the patient in supine position or alternatively corrected for this shift (Raabe *et al.*, 1999). On the other hand, studies investigating intracranial compliance non-invasively,

using brain MRI or mathematical models, have found that intracranial compliance is expected to improve in an upright posture (Alperin *et al.*, 2005b; Gehlen *et al.*, 2017). The controversies around the effect of position on intracranial compliance are further proof of the complexity of CSF dynamics.

As recently discussed by Marek and Zofia Czosnyka, the ICP waveform is 'rich in information' but also not easy to analyse (Czosnyka and Czosnyka, 2020). There are limitations to the current ICP monitoring and compliance measurement techniques that could have contributed to these results. Due to their mechanical characteristics, pneumatic ICP measuring sensors have been described as less reliable for the measurement of intracranial compliance markers (Evensen and Eide, 2020). For this reason, we stratified our results by sensor type but despite this, we found a similar trend for pulse amplitude changes with position in both Spiegelberg (pneumatic system) and Raumedic Neurovent-P (strain-gauge sensor). Additionally, it remains unclear whether time-domain or frequency-domain analysis methods are more reliable for the assessment of intracranial compliance. For this study we used frequency-domain analysis performed through the software ICM+, this type of analysis has been reported to underestimate the ICP pulse amplitude signal compared to time-domain analyses (Holm and Eide, 2008). It is possible that the use of frequency-domain analysis may have played a role in our results, however, this would have presumably affected the analysis of pulse amplitude similarly in all positions. Another limitation is the

retrospective nature of the study; while the analysis is retrospective the data collection has been performed prospectively as part of our local ICP monitoring protocol. Additionally, having information on the capnography waveform and continuous position monitoring would have been useful for the interpretation of the ICP/PA changes, future prospective studies including this information would be valuable.

The venous system has been demonstrated to have a key role for the postural changes of ICP dynamics. When moving from supine to upright posture, the internal jugular veins collapse, causing a shift of the hydrostatic indifferent point (Alperin *et al.*, 2005b; Holmlund *et al.*, 2017; Holmlund *et al.*, 2018). It is possible, that these vascular changes could affect intracranial compliance in upright posture. It should be noted that, our findings are in part in keeping with the observation that at very low ICPs, brain compliance tends to decrease (Qvarlander *et al.*, 2010; Eide *et al.*, 2012).

With the benefit of hindsight, the lack of simultaneous blood pressure measurements during the exercise battery is a significant limitation to the methods of this study and make the interpretation of these findings more uncertain. Changes in posture have known effects on blood pressure, with standing blood pressure being significantly lower compared to supine posture (Eşer *et al.*, 2007). It is possible, that blood pressure changes might have affected the ICP and pulse amplitude changes in different postures. Future

studies on the effect of posture on brain compliance should include this important variable.

As discussed, it is difficult to ascertain the true origin of the increase of pulse amplitude in upright posture. Additionally, these pulse amplitude changes are minimal (about 1 mmHg from supine to sitting) and may not be clinically relevant. However, this finding may be useful for the interpretation of the ICP monitoring results of patients affected by isolated compliance abnormalities (e.g., Chiari malformation I and NPH). Additionally, this information is of importance for studies on non-invasive ICP monitoring techniques that use in their estimations ICP waveform analysis of patients in upright posture (e.g., tympanic membrane displacement) (Evensen and Eide, 2020).

Finally, our study provides information on the ICP and pulse amplitude of patients with no clear abnormality on ICP monitoring results ('normal') in different body postures. Our mean ICP results in supine and upright posture are similar to those described by Andresen *et al.* in 4 'healthy' patients undergoing ICP monitoring after removal of a demarcated, small brain tumour (Andresen and Juhler, 2014). Additionally, we provide data on 'normal' pulse amplitude in different posture that were not previously described. We found that patients with 'normal' ICP tended to have a more stable ICP, with smaller ICP postural changes. This finding is similar to the results of a smaller study by Andresen *et al.* (Andresen *et al.*, 2015) and we

are in agreement with their statement that shunts seem to mimic abnormal ICP dynamics instead of restoring normal ICP physiology.

5.6. Conclusions

This is the largest study investigating the effect of postural changes on ICP dynamics. The results of this study suggest that pulse amplitude (as well as ICP) is significantly associated with posture, increasing in upright positions compared to supine. Moreover, patients with 'normal' ICP monitoring results tend to have a tighter control of their ICP and smaller postural ICP changes.

Chapter 6. Paradoxical response of intracranial pressure to shunt valve setting adjustments

6.1. Abstract

6.1.1. Background

The hydrodynamics of cerebrospinal fluid shunts have been described in vitro; however, knowledge on the response of intracranial pressure (ICP) to valve settings adjustments in vivo is limited. This study describes the effect of adjusting the shunt valve setting on ICP in a cohort of patients with complex symptom management.

6.1.2. Methods

Single-centre retrospective observational study. Patients who underwent ICP-guided valve setting adjustments during 24-hours continuous ICP monitoring, between 2014 and 2019, were included. Patients with suspected shunt malfunction were excluded. Median night ICP before and after the valve adjustments were compared (Δ night ICP). The responses of ICP to valve adjustment were divided into 3 different groups as follows: expected, paradoxical and no response. The frequency of the paradoxical response and its potential predicting factors were investigated.

6.1.3. Results

Fifty-one patients (37 females, 14 males, mean age 38 years) receiving 94 valve setting adjustments met the study inclusion criteria. Patients'

underlying conditions were most commonly hydrocephalus (47%) or idiopathic intracranial hypertension (43%). The response of ICP to valve setting adjustments was classified as 'expected' in 54 cases (57%), 'paradoxical' in 17 cases (18%) and 'no effect' (Δ night ICP <1 mmHg) in 23 cases (24%). There was a significant correlation between the Δ night ICP and the magnitude of valve setting change in both the investigated valves (Miethke ProGAV, $p=0.01$ and Medtronic Strata, $p=0.02$).

6.1.4. Conclusion

Paradoxical ICP changes can occur after shunt valve setting adjustments. This observation should be taken into account when performing ICP-guided valve adjustments and is highly relevant for the future development of "smart" shunt systems.

6.2. Introduction

The management of chronic hydrocephalus and CSF dynamics disorders is often complex. CSF shunt systems provide the possibility to tailor patients' treatment thanks to the availability of adjustable differential pressure valves and, more recently, adjustable gravitational components. The creation of "smart" shunts, able to perform automated adjustments has been pursued and envisioned for years (Lutz *et al.*, 2013). The "smart" shunt is expected to perform automated titration of the CSF flow drainage based on two types of feedback: patients' symptoms (especially headache) and ICP measurements. However, the interpretation of both headache and ICP in

patients with CSF dynamics disorders is challenging. For example, it has been demonstrated that primary headaches are often a comorbidity, making the interpretation of CSF-related headache difficult (e.g., migraine in idiopathic intracranial hypertension) (Mollan *et al.*, 2019). Additionally, evidence on what can be considered normal ICP and therefore which ICP values should be targeted is limited (Andresen and Juhler, 2014).

Another important obstacle for the creation of “smart’ shunts is that detailed information on the effect of valve adjustments on ICP in vivo is lacking. Benchmark laboratory tests are routinely performed to assess shunt systems functionality and they help predict the effect that valve settings adjustments will have on CSF flow and consequently on ICP (Allin *et al.*, 2006; Eklund *et al.*, 2012; Czosnyka *et al.*, 2013; Chari *et al.*, 2014). However, due to the complexity of the CSF dynamics, these predictions can fail in vivo. In the clinical experience of our group, there are also instances in which ICP can react unexpectedly to a valve setting adjustment and change in the opposite direction than predicted.

This study describes the effects of adjusting shunt valve settings on ICP in a cohort of adult patients with complex symptom management. The primary objective was to assess the frequency of paradoxical changes in ICP following valve setting adjustments. The secondary objective was to identify potential predictive factors for this event.

6.3. Methods

This is a single centre retrospective observational study conducted at the National Hospital for Neurology and Neurosurgery (London).

6.3.1. Patients selection

The clinical ICP monitoring database, which is maintained prospectively, was screened to identify patients who underwent continuous 24-hour ICP monitoring between January 2014 and April 2019. Patients who had a shunt valve setting adjustment during the monitoring period and recording of ICP 24 hours before and 24 hours after the valve adjustment were selected. The main exclusion criteria were: (i) incomplete ICP recording (<24 hours) before or after valve setting adjustment, (ii) lack of information about the valve setting adjustment and (iii) suspected shunt blockage/dysfunction addressed with shunt revision surgery in the following 6 months. Additionally, (iv) patients who had valve setting adjustments of gravitational components (e.g., Miethke ProSA), or simultaneous adjustments of more than one shunt component were excluded.

Shunt malfunctions were suspected on the basis of the clinical picture, imaging findings and ICP monitoring results. More specifically, patients who were suspected to have shunt malfunction were excluded from the study in case of imaging evidence of disconnections/misplacements of shunt components, sudden/extreme increase in ventricular size, acute clinical deteriorations and/or shunt reservoir assessment suggesting shunt blockage.

6.3.2. ICP monitoring

ICP monitoring admissions were conducted according to an established local protocol (Chari *et al.*, 2017; Thompson *et al.*, 2017a). Indications for this investigation were discussed in a multidisciplinary context including the opinions of neurosurgeons, neurologists, ophthalmologists and radiologists. Patients selected for this study underwent continuous intraparenchymal ICP monitoring for ICP-guided valve setting adjustments due to their complex symptom management. The 24-hour ICP monitoring data were analysed with the software ICM+ (Cambridge Enterprise, United Kingdom) and the results summarised in terms of median ICP and median pulse amplitude during the 24 hours, daytime and night-time. Further details of this ICP monitoring method have been described in Chapter 2.

6.3.3. Data collection

The following information on patients' baseline characteristics was collected: age, sex, diagnosis, type of shunt (ventriculoperitoneal, lumboperitoneal, other), type of valve, presence of gravitational (or anti siphoning) component, age of shunt (months from insertion or last revision), ventriculomegaly in most recent brain imaging (defined as Evan's index ≥ 0.3).

Valve setting changes were defined as 'upwards' changes when the valve setting was increased and 'downwards' changes when the valve setting was decreased. The difference between post-adjustment and pre-adjustment median night ICP was calculated (Δ night ICP). Compared to median 24-hour

ICP or median daytime ICP, the median night ICP (measured between 00:00 and 06:00 am) is more stable as measured when the patient is supine in bed and not affected by the patient's level of activity. For this reason, the Δ night ICP was chosen as the marker of ICP change for all statistical analysis.

The effect of the valve setting adjustment on night ICP was defined as 'expected', 'paradoxical' or 'no effect':

- 'Expected effect': an 'upwards' valve setting adjustment generating an increase in night median ICP (Δ night ICP > 1 mmHg) or a 'downwards' valve setting adjustment generating a decrease in night median ICP (Δ night ICP < - 1 mmHg);
- 'Paradoxical effect': an 'upwards' valve setting adjustment generating a decrease in night median ICP (Δ night ICP < -1 mmHg) or a 'downwards' valve setting adjustment generating an increase in night median ICP (Δ night ICP > 1 mmHg);
- 'No effect': a valve setting change with negligible impact on night ICP (≤ 1mmHg).

6.3.4. Statistical analysis

Patients' baseline demographic, clinical characteristics, shunt features and ICP monitoring results were summarised. The proportion of valve adjustments resulting in 'expected effect', 'paradoxical effect' and 'no effect' on median night ICP was calculated. Continuous variables were summarised as means (±standard deviation) and categorical variables as percentages.

The difference between the three effect groups ('expected', 'paradoxical' and 'no effect') was tested for the following variables: age, gender, diagnosis (hydrocephalus, idiopathic intracranial hypertension, other), ventricular size (small if Evan's index <0.3, large if Evan's index ≥ 0.3), shunt type (ventriculoperitoneal, lumboperitoneal, other), shunt age, valve type (Miethke ProGAV, Medtronic Strata, other), type of valve setting adjustment (upwards, downwards), baseline median ICP and baseline median pulse amplitude. When available, historical ICP monitoring results preceding the shunt insertion (or the latest revision) were compared to the baseline pre-adjustment ICP monitoring results to provide further evidence of the correct functionality of the shunt system ("Historical" Δ night ICP = pre-adjustment median night ICP minus pre-shunt median night ICP).

Fisher's exact test was used to compare categorical variables. Depending on the normality of distribution, Kruskal-Wallis H test or one-way analysis of variance (ANOVA) were used to compare continuous variables.

For valve types with more than 10 observations, a linear regression analysis was performed to assess the relationship (linearity) between Δ night ICP in mmHg (dependent variable) and magnitude of valve setting adjustment (post-adjustment setting minus baseline setting, independent variable).

Statistical significance level of 0.05 was used. Microsoft® Excel for Mac (version 16.25), Stata© (version 15.0) and GraphPad Prism (version 8.3.1) were used for the data collection, statistical analysis and graphs creation.

6.4. Results

Between January 2014 and April 2019, 867 patients underwent continuous 24-hour ICP monitoring. Figure 6-1 shows the patients selection process and reasons for exclusion. Fifty-one patients receiving 94 valve setting adjustments met the study inclusion criteria.

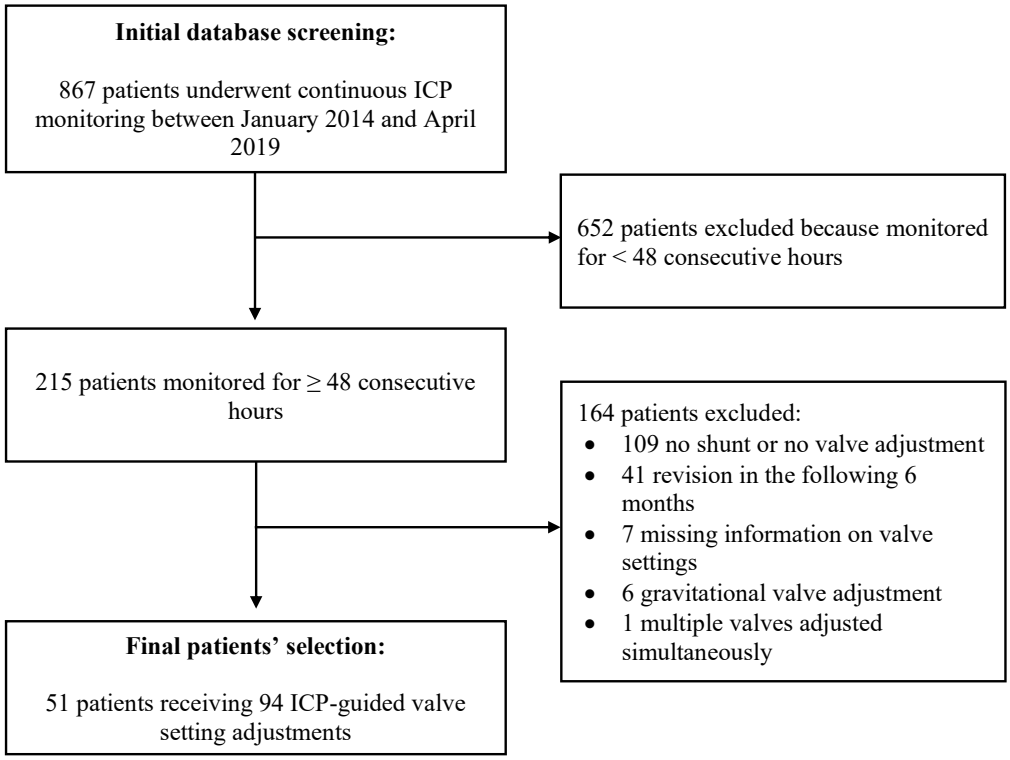


Figure 6-1: Flow diagram of patients' selection process and reasons for exclusion

The population demographic characteristics, diagnosis, shunt features and baseline ICP monitor results are described in

Table 6-1.

Table 6-1: Population baseline characteristics

Sex	**N (%)**
- Female	37 (73)
- Male	14 (27)
Age (years)	**Mean (SD)**
	38 (14)
Diagnosis	**N (%)**
- Hydrocephalus	24 (47)
- Idiopathic Intracranial Hypertension	22 (43)
- Chiari malformation	3 (6)
- LOVA	2 (4)
Shunt type	**N (%)**
- Ventriculoperitoneal	34 (67)
- Lumboperitoneal	12 (24)
- Ventriculoatrial	2 (4)
- Ventriculopleural	1 (2)
- Ventriculoperitoneal and lumboperitoneal	1 (2)
- Ventriculoperitoneal and lumbopleural	1 (2)
Shunt age	**Mean months (SD)**
	32 (39)
Valve type	**N (%)**
- Miethke ProGAV	23 (45)
- Medtronic Strata	19 (37)
- Codman Certas	4 (8)
- Sophysa Polaris	3 (6)
- Codman Hakim Adjustable	1 (2)

- Multiple valves	1 (2)
Ventricles size*	**N (%)**
- Small	43 (84)
- Large	8 (16)
Baseline median ICP (mmHg)	**Mean of the medians (SD)**
- 24-hour	3 (5)
- Night	6 (6)
Baseline median pulse amplitude (mmHg)	**Mean of the medians (SD)**
- 24-hour	5 (2)
- Night	4 (2)

ICP: Intracranial Pressure; LOVA: Longstanding Overt Ventriculomegaly in Adults; SD: Standard Deviation

* Ventricles were considered small if Evan's index <0.3 and large if Evan's index ≥ 0.3.

Valve setting adjustments resulted in the 'expected effect' on median night ICP in 54 cases (57%), 'no effect' in 23 cases (24%) and a 'paradoxical effect' in 17 cases (18%). Pre- and post-valve adjustment night ICP results stratified by effect group are described in Figure 6-2.

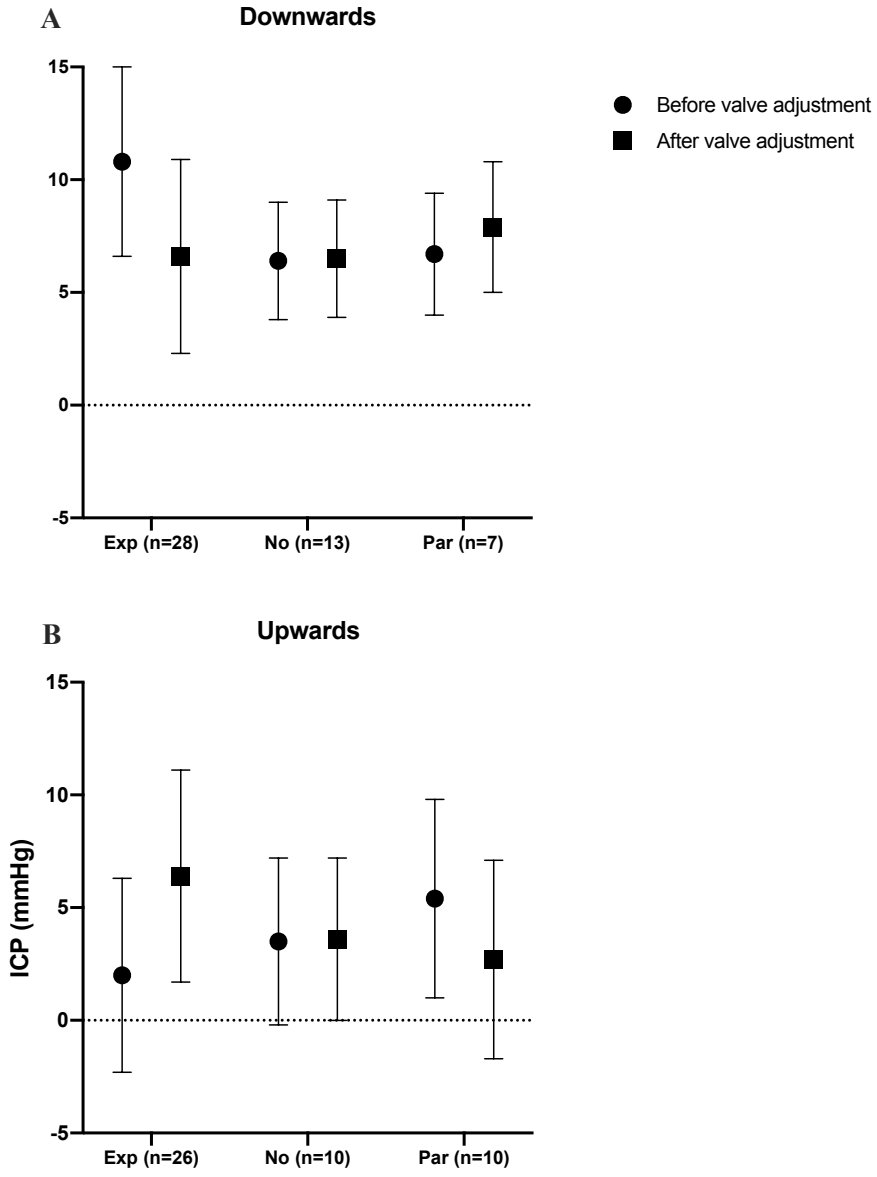


Figure 6-2: Summary of pre- and post-shunt adjustment night ICP (mean and SD) stratified by direction of valve setting adjustment (upwards/downwards) and effect of valve adjustment on ICP (Exp: expected effect, No: no effect, Par: paradoxical effect).

The baseline demographic, clinical, shunt and ICP characteristics did not significantly differ among the three effect groups (see Table 6-2).

Table 6-2: Comparison of baseline demographic, clinical, shunt and intracranial pressure characteristics between three groups of patients with different response to valve setting adjustment: 'expected', 'paradoxical' and 'no effect' groups.

	'Expected effect' group (n=54)[a]	'No effect' group (n=23)[b]	'Paradoxical effect' group (n=17)[c]	p value
Sex, N (row %)				
- Female	37 (54)	18 (26)	13 (19)	
- Male	17 (65)	5 (19)	4 (15)	0.67
Age, Mean (SD)	37 (14)	37 (12)	41 (17)	0.60
Diagnosis, N (row %)				
- Hydrocephalus	29 (62)	9 (19)	9 (19)	
- IIH	23 (53)	12 (28)	8 (19)	
- Other	3 (60)	2 (40)	0 (0)	0.60
Shunt type, N (row %)				
- Lumboperitoneal	9 (56)	5 (31)	2 (13)	
- Ventriculoperitoneal	35 (58)	11 (18)	14 (23)	
- Other	10 (56)	7 (39)	1 (6)	0.25
Shunt age in months, Mean (SD)	38 (40)	23 (15)	17 (21)	0.40
Valve type, N (row %)				
- Medtronic Strata	19 (59)	9 (28)	4 (13)	
- Miethke ProGAV	27 (52)	12 (23)	13 (25)	
- Other	8 (80)	2 (20)	0 (0)	0.32
Ventricles size, N (row %)				

- Small	44 (56)	21 (27)	13 (17)	
- Large	10 (63)	2 (13)	4 (25)	0.52
Baseline median ICP in mmHg, Mean (SD)				
- 24-hour	3 (6)	3 (4)	3 (4)	0.86
- Night	7 (6)	5 (4)	6 (4)	0.56
Baseline median pulse amplitude in mmHg, Mean (SD)				
- 24-hour	4 (2)	5 (1)	5 (2)	0.50
- Night	4 (2)	5 (2)	4 (2)	0.69
Valve setting change type, N (row %)				
- Downwards	28 (58)	13 (27)	7 (15)	
- Upwards	26 (57)	10 (22)	10 (22)	0.66
Δ night ICP in mmHg, Mean (SD) Comparison of pre and post valve adjustment ICP recordings.	4 (3)	1 (0)	4 (3)	<0.01
"Historical" Δ night ICP[d] in mmHg, Mean (SD) Information available for 25 patients only (13 'expected effect', 6 'no effect' and 6 'paradoxical effect')	5 (4)	4 (3)	5 (6)	0.40

[a] 'Expected effect': night ICP change >1 mmHg in the expected/desired direction

[b] 'No effect': negligible night ICP change (≤ 1mmHg).

[c] 'Paradoxical effect': night ICP change >1 mmHg in the unexpected/undesired direction

[d] "Historical" Δ night ICP = pre-adjustment median night ICP - baseline pre-shunt median night ICP

ICP: Intracranial Pressure; IIH: Idiopathic Intracranial Hypertension; SD: Standard deviation

Medtronic Strata and Miethke ProGAV, were the only valves with 10 or more observations. Two unadjusted linear regression models confirmed the association between the magnitude of valve setting adjustment (post-adjustment setting minus baseline setting) and Δ night ICP for both Medtronic Strata (β=1.84; 95% CI 0.30 to 3.38, P=0.02; adjusted R^2=0.14) and Miethke ProGAV valves (β=0.27; 95% CI 0.07 to 0.47, P=0.01; adjusted R^2=0.11). Figure 6-3 and Figure 6-4 display the night ICP change caused by different magnitudes of valve setting adjustments for Medtronic Strata and Miethke ProGAV respectively.

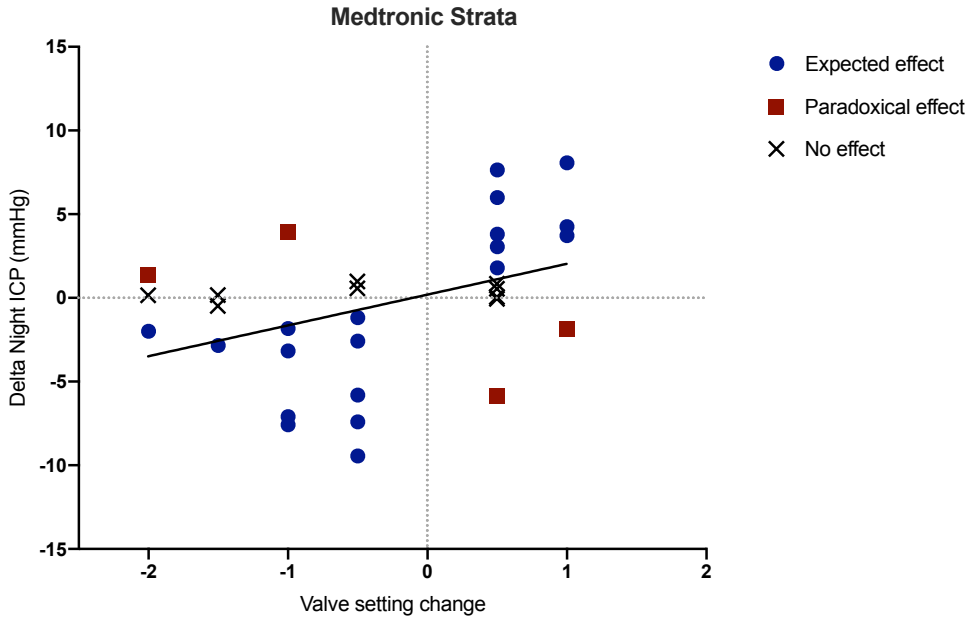


Figure 6-3: Scatter plot and line of best fit of night intracranial pressure change (mmHg) and magnitude of Medtronic Strata setting adjustment (post-adjustment setting minus baseline setting).

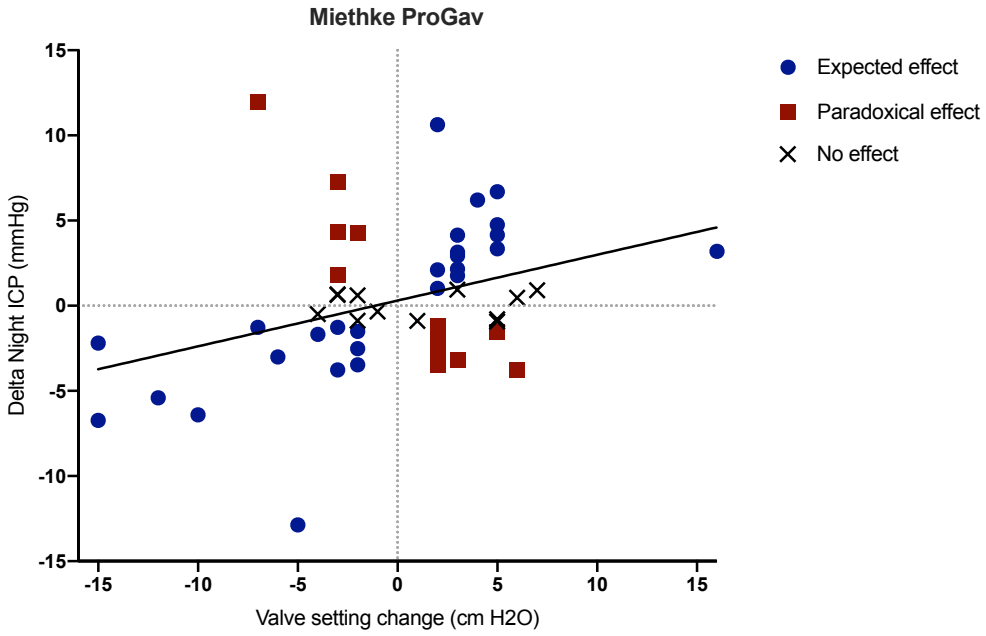


Figure 6-4: Scatter plot and line of best fit of night intracranial pressure change (mmHg) and magnitude of Miethke ProGAV setting adjustment (post-adjustment setting minus baseline setting).

6.5. Discussion

This single centre retrospective observational study describes the effects of 94 shunt valve setting adjustments on ICP in a cohort of patients investigated with continuous 24-hour ICP monitoring. To the best of our knowledge, this is the first description of paradoxical ICP changes following valve setting adjustments of functional shunts in a large cohort of patients. Among 94 valve setting adjustments, paradoxical ICP changes were observed in 18% of the cases, and no significant change in ICP (Δ night ICP <1 mmHg) in 24%. This observation should be taken into account when performing ICP-guided valve setting adjustments and suggests that a paradoxical response to valve

setting adjustments does not always indicate shunt malfunction (only patients with functioning shunts were included in this study). This is further proof of the complexity of CSF drainage shunts in the context of chronic hydrocephalus and other CSF dynamics disorders.

The baseline characteristics of the three effect groups ('expected', 'paradoxical' and 'no effect') did not significantly differ (Table 6-2), making the identification of potential mechanisms for the paradoxical response difficult. It could be hypothesised that in patients with small ventricles (e.g., IIH), 'downwards' valve setting adjustments could cause obstruction of the ventricular catheter lumen secondary to a collapse of the ventricular walls. However, our results did not show any association between paradoxical response and small ventricles or IIH. On the other hand, 'upwards' valve setting adjustments could displace intraluminal debris from a partially blocked ventricular catheter and cause a paradoxical response. While we would expect older shunts to present such intraluminal debris, a significant association between shunt age and paradoxical effect was not found in this study. This theory would be supported by a previous report by Nabbanja *et al.* in which infusion studies allowed the identification of ventricular catheter blockage likely secondary to intraluminal catheter debris in two patients; both patients were successfully treated through the retrograde flush of the ventricular catheter (Nabbanja *et al.*, 2018). Previous experience suggests that, if there are no in-between interventions, different sets of elective 24-hour ICP monitoring measured in the same patient do not significantly differ

(Thompson *et al.*, 2017a). However, the possibility that random ICP changes may have affected the before and/or after valve adjustment ICP results generating a paradoxical ICP response exists. Another hypothesis is that CSF dynamics may require longer times (>24 hours) to adapt to a new valve setting.

The hydrodynamics of valve setting adjustments have been investigated in several in vitro studies (Allin *et al.*, 2006; Eklund *et al.*, 2012; Czosnyka *et al.*, 2013; Chari *et al.*, 2014). Information on the effect of valve setting adjustments on ICP in vivo is scarce. Farahmand *et al.* looked at the impact of Medtronic Strata valve adjustments on ICP in a group of 15 patients with communicating hydrocephalus concluding that the ICP change between different valve settings was smaller than the difference previously observed in vitro (Farahmand *et al.*, 2014). Antes *et al.* found that the patients who do not benefit from ICP-guided adjustments are those who do not demonstrate a significant ICP change (follow-up compared to baseline ICP) (Antes *et al.*, 2018). These studies corroborate our finding that there is a group of patients in whom the valve setting adjustment of a functional shunt generates minimal ICP change, not exceeding 1 mmHg ('no effect group'). Similarly, Bergsneider *et al.* demonstrated that ICP at different Codman Hakim programmable valve settings were lower than predicted with a linear mathematical model in 11 normal pressure hydrocephalus patients (Bergsneider *et al.*, 2004). The previously published studies have an important limitation: they measured ICP for a short period time (minutes) or

shortly after a postural change, possibly before the achievement of the ICP 'steady state' (Bergsneider *et al.*, 2004; Farahmand *et al.*, 2014; Antes *et al.*, 2018). To overcome this limitation, we have used median night ICP, this value is obtained from a 6-hour continuous measurement recorded at standard times (00:00 - 06:00) when the patient is expected to be supine in bed. In 2008, Eide and Sorteberg used a similar methodology to describe the effect of valve setting adjustments in the ICP of 2 normal pressure hydrocephalus patients (Eide and Sorteberg, 2008). Interestingly, their data shows one episode of ICP increase after a downward valve setting adjustment in a patient with functional shunt, this is in keeping with what we define as a 'paradoxical effect'.

The main limitation of our study is the retrospective analysis of prospectively collected data; however, the standardised approach for ICP monitoring data recording, analysis and storage might have reduced the disadvantages of this design. Whilst valve settings adjustments were performed by trained staff, human error might have occurred in the process of changing or checking the valve setting. In this retrospective study, post-adjustment skull x-rays were not routinely performed, unless suspicion of shunt and/or valve malfunction was raised. As a result, the possibility that some of these valve setting adjustments were unsuccessful cannot be excluded. Prospective studies testing the effect of valve setting adjustments on ICP should include standard procedures to ensure successful valve adjustments, for example with routine post-adjustment x-rays.

In addition, body position has known effects on ICP (Andresen *et al.*, 2015), different postures in the pre and post valve adjustment readings could have affected our results. This is the reason why we used the median night ICP, which is recorded between 00:00 and 06:00 am when the patients were supine. Technical issues with ICP monitoring could have occurred, but they are unlikely since a routine raw ICP data quality assessment was performed before each 24-hour ICP monitoring analysis. The lack of detailed information on the patients' symptoms and their changes in relation to the valve setting adjustments as well as intrabdominal pressure measurements are further shortcomings. Despite being the largest study on this topic, a larger cohort of patients would have allowed a better understanding of potential predictors of the response to valve adjustments. Moreover, the possibility that some of the shunts in the 'no/paradoxical effect' groups were non-functional cannot be excluded with absolute certainty. Nevertheless, we did not find any clinical evidence of malfunctioning (imaging and reservoir assessment) and there was no statistical difference among groups in any of the tested variables including the "historical" Δ night ICP. Future studies should also include measurements of clinical outcomes (i.e., verbal reporting scale for headache) to investigate potential association of clinical findings and ICP changes in the context of valve setting adjustments. Due to the retrospective nature of the study, measurements of clinical findings were not available adding to the limitation of this work. Finally, there is a selection bias due to fact that only patients with complex symptom management were

included in this study and this aspect should be taken into account when interpreting these results.

Future prospective studies employing implantable telemetric ICP monitoring devices such as M.Scio (Miethke, Potsdam, Germany) and Neurovent-P-Tel (Raumedic AG, Helbrechts, Germany), might be able to assess the effect of valve settings adjustments on ICP for longer periods of time and clarify predicting factors for 'paradoxical' ICP response to adjustment. Due to the limited number of cases, it was not possible to describe the effect of gravitational valve adjustments on ICP and this aspect should also be addressed by future research. A better understanding of the dynamics of CSF shunts in vivo is essential for the future development of smart shunts able to generate automated responses to patients' symptoms and ICP.

Paradoxical ICP changes can occur in the 24 hours following shunt valve setting adjustments. This observation should be taken into account when performing ICP-guided valve adjustments and is highly relevant for the future development of "smart" shunt systems.

Chapter 7. Association of Intracranial Pressure and Spontaneous Retinal Venous Pulsation

7.1. Abstract

7.1.1. Background

A reliable method for non-invasive intracranial pressure assessments is desirable to reduce the need for invasive procedures (e.g., intracranial pressure monitoring and lumbar punctures) and allow clinicians to identify and treat patients with intracranial hypertension in a timely manner. The aim of this study was to determine whether infrared video assessment of spontaneous retinal venous pulsation is a valid tool to indicate the presence or absence of raised intracranial pressure.

7.1.2. Methods

This is a single-centre prospective observational study. Patients consecutively admitted for elective invasive intracranial pressure monitoring had ophthalmic review including infrared video recording of their spontaneous venous pulsation. Two neuro-ophthalmologists, who were masked to the intracranial pressure monitoring results, independently graded the spontaneous venous pulsation. The correlation between simultaneously recorded intracranial pressure and spontaneous venous pulsation (present/absent) was evaluated using a multiple linear regression model.

7.1.3. Results

Of 105 patients, the mean (SD) age was 39 (±14) years, and 79 (75%) were women. The mean (SD) simultaneous intracranial pressure was 1 (±5) mm Hg for 91 patients (86.7%) with spontaneous venous pulsations and 13 (±14) mm Hg for 14 patients (13.3%) without spontaneous venous pulsations. A multiple linear regression model adjusted for 7 potential confounders confirmed a statistically significant association between intracranial pressure and spontaneous venous pulsation (β = –9.1; 95% CI, –13.7 to –4.6; P < .001; adjusted R2 = 0.42).

7.1.4. Conclusions

The absence of spontaneous venous pulsation on retinal infrared video recordings is significantly associated with higher levels of intracranial pressure and should raise the suspicion of intracranial hypertension.

7.2. Background

Spontaneous retinal venous pulsation (SVP) is the rhythmic constriction and redilation in the calibre of the retinal veins at or near the optic disc, synchronised to the cardiac cycle. It was first described by Coccius in 1853 (Coccius, 1853). It is thought to occur due to the pressure gradient between the retinal veins within the eye and the lower pressure in the retrobulbar portion of the central retinal vein, the latter being determined by the pressure of the cerebrospinal fluid (CSF) as the vein crosses the subarachnoid space within the optic nerve sheath. This pressure gradient causes pulsatile flow through the veins, with visible collapse of the compliant venous walls during each cardiac cycle (Hedges *et al.*, 1994; Levine, 1998; Jacks and Miller, 2003; Kim *et al.*, 2014; Levine and Bebie, 2016; Morgan *et al.*, 2016).

SVP tends to disappear when the CSF pressure is high due to loss of the physiological pressure gradient and distention of the retinal veins. The presence of SVP could therefore be regarded as a reassuring sign that excludes raised intracranial pressure (ICP) (Walsh *et al.*, 1969; Levin, 1978; Jacks and Miller, 2003). However, SVP assessments using a direct ophthalmoscope have been shown to have limited sensitivity, specificity and interrater reliability (Wong and White, 2013) with authors reporting that SVP cannot be observed in 7-23% of healthy individuals (9, 11-13). Moreover, in previous studies CSF pressure has been measured by lumbar puncture and the SVP evaluation has typically been made at a different time point, with the patient in a different posture than the ICP measurement.

Motion-stabilised infrared (IR) video, recorded using the Heidelberg Spectralis OCT system (Heidelberg engineering GmbH, Germany) is a highly sensitive method for detecting SVP, being able to detect SVP in many more subjects with normal ICP (99%) than conventional SVP examination via slit lamp or direct ophthalmoscopy (77-93%) and with a high level of interobserver concordance in grading SVP (Cohen's kappa 0.89) (McHugh *et al.*, 2020). This implies that in those healthy patients where SVP is not observable via slit lamp or direct ophthalmoscopy, SVP is likely to be present but just cannot be readily visualised due to its small amplitude which is masked by patient and eye movements.

This prospective observational study investigated the correlation between SVP and ICP using the same SVP assessment technique (McHugh *et al.*, 2020). Motion-stabilised IR retinal video recordings of SVP were obtained in patients undergoing continuous invasive ICP monitoring, thereby enabling simultaneous estimations of SVP and ICP. We ascertained the correlation between SVP and ICP and determined the reliability of this assessment method as a screening test for elevated ICP.

7.3. Methods

This study has been approved by the South West (Central Bristol) Human Research Ethics Committee (18/NW/0208).

7.3.1. Patient selection

Consecutive patients admitted at the National Hospital for Neurology and Neurosurgery (NHNN) with a clinical indication for elective invasive continuous ICP monitoring were prospectively identified. All patients who had simultaneous ICP monitoring and an ophthalmology assessment including IR video recording of SVP were included. Children (<18 years) and patients with ocular co-morbidity that could interfere with the validity of the data (e.g., central retinal vein occlusion, ocular media opacity, glaucoma) were excluded.

7.3.2. ICP monitoring methods

ICP monitoring was performed following an established local protocol (Chari *et al.*, 2017). The clinical decision to admit a patient for invasive ICP monitoring was based on a multidisciplinary team discussion including neurosurgeons, neurologists and neuroradiologists. An intraparenchymal ICP probe was implanted in the operating theatre under local anaesthesia with or without sedation. All patients were continuously monitored for at least 24 hours (Thompson *et al.*, 2017a). The ICP data results were routinely analysed and summarised in terms of median ICP and pulse amplitude (in mmHg) (Chari *et al.*, 2017). Further details on the ICP monitoring methods are described in Chapter 2.

7.3.3. Ophthalmology assessments and IR video recording of SVP

Patients admitted for elective ICP monitoring at NHNN underwent ophthalmology assessment during the ICP monitoring period. This included slit lamp biomicroscopy of the anterior and posterior segments of the eye (including Frisen grading of papilloedema, and clinical determination of the presence or absence of SVP) and measurement of intraocular pressure (IOP) by applanation tonometry. The retina and optic disc were then examined using the SPECTRALIS® Optic Coherence Tomography (OCT) system (Heidelberg Engineering Ltd, Germany). This included automated measurements of the mean thickness of the retinal nerve fiber layer (RNFLT) in a 1.7mm circle around each disc, the vertical diameter and maximum elevation of each disc and an objective measurement of the cup-to-disc diameter ratio (CDR). According to the usual NHNN protocol, ten-second IR videos of the patients' optic discs were recorded in High Speed (HS) mode. Blood pressure (systolic, diastolic and the derived estimation of mean arterial pressure MAP) was measured immediately after the fundus video recording. The whole ophthalmology examination was performed with the patient in a sitting position.

7.3.4. Data collection

During the ophthalmic assessments, the timestamp of both the ICP monitor and OCT system was noted at the start of each 10 second SVP video. At the end of the 24-hour ICP monitoring period, the ICP measurements

corresponding to the time of each fundus video recording were extracted for subsequent analysis. We have defined 'simultaneous ICP' as the average ICP (in mmHg) measured over the same minute as the IR video recordings of SVP.

The IR retinal video recordings were subsequently assessed independently by two neuro-ophthalmologists masked to these ICP results. For each eye, SVP was graded using the system first proposed by Hedges (Hedges *et al.*, 1994): '0' (SVP absent), '1' (up to 33% change in vessel diameter, i.e. 'equivocal SVP'), '2' (33-66% change, i.e. 'definite SVP'), or '3' (>66% change, i.e. complete collapse of the vein). This system was also used for grading SVP observed with the slit lamp. In cases where there was discordance between the SVP grade in the two eyes, the higher of the grades was used for subsequent analysis. Only those patients with no observable SVP (grade 0) in both eyes, when assessed by both examiners, were considered to have absent SVP for the purposes of analysis.

7.3.5. Statistical analysis

The association between ICP (in mmHg) and SVP (present or absent) was assessed using a multiple linear regression model, estimated using a stepwise approach. Due to the limited published literature on this topic and to the novel approach to this research question, a pragmatic sample size calculation was conducted. A P value of 0.05 was the statistical significance threshold. The following covariates were included in the model: age, sex, ICP

pulse amplitude, presence of a CSF diversion shunt, IOP, MAP, RNFLT, cup-to-disc ratio (CDR) and indication for ICP monitoring. To assess the predictive value of the absence of SVP, a receiver operating characteristics curve was built, and the area under the curve calculated. Stata© (version 15.0) was used for the statistical analysis.

7.4. Results

Between January 2017 and May 2018, 105 consecutive patients were recruited according to the inclusion criteria. The mean age was 39 years (SD=14, range 18 to 78), and 79 patients were female (75%). The clinical indications for invasive ICP monitoring were as follows: 30 hydrocephalus (28.6%), 29 idiopathic intracranial hypertension (27.6%), 16 intractable headache of unknown aetiology (15.2%), 16 Chiari malformation (15.2%), 12 suspected low CSF pressure/volume syndrome (11.5%) and 2 suspected normal pressure hydrocephalus (1.9%).

ICP bolts are rarely used in patients with optic disc swelling, except where there is a suspicion of pseudopapilloedema/optic nerve head drusen in the context of symptoms suggesting high ICP. Of the 105 patients, 91 had Frisen grade 0 and 14 had Frisen grade 1. IOP was recorded in 100 patients (average IOP 15.3 mmHg ± 3.0) and was within the normal range in most cases (92%). The lowest recorded IOP was 6 mmHg, in a patient without disc swelling; there were no cases of elevated IOP (>22mmHg) in this cohort.

SVP was initially assessed by slit lamp examination and recorded as absent in 52 patients (bilateral SVP grade 0), present in 51 patients (SVP grade 1 or more in at least one eye), and difficult to assess in 2 patients. When SVP was assessed using IR video recordings, only 14 patients had absent SVP (grade 0 bilaterally), the remaining 91 patients had SVP (at least grade 1 SVP in at least one eye). The inter-rater reliability between 2 independent observers in grading infrared video SVP assessments was 0.81 (Cohen's kappa coefficient). The two observers assigned the same SVP grade to 69.7% of the eyes, and in all the remaining cases the discrepancy was a single SVP grade (30.3%).

Table 7-1: Results of ICP monitoring and ophthalmic assessments

	SVP Absent	SVP Present	P values
No. (%) of patients	14 (13%)	91 (87%)	
Simultaneous ICP, mean (SD), mmHg [a]	13 (±14)	1 (±5)	<0.001
Simultaneous ICP, range, mmHg [a]	-12 to +36	-17 to +14	
Simultaneous ICP pulse amplitude, mean (SD), mmHg [b]	10 (±5)	5 (±2)	<0.001
24-hour ICP, mean (SD), mmHg	16 (±11)	4 (±5)	<0.001
24-hour ICP, range, mmHg	-5 to +30	-11 to +24	
24-hour pulse amplitude, mean (SD), mmHg	9 (±4)	5 (±2)	<0.001
Night ICP (supine), mean (SD), mmHg	21 (±8)	8 (±5)	<0.001
Night ICP (supine), range, mmHg	1 to 31	-5 to 25	
MAP, mean (SD), mmHg	89 (±13)	92 (±9)	0.28
IOP, mean (SD), mmHg	16 (±3)	15 (±3)	0.25

[a] Simultaneous ICP is the mean ICP (in mmHg) over the same minute as the IR video recording

[b] Simultaneous pulse amplitude is the mean ICP pulse amplitude (in mmHg) over the same minute as the IR video recording

ICP: Intracranial pressure; CSF: Cerebrospinal Fluid; SVP: Spontaneous venous pulsation; MAP: Mean arterial pressure; IOP: Intraocular pressure.

Simultaneous ICP measurements by SVP grade are displayed in Table 7-1 and Figure 7-1. Ranked simultaneous ICPs, stratified by presence or

absence of SVP can be seen in Figure 7-2. The average simultaneous ICP was significantly higher in the group of patients with absent SVP (95%CI -16.3 to -8.4, P<.001).

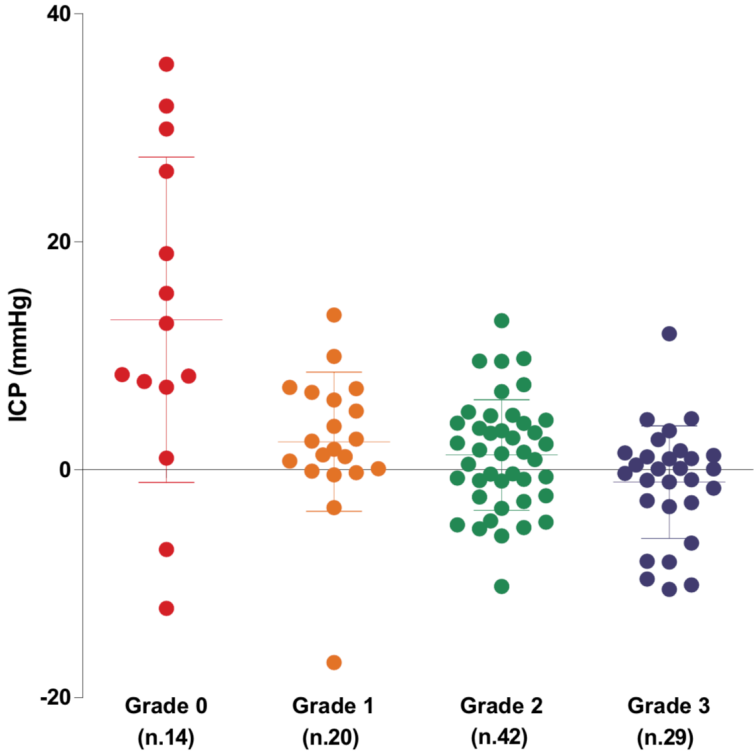


Figure 7-1: Mean (SD) Simultaneous Intracranial Pressure (ICP) Measurements by Spontaneous Venous Pulsation Grade

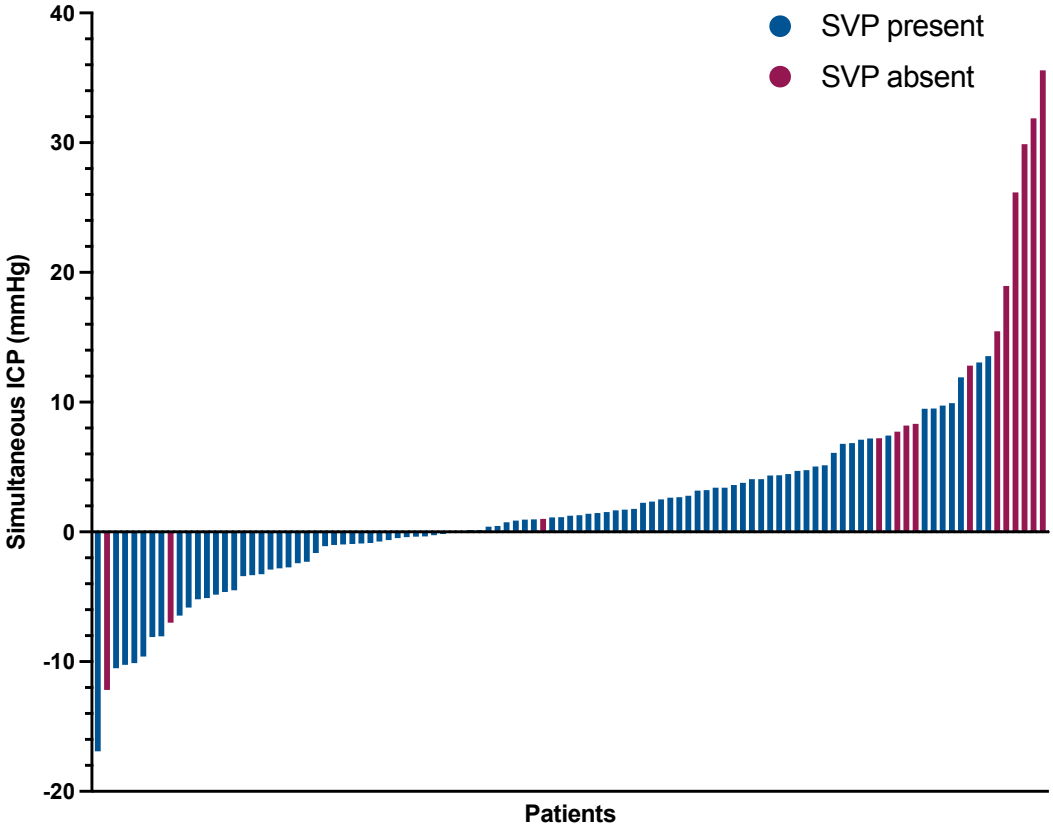


Figure 7-2: Ranked simultaneous ICP stratified by presence or absence of SVP

An unadjusted linear regression model showed a significant correlation between simultaneous ICP and SVP group (95% CI -16.4 to -8.3, P<0.001, R-squared 0.26). The multiple linear regression also confirmed the validity of this correlation after adjusting for the 9 potential confounders (95%CI -11.8 to -1.1, P=0.019, R-squared 0.43). Of these 9 covariates, a diagnosis of IIH and the simultaneous ICP pulse amplitude were also significantly correlated to the mean ICP (P=0.033 in both cases).

The receiver operating characteristics analysis showed an area under the curve of 0.80 (SE, 0.09; 95% CI, 0.62-0.99, see Figure 7-3).

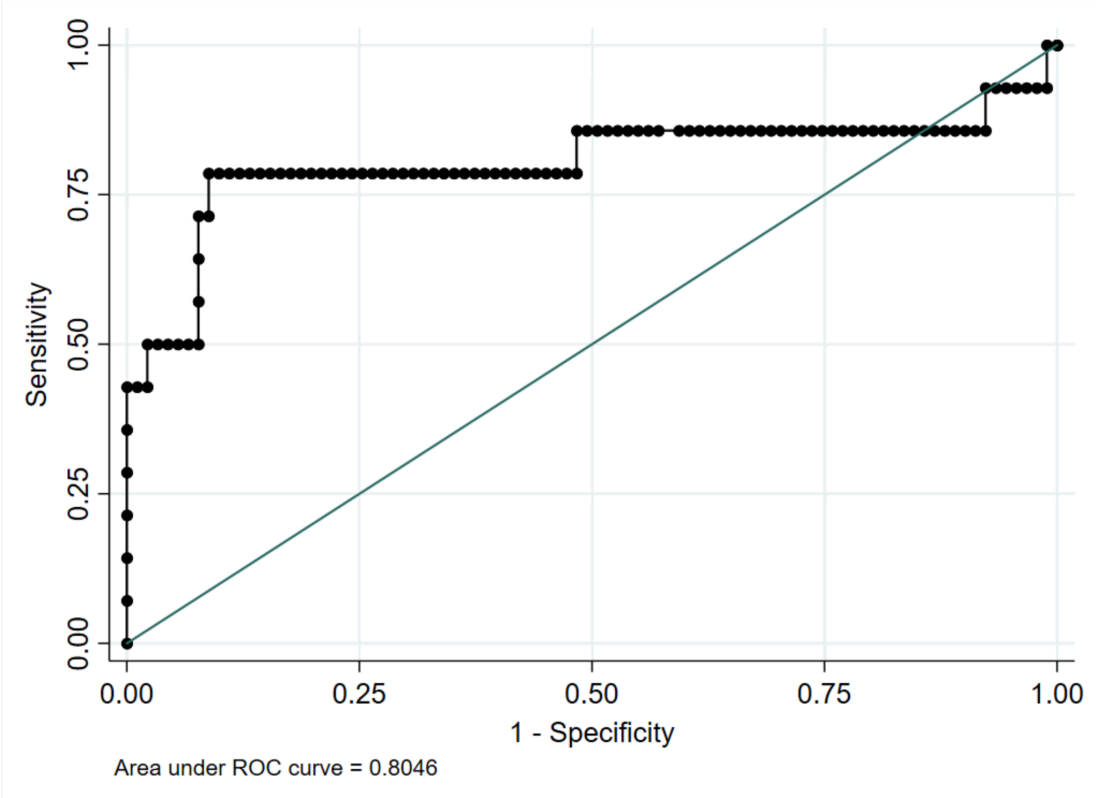


Figure 7-3: Receiver Operating Characteristics Curve Plotting the Predictive Value of Spontaneous Venous Pulsation in Determining Intracranial Pressure

7.5. Discussion

The debate about the validity and usefulness of the relationship between SVP and ICP is longstanding. Five studies have investigated the correlation between SVP and ICP using direct CSF pressure measurements (Walsh *et al.*, 1969; Levin, 1978; Van Uitert and Eisenstadt, 1978; McKee and Ahad,

2004; Wong and White, 2013). Walsh and Levin manipulated their patients' CSF pressure through Queckenstedt manoeuvre (Walsh *et al.*, 1969) or CSF drainage (Levin, 1978); they both reached similar conclusions, namely that SVP disappears when the CSF pressure rises above 204 and 180 mmH2O respectively. However, other authors have reported isolated cases of patients with convincing SVP despite higher CSF pressure (Van Uitert and Eisenstadt, 1978; McKee and Ahad, 2004; Wong and White, 2013).

In the largest published series, Wong and White evaluated SVP and ICP in 106 consecutive patients admitted to hospital for lumbar puncture (Wong and White, 2013). They found that 85% of patients with raised ICP (which they defined as ≥30 cmH2O, equivalent to 22 mmHg) still had SVP, while 11% of patients with normal ICP had absent SVP, concluding that SVP (assessed with a direct ophthalmoscope) is not a reliable predictor of ICP. A significant limitation of Wong's study, and the other studies mentioned above is that CSF pressure was measured in the lateral decubitus position through lumbar punctures whereas SVP was assessed at a different time in either the supine or upright position. It is known that ICP drops when moving from supine to an upright position (Andresen *et al.*, 2015), and it is therefore possible that a previously obliterated SVP whilst supine could reappear on sitting up; this might explain a number of reported cases in which patients with SVP were reported to have high lumbar puncture opening pressures (Van Uitert and Eisenstadt, 1978; McKee and Ahad, 2004; Wong and White, 2013). Our study overcomes this issue through the simultaneous assessment of ICP and

SVP in the same (sitting) position, and the results confirm that under these conditions there is a significant correlation between ICP and SVP (95%CI -11.8 to -1.1, P=0.019, R-squared 0.43).

As with any clinical parameter, we would expect the ICP cut-off at which SVP is obliterated to vary between different individuals according to their individual anatomy and physiology. We found that SVP was invariably absent in patients with an ICP above 14 mmHg, and present in the great majority (95%) of patients whose ICP was below 7 mmHg (see Figure 7-2). In those patients with sitting ICP between 7 and 14 mmHg, around half (47%) had absent SVP, which might mean that in this range of moderately elevated ICP, anatomical variations play an important role in determining whether SVP is obliterated. Further studies on ICP dynamics in different positions are needed to resolve the physiological question of what upper limit of normal ICP should apply and what level of ICP is associated with morbidity.

While the use of infrared video recordings obtained with OCT machines has been occasionally reported before (Lee *et al.*, 2017), this is the first time that this approach has been validated by investigating the correlation between SVP and ICP. This technique has various advantages: it allows motion stabilisation, revealing subtle SVP while removing artefacts due to eye movements which could be mistaken for SVP; it allows comparison of videos from a given patient at different time points; and it allows ready assessment by different observers. In our cohort, IR video assessment of the SVP had a

high inter-rater reliability (kappa=0.81), much higher than that reported with a direct ophthalmoscope by Wong and White (kappa = 0.42) (Wong and White, 2013). Clearly, assessment of SVP through IR video recordings remains subjective and highly dependent on the examiner's experience and techniques to objectively measure SVP in these recordings will be needed in the future.

Our results also suggest that a patient without SVP (as judged using IR video recordings) is very likely to have an ICP above 7 mmHg in the sitting position. However, we also observed 3 cases in which SVP was absent despite the ICP being below 7 mmHg (i.e., a 'false positive' sign); indeed 2 of these patients had extremely negative sitting ICP (-12 and -7 mmHg respectively) requiring further management with shunt valve adjustment. Both these patients had severe optic atrophy from previous episodes of papilloedema. It has previously been found that advanced glaucomatous cupping is associated with absent SVP, possibly due to anatomical changes affecting venous resistance posterior to the lamina cribrosa (Morgan *et al.*, 2004), but no association between the absence of SVP and optic atrophy has been described in the literature. Alternatively, this could suggest the possibility that an excessively low ICP (as well as an abnormally elevated ICP) could alter the balance between CSF pressure and IOP obliterating SVP. All patients with SVP on IR video in this cohort had an ICP below 14mmHg (sitting) at the time of video recording, and a 24 hour mean ICP below 17.5mmHg (equivalent to 240mmH2O). Thus, the presence of SVP on

IR video does not exclude mildly elevated ICP but can help to exclude moderate-severe ICP elevation.

This study also reminds us that the absence of papilloedema does not exclude elevated ICP. The highest mean 24-hour ICP in a patient without any degree of disc swelling on OCT was 25.8mmHg (350mmH2O).

The main limitation of the IR video assessment technique is that the Spectralis and comparable imaging systems are not portable and can only examine patients in a sitting position; the technique is thus limited in its applicability to severely ill patients. Further work is needed to develop the use of portable imaging systems to allow SVP assessment in a wider range of clinical environments. Moreover, fundus video interpretation requires experienced assessors to identify SVP. Automated interpretation of fundus video recordings to quantify SVP would reduce dependence on expert assessors, potentially facilitating its application in environments with limited access to experienced clinicians. Further limitations are the small number of patients with absent SVP and the heterogeneity of the group. Larger studies including more patients without SVP and higher numbers of representatives for each clinical group would allow a more precise interpretation of the validity of SVP as a diagnostic sign.

7.6. Conclusions

In conclusion, our results confirm that there is a significant correlation between SVP and ICP and support the utility of performing SVP

assessments using OCT IR video recordings in patients with suspected abnormal CSF pressure. Further work is needed to develop a technique that could be used in bed-bound patients and to automate the assessment of SVP.

Chapter 8. Brain MRI and ophthalmic biomarkers of intracranial pressure

8.1. Abstract

8.1.1. Background

Currently available intracranial pressure (ICP) monitoring techniques are invasive. Biomarkers of intracranial hypertension could provide a non-invasive alternative for the investigation of patients with suspected cerebrospinal fluid (CSF) dynamics disturbances. This is the first study using a combination of ophthalmic and imaging biomarkers for the prediction of intracranial hypertension. Additionally, for the first time the intracranial compliance (using pulse amplitude as a marker) of patients with and without abnormal biomarkers was described.

8.1.2. Methods

This single-centre observational study includes patients who underwent 24-hour ICP monitoring, brain MRI (within three months) and ophthalmic assessment (during ICP monitoring). Six biomarkers were investigated: pituitary gland shape, vertical tortuosity of the optic nerve, distension of the optic nerve sheath, optic disc protrusion (MRI), papilloedema (slit lamp biomicroscopy) and spontaneous venous pulsations (SVP, infrared video recordings).

8.1.3. Results

Forty-five patients (mean age 39±14SD, 38 females) met the inclusion criteria. All 6 biomarkers had a significant association with 24-hour ICP. Concave pituitary gland was observed with moderately elevated median ICP. Protrusion of the optic disc (MRI), papilloedema and absence of SVP were associated with the highest median ICP values. Pulse amplitude was also significantly higher for patients with abnormal biomarkers (except for distension of the optic nerve sheath). Twenty patients had raised ICP (median 24-hour ICP>5.96 mmHg, cut-off obtained through Youden index calculation). Patients with all normal biomarkers had normal median ICP in 94% (St.Err.=6%) of the cases. All the patients with 3 or more abnormal biomarkers had intracranial hypertension. The combination of at least one abnormal biomarker in MRI and ophthalmic assessments was highly suggestive of intracranial hypertension (AUC 0.94, 95% CI 0.93-0.94).

8.1.4. Conclusions

Brain MRI and ophthalmic biomarkers can non-invasively guide the management of patients with suspected CSF dynamics abnormalities. Patients with multiple abnormal biomarkers (≥3) or a combination of abnormal MRI and ophthalmic biomarkers are likely to have intracranial hypertension and should be managed promptly.

8.2. Introduction

Intracranial pressure (ICP) is an important physiological parameter and its measurement assists clinicians in the diagnosis and management of a

variety of diseases. To this date, ICP assessment still requires invasive methods including lumbar punctures and intraparenchymal ICP monitoring with intracranial bolts. Several non-invasive methods to detect intracranial hypertension have been suggested, however, none of these techniques has yet been able to replace invasive ICP measurements (Raboel *et al.*, 2012; Canac *et al.*, 2020; Price *et al.*, 2020).

Brain MRIs and ophthalmic exams are non-invasive assessments commonly performed in elective patients with suspected raised ICP and are accessible in most non-emergency clinical settings. Brain MRI markers such as the shape of the pituitary gland, vertical tortuosity of the optic nerves and distension of the optic nerve sheath can be useful signs of raised ICP in patients with Idiopathic Intracranial Hypertension (IIH) (Brodsky and Vaphiades, 1998; Yuh *et al.*, 2000; Agid *et al.*, 2006; Rohr *et al.*, 2011; Passi *et al.*, 2013; Bidot *et al.*, 2015; Holbrook and Saindane, 2017; Moreno-Ajona *et al.*, 2020; Rehder, 2020). In addition to the presence of papilloedema (Funnell *et al.*, 2018), the absence of spontaneous venous pulsations (SVP) on infrared videography has been shown to have a strong correlation with raised ICP and represents a good ophthalmic marker for the prediction of intracranial hypertension (D'Antona *et al.*, 2019b).

Previous studies have separately looked at ophthalmic or brain MRI correlates of ICP and in most cases relied on lumbar punctures for the measurement of ICP. To our knowledge this is the first study assessing both

brain MRI and ophthalmic biomarkers of ICP in a population of patients undergoing elective 24-hour ICP monitoring for suspected cerebrospinal fluid (CSF) dynamics abnormalities. This is also the first time that the association of such biomarkers and pulse amplitude (PA) is investigated. PA is recognised as a good marker of intracranial compliance and can help in the identification of patients with isolated abnormal intracranial compliance without intracranial hypertension (e.g., Chiari malformation type I and NPH) (Chari *et al*., 2017; Evensen and Eide, 2020). The primary objective of this study is to identify which biomarkers are associated with the highest levels of ICP, and the secondary objective is to determine which biomarkers have the best positive and negative predictive values for detecting elevated ICP. Finally, a description of the pulse PA in patients with and without abnormal biomarkers is provided.

8.3. Methods

This is a single centre retrospective observational study conducted at the National Hospital for Neurology and Neurosurgery (London, UK). This study has been approved by the North East-Newcastle & North Tyneside 2 Research Ethics Committee and the Health Research Authority (20/NE/0127). Due to its retrospective nature, written consent was waived.

8.3.1. Participants

This study includes a consecutive series of patients investigated with elective 24-hour ICP monitoring in the period between January 2017 and February

2020. We searched our ICP monitoring database to identify patients meeting the following eligibility criteria: (i) investigated with elective 24-hour ICP monitoring for suspected CSF dynamics disorder (e.g., IIH, Chiari, hydrocephalus, spontaneous intracranial hypotension, shunt malfunction), (ii) brain MRI performed within 3 months of the ICP monitoring with no intervention performed in between events and (iii) ophthalmic examination performed by an ophthalmologist during the 24-hour ICP monitoring period including assessment of papilloedema (by slitlamp biomicroscopy) and SVP (by infrared video recordings) (D'Antona *et al.*, 2019b; McHugh *et al.*, 2020).

8.3.2. ICP monitoring

The clinical indications for 24-hour ICP monitoring were routinely discussed within a multidisciplinary team including neurosurgeons, neurologists and ophthalmologists. ICP monitoring was performed according to an established standardised protocol (Chari *et al.*, 2017; Thompson *et al.*, 2017a). On the morning of admission, the patients had a right frontal intraparenchymal ICP measuring sensor inserted in the operating theatre under local anaesthesia. High frequency ICP data (100 Hz) were collected for a continuous period of 24 hours. During the daytime monitoring period, patients were encouraged to mobilise to simulate their usual level of activity. At the end of the 24 hours, the ICP raw data were downloaded and processed through the software ICM+© (University of Cambridge, UK). This analysis resulted in a mean ICP and PA value for each minute of recording (minute-by-minute results). The results were then summarised in terms of median ICP and PA over the entire

24 hours. A detailed description of the 24-hour ICP monitoring procedure employed at our institution can be found above (page 100). For the interpretation of the ICP monitoring results, it should be noted that patients considered to have 'normal' ICP monitoring results with this technique have previously been reported to have a median 24-hour ICP of 3.21 mmHg (95% CI 2.29–4.13) and a median 24-hour PA of 4.12 mmHg (95% CI 3.72-4.52) (Chari *et al.*, 2017).

8.3.3. Brain MRI imaging assessment

Brain MRIs performed within 3 months of the ICP monitoring period were selected. The imaging evaluation was performed by two independent trained assessors (Mr Hasan Asif and Miss Claudia L. Craven) masked to the 24-hour ICP results. Discordances between the two assessors were settled through consensus. Four imaging markers were assessed and graded as binary variables (normal/abnormal): pituitary gland shape, vertical tortuosity of the optic nerves, protrusion of the optic disc and distension of the optic nerve sheath (Holbrook and Saindane, 2017). Figure 8-1 shows examples of the brain MRI biomarkers of intracranial hypertension. The pituitary gland shape was assessed according to the classification proposed by Yuh *et al.* in 2000 (Yuh *et al.*, 2000). A concavity of the pituitary gland of more than 1/3 of the height of the sella was considered abnormal, this corresponds to categories III, IV and V of the Yuh classification system and includes both empty and partially empty sella (Figure 8-1 A). Protrusion of the optic disc was confirmed when the sclera was concave at the point of attachment of the

optic nerve with associated intraocular protrusion of the disc (Figure 8-1 B) (Agid *et al.*, 2006; Passi *et al.*, 2013). The vertical tortuosity of the optic nerve was defined as a 'S-shaped' appearance of the optic nerve on sagittal views (Figure 8-1 C) (Agid *et al.*, 2006). Similarly, to Agid *et al.*, the optic nerve sheath was considered distended when the CSF in the subarachnoid space surrounding the optic nerve was wider than 2 mm at any point within the 10 mm behind the globe (Figure 8-1 B) (Agid *et al.*, 2006). Distension of the optic nerve sheath, optic nerve sheath protrusion and vertical tortuosity of the optic nerve were classified as abnormal whether present unilaterally or bilaterally. T1-weighted sagittal MRI sequences were used to assess pituitary gland shape and vertical tortuosity of the optic nerves, while T2-weighted axial MRI sequences (non-fat-suppressed) were used to assess optic disc protrusion and optic nerve sheath distension.

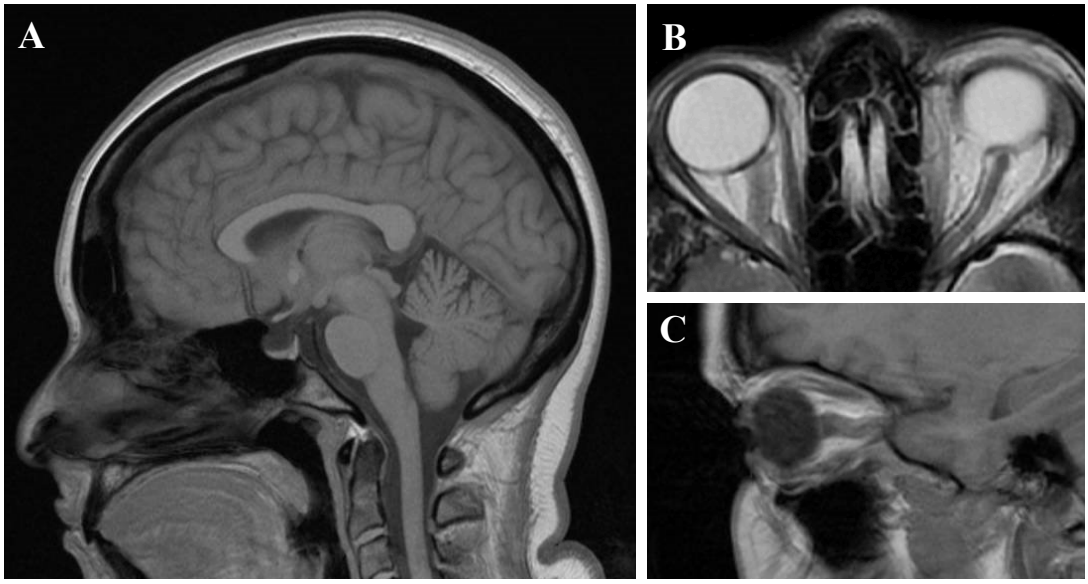


Figure 8-1: Example of the brain MRI biomarkers of intracranial hypertension.

(A) T1-weighted sagittal brain MRI showing a partially empty sella; (B) T2-weighted axial brain MRI showing protrusion of the left optic nerve head and optic nerve sheath distension; (C) T1-weighted sagittal brain MRI showing vertical tortuosity of the optic nerve.

8.3.4. Ophthalmic Assessment

Ophthalmic assessments were performed during the 24-hour ICP monitoring period and included slit lamp assessment of papilloedema (Frisén grading), intraocular pressure (IOP) and motion-stabilised SVP infrared videography. Papilloedema was defined as Frisén grade 2 or greater during slit lamp exam in at least one eye. The SVP videos were graded by two independent assessors (Mr James A. McHugh and Mr Fion Bremner) according to the grading system proposed by Hedges *et al.* (Hedges *et al.*, 1994). The two assessors were masked to the ICP results. Absence of SVP was defined as grade 0 SVP bilaterally as judged by both the assessors. Further details on

the methods of assessment and interpretation of SVP were previously published (D'Antona *et al.*, 2019b; McHugh *et al.*, 2020).

8.3.5. Statistical analysis

8.3.5.1. Association between biomarkers and ICP

The mean 24-hour ICP of the patients with normal and abnormal biomarkers were compared (Mann-Whitney U test). The strength of the association between ICP and the 6 biomarkers was evaluated through Receiver Operating Characteristic (ROC) curves and Areas Under the Curves (AUC). The strength of the associations was defined as acceptable (AUC 0.7 to 0.8), excellent (AUC 0.8 to 0.9) or outstanding (AUC >0.9). Frequency distribution analyses were used to describe the time-ICP burden for each biomarker and identify the biomarkers associated with the highest (and lowest) level of ICP. ROC and frequency distribution analyses were performed using the patients' minute-by-minute ICP monitoring results (about 1440 ICP values per patient).

8.3.5.2. Association between biomarkers and PA

Similar analyses were performed to test the association of the 6 biomarkers with 24-hour PA values. In particular, ROC and AUC were built to assess the strength of associations and frequency distribution analyses to describe the time-PA burden for each biomarker.

8.3.5.3. Predictive value of the 6 biomarkers

A ROC curve analysis using mean minute-by-minute ICP data (predictor) and normal versus abnormal biomarkers (binary classifier) was performed to identify the optimal median 24-hour ICP cut-off (Youden index). The positive and negative predictive values (PPV and NPV) of the biomarkers in identifying intracranial hypertension were calculated.

Due to the exploratory and retrospective nature of the study a formal sample size calculation was not performed and all eligible patients were identified and included in the study. Continuous variables were summarised as means (standard deviation) and categorical variables as percentages. A significance level 0.05 was used. Microsoft® Excel for Mac (version 16.25), Stata© (version 15.0) and GraphPad Prism for macOS (version 8.4.1) were used for the data collection and statistical analysis.

8.4. Results

Between January 2017 and February 2020, 400 patients underwent elective continuous 24-hour ICP monitoring. Forty-five patients met the eligibility criteria and were included in the study (Figure 8-2).

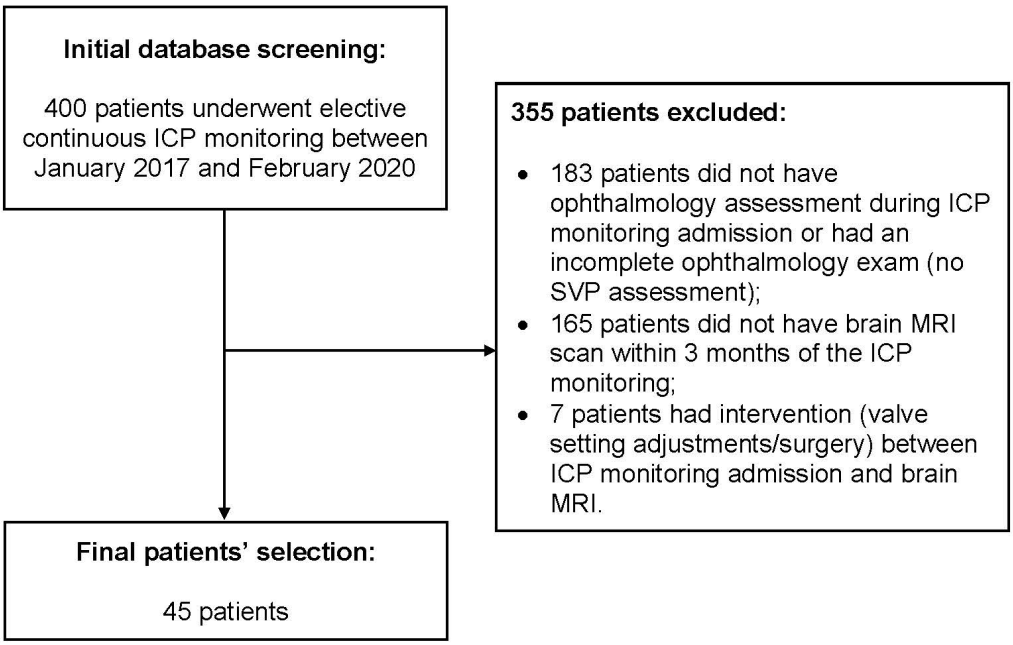


Figure 8-2: Flowchart of patients' screening and inclusion

The baseline demographic characteristics, indications for 24-hour ICP monitoring, results of ICP monitoring, brain MRI features and ophthalmology findings are summarised in Table 8-1. The average interval time between brain MRI and 24-hour ICP monitoring was 36 (SD 31) days, while all ophthalmology exams were performed during the ICP monitoring period.

Table 8-1: Baseline patients' characteristics

Demographic characteristics	
Age, mean (SD)	39 (14)
Sex, n (%)	
- Females, n (%)	38 (84)
- Males, n (%)	7 (16)
Clinical indications for 24-hour ICP monitoring	
- Suspected CSF dynamics disorder causing headache (e.g., IIH, SIH)	22 (49)
- Suspected CSF shunt malfunction	12 (27)
- Hydrocephalus	7 (16)
- Chiari malformation	3 (7)
- Suspected NPH	1 (2)
ICP monitoring results in mmHg	
- 24-hour ICP, mean[a] (SD)	7.8 (8)
- 24-hour PA, mean[a] (SD)	6.3 (3.2)
Brain MRI results	
- Concave pituitary gland or empty sella, n (%)	24 (53)
- Optic nerve sheath distension, n (%)	15 (33)

- Vertical tortuosity of optic nerves, n (%)	13 (29)
- Protrusion of the optic disc, n (%)	4 (9)
Ophthalmology results	
- Absence of SVP, n (%)	10 (22)
- Papilloedema, n (%)	2 (4)
- IOP in mmHg, mean[b] (SD)	15.3 (3)

[a] Mean of the patients' median results; [b] Mean of all eyes.

CSF: Cerebrospinal Fluid; ICP: Intracranial Pressure; IIH: Idiopathic Intracranial Hypertension; SD: Standard Deviations; SIH: Spontaneous Intracranial Hypotension; SVP: Spontaneous Venous Pulsation

8.4.1. ICP monitoring results by normal/abnormal biomarker

Table 8-2, Figure 8-3 and Figure 8-4 describe the mean (SD) ICP and PA results of the patients stratified by imaging and ophthalmic findings. 24-hour median ICP results were significantly higher in patients with abnormal biomarkers compared to patients in whom the markers were normal (Mann-Whitney U, $p<0.05$ in all 6 analyses, Table 8-2). 24-hour median PA results were significantly higher in patients with abnormal pituitary gland shape, vertical tortuosity of the optic nerves, protrusion of the optic disc, absence of SVP and papilloedema (Mann-Whitney U, $p<0.05$, Table 8-2).

Table 8-2: Intracranial pressure monitoring results (in mmHg) stratified by imaging and ophthalmic biomarkers

	Normal marker	**Abnormal marker**	**P value[b]**
Pituitary gland shape	N=21	N=24	
- 24-hour ICP, mean[a] (SD)	2.4 (3.4)	12.6 (8.1)	<0.001
- 24-hour PA, mean[a] (SD)	4.6 (1.6)	7.8 (3.4)	<0.001
Optic nerve sheath distension	N=30	N=15	
- 24-hour ICP, mean[a] (SD)	4.7 (5.7)	14.0 (8.9)	<0.001
- 24-hour PA, mean[a] (SD)	5.5 (2.0)	7.9 (4.3)	0.10
Vertical tortuosity of optic	N=32	N=13	

nerves			
- 24-hour ICP, mean[a] (SD)	4.6 (5.9)	15.9 (7.4)	<0.001
- 24-hour PA, mean[a] (SD)	5.4 (2.5)	8.5 (3.4)	0.001
Protrusion of the optic disc	N= 41	N= 4	
- 24-hour ICP, mean[a] (SD)	6.2 (6.5)	24.2 (4.3)	0.002
- 24-hour PA, mean[a] (SD)	5.6 (2.2)	13.3 (2.8)	<0.001
Spontaneous venous pulsation	N=35	N=10	
- 24-hour ICP, mean[a] (SD)	4.7 (4.1)	18.9 (9.1)	<0.001
- 24-hour PA, mean[a] (SD)	5.2 (1.7)	10.3 (3.8)	<0.001
Papilloedema	N=43	N=2	
- 24-hour ICP, mean[a] (SD)	7.1 (7.4)	23.1 (9.6)	0.04
- 24-hour PA, mean[a] (SD)	6.0 (2.8)	12.8 (4.2)	0.024

[a] Mean of the patients' median results; [b] Mann-Whitney U test; ICP: Intracranial Pressure; PA: Pulse Amplitude.

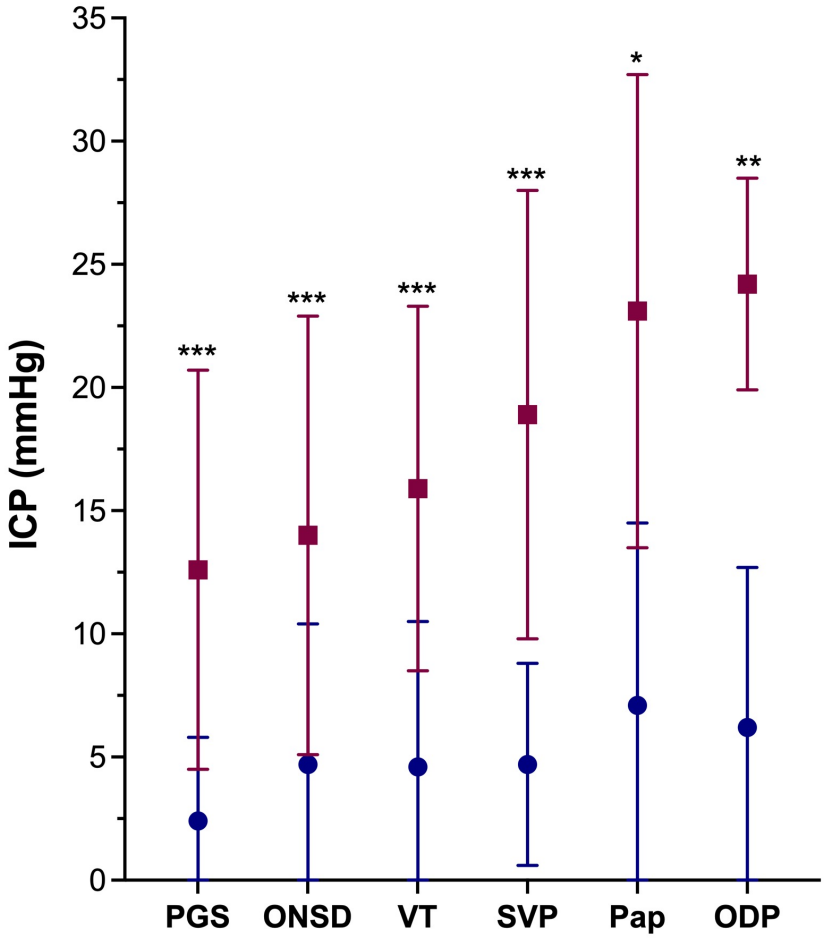


Figure 8-3: Mean (SD) intracranial pressure (ICP) stratified by normal (blue) and abnormal (red) biomarkers

ICP: Intracranial Pressure, PGS: Pituitary Gland Shape, ONSD: Optic Nerve Sheath Distension, VT: Vertical Tortuosity of the Optic Nerves, SVP: Spontaneous Venous Pulsation, Pap: Papilloedema, ODP: Optic Disc Protrusion.

Mann-Whitney U test comparing mean ICP in patients with normal versus abnormal biomarker. *p <0.05, **p<0.01, ***p<0.001

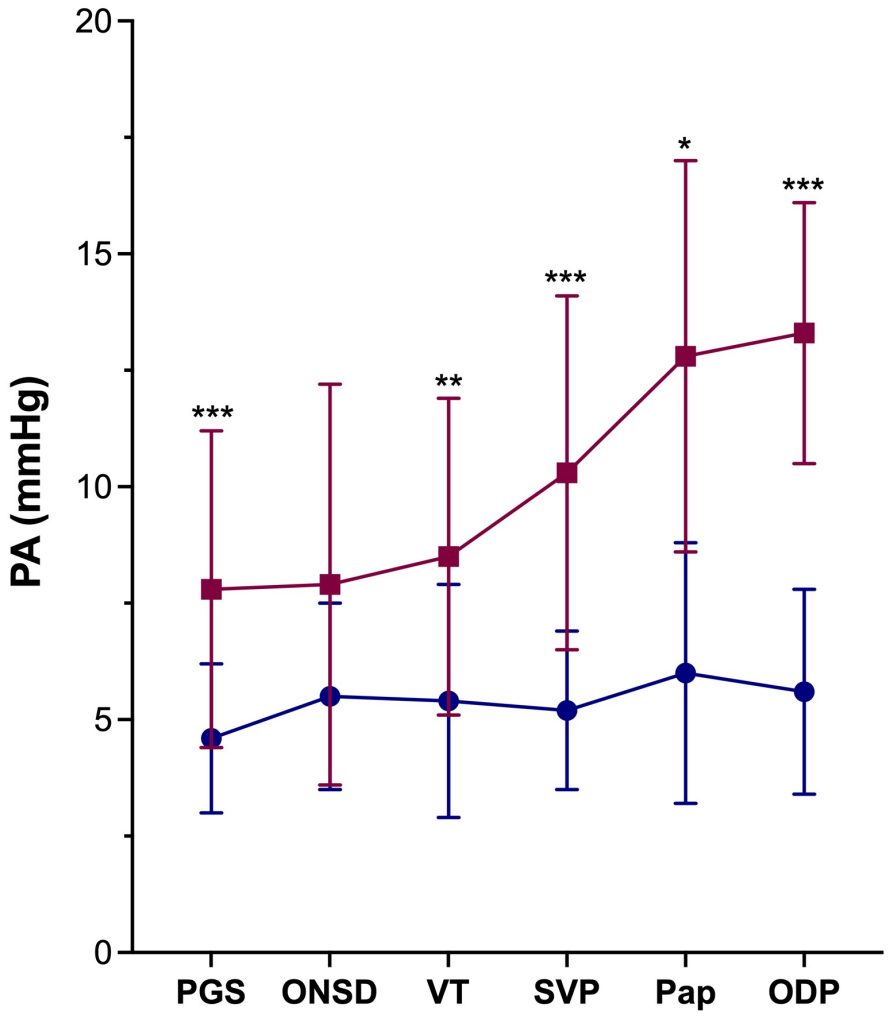


Figure 8-4: Mean (SD) pulse amplitude (PA) stratified by normal (blue) and abnormal (red) biomarkers

PA: Pulse Amplitude, PGS: Pituitary Gland Shape, ONSD: Optic Nerve Sheath Distension, VT: Vertical Tortuosity of the Optic Nerves, SVP: Spontaneous Venous Pulsation, Pap: Papilloedema, ODP: Optic Disc Protrusion.

Mann-Whitney U test comparing mean PA in patients with normal versus abnormal biomarker. *p <0.05, **p<0.01, ***p<0.001

8.4.2. Time-ICP burden analysis

The minute-by-minute patients' ICP values (70,467 observations) were extracted and plotted in frequency distribution graphs according to biomarker results (normal/abnormal). Patients with an abnormal (concave) pituitary gland shape (or empty sella) had a median ICP of 10 mmHg (Figure 8-5); this value indicates intracranial hypertension but is lower than the median ICP levels associated with other abnormal biomarkers (Figure 8-6, Figure 8-7, Figure 8-8, Figure 8-9 and Figure 8-10). Protrusion of the optic disc detected on MRI imaging and papilloedema were associated with the highest ICP levels and the patients with either one of these signs had a median ICP of 24 mmHg (Figure 8-9 and Figure 8-10).

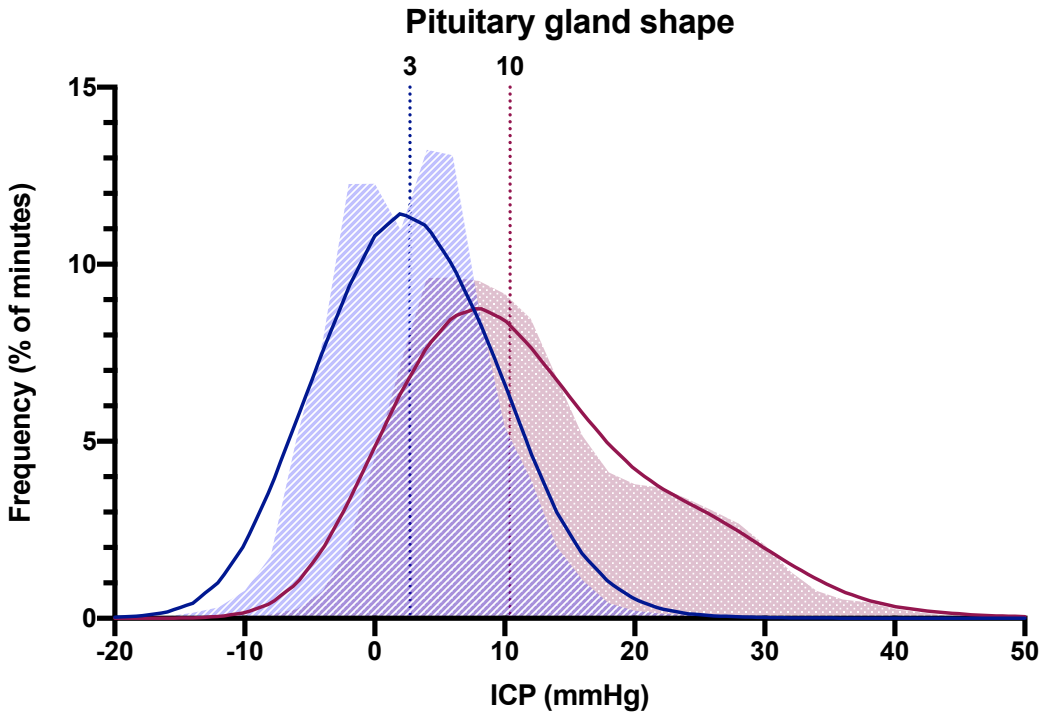


Figure 8-5: Frequency distribution of minute-by-minute Intracranial Pressure (ICP) measurements in patients presenting with normal (blue) and abnormal (red) pituitary gland shape.

LOWESS smoothing line and median ICP are marked.

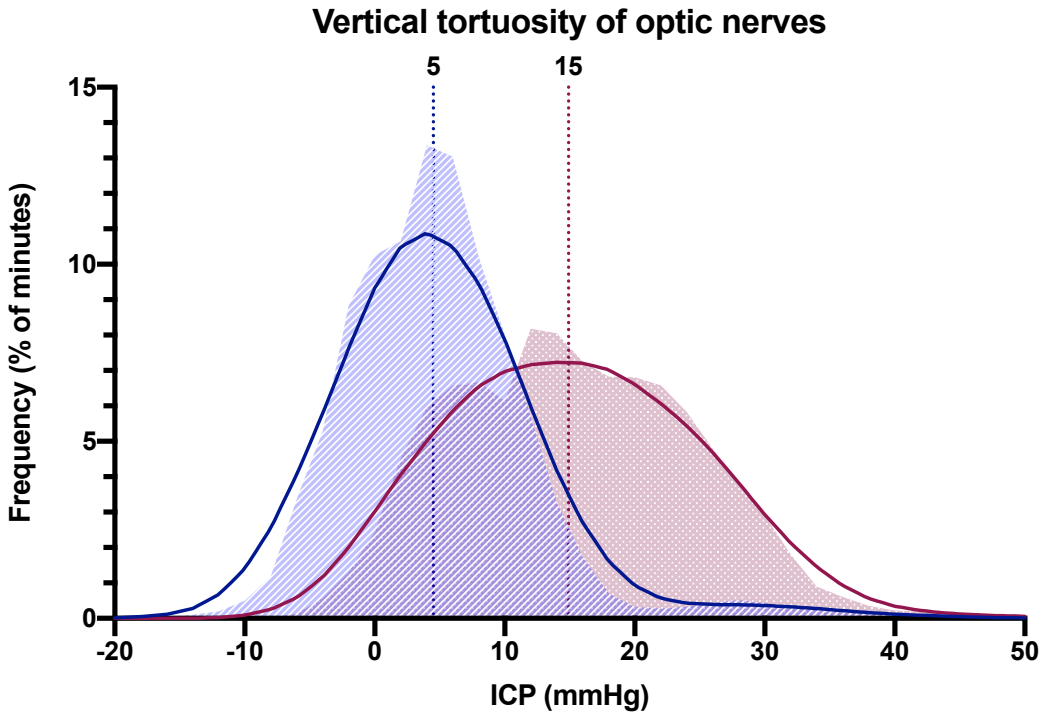


Figure 8-6: Frequency distribution of minute-by-minute Intracranial Pressure (ICP) measurements in patients without (blue) and with vertical tortuosity of the optic nerves (red).

LOWESS smoothing line and median ICP are marked.

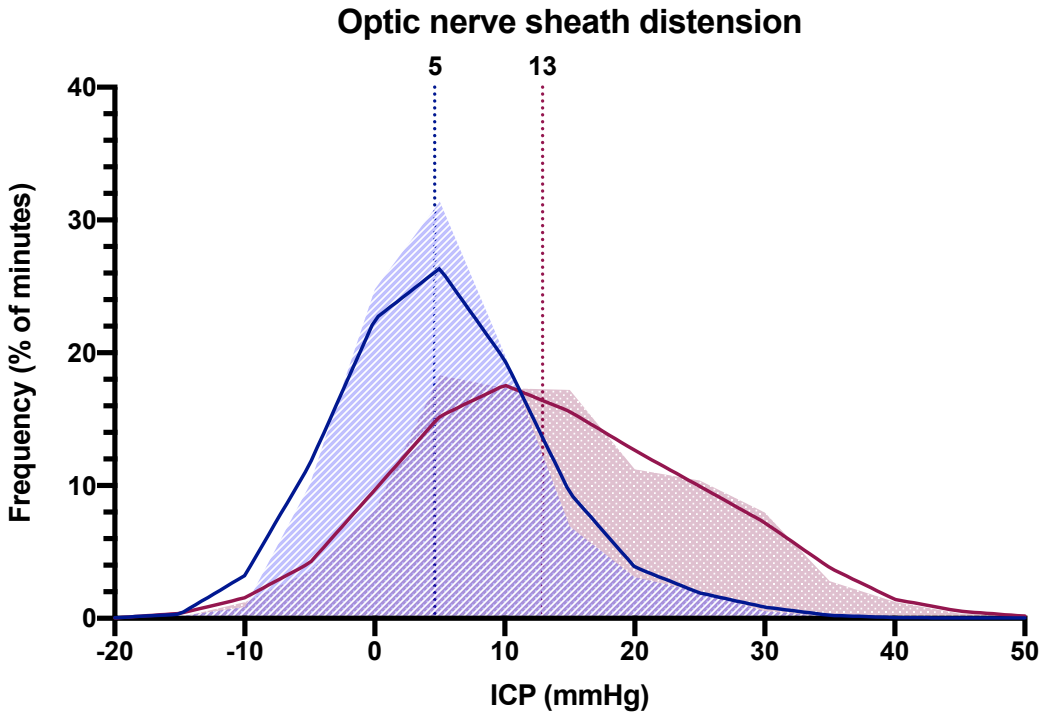


Figure 8-7: Frequency distribution of minute-by-minute Intracranial Pressure (ICP) measurements in patients without (blue) and with optic nerve sheath distension (red).

LOWESS smoothing line and median ICP are marked.

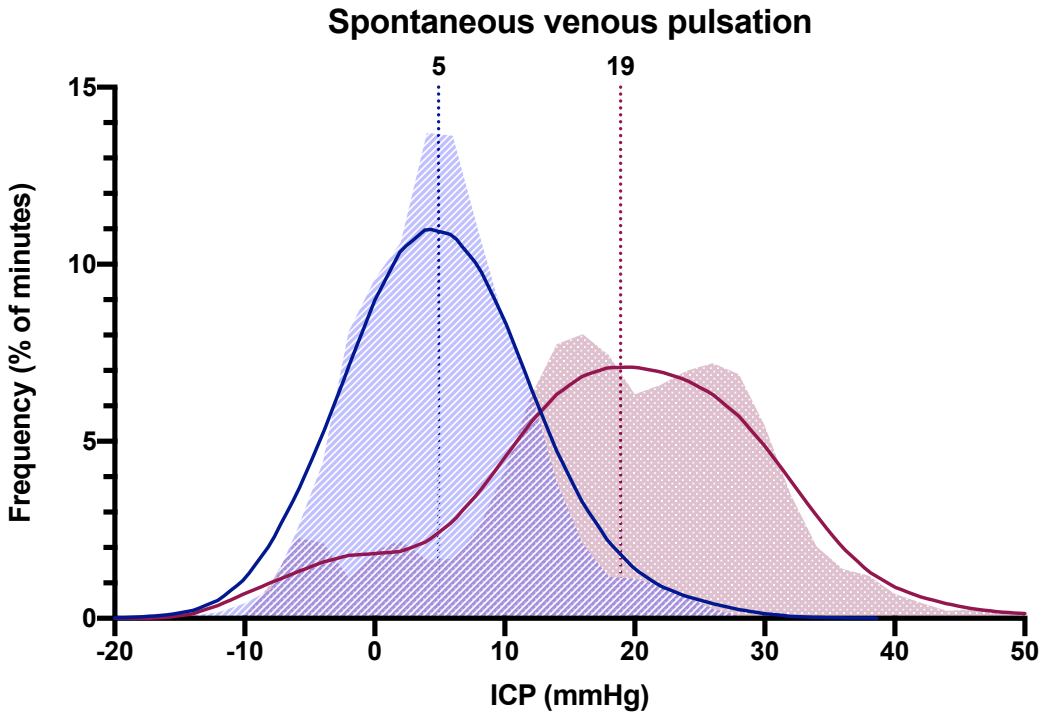


Figure 8-8: Frequency distribution of minute-by-minute Intracranial Pressure (ICP) measurements in patients with presence (blue) and absence of spontaneous venous pulsations (red).

LOWESS smoothing line and median ICP are marked.

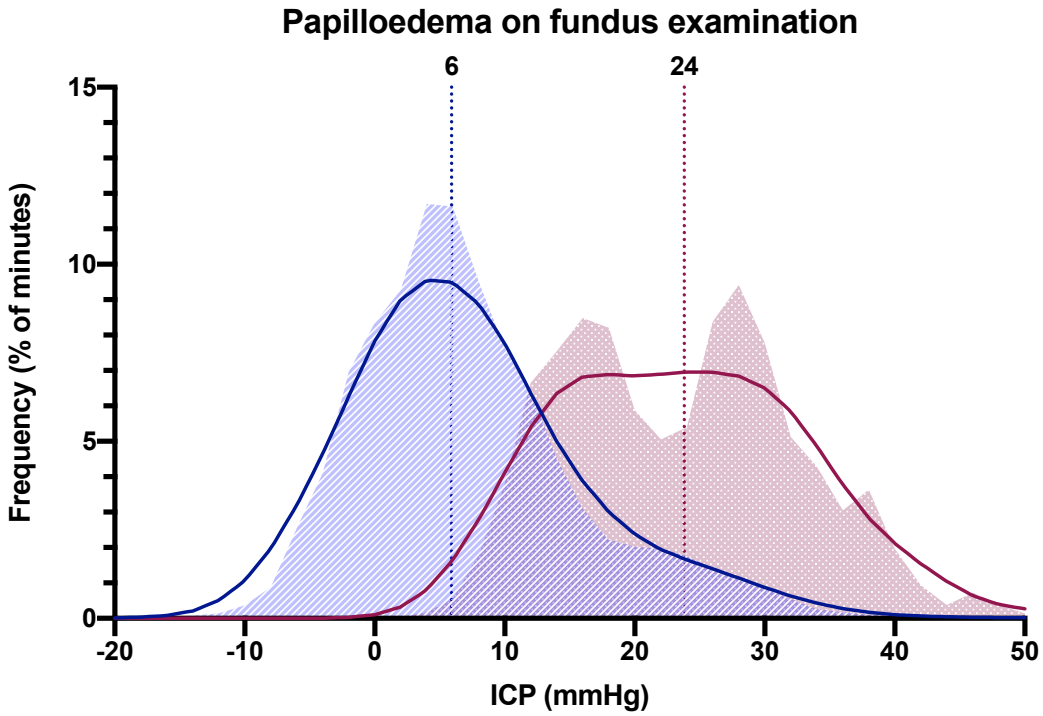


Figure 8-9: Frequency distribution of minute-by-minute Intracranial Pressure (ICP) measurements in patients without (blue) and with papilloedema (red).

LOWESS smoothing line and median ICP are marked.

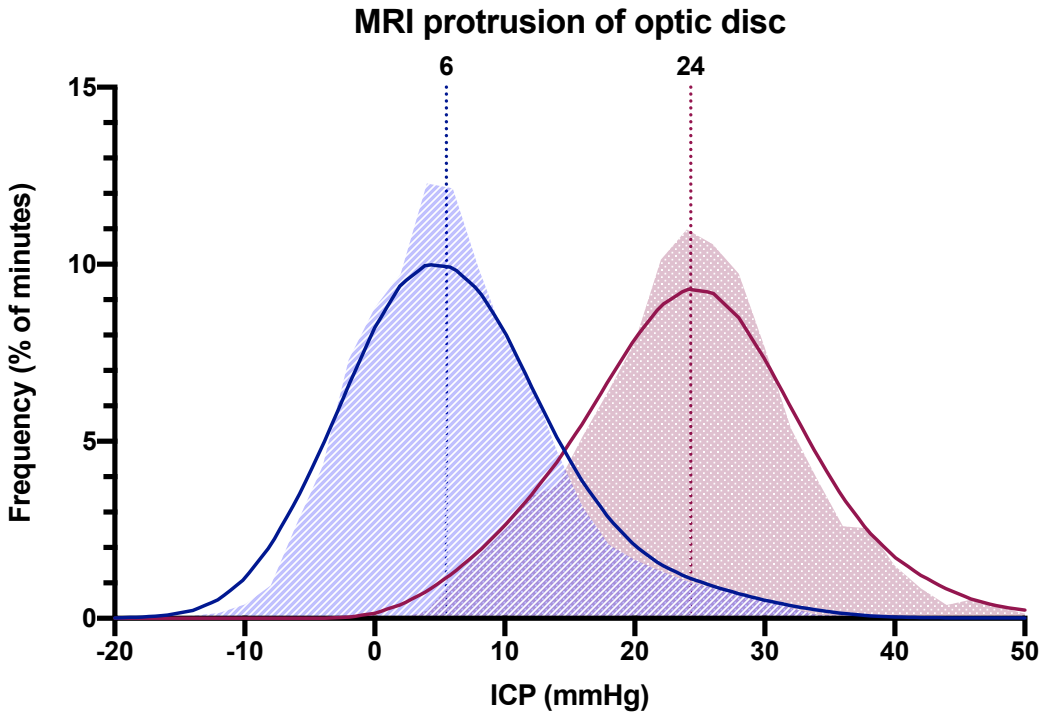


Figure 8-10: Frequency distribution of minute-by-minute Intracranial Pressure (ICP) measurements in patients without (blue) and with protrusion of the optic disc on MRI imaging (red).

LOWESS smoothing line and median ICP are marked.

8.4.3. Time-PA burden analysis

The minute-by-minute patients' PA values (70,467 observations) were extracted and plotted in frequency distribution graphs according to their biomarker results. Patients with absence of SVP, papilloedema or optic disc protrusion on MRI imaging spent most of the time with PA levels above 10 mmHg, which are clearly high (Figure 8-14, Figure 8-15 and Figure 8-16) (Chari *et al.*, 2017). Also patients with abnormal pituitary gland shape, vertical tortuosity of the optic nerves and/or optic nerve sheath distension

had high pulse amplitude (Figure 8-11, Figure 8-12 and Figure 8-13), but in these cases the median PA was lower compared to the other biomarkers.

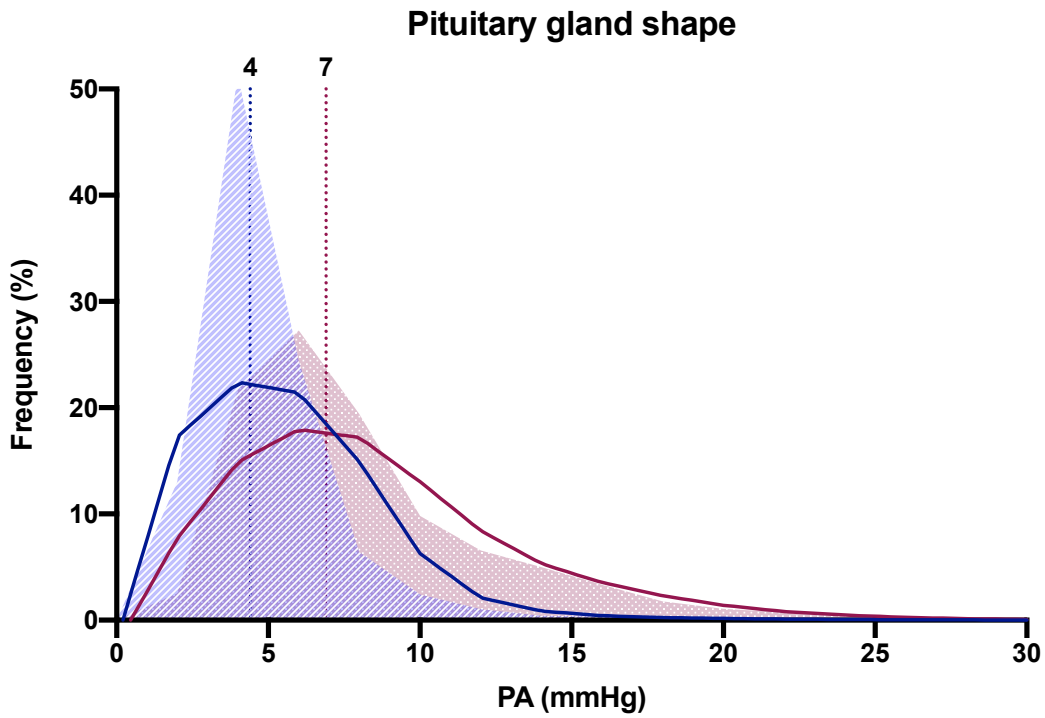


Figure 8-11: Frequency distribution of minute-by-minute Pulse Amplitude (PA) measurements in patients presenting with normal (blue) and abnormal (red) pituitary gland shape.

LOWESS smoothing line and median PA are marked.

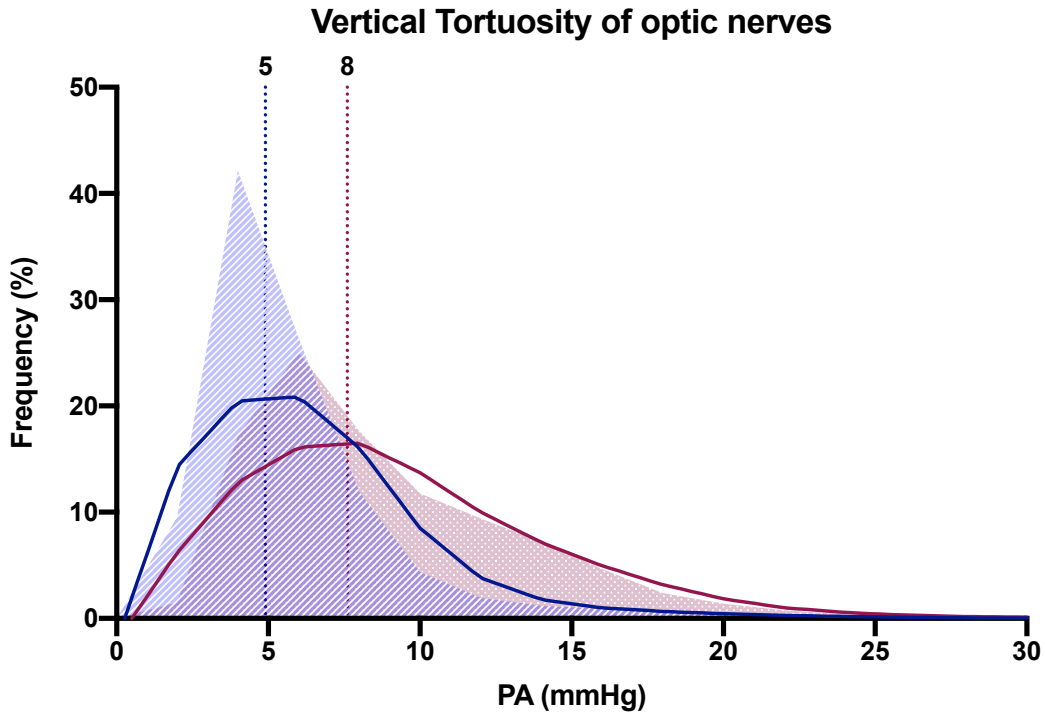


Figure 8-12: Frequency distribution of minute-by-minute Pulse Amplitude (PA) measurements in patients without (blue) and with vertical tortuosity of the optic nerves (red).

LOWESS smoothing line and median PA are marked.

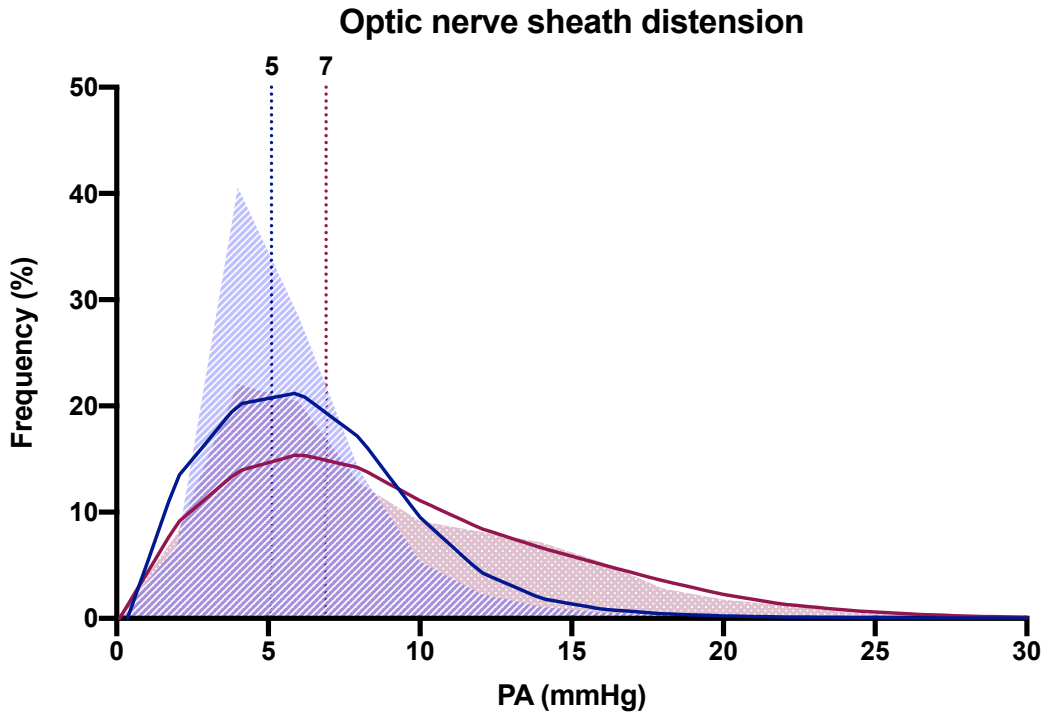


Figure 8-13: Frequency distribution of minute-by-minute Pulse Amplitude (PA) measurements in patients without (blue) and with optic nerve sheath distension (red).

LOWESS smoothing line and median PA are marked.

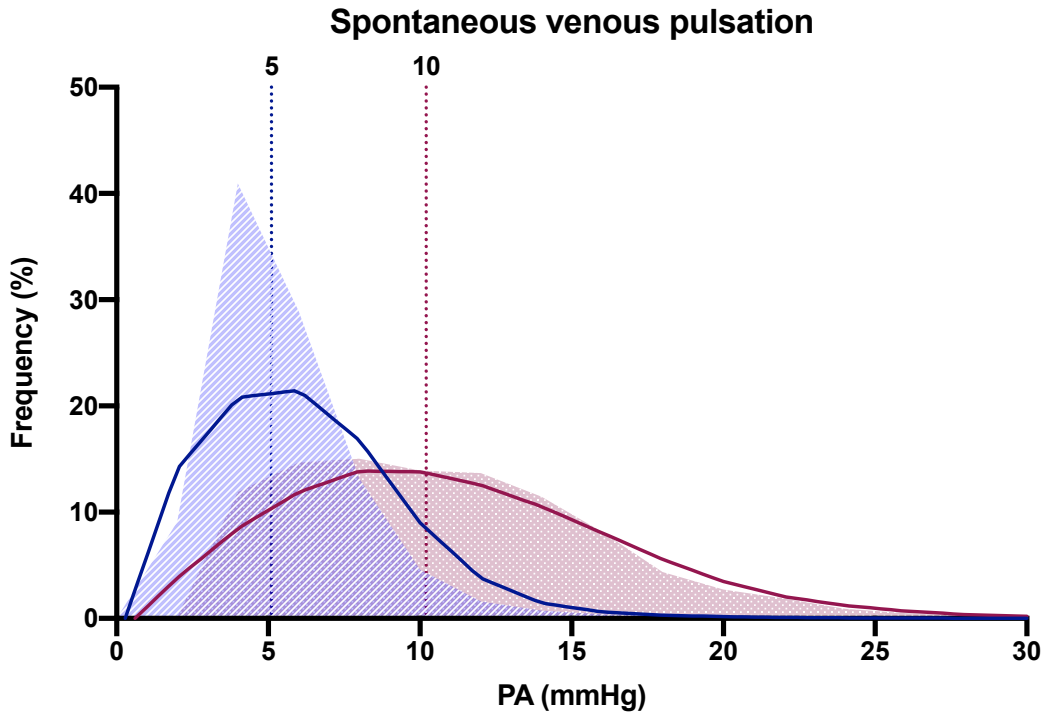


Figure 8-14: Frequency distribution of minute-by-minute Pulse Amplitude (PA) measurements in patients with presence (blue) and absence of spontaneous venous pulsations (red).

LOWESS smoothing line and median PA are marked.

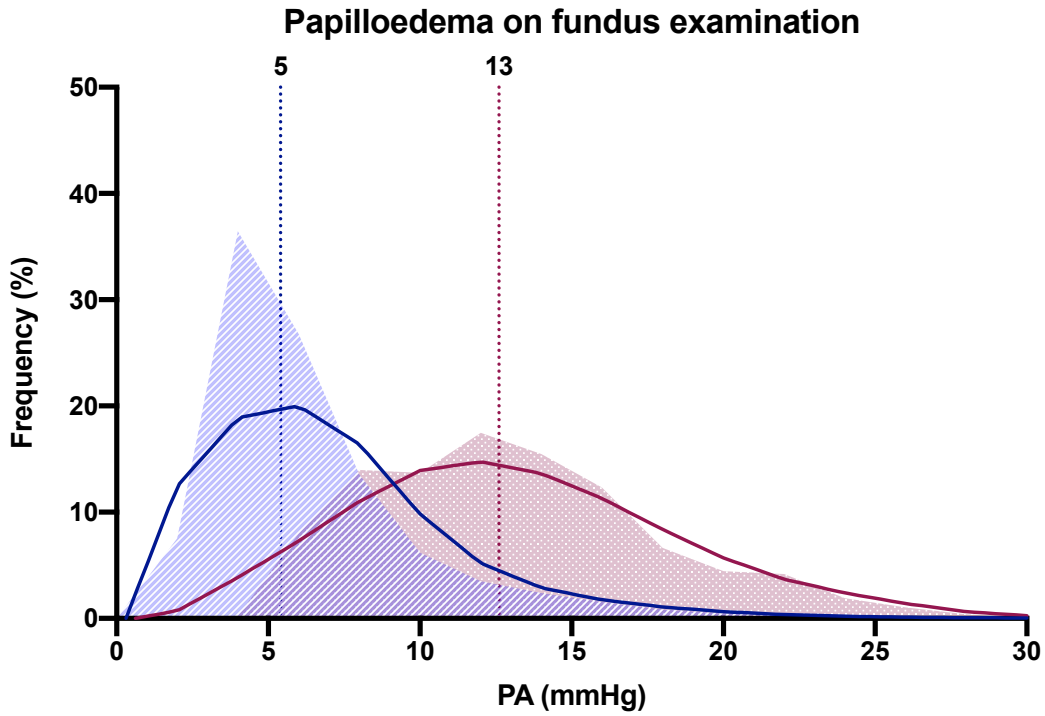


Figure 8-15: Frequency distribution of minute-by-minute Pulse Amplitude (PA) measurements in patients without (blue) and with papilloedema (red).

LOWESS smoothing line and median PA are marked.

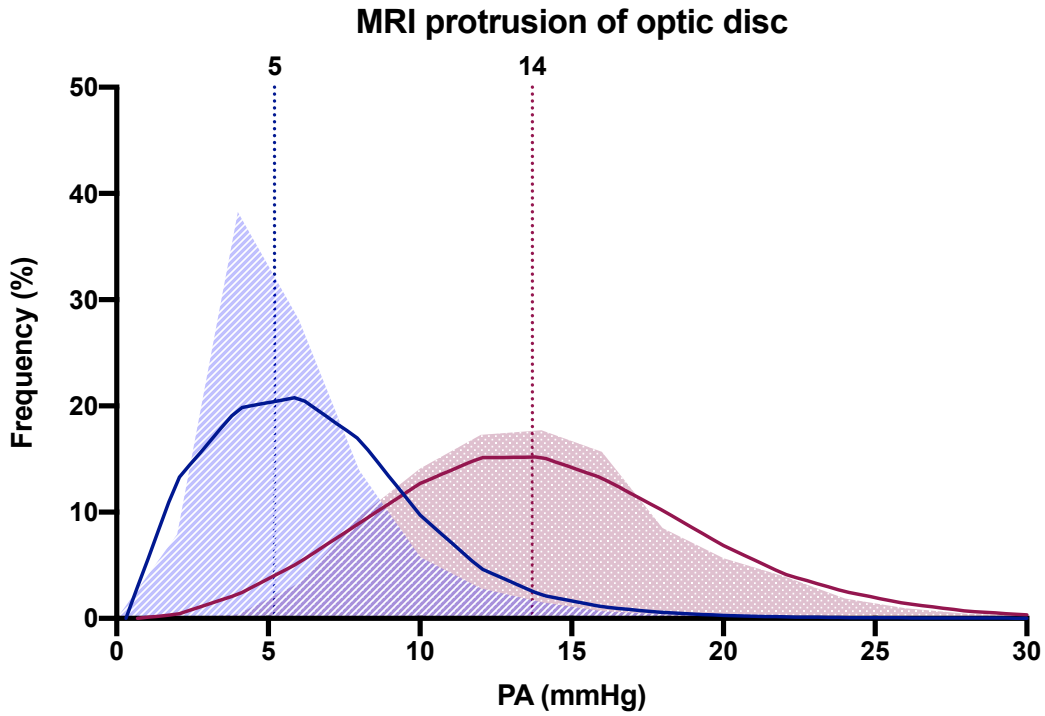


Figure 8-16: Frequency distribution of minute-by-minute Pulse Amplitude (PA) measurements in patients without (blue) and with protrusion of the optic disc on MRI imaging (red).

LOWESS smoothing line and median PA are marked.

8.4.4. Biomarkers and their association with ICP

ROC curve analyses showed that ICP measurements (minute-by-minute) had an outstanding association (AUC > 0.90) with optic disc protrusion detected on MRI imaging (AUC=0.94, 95% CI 0.93-0.94). The associations with ICP (minute-by-minute) were excellent (AUC between 0.8 and 0.9) for vertical tortuosity of the optic nerves (AUC=0.82, 95% CI 0.81-0.82) and pituitary gland shape (AUC=0.80, 95% CI 0.79-0.81). The association with

ICP (minute-by-minute) was acceptable (AUC between 0.70 and 0.80) for the distension of the optic nerve sheath (AUC=0.75, 95% CI 0.74-0.75).

Patients with absence of SVP (n=10) had a mean ICP of 19 mmHg and patients with papilloedema (n=2) had a mean ICP of 23 mmHg (Table 8-2). The minute-by-minute ICP had an excellent association (AUC between 0.80 and 0.90) with both papilloedema (AUC=0.90, 95% CI 0.90-0.91) and absence of SVP (AUC=0.85, 95% CI 0.84-0.85).

Figure 8-17 and Figure 8-18 show the ROC curve analyses and AUCs of the 6 biomarkers.

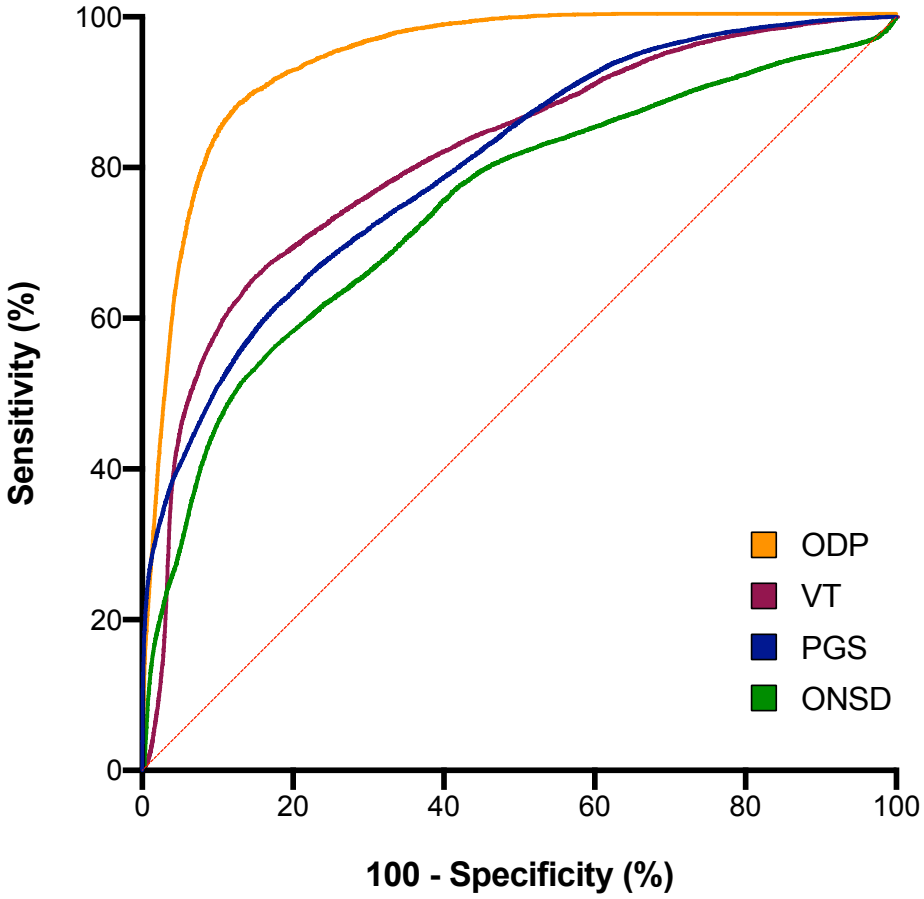


Figure 8-17: Receiver Operating Characteristic (ROC) curves and Areas Under the Curves (AUC) representing the association of Intracranial Pressure (ICP) with the MRI biomarkers.

Brain MRI biomarkers: pituitary gland shape (PGS, AUC=0.80), Vertical Tortuosity of the optic nerves (VT, AUC= 0.82), Optic Nerve Sheath Distension (ONSD, AUC= 0.75), Optic Disc Protrusion (ODP, AUC=0.94).

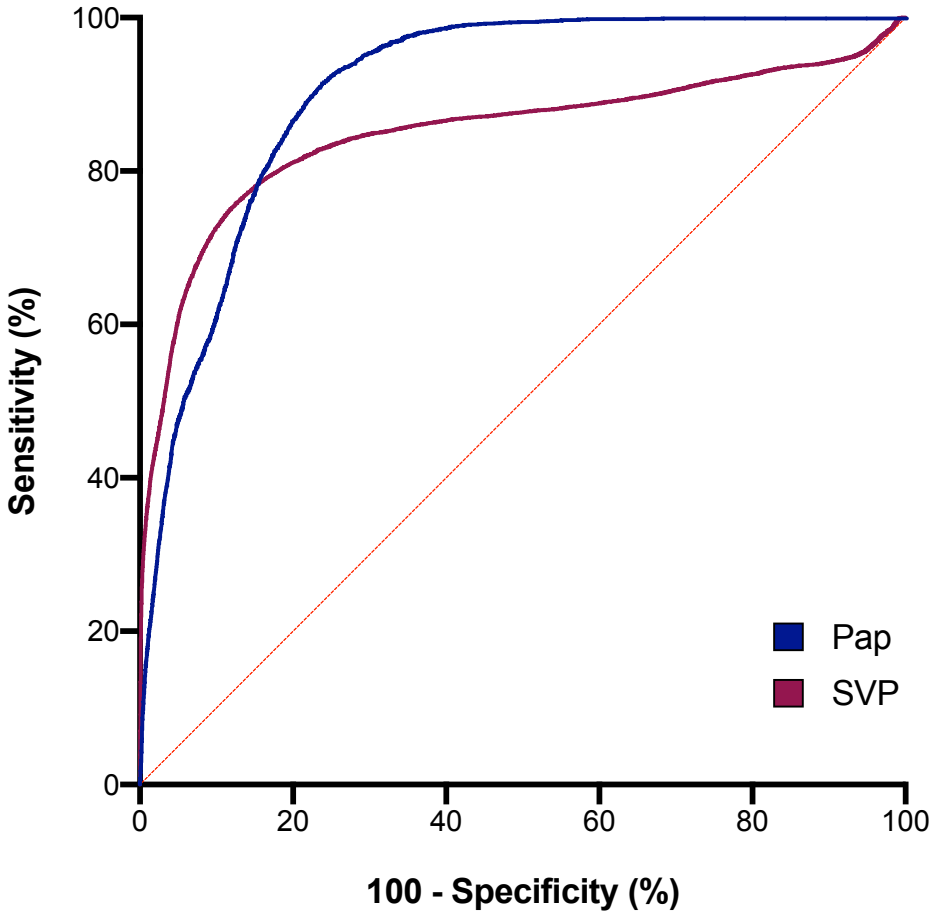


Figure 8-18: Receiver Operating Characteristic (ROC) curves and Areas Under the Curves (AUC) representing the association of Intracranial Pressure (ICP) with the ophthalmic biomarkers.

Ophthalmic biomarkers: papilloedema (Pap, AUC=0.90), Spontaneous Venous Pulsation (SVP, AUC= 0.85).

8.4.5. Positive and negative predictive value of the 6 biomarkers

Sixteen patients (36%) in this study had no abnormal biomarkers on MRI or ophthalmic examination. The mean 24-hour ICP in this subgroup of patients was 2.7 mmHg (SD 5.6). The ROC curve analysis identified 5.96 mmHg as the optimal median 24-hour ICP threshold distinguishing patients with normal

biomarkers from patients with 1 or more abnormal biomarkers (based on Youden index calculation).

Based on this ICP threshold, the biomarker with the best negative predictive value was the pituitary gland shape; a normal pituitary gland shape predicted normal ICP (median 24-hour ICP < 5.96 mmHg) in 86% of the cases. The biomarkers with the best positive predictive values were SVP, papilloedema and protrusion of the optic disc; if abnormal these markers identified raised ICP (median 24-hour ≥ 5.96 mmHg) in 90%, 100% and 100% of the study patients respectively.

ICP was elevated (median 24-hour ICP > 5.96 mm Hg) in 6% of patients with no abnormal markers, 46% of patients with 1 abnormal marker, 50% of patients with 2 abnormal markers, and 100% of patients with 3 or more abnormal markers. The sensitivity, specificity, positive predictive value and negative predictive value of the biomarkers (test) for the identification of patients with raised ICP (disease, median 24-hour ≥ 5.96 mmHg) are displayed in Table 8-3.

Table 8-3: Sensitivity, specificity, Positive Predictive Value (PPV) and Negative Predictive Value (NPV) of the biomarkers for the identification of raised intracranial pressure.

Number of abnormal biomarkers	Sensitivity	Specificity	PPV	NPV
1 or more	95%	60%	65%	94%
2 or more	65%	88%	81%	76%
3 or more	50%	100%	100%	71%
4 or more	40%	100%	100%	68%
5 or more	25%	100%	100%	63%
6 or more	NA	NA	NA	NA

Sensitivity: % of patients who had a positive test (abnormal biomarkers) among diseased patients (intracranial hypertension). Specificity: % of patients who had a negative test (normal biomarkers) among patients who did not have the disease (normal intracranial pressure). PPV: % of patients with the disease (intracranial hypertension) among patients with a positive test (abnormal biomarkers). NPV: % of patients without the disease (normal intracranial pressure) among patients with a negative test (normal biomarkers).

8.4.6. A comparison of brain MRI and ophthalmic biomarkers domains

Among the 45 patients, 28 had at least 1 abnormal biomarker in the brain MRI domain, 10 had at least 1 abnormal biomarker in the ophthalmic domain and 9 had at least 1 abnormal biomarker in each of the 2 domains (brain MRI

and ophthalmic). Patients with at least one abnormal biomarker in the brain MRI domain had a median ICP of 9.4 mmHg, while patients with at least 1 abnormal biomarker in the ophthalmic domain had a median ICP of 18.9 mmHg (Figure 8-19 A and B). Patients with at least one abnormal biomarker in each of the two domains had the highest median ICP (20.7 mmHg, Figure 8-19 C). The combination of one abnormal biomarker in each of the two domains achieved the strongest association with ICP (AUC 0.94, 95% CI 0.93 to 0.94, Figure 8-20).

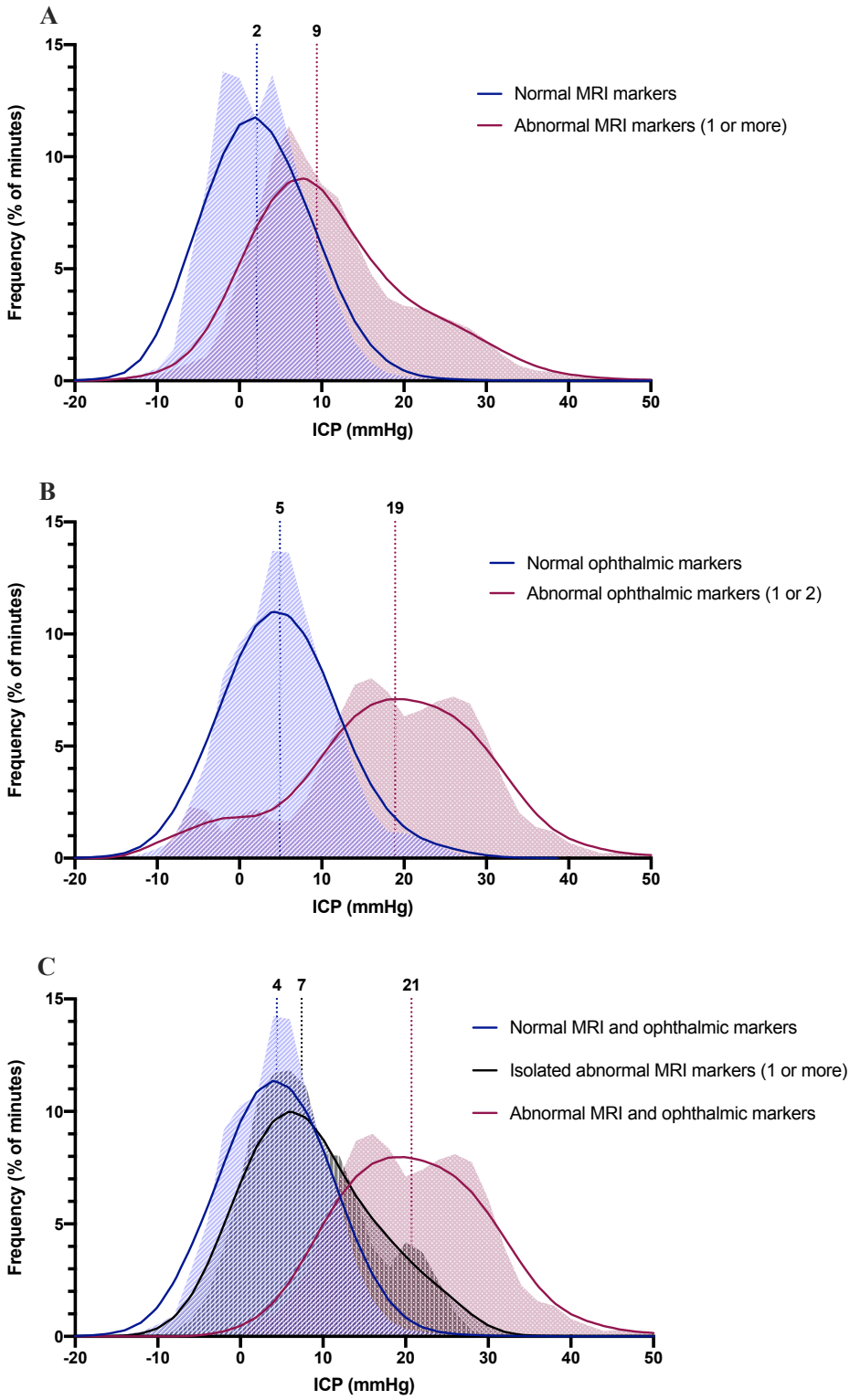


Figure 8-19: Frequency distribution of minute-by-minute Intracranial Pressure (ICP) measurements in patients presenting with normal (blue) and abnormal (red) biomarkers stratified by ophthalmic and MRI domains. LOWESS smoothing lines and median ICP are marked.

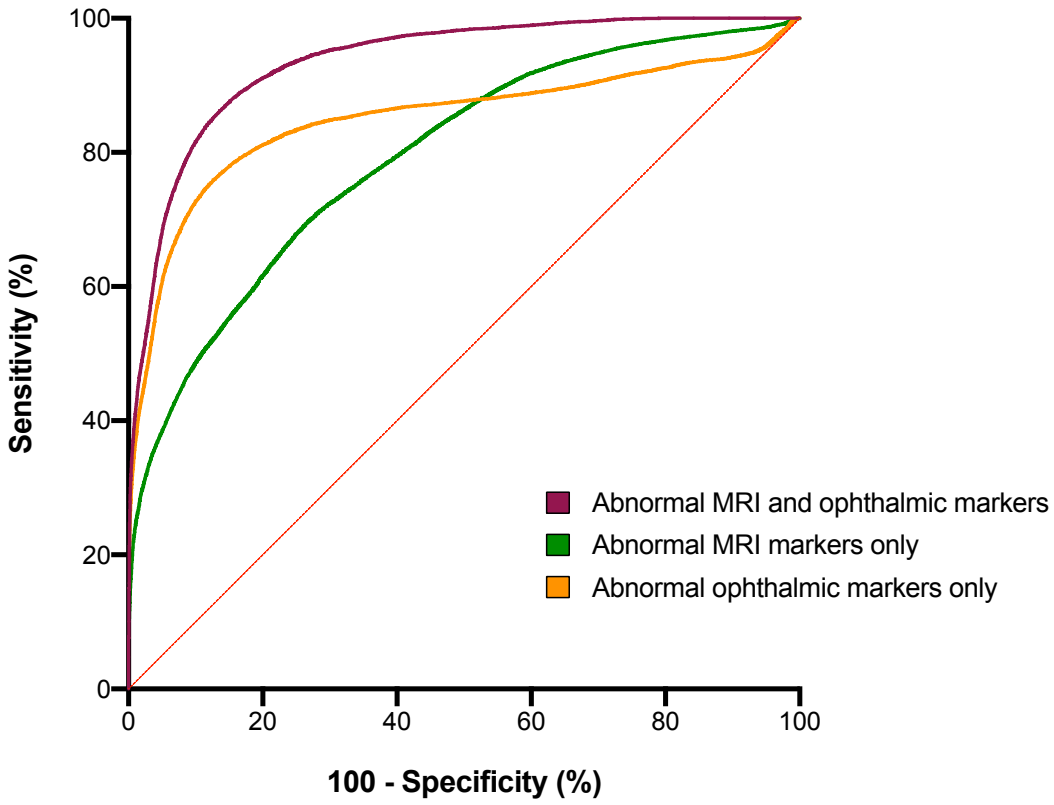


Figure 8-20: Receiver Operating Characteristic (ROC) curves representing the association of ICP with the biomarkers classified by domains (brain MRI and ophthalmic).

8.5. Discussion

This observational study describes the association of ICP with brain MRI and ophthalmic biomarkers of intracranial hypertension in a group of 45 patients with suspected CSF dynamics disorders. Our predictive values analysis demonstrated that patients with 3 (or more) abnormal biomarkers invariably had high median 24-hour ICP (100% PPV). Patients without any abnormal biomarker had normal ICP in 94% of the cases. There was only 1 patient with

raised ICP and normal biomarkers, he had a median 24-hour ICP of 6.5 mmHg, this value is very close to the optimal ICP cut-off considered for this analysis.

Patients with optic disc protrusion identified with brain MRI, papilloedema and/or absence of SVP on infrared videography had higher ICP levels compared to patients with other abnormal biomarkers (Figure 8-3). A concave pituitary gland (or empty sella) was associated with the lowest ICP levels. This may represent an earlier marker of elevated ICP than other biomarkers, although this study's design did not permit this hypothesis to be directly tested. The simultaneous presence of at least one abnormal marker in the brain MRI domain and at least one abnormal marker in the ophthalmic domain achieved the strongest association with ICP readings (AUC 0.94, 95% CI 0.93 to 0.94, Figure 8-20).

For ethical reasons, continuous ICP monitoring has not been performed in healthy subjects, therefore there is uncertainty about the level of median 24-hour ICP that can be considered normal. Our calculation of an optimal ICP cut-off is not intended as a definition of normal/abnormal ICP values, but rather as the ICP threshold above which increased ICP became increasingly associated with MRI and ophthalmic biomarkers of intracranial hypertension in a group of patients undergoing clinically indicated investigations. As most physiological parameters, we expect ICP to vary among different people and a normal ICP to be best defined by ranges rather than a specific cut-off

value. Moreover, this value was obtained from a population of patients who had a clinical indication for ICP monitoring, therefore they cannot be considered representative of a completely healthy population. However, this calculation was necessary for the evaluation of the utility of the 6 biomarkers in clinical practice. The cut-off obtained with this analysis is very close to the 'normal' ICP previously obtained by Chari *et al.* through the principal component analysis of a large group of patients undergoing 24-hour ICP monitoring (Chari *et al.*, 2017).

Interestingly, of the four patients with disc protrusion on MRI, only two were found to have papilloedema with fundoscopy. The sensitivity of MRI scan for the detection of signs of papilloedema could potentially be higher than direct fundoscopy because of its repeatability (the same MRI can be assessed many times and by different observers) while fundoscopy exams lead to a decision on papilloedema formulated there and then. This hypothesis is outside the primary aim of this study and could only be confirmed by a study specifically designed for this purpose.

Bilateral stenosis of the transverse sinuses on post gadolinium brain MRI has been reported to have the highest sensitivity for the diagnosis of IIH among other imaging biomarkers (Morris *et al.*, 2017). Due to the lack of availability of MRI with contrast (not routinely performed for this patient cohort in our institution) and to the heterogenous indications for ICP monitoring (not only IIH) of this patients' cohort, this sign could not be assessed in this study.

However, it should be considered for the assessment of patients with IIH and in the design of future prospective studies. Patterson *et al.* suggested that the ability to non-invasively predict ICP is improved by multimodal assessment combining an orbital ultrasound measurement of optic nerve sheath diameter and MRI pituitary-to-sella ratio (Patterson *et al.*, 2018). Compared to other previous studies investigating the role of brain MRI markers as predictors of ICP where 'snapshot' ICP estimates were made by lumbar puncture, our study has the advantage of relying on continuous ICP monitoring data (Brodsky and Vaphiades, 1998; Yuh *et al.*, 2000; Agid *et al.*, 2006; Rohr *et al.*, 2011; Bidot *et al.*, 2015; Holbrook and Saindane, 2017; Rehder, 2020). This allowed us to achieve a better overview of the time-ICP burden in each patient group. Additionally, it allowed an analysis of the association of these biomarkers with PA, demonstrating that higher levels of PA are found in patients with abnormal biomarkers (all except for distension of the optic nerve sheath, Table 8-2). The lack of association between PA and distension of the optic nerve sheath may be secondary to the small sample size, but it could also result from the reduced compliance preventing the sheath distension. The PA analysis is particularly relevant for those conditions in which there is isolated abnormal intracranial compliance not accompanied by clearly raised ICP (e.g., Chiari malformation type I and NPH). These aspects were previously discussed in the introduction chapter (see sections 1.3.3.5 and 1.3.4.5). The limitations of lumbar puncture opening pressures in this context have been previously exposed by Tuncel *et al.* who did not find any correlation between lumbar puncture opening

pressures and imaging markers of intracranial hypertension (Tuncel *et al.*, 2017).

Another important difference compared to previous studies is the inclusion of patients undergoing ICP monitoring for a variety of clinical indications, not only IIH (Table 8-1). Whilst this heterogeneity within the studied cohort may increase the 'noisiness' of the data, it does allow us to draw useful conclusions not only for IIH patients, but for any patient with suspected intracranial hypertension in a non-emergency setting.

An important limitation of this study is the fact that, while ophthalmic assessments were performed during the ICP monitoring period, brain MRIs were conducted at an average interval time of 36 days from the 24-hour ICP monitoring. The resulting risk of bias was addressed by only selecting patients who did not have any change in clinical picture or any type of intervention (including medical treatments) in between the two events. It is unlikely that a clinical change would go unnoticed as patients attend multiple perioperative clinical appointments around the time of ICP monitoring and are encouraged to report any clinical change to the care team through a dedicated telephone line (and/or email address). Additionally, it should be noted that for 37 patients (82%) the brain MRI was performed before the ICP monitoring procedure. At our institution, patients who undergo ICP monitoring are those in whom there is diagnostic uncertainty and would not be treated solely on the basis of brain MRI imaging before confirmation of intracranial

hypertension. The remaining eight patients had a brain MRI performed after the ICP monitoring as well as baseline brain imaging (either CT or MRI) performed before the time of ICP monitoring. For the purpose of the study, when multiple eligible brain MRIs were available, the imaging closest to the time of ICP monitoring was selected. The association between ICP and biomarkers was similar when comparing these eight patients to the rest of the cohort.

There are other limitations to this study. First of all, both ophthalmic and brain MRI imaging assessments are operator-dependent; however, there were two trained independent observers for each assessment, and they were masked to the ICP results at all times. The retrospective design of the study is another obvious limitation. A prospective study would have permitted the reduction of the interval between the investigations and to recruit a larger group of patients. Additionally, a prospective design would have resulted in the possibility of including different types of brain MRI sequences reported to be helpful in the literature. For example, our brain MRI assessment of the optic nerve features was not performed on fat-suppressed sequences. Fat-suppressed sequences can facilitate the assessment of the optic nerve sheath diameter, but they are not mandatory (Shofty *et al.*, 2012; Holbrook and Saindane, 2017). This type of sequence was not available for most of the patients in this study as not routinely performed. Whilst it is possible that the predictive value of this marker would improve with the use of fat-suppressed MRI sequences, the visualisation of the optic nerve sheaths was

deemed satisfactory by both the assessors for all the included MRIs. Finally, it is important to consider that ICP is affected by body position and while slit lamp examination and OCT scans are performed with the patient upright, MRIs are performed in the supine position (Farahmand *et al.*, 2014; Andresen *et al.*, 2015). We have partially addressed this issue by using continuous 24-hour ICP monitoring readings as these will include ICP values measured in both body positions. These are the conditions (supine MRI and upright ophthalmic assessments) in which outpatients are routinely investigated for suspected abnormalities of ICP, and the significance of abnormal biomarkers observed in these positions is therefore relevant to real-world clinical practice.

Future research could improve our understanding on the utility of these biomarkers as predictors of intracranial hypertension by conducting large, prospective studies and should investigate the specificity of the MRI biomarkers in a large population of healthy controls.

8.6. Conclusions

MRI biomarkers of elevated ICP (arachnoid herniation into the sella, a distended optic nerve sheath, vertical optic nerve tortuosity, and optic disc protrusion) and ophthalmic biomarkers (absent spontaneous venous pulsation on infrared fundus video, disc swelling) are strongly associated with higher intracranial pressure. Patients with multiple abnormal biomarkers (≥3) or a combination of abnormal MRI and ophthalmic biomarkers are likely to

have intracranial hypertension, therefore patients presenting this characteristic should be managed promptly.

Chapter 9. Discussion

ICP monitoring has been used for decades for the management of traumatic brain injury patients. More recently, it has proved its utility for the investigation and management of patients with non-acute CSF dynamics disturbances (e.g., IIH, Chiari malformation, hydrocephalus, NPH) (see section 1.3). The invasive nature of this investigation does not allow its use for research purposes in healthy individuals, for this reason we are still unsure of the normal limits for ICP and pulse amplitude. Despite the lack of studies employing ICP monitoring in healthy individuals, the variety of clinical studies employing this investigation in patients with suspected clinical problems has led to improvements in our understanding of CSF dynamics. There are numerous gaps in our knowledge of ICP physiology and CSF dynamics, this PhD thesis further advances the knowledge in this field, answering some of these research questions, through the use of invasive ICP monitoring in patients with suspected CSF dynamics disturbances.

9.1. Evidence on spontaneous intracranial hypotension

Research on CSF dynamics disturbances has mainly focused on conditions that cause high ICP or abnormal brain compliance, whilst only sparse attention has been centred on low CSF pressure/volume states. Compared to intracranial hypertension, diseases causing low CSF pressure/volume states are perceived as less risky being less likely to cause death, permanent disability, or blindness. However, more recent evidence suggests that

patients with low CSF pressure/volume states can suffer severe symptoms with many reports of loss of consciousness and coma, often secondary to large subdural collections (Schievink *et al.*, 2018b; Takai *et al.*, 2019). In addition, a recent survey conducted on patients diagnosed with SIH in the UK has demonstrated the significant impact that such disease can have on the patients' economical health and quality of life (Cheema *et al.*, 2022). Chapter 3 and Chapter 4 of this thesis are focused on SIH, probably the less understood of the low CSF pressure/volume syndromes.

The systematic review and meta-analysis of SIH in Chapter 3 is the first comprehensive objective summary on the clinical presentation, investigations and treatment outcomes for this disease. This chapter provides an objective quantification of the proportion of clinical signs/symptoms and brain MRI findings in patients with diagnosis of SIH (Table 3-5, Figure 3-4, Figure 3-35). This work demonstrates that despite most patients with SIH having orthostatic headaches, a significant minority do not have this classical presentation. The systematic review showed that 7% of the patients with SIH had a non-orthostatic headache and 3% did not experience headaches at all. Another important finding is that a diagnosis of SIH cannot be excluded based on a normal brain MRI; in fact brain MRI results were normal in 19% of the patients. Patients who have SIH, but normal imaging pose a major diagnostic challenge and the following chapter (Chapter 4) focuses on this patient category.

The meta-analysis on lumbar puncture opening pressures demonstrated the relatively low diagnostic yield of this investigation with a sensitivity of 67% (section 3.4.4.5). This investigation could still be offered to patients with strong clinical suspicion for SIH and non-conclusive/normal imaging; however, this should be conducted with caution, as there is a risk of worsening SIH. Moreover, SIH should not be excluded on the basis of a normal lumbar puncture opening pressure, as this can occur in up to 32% of patients with SIH (Figure 3-52).

In addition, the meta-analyses compared the sensitivity of different spinal imaging techniques in the identification of a spontaneous CSF leak and the efficacy of different EBP techniques for the treatment of SIH (Figure 3-36, Figure 3-56, Table 3-6). Spinal investigations were able to identify extradural CSF in 48-76% of the patients, and the investigations with the highest sensitivity for the identification of the exact leak site were the MRI myelography with intrathecal gadolinium and the DSM (Figure 3-36). While the identification of the exact leak site is important in patients who do not respond well to non-targeted treatment, it is not essential for most patients. In fact, one epidural blood patch was successful for 64% of the patients (non-targeted in most cases), the success rate was even higher when large volume blood patches (20 ml) were used (77%). These results suggest that non-targeted epidural blood patches could be attempted at early stages, whereas specialised spinal imaging (e.g., DSM, MRM with intrathecal

gadolinium) could be reserved for those patients who do not respond to non-targeted treatment (Figure 3-62).

The vast heterogeneity of the literature on SIH, as well as the lack of randomised controlled trials are important limitations of this work and could have significantly affected the results of the meta-analyses. Despite its limitations, this systematic review offers a comprehensive summary that could guide clinicians (and patients) approaching SIH for the first time and provide support to more experienced clinicians and researchers who, through this review, could identify useful targets for their future research.

9.2. The role of ICP monitoring in spontaneous intracranial hypotension

In most cases SIH is diagnosed through non-invasive (or minimally invasive) investigations and successfully treated with EBPs (Figure 3-56). There are instances in which making a diagnosis of SIH can be challenging due to patients presenting with atypical features, for example without the typical imaging findings on brain MRI (Figure 3-35), without evidence of a CSF leak on spinal imaging (Figure 3-36) or with normal lumbar puncture opening pressures (see above 3.4.4.5). In other cases, despite meeting the diagnostic criteria for SIH, patients do not respond to treatment with EBPs raising doubts on the accuracy of the diagnosis.

Chapter 4 is an observational study that studied the utility of invasive ICP monitoring when there is diagnostic uncertainty for SIH. ICP monitoring has

traditionally been used for the identification of high ICP states, this study has investigated this less known and less studied aspect of CSF dynamics.

This study demonstrates that, in selected cases in which a diagnosis of SIH is strongly suspected but difficult to confirm, ICP monitoring can be useful and confirm a low-pressure state in 8% of the cases. An additional 16% of these patients benefit from ICP monitoring because they can be diagnosed with a high-pressure state despite this paradoxical presentation with orthostatic headache (Table 4-3). Except for a few case reports, this is the first study investigating the role of ICP monitoring in the diagnostic pathway for SIH (Eide *et al.*, 2012; Fichtner *et al.*, 2012; Jensen *et al.*, 2021).

9.3. Effect of position and valve setting changes on CSF dynamics

In addition to being a useful diagnostic tool, ICP monitoring can provide guidance for the treatment of patients when adjustable shunt systems are implanted. ICP monitoring can help choose the right shunt system (number, type and initial setting of shunt valves) as well as tailoring the shunt settings when patients' requirements change through the years of treatment. Current shunt systems rely on the correct interpretation of symptoms, ophthalmic signs, imaging signs and CSF pressure measurements for the selection of the correct shunt settings. The advent of telemetric ICP implantable readers as M.Scio (Miethke, Potsdam, Germany) and Neurovent-P-Tel (Raumedic AG, Helbrechts, Germany) has the potential of improving shunt technologies making a closed loop shunt system, or 'smart shunt', a possibility for the near

future. The programming of a closed loop shunt system will however require a certain knowledge on how ICP and brain compliance respond to external variables, including changes in posture and shunt setting changes.

Chapter 5 is a retrospective observational study that describes the changes of CSF dynamics parameters (ICP and pulse amplitude) with different postures, it demonstrates that pulse amplitude is higher in upright posture suggesting a possible lower brain compliance in sitting/standing position. While the effect of posture on ICP has been described before, its effect on pulse amplitude (and brain compliance) had never been described in a large cohort.

Chapter 6 is a retrospective observational study investigating the effect of valve setting changes on median 24-hour ICP measured through continuous monitoring with an intraparenchymal probe. This study reports paradoxical changes in ICP following differential pressure valves setting changes. One of the limitations of this work was the lack of data on clinical outcomes. While we are unsure on how (or if) these ICP changes correlate with clinical outcomes, the results of this study suggest that valve settings should be altered with caution as they can result in a paradoxical response.

The information derived from the studies described in chapters 5 and 6 may be useful for the future development of patient-tailored treatment with programmable closed loop shunts but large prospective studies observing

ICP for longer periods of time (>24 hours) including information on clinical outcomes will be needed to improve our understanding of CSF dynamics.

9.4. Ophthalmic and imaging markers of raised ICP

ICP monitoring has been demonstrated to be a safe procedure at NHNN (Chari *et al.*, 2015); however it remains an invasive treatment and as such it carries risks for the patients. These risks, even if rare, should be avoided whenever possible and non-invasive ICP measuring methods are desirable. Chapters 7 and 8 of this thesis investigate the possibility of replacing invasive ICP monitoring with non-invasive biomarkers of raised ICP. Chapter 7 demonstrated the association between higher ICP measurements and the absence of SVPs detected with infrared video recordings. This method has the limitation of being observer-dependent and requires an OCT system that includes an infrared video recording module. Despites these weaknesses, providing proof of this association opens the possibility of testing other fundus video recordings techniques that may be more accessible and readily available (e.g., mobile cameras). Future studies should also focus on the development of automated SVP videos assessment methods. Chapter 8 demonstrates the utility of integrating ophthalmic and imaging biomarkers to predict raised ICP. This study provides useful information for the triage of patients with suspected raised ICP and the results suggest that patients with three or more biomarkers, especially if a mix of ophthalmic and imaging biomarkers is present, are likely to have intracranial hypertension and should be managed promptly.

9.5. Future directions

SIH is highly debilitating and not uncommon; the heterogeneity of the studies included in the systematic review and meta-analyses (Chapter 3) highlights the lack of consensus in the way that this disorder is diagnosed and managed. The limited understanding of the exact aetiology and pathophysiology of SIH significantly contributes to the clinical uncertainty. In addition, most of the knowledge on SIH is based on case reports and case series with very few examples of high-quality research. Future studies should focus on understanding why patients get SIH, defining whether a CSF leak (or CSF-venous fistula) is always the cause for this disorder, and what is the cascade of events leading to the debilitating symptoms that affect SIH patients. Experimental studies could employ a combination of dynamic imaging (supine and upright imaging) and CSF dynamics tests (infusion studies and/or ICP monitoring) to improve our understanding on the pathophysiology of SIH. Prospective randomised controlled studies could also improve our knowledge on the most effective epidural blood patch technique (targeted or non-targeted, volume, content of the patch) and the most sensitive specialised spinal imaging to identify the exact leak site.

The creation of truly programmable CSF shunts is another important aim for the management of patients with CSF dynamics disorders. Current CSF shunt systems are in some ways outdated; this is because they heavily rely on an operator to program them correctly. Future closed loop shunts, also called ‘smart shunts’, should have the ability to self-adjust rapidly based on

the factors that influence CSF dynamics (e.g., position, activity, shunt valve settings). Chapters 5 and 6 demonstrate that there are many gaps in knowledge on how external factors influence CSF dynamics. Future prospective studies should look at the effect of position on CSF dynamics in a more precise way, possibly with the use of accelerometers or video-recording analysis that allow constant monitoring of posture and activities. In addition, the studies described in chapters 5 and 6 only observed ICP for short time periods, future research should look at CSF dynamics for longer time periods (days, months or years), this could be achieved, for example, through the use of implantable telemetric ICP reading devices (e.g., M.Scio, Miethke, Potsdam, Germany; Neurovent-P-Tel, Raumedic AG, Helbrechts, Germany). Most importantly, future research should aim at the identification of normal ranges for ICP and pulse amplitude in healthy individuals and at the correlation of CSF dynamics parameters with patients' symptoms, without this information it will be difficult to efficiently program a 'smart shunt'.

Non-invasive ICP measuring techniques and biological markers will hopefully become more reliable for the prediction of CSF dynamics parameters, making invasive ICP monitoring less necessary. The studies described in chapters 7 and 8 demonstrated the utility of some imaging and ophthalmic biomarkers for the prediction of raised ICP. Infrared video recordings of spontaneous retinal venous pulsations can help predict intracranial hypertension; however, the technique used in this study requires specialised equipment that may not be available in some centres. Future research

should investigate whether similar results can be obtained with widely available (possibly low cost) cameras. In addition, it is essential for future studies to develop automated systems able to detect the signs of raised ICP in both brain imaging and retina video recordings without the need for a trained observer.

Chapter 10. Appendices

Table 10-1: Diagnostic criteria for spontaneous intracranial hypotension

ICHD-II (2004)	ICHD-3 beta (2013)	ICHD-III (2018)	Schievink 2008 (Schievink *et al.*, 2008)	Schievink 2011 (Schievink *et al.*, 2011)
A. Diffuse and/or dull headache that worsens within 15 minutes after sitting or standing, with at least one of the following and fulfilling criterion D: 1. neck stiffness 2. tinnitus 3. hypoacusia 4. photophobia, nausea. B. At least one of the following: 1. evidence of low CSF pressure on MRI 2. evidence of CSF leakage on conventional myelography, CT myelography or cisternography 3. CSF opening pressure <60 mm H_20 in sitting position C. No history of dural puncture or other cause of CSF fistula D. Headache resolves within 72 hours after epidural blood patching	A. Any headache fulfilling criterion C B. Low CSF pressure (<60 mm CSF) and/or evidence of CSF leakage on imaging C. Headache has developed in temporal relation to the low CSF pressure or CSF leakage, or has led to its discovery D. Not better accounted for by another ICHD-III beta diagnosis	A. Headache fulfilling criteria 7.2 (see below) and criterion C B. Absence of a procedure or trauma known to be able to cause CSF leakage C. Headache has developed in temporal relation to occurrence of low CSF pressure or CSF leakage, or has led to its discovery D. Not better accounted for by any other ICHD-III diagnosis Criteria 7.2 A. Any headache1 fulfilling criterion C B. Either or both of the following: 1. low cerebrospinal fluid (CSF) pressure (< 60 mm CSF) 2. evidence of CSF leakage on imaging2 C. Headache has developed in temporal relation to the low CSF pressure or CSF leakage, or led to its discovery D. Not better accounted for by another ICHD-III diagnosis.	Criterion A, demonstration of a spinal CSF leak or, if criterion A not met: Criterion B, cranial MR imaging changes of intracranial hypotension and the presence of at least one of the following: 1) low opening pressure (<60 mm H2O); 2) spinal meningeal diverticulum; 3) improvement of symptoms after epidural blood patching; or, if criteria A and B not met: Criterion C, the presence of all of the following or at least 2 of the following if typical orthostatic headaches are present: 1) low opening pressure (!60 mm H_2O), 2) spinal meningeal diverticulum, and 3) improvement of symptoms after epidural blood patching.	A) Orthostatic headache B) The presence of at least one of the following: 1. Low opening pressure (<60 mm H_2O) 2. Sustained improvement of symptoms after epidural blood patching 3. Demonstration of an active spinal CSF leak 4. Cranial MRI changes of intracranial hypotension C) No recent history of dural puncture D) Not attributable to another disorder
CSF: Cerebrospinal Fluid, ICHD: International Classification of Headache Disorders				

Table 10-2: List of selected studies and inclusion for meta-analyses

Reference	Author (year)	Quality grading[a]	Patients (n)	Meta-analyses
(Cebeci *et al.*, 2020)	Cebeci et al (2020)	Fair	20	Age, sex, other symptoms, MRMG, leak location
(Davies *et al.*, 2020)	Davies et al (2020)	Good	86	Sex, other symptoms, conservative treatment
(Wang *et al.*, 2020)	Wang et al (2020)	Good	20	
(Dobrocky *et al.*, 2019)	Dobrocky et al (2019)	Good	56	Age, sex, brain MRI
(Li *et al.*, 2019)	Li et al (2019)	Fair	40	Age, sex, clinical presentation, brain MRI, LPOP
(Levi *et al.*, 2019)	Levi et al (2019)	Good	101	Age, sex, headache, other symptoms, non-targeted EBP, small EBP
(Kim *et al.*, 2019)	Kim et al (2019)	Good	43	Age, sex, symptoms duration, headache, other symptoms, brain MRI
(Schievink *et al.*, 2019a)	Schievink et al (2019)	Good	113	Age, symptoms duration, headache
(Schievink *et al.*, 2019b)	Schievink et al (2019)	Good	49	DSM
(Pagani-Estevez *et al.*, 2019a)	Pagani-Estévez et al (2019)	Fair	202	First EBP
(Fichtner *et al.*, 2019)	Fichtner et al (2019)	Fair	27	LPOP, leak location
(Martin *et al.*, 2019)	Martin et al (2019)	Fair	94	Other symptoms, first EBP
(Kinsman *et al.*, 2019)	Kinsman et al (2019)	Fair	144	Sex
(Farb *et al.*, 2019)	Farb et al (2019)	Fair	31	Sex, brain MRI, spine MRI, DSM, leak location
(Griffin *et al.*, 2019)	Griffin et al (2019)	Good	92	
(Ohtonari *et al.*, 2018)	Ohtonary et al (2018)	Fair	19	Age, sex, headache, other symptoms, LPOP, leak location, conservative,

Reference	Author (year)	Quality grading[a]	Patients (n)	Meta-analyses
(Murakami *et al.*, 2018)	Murakami et al (2018)	Good	38	Age, sex
(Lee *et al.*, 2018)	Lee et al (2018)	Fair	62	Age, sex, leak location, first EBP, targeted EBP
(Schievink *et al.*, 2018a)	Schievink et al (2018)	Good	29	Conservative treatment
(Xia *et al.*, 2018)	Xia et al (2018)	Good	156	Conservative treatment
(Ahn *et al.*, 2019)	Ahn et al (2018)	Good	116	Sex, brain MRI, spine MRI, CTM, leak location, first EBP, non-targeted EBP, targeted EBP
(Yagi *et al.*, 2018)	Yagi et al (2018)	Fair	37	Sex, symptoms duration, other symptoms, brain MRI, leak location, conservative, first EBP, large EBP
(Tsai *et al.*, 2018)	Tsai et al (2018)	Fair	27	Symptoms duration, brain MRI
(Takai *et al.*, 2019)	Takai et al (2018)	Fair	11	Symptoms duration, LPOP
(Dobrocky *et al.*, 2018)	Dobrocky et al (2018)	Fair	14	
(Clark *et al.*, 2018)	Clark et al (2018)	Fair	101	
(Ferrante *et al.*, 2018)	Ferrante et al (2018)	Fair	35	
(Beck *et al.*, 2019)	Beck et al (2018)	Fair	47	
(Schievink *et al.*, 2018b)	Schievink et al (2018)	Fair	15	
(Yao and Hu, 2017)	Yao et al (2017)	Fair	206	Age, sex, symptoms duration, headache, brain MRI, LPOP
(Wu *et al.*, 2017)	Wu et al (2017)	Good	150	Age, sex, symptoms duration, headache, other symptoms, brain MRI, MRM, leak location, first EBP, targeted EBP
(Beck *et al.*, 2017)	Beck et al (2017)	Good	31	Other symptoms

Reference	Author (year)	Quality grading[a]	Patients (n)	Meta-analyses
(He *et al.*, 2018)	He et al (2017)	Good	165	Other symptoms, CTM, MRM, leak location, conservative, first EBP, targeted EBP, small EBP
(Choi *et al.*, 2018)	Choi et al (2017)	Good	95	Sex, headache, other symptoms, brain MRI, leak location, first EBP, Non-tageted EBP, targeted EBP, small EBP
(Kim *et al.*, 2017)	Kim et al (2017)	Fair	128	Sex, headache, headache location, other symptoms, brain MRI, first EBP
(Kranz *et al.*, 2017)	Kranz et al (2017)	Good	22	
(Chen *et al.*, 2017a)	Chen et al (2017)	Good	19	
(Chen *et al.*, 2017b)	Chen et al (2017)	Good	23	
(Chen *et al.*, 2016)	Chen et al (2016)	Fair	45	Age, sex, headache, other symptoms, conservative, first EBP
(So *et al.*, 2016)	So et al (2016)	Fair	34	Age, sex, symptoms duration, headache, leak location, first EBP, small EBP
(Amemiya *et al.*, 2016)	Amemiya et al (2016)	Good	15	Age, symptoms duration, other symptoms
(Kranz *et al.*, 2016c)	Kranz et al (2016)	Good	99	CTM
(Schievink *et al.*, 2016b)	Schievink et al (2016)	Good	53	DSM
(Ferrante *et al.*, 2016b)	Ferrante et al (2016)	Fair	106	First EBP, large EBP
(Amrhein *et al.*, 2016)	Amrhein et al (2016)	Fair	35	First EBP, targeted EBP, small EBP
(Fichtner *et al.*, 2016)	Fichtner et al (2016)	Good	39	Headache
(Monteith *et al.*, 2016)	Monteith et al (2016)	Fair	12	Headache, brain MRI, RIC
(Schievink *et al.*, 2016a)	Schievink et al (2016)	Good	568	Sex

Reference	Author (year)	Quality grading[a]	Patients (n)	Meta-analyses
(Hori *et al.*, 2016)	Hori et al (2016)	Good	22	Sex, brain MRI
(Karm *et al.*, 2016)	Karm et al (2016)	Fair	104	Sex, brain MRI, first EBP, targeted EBP
(Ansel *et al.*, 2016)	Ansel et al (2016)	Fair	16	Sex, brain MRI, spine MRI, leak location, first EBP, non-targeted EBP, small EBP
(Takahashi *et al.*, 2016)	Takahashi et al (2016)	Fair	169	Sex, headache, brain MRI, RIC, LPOP, leak location, conservative, first EBP
(Capizzano *et al.*, 2016)	Capizzano et al (2016)	Fair	41	Sex, headache, other symptoms, brain MRI
(Tanaka *et al.*, 2016)	Tanaka et al (2016)	Good	40	Sex, headache, other symptoms, brain MRI
(Kim *et al.*, 2016)	Kim et al (2016)	Fair	140	Sex, headache, other symptoms, brain MRI, spine MRI, conservative, first EBP, small EBP
(Choi *et al.*, 2016)	Choi et al (2016)	Fair	18	Sex, leak location, first EBP, targeted EBP
(Kranz *et al.*, 2016a)	Kranz et al (2016)	Good	89	Symptoms duration
(Ferrante *et al.*, 2016a)	Ferrante et al (2016)	Good	28	Symptoms duration, headache location
(Beck *et al.*, 2016a)	Beck et al (2016)	Good	15	
(Verdoorn *et al.*, 2016)	Verdoorn et al (2016)	Fair	129	
(Wan *et al.*, 2016)	Wan et al (2016)	Fair	15	
(Kranz *et al.*, 2016b)	Kranz et al (2015)	Good	106	Age, sex, brain MRI, LPOP
(Idrissi *et al.*, 2015)	Idrissi et al (2015)	Fair	24	Age, sex, headache, headache location, other symptoms, brain MRI, spine MRI, RIC, leak location, conservative, first EBP,
(Thielen *et al.*, 2015)	Thielen et al (2015)	Fair	14	Leak location
(Joo *et al.*, 2015)	Joo et al (2015)	Fair	76	Leak location, small EBP

Reference	Author (year)	Quality grading[a]	Patients (n)	Meta-analyses
(Feltracco *et al.*, 2015)	Feltracco et al (2015)	Fair	18	Sex, brain MRI, first EBP, non-targeted EBP
(Schievink *et al.*, 2015a)	Schievink et al (2015)	Fair	13	
(Schievink *et al.*, 2015b)	Schievink et al (2015)	Good	42	
(Xia *et al.*, 2015)	Xia et al (2015)	Fair	93	
(Yoshida *et al.*, 2014)	Yoshida et al (2014)	Fair	12	Age, sex, headache, other symptoms, brain MRI, leak location, first EBP, targeted EBP, small EBP
(Chazen *et al.*, 2014)	Chazen et al (2014)	Good	24	Sex, CTM, MRMG, LPOP
(Pimienta *et al.*, 2014)	Pimienta et al (2014)	Fair	50	
(Schievink *et al.*, 2014a)	Schievink et al (2014)	Fair	338	
(Tung *et al.*, 2014)	Tung et al (2014)	Good	17	
(Hashizume *et al.*, 2013)	Hashizume et al (2013)	Fair	29	Age, sex, other symptoms, brain MRI, RIC, LPOP, conservative, first EBP, targeted EBP
(Schievink *et al.*, 2013b)	Schievink et al (2013)	Fair	24	Headache location
(Hosoya *et al.*, 2013)	Hosoya et al (2013)	Fair	100	Spine MRI, MRM
(Ferrante *et al.*, 2013)	Ferrante et al (2013)	Fair	10	
(Franzini *et al.*, 2013)	Franzini et al (2013)	Fair	80	
(Kranz *et al.*, 2013)	Kranz et al (2013)	Good	19	
(Reinstein *et al.*, 2013)	Reinstein et al (2013)	Good	50	

Reference	Author (year)	Quality grading[a]	Patients (n)	Meta-analyses
(Albes *et al.*, 2012)	Albes et al (2012)	Fair	26	Age, sex, CTM, leak location, first EBP, targeted EBP, large EBP
(Hasiloglu *et al.*, 2012)	Hasiloglu et al (2012)	Good	25	Age, sex, headache, LPOP, leak location
(Hashizume *et al.*, 2012)	Hashizume et al (2012)	Fair	12	Leak location
(Akbar *et al.*, 2012)	Akbar et al (2012)	Fair	41	MRMG
(Luetmer *et al.*, 2012)	Luetmer et al (2012)	Fair	151	Spine MRI
(Balkan *et al.*, 2012)	Balkan et al (2012)	Fair	11	Symptoms duration, other symptoms, brain MRI, first EBP, targeted EBP
(Schievink *et al.*, 2012)	Schievink et al (2012)	Good	33	
(Schievink *et al.*, 2013a)	Schievink et al (2012)	Fair	20	
(Takeuchi *et al.*, 2012)	Takeuchi et al (2012)	Fair	15	
(Yoon *et al.*, 2011)	Yoon et al (2011)	Fair	30	LPOP
(Cho *et al.*, 2011)	Cho et al (2011)	Good	56	Sex, headache, brain MRI, leak location, first EBP, non-targeted EBP, targeted EBP, small EBP
(Bonetto *et al.*, 2011)	Bonetto et al (2011)	Fair	17	Sex, symptoms duration, headache, other symptoms, brain MRI, conservative, first EBP, non-targeted EBP
(Watanabe *et al.*, 2011)	Watanabe et al (2011)	Fair	13	Symptoms duration, headache, small EBP
(Franzini *et al.*, 2011)	Franzini et al (2011)	Fair	74	
(Liu *et al.*, 2011)	Liu et al (2011)	Good	55	
(Franzini *et al.*, 2010)	Franzini et al (2010)	Fair	28	Leak location
(Medina *et*	Medina et al	Fair	13	Sex, headache, spine MRI, first EBP

Reference	Author (year)	Quality grading[a]	Patients (n)	Meta-analyses
al., 2010)	(2010)			
(Ferrante *et al*., 2010)	Ferrante et al (2010)	Fair	42	Spine MRI, MRM, RIC
(Horikoshi *et al*., 2010)	Horikoshi et al (2010)	Fair	16	Targeted EBP
(Adachi *et al*., 2009)	Adachi et al (2009)	Fair	10	Age, sex, headache, other symptoms
(Park and Kim, 2009)	Park et al (2009)	Fair	12	Age, sex, headache, other symptoms, brain MRI, RIC, LPOP, conservative
(Su *et al*., 2009)	Su et al (2009)	Fair	11	Age, sex, headache, other symptoms, brain MRI, spine MRI, leak location, first EBP, non-targeted EBP
(Mea *et al*., 2009b)	Mea et al (2009)	Good	90	Brain MRI
(Wang *et al*., 2009)	Wang et al (2009)	Fair	19	CTM
(Shankar *et al*., 2009)	Shankar et al (2009)	Good	17	Sex, brain MRI
(Mea *et al*., 2009a)	Mea et al (2009)	Fair	90	
(Watanabe *et al*., 2009)	Watanabe et al (2008)	Fair	18	Age, headache, spine MRI, LPOP
(Schievink *et al*., 2008)	Schievink et al (2008)	Fair	94	Brain MRI, LPOP
(Yoo *et al*., 2008)	Yoo et al (2008)	Fair	15	MRM, RIC, first EBP
(Albayram *et al*., 2008a)	Albayram et al (2008)	Good	19	MRMG
(Hyun *et al*., 2008)	Hyun et al (2008)	Good	30	Sex, headache, other symptoms, brain MRI, RIC, LPOP, leak location, conservative, first EBP, small EBP
(Tomoda *et al*., 2008)	Tomoda et al (2008)	Fair	27	Sex, other symptoms, conservative treatment, MRM, LPOP, first EBP
(Fuh *et al*., 2008)	Fuh et al (2008)	Fair	53	

Reference	Author (year)	Quality grading[a]	Patients (n)	Meta-analyses
(Mea *et al.*, 2008)	Mea et al (2008)	Fair	70	
(Mea *et al.*, 2007)	Mea et al (2007)	Good	59	Sex
(Chung *et al.*, 2007)	Chung et al (2007)	Fair	10	
(Farb *et al.*, 2007)	Farb et al (2007)	Good	12	
(Lai *et al.*, 2007)	Lai et al (2007)	Fair	40	
(Schievink *et al.*, 2007)	Schievink et al (2007)	Fair	11	
(Schievink and Louy, 2007)	Schievink et al (2007)	Fair	80	
(Tsai *et al.*, 2007)	Tsai et al (2007)	Fair	17	
(Wiesemann *et al.*, 2006)	Wiesemann et al (2006)	Fair	10	Age, sex, symptoms duration, headache, other symptoms, brain MRI, LPOP, conservative
(Chung *et al.*, 2006)	Chung et al (2006)	Fair	67	RIC
(Hannerz *et al.*, 2006)	Hannerz et al (2006)	Fair	12	Sex, headache, other symptoms, brain MRI, conservative, first EBP, non-targeted EBP, large EBP
(Cohen-Gadol *et al.*, 2006)	Cohen-Gadol et al (2006)	Fair	13	Sex, headache, other symptoms, brain MRI, leak location
(Chung *et al.*, 2005)	Chung et al (2005)	Fair	53	Age, spine MRI, conservative treatment
(Kong *et al.*, 2005)	Kong et al (2005)	Fair	13	Age, symptoms duration, spine MRI, CTM, RIC, LPOP, conservative
(Schievink *et al.*, 2005a)	Schievink et al (2005)	Fair	33	Leak location
(Schievink *et al.*, 2005b)	Schievink et al (2005)	Fair	20	

Reference	Author (year)	Quality grading[a]	Patients (n)	Meta-analyses
(Ferrante *et al*., 2004b)	Ferrante et al (2004)	Fair	18	LPOP
(Berroir *et al*., 2004)	Berrior et al (2004)	Fair	33	Sex, symptoms duration, headache, other symptoms, brain MRI, first EBP, non-targeted EBP
(Ferrante *et al*., 2004a)	Ferrante et al (2004)	Fair	12	
(Schievink *et al*., 2004a)	Schievink et al (2004)	Good	18	
(Schievink *et al*., 2004b)	Schievink et al (2004)	Good	25	
(Miyazawa *et al*., 2003)	Miyazawa et al (2003)	Fair	10	Age, headache, other symptoms, brain MRI, RIC, LPOP, leak location
(Chen *et al*., 2003b)	Chen et al (2003)	Fair	13	
(Schievink, 2003)	Schievink et al (2003)	Good	18	
(Lin *et al*., 2002)	Lin et al (2002)	Fair	15	LPOP
(Schrijver *et al*., 2002)	Schrijver et al (2002)	Good	20	
(Chung *et al*., 2000)	Chung et al (2000)	Fair	30	Headache location
(Chen *et al*., 1999)	Chen et al (1999)	Good	13	
(Schievink *et al*., 1998)	Schievink et al (1998)	Good	10	
(Schievink *et al*., 1996)	Schievink et al (1996)	Fair	11	Spine MRI, RIC

[a]Based on NIH Quality Assessment Tool for Case Series Studies

CTM: CT myelography, EBP: Epidural Blood Patch, LPOP: Lumbar Puncture Opening Pressure, MRM: MR Myelography, MRMG: MR myelography with intrathecal Gadolinium, RIC: Radionuclide Cisternography

Chapter 11. Bibliography

The International Classification of Headache Disorders: 2nd edition. Cephalalgia 2004; 24 Suppl 1: 9-160.

The International Classification of Headache Disorders, 3rd edition (beta version). Cephalalgia 2013; 33(9): 629-808.

Headache Classification Committee of the International Headache Society (IHS) The International Classification of Headache Disorders, 3rd edition. Cephalalgia 2018; 38(1): 1-211.

National Institutes of Health (NIH). Quality Assessment Tool for Case Series Studies. 2021 [cited 2020; Available from: https://www.nhlbi.nih.gov/health-topics/study-quality-assessment-tools

Abbott NJ. Evidence for bulk flow of brain interstitial fluid: significance for physiology and pathology. Neurochem Int 2004; 45(4): 545-52.

Adachi M, Mugikura S, Shibata A, Kawaguchi E, Sato T, Takahashi S. Relative decrease in signal intensity of subcortical white matter in spontaneous intracranial hypotension on fluid-attenuated inversion recovery images. AJNR Am J Neuroradiol 2009; 30(5): 906-10.

Adams RD, Fisher CM, Hakim S, Ojemann RG, Sweet WH. Symptomatic Occult Hydrocephalus with Normal Cerebrospinal-Fluid Pressure. New England Journal of Medicine 1965; 273(3): 117-26.

Agid R, Farb RI, Willinsky RA, Mikulis DJ, Tomlinson G. Idiopathic intracranial hypertension: the validity of cross-sectional neuroimaging signs. Neuroradiology 2006; 48(8): 521-7.

Ahn C, Lee E, Lee JW, Chee CG, Kang Y, Kang HS. Two-site blind epidural blood patch versus targeted epidural blood patch in spontaneous intracranial hypotension. J Clin Neurosci 2019; 62: 147-54.

Akbar JJ, Luetmer PH, Schwartz KM, Hunt CH, Diehn FE, Eckel LJ. The role of MR myelography with intrathecal gadolinium in localization of spinal CSF leaks in patients with spontaneous intracranial hypotension. AJNR Am J Neuroradiol 2012; 33(3): 535-40.

Albayram S, Kilic F, Ozer H, Baghaki S, Kocer N, Islak C. Gadolinium-enhanced MR cisternography to evaluate dural leaks in intracranial hypotension syndrome. AJNR Am J Neuroradiol 2008a; 29(1): 116-21.

Albayram S, Ulu MO, Hanimoglu H, Kaynar MY, Hanci M. Intracranial hypotension following scoliosis surgery: dural penetration of a thoracic pedicle screw. Eur Spine J 2008b; 17 Suppl 2(Suppl 2): S347-50.

Albes G, Weng H, Horvath D, Musahl C, Bazner H, Henkes H. Detection and treatment of spinal CSF leaks in idiopathic intracranial hypotension. Neuroradiology 2012; 54(12): 1367-73.

Allin DM, Czosnyka ZH, Czosnyka M, Richards HK, Pickard JD. In vitro hydrodynamic properties of the Miethke ProGAV hydrocephalus shunt. Cerebrospinal Fluid Res 2006; 3: 9.

Alperin N, Hushek SG, Lee SH, Sivaramakrishnan A, Lichtor T. MRI study of cerebral blood flow and CSF flow dynamics in an upright posture: the effect of posture on the intracranial compliance and pressure. Acta Neurochir Suppl 2005a; 95: 177-81.

Alperin N, Lee SH, Sivaramakrishnan A, Hushek SG. Quantifying the effect of posture on intracranial physiology in humans by MRI flow studies. J Magn Reson Imaging 2005b; 22(5): 591-6.

Amemiya S, Takahashi K, Mima T, Yoshioka N, Miki S, Ohtomo K. Reversible alterations of the neuronal activity in spontaneous intracranial hypotension. Cephalalgia 2016; 36(2): 162-71.

Amorim JA, Gomes de Barros MV, Valença MM. Post-dural (post-lumbar) puncture headache: risk factors and clinical features. Cephalalgia 2012; 32(12): 916-23.

Amrhein TJ, Befera NT, Gray L, Kranz PG. CT Fluoroscopy-Guided Blood Patching of Ventral CSF Leaks by Direct Needle Placement in the Ventral Epidural Space Using a Transforaminal Approach. AJNR Am J Neuroradiol 2016; 37(10): 1951-6.

Andersson J, Rosell M, Kockum K, Lilja-Lund O, Söderström L, Laurell K. Prevalence of idiopathic normal pressure hydrocephalus: A prospective, population-based study. PLoS One 2019; 14(5): e0217705.

Andrén K, Wikkelsø C, Tisell M, Hellström P. Natural course of idiopathic normal pressure hydrocephalus. Journal of Neurology, Neurosurgery & Psychiatry 2014; 85(7): 806-10.

Andresen M, Hadi A, Petersen LG, Juhler M. Effect of postural changes on ICP in healthy and ill subjects. Acta Neurochir (Wien) 2015; 157(1): 109-13.

Andresen M, Juhler M. Intracranial pressure following complete removal of a small demarcated brain tumor: a model for normal intracranial pressure in humans. J Neurosurg 2014; 121(4): 797-801.

Ansel S, Rae A, Tyagi A. Efficacy of epidural blood patches for spontaneous low-pressure headaches: a case series. J R Coll Physicians Edinb 2016; 46(4): 234-7.

Antes S, Stadie A, Muller S, Linsler S, Breuskin D, Oertel J. Intracranial Pressure-Guided Shunt Valve Adjustments with the Miethke Sensor Reservoir. World Neurosurg 2018; 109: e642-e50.

Arnautovic A, Splavski B, Boop FA, Arnautovic KI. Pediatric and adult Chiari malformation Type I surgical series 1965–2013: a review of demographics, operative treatment, and outcomes. Journal of Neurosurgery: Pediatrics PED 2015; 15(2): 161.

Bakker E, Naessens DMP, VanBavel E. Paravascular spaces: entry to or exit from the brain? Exp Physiol 2019; 104(7): 1013-7.

Balkan, II, Albayram S, Ozaras R, Yilmaz MH, Ozbayrak M, Mete B*, et al.* Spontaneous intracranial hypotension syndrome may mimic aseptic meningitis. Scand J Infect Dis 2012; 44(7): 481-8.

Barron SA, Jacobs L, Kinkel WR. Changes in size of normal lateral ventricles during aging determined by computerized tomography. Neurology 1976; 26(11): 1011-3.

Bateman GA. The reversibility of reduced cortical vein compliance in normal-pressure hydrocephalus following shunt insertion. Neuroradiology 2003; 45(2): 65-70.

Bateman GA. Pulse wave encephalopathy: a spectrum hypothesis incorporating Alzheimer's disease, vascular dementia and normal pressure hydrocephalus. Med Hypotheses 2004; 62(2): 182-7.

Beck J, Fung C, Ulrich CT, Fiechter M, Fichtner J, Mattle HP*, et al.* Cerebrospinal fluid outflow resistance as a diagnostic marker of spontaneous cerebrospinal fluid leakage. J Neurosurg Spine 2017; 27(2): 227-34.

Beck J, Raabe A, Schievink WI, Fung C, Gralla J, Piechowiak E*, et al.* Posterior Approach and Spinal Cord Release for 360 degrees Repair of Dural Defects in Spontaneous Intracranial Hypotension. Neurosurgery 2019; 84(6): E345-E51.

Beck J, Ulrich CT, Fung C, Fichtner J, Seidel K, Fiechter M*, et al.* Diskogenic microspurs as a major cause of intractable spontaneous intracranial hypotension. Neurology 2016a; 87: 1220-6.

Beck J, Ulrich CT, Fung C, Fichtner J, Seidel K, Fiechter M*, et al.* Diskogenic microspurs as a major cause of intractable spontaneous intracranial hypotension. Neurology 2016b; 87.

Bergsneider M, Yang I, Hu X, McArthur DL, Cook SW, Boscardin WJ. Relationship between valve opening pressure, body position, and intracranial pressure in normal pressure hydrocephalus: paradigm for selection of

programmable valve pressure setting. Neurosurgery 2004; 55(4): 851-8; discussion 8-9.

Berroir S, Loisel B, Ducros A, Boukobza M, Tzourio C, Valade D*, et al.* Early epidural blood patch in spontaneous intracranial hypotension. Neurology 2004; 63: 1950-1.

Bidot S, Saindane AM, Peragallo JH, Bruce BB, Newman NJ, Biousse V. Brain Imaging in Idiopathic Intracranial Hypertension. J Neuroophthalmol 2015; 35(4): 400-11.

Bonetto N, Manara R, Citton V, Cagnin A. Spinal subtraction MRI for diagnosis of epidural leakage in SIH. Neurology 2011; 77: 1873-6.

Boon AJ, Tans JT, Delwel EJ, Egeler-Peerdeman SM, Hanlo PW, Wurzer HA*, et al.* Dutch normal-pressure hydrocephalus study: prediction of outcome after shunting by resistance to outflow of cerebrospinal fluid. J Neurosurg 1997; 87(5): 687-93.

Bothwell SW, Janigro D, Patabendige A. Cerebrospinal fluid dynamics and intracranial pressure elevation in neurological diseases. Fluids and Barriers of the CNS 2019a; 16(1): 9.

Bothwell SW, Janigro D, Patabendige A. Cerebrospinal fluid dynamics and intracranial pressure elevation in neurological diseases. Fluids Barriers CNS 2019b; 16(1): 9.

Bradbury MW. Physiopathology of the blood-brain barrier. Adv Exp Med Biol 1976; 69: 507-16.

Brean A, Eide PK. Assessment of idiopathic normal pressure patients in neurological practice: the role of lumbar infusion testing for referral of patients to neurosurgery. Eur J Neurol 2008; 15(6): 605-12.

Brean A, Eide PK, Stubhaug A. Comparison of intracranial pressure measured simultaneously within the brain parenchyma and cerebral ventricles. J Clin Monit Comput 2006; 20(6): 411-4.

Bridges KJ, Raslan AM. Utility of Intracranial Pressure Monitoring for Diagnosis of Idiopathic Intracranial Hypertension in the Absence of Papilledema. World Neurosurg 2018; 111: e221-e7.

Brinker T, Lüdemann W, Berens von Rautenfeld D, Samii M. Dynamic properties of lymphatic pathways for the absorption of cerebrospinal fluid. Acta Neuropathol 1997; 94(5): 493-8.

Brinker T, Stopa E, Morrison J, Klinge P. A new look at cerebrospinal fluid circulation. Fluids and Barriers of the CNS 2014; 11(1): 10.

Brodsky MC, Vaphiades M. Magnetic resonance imaging in pseudotumor cerebri. Ophthalmology 1998; 105(9): 1686-93.

Brown PD, Davies SL, Speake T, Millar ID. Molecular mechanisms of cerebrospinal fluid production. Neuroscience 2004; 129(4): 957-70.

Bruce BB, Kedar S, Van Stavern GP, Monaghan D, Acierno MD, Braswell RA*, et al.* Idiopathic intracranial hypertension in men. Neurology 2009; 72(4): 304-9.

Budohoski KP, Schmidt B, Smielewski P, Kasprowicz M, Plontke R, Pickard JD*, et al.* Non-invasively estimated ICP pulse amplitude strongly correlates with outcome after TBI. Acta Neurochir Suppl 2012; 114: 121-5.

Bulat M, Klarica M. Recent insights into a new hydrodynamics of the cerebrospinal fluid. Brain Res Rev 2011; 65(2): 99-112.

Canac N, Jalaleddini K, Thorpe SG, Thibeault CM, Hamilton RB. Review: pathophysiology of intracranial hypertension and noninvasive intracranial pressure monitoring. Fluids and Barriers of the CNS 2020; 17(1): 40.

Capizzano AA, Lai L, Kim J, Rizzo M, Gray L, Smoot MK*, et al.* Atypical Presentations of Intracranial Hypotension: Comparison with Classic Spontaneous Intracranial Hypotension. AJNR Am J Neuroradiol 2016; 37(7): 1256-61.

Carey M, Fuell W, Harkey T, Albert GW. Natural history of Chiari I malformation in children: a retrospective analysis. Child's Nervous System 2020; 37(4): 1185-90.

Cebeci H, Bilgin C, Candan S, Demir AB, Hakyemez B. Spinal Cerebrospinal Fluid Leakage in Spontaneous Intracranial Hypotension: An Intrathecal Gadolinium Enhanced MR-Myelography Study. J Belg Soc Radiol 2020; 104(1): 6.

Chambers IR, Siddique MS, Banister K, Mendelow AD. Clinical comparison of the Spiegelberg parenchymal transducer and ventricular fluid pressure. Journal of Neurology, Neurosurgery & Psychiatry 2001; 71(3): 383-5.

Chari A, Czosnyka M, Richards HK, Pickard JD, Czosnyka ZH. Hydrocephalus shunt technology: 20 years of experience from the Cambridge Shunt Evaluation Laboratory. J Neurosurg 2014; 120(3): 697-707.

Chari A, Dasgupta D, Smedley A, Craven C, Dyson E, Matloob S*, et al.* Intraparenchymal intracranial pressure monitoring for hydrocephalus and cerebrospinal fluid disorders. Acta Neurochir (Wien) 2017; 159(10): 1967-78.

Chari A, Dyson EW, Stevens AR, Thompson SD, Craven C, Matloob SA*, et al.* Three-hundred cases of Spiegelberg ICP monitoring for hydrocephalus and CSF disorders: the Queen Square experience. Fluids and Barriers of the CNS 2015; 12(Suppl 1).

Chatrath A, Marino A, Taylor D, Elsarrag M, Soldozy S, Jane JA, Jr. Chiari I malformation in children-the natural history. Childs Nerv Syst 2019; 35(10): 1793-9.

Chazen JL, Talbott JF, Lantos JE, Dillon WP. MR myelography for identification of spinal CSF leak in spontaneous intracranial hypotension. AJNR Am J Neuroradiol 2014; 35(10): 2007-12.

Cheema S, Joy C, Pople J, Snape-Burns J, Trevarthen T, Matharu M. Patient experience of diagnosis and management of spontaneous intracranial hypotension: a cross-sectional online survey. BMJ Open 2022; 12(1): e057438.

Chen C-C, Luo C-L, Wang S-J, Chern C-M, Fuh J-L, Lin S-H*, et al.* Colour doppler imaging for diagnosis of intracranial hypotension. The Lancet 1999; 354(9181): 826-9.

Chen CH, Chen JH, Chen HC, Chai JW, Chen PL, Chen CC. Patterns of cerebrospinal fluid (CSF) distribution in patients with spontaneous intracranial hypotension: Assessed with magnetic resonance myelography. J Chin Med Assoc 2017a; 80(2): 109-16.

Chen HC, Chen PL, Tsai YH, Chen CH, Chen CC, Chai JW. Quantitative Measurement of CSF in Patients with Spontaneous Intracranial Hypotension. AJNR Am J Neuroradiol 2017b; 38(5): 1061-7.

Chen WT, Fuh JL, Lirng JF, Lu SR, WU ZA, Wang SJ. Collapsed superior ophthalmic veins in patients with spontaneous intracranial hypotension. Neurology 2003a; 61.

Chen WT, Fuh JL, Lirng JF, Lu SR, Wu ZA, Wang SJ. Collapsed superior ophthalmic veins in patients with spontaneous intracranial hypotension. Neurology 2003b; 61: 1265-7.

Chen YC, Wang YF, Li JY, Chen SP, Lirng JF, Hseu SS*, et al.* Treatment and prognosis of subdural hematoma in patients with spontaneous intracranial hypotension. Cephalalgia 2016; 36(3): 225-31.

Cho KI, Moon HS, Jeon HJ, Park K, Kong DS. Spontaneous intracranial hypotension: Efficacy of radiologic targeting vs blind blood patch. Neurology 2011; 76: 1139-44.

Choi H, Lee MJ, Choi HA, Cha J, Chung CS. Intracranial structural alteration predicts treatment outcome in patients with spontaneous intracranial hypotension. Cephalalgia 2018; 38(2): 323-31.

Choi SW, Ahn JM, Lee JW, Park KS, Kang HS. The usefulness of MDCT-myelography for patients with spontaneous intracranial hypotension. Springerplus 2016; 5: 424.

Chung SJ, Ki CS, Lee MC, Lee JH. Fibrillin-1 gene analysis of Korean patients with spontaneous CSF hypovolemia. Headache 2007; 47(1): 111-5.

Chung SJ, Kim JS, Lee MC. Syndrome of cerebral spinal fluid hypovolemia: Clinical and imaging features and outcome. Neurology 2000; 55: 1321-7.

Chung SJ, Lee JH, Im JH, Lee MC. Short- and long-term outcomes of spontaneous CSF hypovolemia. Eur Neurol 2005; 54(2): 63-7.

Chung SJ, Lee JH, Kim SJ, Kwun BD, Lee MC. Subdural hematoma in spontaneous CSF hypovolemia. Neurology 2006; 67: 1088-9.

Cipriani D, Rodriguez B, Häni L, Zimmermann R, Fichtner J, Ulrich CT*, et al.* Postural changes in optic nerve and optic nerve sheath diameters in postural orthostatic tachycardia syndrome and spontaneous intracranial hypotension: A cohort study. PLOS ONE 2019; 14(10): e0223484.

Citerio G, Piper I, Chambers IR, Galli D, Enblad P, Kiening K*, et al.* Multicenter clinical assessment of the Raumedic Neurovent-P intracranial pressure sensor: a report by the BrainIT group. Neurosurgery 2008; 63(6): 1152-8; discussion 8.

Citerio G, Piper I, Cormio M, Galli D, Cazzaniga S, Enblad P*, et al.* Bench test assessment of the new Raumedic Neurovent-P ICP sensor: a technical report by the BrainIT group. Acta Neurochir (Wien) 2004; 146(11): 1221-6.

Clark MS, Diehn FE, Verdoorn JT, Lehman VT, Liebo GB, Morris JM*, et al.* Prevalence of hyperdense paraspinal vein sign in patients with spontaneous

intracranial hypotension without dural CSF leak on standard CT myelography. Diagn Interv Radiol 2018; 24(1): 54-9.

Coccius EA. Ueber die Anwendung des Augen-spiegels nebst Angabe eines neuen Instrumentes: I. Muller; 1853.

Cohen-Gadol AA, Mokri B, Piepgras DG, Meyer FB, Atkinson JL. Surgical anatomy of dural defects in spontaneous spinal cerebrospinal fluid leaks. Neurosurgery 2006; 58(4 Suppl 2): ONS-238-45; discussion ONS-45.

Craven C, Toma AK, Khan AA, Watkins LD. The role of ICP monitoring in patients with persistent cerebrospinal fluid leak following spinal surgery: a case series. Acta Neurochirurgica 2016a; 158(9): 1813-9.

Craven CL, Toma AK, Mostafa T, Patel N, Watkins LD. The predictive value of DESH for shunt responsiveness in idiopathic normal pressure hydrocephalus. J Clin Neurosci 2016b; 34: 294-8.

Cushing H. Studies on the Cerebro-Spinal Fluid : I. Introduction. J Med Res 1914; 31(1): 1-19.

Czosnyka M, Czosnyka Z. Origin of intracranial pressure pulse waveform. Acta Neurochir (Wien) 2020; 162(8): 1815-7.

Czosnyka M, Guazzo E, Whitehouse M, Smielewski P, Czosnyka Z, Kirkpatrick P*, et al.* Significance of intracranial pressure waveform analysis

after head injury. Acta Neurochir (Wien) 1996; 138(5): 531-41; discussion 41-2.

Czosnyka M, Pickard JD. Monitoring and interpretation of intracranial pressure. J Neurol Neurosurg Psychiatry 2004; 75(6): 813-21.

Czosnyka M, Steiner L, Balestreri M, Schmidt E, Smielewski P, Hutchinson PJ*, et al.* Concept of "true ICP" in monitoring and prognostication in head trauma. Acta Neurochir Suppl 2005; 95: 341-4.

Czosnyka Z, Czosnyka M. Long-term monitoring of intracranial pressure in normal pressure hydrocephalus and other CSF disorders. Acta Neurochir (Wien) 2017; 159(10): 1979-80.

Czosnyka Z, Pickard JD, Czosnyka M. Hydrodynamic properties of the Certas hydrocephalus shunt. J Neurosurg Pediatr 2013; 11(2): 198-204.

D'Antona L, Blamey SC, Craven CL, Sewell D, Manohara S, Leemans M*, et al.* Early Postoperative Outcomes of Normal Pressure Hydrocephalus: Results of a Service Evaluation. J Neurosurg Anesthesiol 2019a.

D'Antona L, McHugh JA, Ricciardi F, Thorne LW, Matharu MS, Watkins LD*, et al.* Association of Intracranial Pressure and Spontaneous Retinal Venous Pulsation. JAMA Neurol 2019b; 76(12): 1502-5.

D'Antona L, Thompson SD, Thorne L, Watkins LD, Toma AK. Letter: Thirty-Day Hospital Readmission and Surgical Complication Rates for Shunting in Normal Pressure Hydrocephalus: A Large National Database Analysis. Neurosurgery 2020.

Dandy WE. Experimental Hydrocephalus. Ann Surg 1919; 70(2): 129-42.

Dandy WE. Intracranial pressure without brain tumor: diagnosis and treatment. Ann Surg 1937; 106(4): 492-513.

Davies MJ, Davies MA, Sharpe R, Cordato D, Schwartz R. Epidural Blood Patch as a Diagnostic and Therapeutic Intervention in Spontaneous Intracranial Hypotension: A Novel Approach to Management. World Neurosurg 2020; 137: e242-e50.

Delwel EJ, de Jong DA, Avezaat CJJ. The prognostic value of clinical characteristics and parameters of cerebrospinal fluid hydrodynamics in shunting for idiopathic normal pressure hydrocephalus. Acta Neurochirurgica 2005; 147(10): 1037-43.

Dobrocky T, Grunder L, Breiding PS, Branca M, Limacher A, Mosimann PJ*, et al.* Assessing Spinal Cerebrospinal Fluid Leaks in Spontaneous Intracranial Hypotension With a Scoring System Based on Brain Magnetic Resonance Imaging Findings. JAMA Neurol 2019; 76(5): 580-7.

Dobrocky T, Mosimann PJ, Zibold F, Mordasini P, Raabe A, Ulrich CT*, et al.* Cryptogenic Cerebrospinal Fluid Leaks in Spontaneous Intracranial Hypotension: Role of Dynamic CT Myelography. Radiology 2018; 289(3): 766-72.

Dobrocky T, Winklehner A, Breiding PS, Grunder L, Peschi G, Häni L*, et al.* Spine MRI in Spontaneous Intracranial Hypotension for CSF Leak Detection: Nonsuperiority of Intrathecal Gadolinium to Heavily T2-Weighted Fat-Saturated Sequences. American Journal of Neuroradiology 2020; 41(7): 1309-15.

Dubost C, Le Gouez A, Zetlaoui PJ, Benhamou D, Mercier FJ, Geeraerts T. Increase in optic nerve sheath diameter induced by epidural blood patch: a preliminary report. Br J Anaesth 2011; 107(4): 627-30.

Dyson EW, Chari A, Toma AK, Thorne LW, Watkins LD. Failed Foramen Magnum Decompression in Chiari I Malformation Is Associated With Failure to Restore Normal Intracranial Compliance: An Observational Cohort Study. Neurosurgery 2020; 86(6): E552-E7.

Edsbagge M, Tisell M, Jacobsson L, Wikkelso C. Spinal CSF absorption in healthy individuals. Am J Physiol Regul Integr Comp Physiol 2004; 287(6): R1450-5.

Egnor MR. The Cerebral Windkessel as a Dynamic Pulsation Absorber. BIO-Complexity 2019.

Eide PK. The pathophysiology of chronic noncommunicating hydrocephalus: lessons from continuous intracranial pressure monitoring and ventricular infusion testing. J Neurosurg 2018; 129(1): 220-33.

Eide PK, Brean A. Cerebrospinal fluid pulse pressure amplitude during lumbar infusion in idiopathic normal pressure hydrocephalus can predict response to shunting. Cerebrospinal Fluid Res 2010; 7: 5.

Eide PK, Kerty E. Static and pulsatile intracranial pressure in idiopathic intracranial hypertension. Clin Neurol Neurosurg 2011; 113(2): 123-8.

Eide PK, Sorteberg A, Meling TR, Sorteberg W. The effect of baseline pressure errors on an intracranial pressure-derived index: results of a prospective observational study. Biomed Eng Online 2014; 13: 99.

Eide PK, Sorteberg W. Changes in intracranial pulse pressure amplitudes after shunt implantation and adjustment of shunt valve opening pressure in normal pressure hydrocephalus. Acta Neurochir (Wien) 2008; 150(11): 1141-7; discussion 7.

Eide PK, Sorteberg W. Diagnostic intracranial pressure monitoring and surgical management in idiopathic normal pressure hydrocephalus: a 6-year review of 214 patients. Neurosurgery 2010; 66(1): 80-91.

Eide PK, Sroka M, Wozniak A, Sæhle T. Morphological characterization of cardiac induced intracranial pressure (ICP) waves in patients with overdrainage of cerebrospinal fluid and negative ICP. Med Eng Phys 2012; 34(8): 1066-70.

Eklund A, Koskinen LO, Williams MA, Luciano MG, Dombrowski SM, Malm J. Hydrodynamics of the Certas programmable valve for the treatment of hydrocephalus. Fluids Barriers CNS 2012; 9(1): 12.

Enzmann DR, Pelc NJ. Normal flow patterns of intracranial and spinal cerebrospinal fluid defined with phase-contrast cine MR imaging. Radiology 1991; 178(2): 467-74.

Eşer I, Khorshid L, Güneş UY, Demir Y. The effect of different body positions on blood pressure. J Clin Nurs 2007; 16(1): 137-40.

Evensen KB, Eide PK. Measuring intracranial pressure by invasive, less invasive or non-invasive means: limitations and avenues for improvement. Fluids Barriers CNS 2020; 17(1): 34.

Farahmand D, Qvarlander S, Malm J, Wikkelso C, Eklund A, Tisell M. Intracranial pressure in hydrocephalus: impact of shunt adjustments and body positions. J Neurol Neurosurg Psychiatry 2014; 86.

Farb RI, Forghani R, Lee SK, Mikulis DJ, Agid R. The venous distension sign: a diagnostic sign of intracranial hypotension at MR imaging of the brain. AJNR Am J Neuroradiol 2007; 28(8): 1489-93.

Farb RI, Nicholson PJ, Peng PW, Massicotte EM, Lay C, Krings T*, et al.* Spontaneous Intracranial Hypotension: A Systematic Imaging Approach for CSF Leak Localization and Management Based on MRI and Digital Subtraction Myelography. AJNR Am J Neuroradiol 2019; 40(4): 745-53.

Feinberg DA, Mark AS. Human brain motion and cerebrospinal fluid circulation demonstrated with MR velocity imaging. Radiology 1987; 163(3): 793-9.

Feltracco P, Galligioni H, Barbieri S, Ori C. Thoracic epidural blood patches in the treatment of spontaneous intracranial hypotension: a retrospective case series. Pain Physician 2015; 18: 343-8.

Ferrante E, Arpino I, Citterio A, Wetzl R, Savino A. Epidural blood patch in Trendelenburg position pre-medicated with acetazolamide to treat spontaneous intracranial hypotension. Eur J Neurol 2010; 17(5): 715-9.

Ferrante E, Olgiati E, Sangalli V, Rubino F. Early pain relief from orthostatic headache and hearing changes in spontaneous intracranial hypotension after epidural blood patch. Acta Neurol Belg 2016a; 116(4): 503-8.

Ferrante E, Regna-Gladin C, Arpino I, Rubino F, Porrinis L, Ferrante MM*, et al.* Pseudo-subarachnoid hemorrhage: a potential imaging pitfall associated with spontaneous intracranial hypotension. Clin Neurol Neurosurg 2013; 115(11): 2324-8.

Ferrante E, Rubino F, Beretta F, Regna-Gladin C, Ferrante MM. Treatment and outcome of subdural hematoma in patients with spontaneous intracranial hypotension: a report of 35 cases. Acta Neurol Belg 2018; 118(1): 61-70.

Ferrante E, Rubino F, Mongelli M, Arpino I. Subarachnoideal blood spread following epidural blood patch given to treat spontaneous intracranial hypotension: Can it cause neurological complications? Clin Neurol Neurosurg 2016b; 140: 43-6.

Ferrante E, Savino A, Sances G, Nappi G. Spontaneous intracranial hypotension syndrome: report of twelve cases. Headache 2004a: 615-22.

Ferrante E, Wetzl R, Savino A, Citterio A, Protti A. Spontaneous cerebrospinal fluid leak syndrome: report of 18 cases. Neurol Sci 2004b; 25 Suppl 3: S293-5.

Fichtner J, Fung C, Z'Graggen W, Raabe A, Beck J. Lack of increase in intracranial pressure after epidural blood patch in spinal cerebrospinal fluid leak. Neurocrit Care 2012; 16(3): 444-9.

Fichtner J, Ulrich CT, Fung C, Cipriani D, Gralla J, Piechowiak EI*, et al.* Sonography of the optic nerve sheath diameter before and after microsurgical closure of a dural CSF fistula in patients with spontaneous intracranial hypotension - a consecutive cohort study. Cephalalgia 2019; 39(2): 306-15.

Fichtner J, Ulrich CT, Fung C, Knuppel C, Veitweber M, Jilch A*, et al.* Management of spontaneous intracranial hypotension - Transorbital ultrasound as discriminator. J Neurol Neurosurg Psychiatry 2016; 87(6): 650-5.

Franzini A, Messina G, Chiapparini L, Bussone G. Treatment of spontaneous intracranial hypotension: evolution of the therapeutic and diagnostic modalities. Neurol Sci 2013; 34 Suppl 1: S151-5.

Franzini A, Messina G, Mea E, Chiapparini L, Bussone G. Spontaneous intracranial hypotension: diagnostic and therapeutic implications in neurosurgical practice. Neurol Sci 2011; 32 Suppl 3: S287-90.

Franzini A, Messina G, Nazzi V, Mea E, Leone M, Chiapparini L*, et al.* Spontaneous intracranial hypotension syndrome: a novel speculative physiopathological hypothesis and a novel patch method in a series of 28 consecutive patients. J Neurosurg 2010; 112(2): 300-6.

Fric R, Eide PK. Comparative observational study on the clinical presentation, intracranial volume measurements, and intracranial pressure scores in patients with either Chiari malformation Type I or idiopathic intracranial hypertension. J Neurosurg 2017; 126(4): 1312-22.

Frič R, Eide PK. Comparison of pulsatile and static pressures within the intracranial and lumbar compartments in patients with Chiari malformation type 1: a prospective observational study. Acta Neurochir (Wien) 2015; 157(8): 1411-23; discussion 23.

Frič R, Eide PK. Chiari type 1—a malformation or a syndrome? A critical review. Acta Neurochirurgica 2020; 162(7): 1513-25.

Fridley J, Foroozan R, Sherman V, Brandt ML, Yoshor D. Bariatric surgery for the treatment of idiopathic intracranial hypertension. J Neurosurg 2011; 114(1): 34-9.

Friedman DI, Liu GT, Digre KB. Revised diagnostic criteria for the pseudotumor cerebri syndrome in adults and children. Neurology 2013; 81(13): 1159-65.

Friedman DI, Rausch EA. Headache diagnoses in patients with treated idiopathic intracranial hypertension. Neurology 2002; 58(10): 1551-3.

Fuh JL, Wang SJ, Lai TH, Hseu SS. The timing of MRI determines the presence or absence of diffuse pachymeningeal enhancement in patients with spontaneous intracranial hypotension. Cephalalgia 2008; 28(4): 318-22.

Funnell JP, Craven CL, D'Antona L, Thompson SD, Chari A, Thorne L*, et al.* Intracranial pressure in patients with papilloedema. Acta Neurol Scand 2018; 138(2): 137-42.

Gehlen M, Kurtcuoglu V, Schmid Daners M. Is posture-related craniospinal compliance shift caused by jugular vein collapse? A theoretical analysis. Fluids and Barriers of the CNS 2017; 14(1): 5.

Gergelé L, Manet R. Postural Regulation of Intracranial Pressure: A Critical Review of the Literature. Acta Neurochir Suppl 2021; 131: 339-42.

Girard F, Moumdjian R, Boudreault D, Chouinard P, Bouthilier A, Ruel M. The effect of sedation on intracranial pressure in patients with an intracranial space-occupying lesion: remifentanil versus propofol. Anesth Analg 2009; 109(1): 194-8.

Girard F, Moumdjian R, Boudreault D, Chouinard P, Bouthilier A, Sauvageau E*, et al.* The effect of propofol sedation on the intracranial pressure of patients with an intracranial space-occupying lesion. Anesth Analg 2004; 99(2): 573-7, table of contents.

Greitz D. Unraveling the riddle of syringomyelia. Neurosurgical Review 2006; 29(4): 251-64.

Griffin AS, Lu L, Peacock S, Gray L, Kranz PG, Amrhein TJ. CSF volume provocation maneuvers during lumbar puncture as a possible predictive tool for diagnosing spontaneous intracranial hypotension. Clin Neurol Neurosurg 2019; 186: 105552.

Hall A, O'Kane R. The best marker for guiding the clinical management of patients with raised intracranial pressure-the RAP index or the mean pulse amplitude? Acta Neurochir (Wien) 2016; 158(10): 1997-2009.

Hallaert GG, Vanhauwaert DJ, Logghe K, Broecke CVd, Baert E, Roost DV*, et al.* Endoscopic coagulation of choroid plexus hyperplasia. Journal of Neurosurgery: Pediatrics PED 2012; 9(2): 169.

Häni L, Fung C, Jesse CM, Ulrich CT, Miesbach T, Cipriani DR*, et al.* Insights into the natural history of spontaneous intracranial hypotension from infusion testing. Neurology 2020; 95(3): e247-e55.

Hannerz J, Dahlgren G, Irestedt L, Meyerson B, Ericson K. Treatment of idiopathic intracranial hypotension: cervicothoracic and lumbar blood patch and peroral steroid treatment. Headache 2006; 46(3): 508-11.

Harary M, Dolmans RGF, Gormley WB. Intracranial Pressure Monitoring-Review and Avenues for Development. Sensors (Basel) 2018; 18(2).

Hashimoto M, Ishikawa M, Mori E, Kuwana N. Diagnosis of idiopathic normal pressure hydrocephalus is supported by MRI-based scheme: a prospective cohort study. Cerebrospinal Fluid Res 2010; 7: 18.

Hashizume K, Watanabe K, Kawaguchi M, Fujiwara A, Furuya H. Evaluation on a clinical course of subdural hematoma in patients undergoing epidural blood patch for spontaneous cerebrospinal fluid leak. Clin Neurol Neurosurg 2013; 115(8): 1403-6.

Hashizume K, Watanabe K, Kawaguchi M, Taoka T, Shinkai T, Furuya H. Comparison of computed tomography myelography and radioisotope cisternography to detect cerebrospinal fluid leakage in spontaneous intracranial hypotension. Spine (Phila Pa 1976) 2012; 37(4): E237-42.

Hasiloglu ZI, Albayram S, Gorucu Y, Selcuk H, Cagil E, Erdemli HE*, et al.* Assessment of CSF flow dynamics using PC-MRI in spontaneous intracranial hypotension. Headache 2012; 52(5): 808-19.

He FF, Li L, Liu MJ, Zhong TD, Zhang QW, Fang XM. Targeted Epidural Blood Patch Treatment for Refractory Spontaneous Intracranial Hypotension in China. J Neurol Surg B Skull Base 2018; 79(3): 217-23.

Hedges TR, Jr., Baron EM, Hedges TR, 3rd, Sinclair SH. The retinal venous pulse. Its relation to optic disc characteristics and choroidal pulse. Ophthalmology 1994; 101(3): 542-7.

Hindmarsh T. Computer cisternography for evaluation of CSF flow dynamics. Further experiences. Acta Radiol Suppl 1977; 355: 269-79.

Hirzallah MI, Lochner P, Hafeez MU, Lee AG, Krogias C, Dongarwar D*, et al.* Quality assessment of optic nerve sheath diameter ultrasonography: Scoping literature review and Delphi protocol. J Neuroimaging 2022.

Holbrook J, Saindane AM. Imaging of Intracranial Pressure Disorders. Neurosurgery 2017; 80(3): 341-54.

Holbrook JF, Hudgins PA, Bruce BB, Saindane AM. Novel orbital findings of intracranial hypotension. Clin Imaging 2017; 41: 125-31.

Holm S, Eide PK. The frequency domain versus time domain methods for processing of intracranial pressure (ICP) signals. Med Eng Phys 2008; 30(2): 164-70.

Holmlund P, Eklund A, Koskinen LD, Johansson E, Sundström N, Malm J*, et al.* Venous collapse regulates intracranial pressure in upright body positions. Am J Physiol Regul Integr Comp Physiol 2018; 314(3): R377-r85.

Holmlund P, Johansson E, Qvarlander S, Wåhlin A, Ambarki K, Koskinen LD*, et al.* Human jugular vein collapse in the upright posture: implications for postural intracranial pressure regulation. Fluids Barriers CNS 2017; 14(1): 17.

Hori S, Taoka T, Miyasaka T, Ochi T, Sakamoto M, Wada T*, et al.* Dural Thickening of the Internal Auditory Canal in Patients With Spontaneous Intracranial Hypotension Syndrome. J Comput Assist Tomogr 2016; 40(2): 297-300.

Horikoshi T, Watanabe A, Uchida M, Kinouchi H. Effectiveness of an epidural blood patch for patients with intracranial hypotension syndrome and persistent spinal epidural fluid collection after treatment. J Neurosurg 2010; 113(5): 940-6.

Hosoya T, Hatazawa J, Sato S, Kanoto M, Fukao A, Kayama T. Floating dural sac sign is a sensitive magnetic resonance imaging finding of spinal cerebrospinal fluid leakage. Neurol Med Chir (Tokyo) 2013; 53: 207-12.

Hyun SH, Lee KH, Lee SJ, Cho YS, Lee EJ, Choi JY*, et al.* Potential value of radionuclide cisternography in diagnosis and management planning of spontaneous intracranial hypotension. Clin Neurol Neurosurg 2008; 110(7): 657-61.

Ibañez-Tallon I, Pagenstecher A, Fliegauf M, Olbrich H, Kispert A, Ketelsen UP*, et al.* Dysfunction of axonemal dynein heavy chain Mdnah5 inhibits ependymal flow and reveals a novel mechanism for hydrocephalus formation. Hum Mol Genet 2004; 13(18): 2133-41.

Idrissi AL, Lacour JC, Klein O, Schmitt E, Ducrocq X, Richard S. Spontaneous Intracranial Hypotension: Characteristics of the Serious Form in a Series of 24 Patients. World Neurosurg 2015; 84(6): 1613-20.

Iliff JJ, Wang M, Liao Y, Plogg BA, Peng W, Gundersen GA*, et al.* A paravascular pathway facilitates CSF flow through the brain parenchyma and the clearance of interstitial solutes, including amyloid β. Sci Transl Med 2012; 4(147): 147ra11.

Iliff JJ, Wang M, Zeppenfeld DM, Venkataraman A, Plog BA, Liao Y*, et al.* Cerebral arterial pulsation drives paravascular CSF-interstitial fluid exchange in the murine brain. J Neurosci 2013; 33(46): 18190-9.

Ishii K, Kanda T, Harada A, Miyamoto N, Kawaguchi T, Shimada K*, et al.* Clinical impact of the callosal angle in the diagnosis of idiopathic normal pressure hydrocephalus. Eur Radiol 2008; 18(11): 2678-83.

Jacks AS, Miller NR. Spontaneous retinal venous pulsation: aetiology and significance. J Neurol Neurosurg Psychiatry 2003; 74(1): 7-9.

Jacobsen HH, Jørstad Ø K, Moe MC, Petrovski G, Pripp AH, Sandell T*, et al.* Noninvasive Estimation of Pulsatile and Static Intracranial Pressure by Optical Coherence Tomography. Transl Vis Sci Technol 2022; 11(1): 31.

Jacobsson J, Qvarlander S, Eklund A, Malm J. Comparison of the CSF dynamics between patients with idiopathic normal pressure hydrocephalus and healthy volunteers. J Neurosurg 2018: 1-6.

Jamjoom AAB, Joannides AJ, Poon MT, Chari A, Zaben M, Abdulla MAH*, et al.* Prospective, multicentre study of external ventricular drainage-related infections in the UK and Ireland. J Neurol Neurosurg Psychiatry 2018; 89(2): 120-6.

Jaraj D, Agerskov S, Rabiei K, Marlow T, Jensen C, Guo X*, et al.* Vascular factors in suspected normal pressure hydrocephalus: A population-based study. Neurology 2016; 86(7): 592-9.

Jensen TSR, Rekate HL, Juhler M. Long-term telemetric intracerebral pressure monitoring as a tool in intracranial hypotension. Acta Neurochir (Wien) 2021; 163(3): 733-7.

Jeon JP, Lee SU, Kim SE, Kang SH, Yang JS, Choi HJ*, et al.* Correlation of optic nerve sheath diameter with directly measured intracranial pressure in Korean adults using bedside ultrasonography. PLoS One 2017; 12(9): e0183170.

Johanson CE, Duncan JA, Klinge PM, Brinker T, Stopa EG, Silverberg GD. Multiplicity of cerebrospinal fluid functions: New challenges in health and disease. Cerebrospinal Fluid Research 2008; 5(1): 10.

Joo EY, Hwang BY, Kong YG, Lee JH, Hwang BS, Suh JH. Retrospective study of epidural blood patch use for spontaneous intracranial hypotension. Reg Anesth Pain Med 2015; 40(1): 58-61.

Kameda M, Yamada S, Atsuchi M, Kimura T, Kazui H, Miyajima M*, et al.* Cost-effectiveness analysis of shunt surgery for idiopathic normal pressure hydrocephalus based on the SINPHONI and SINPHONI-2 trials. Acta Neurochirurgica 2017; 159(6): 995-1003.

Karm MH, Choi JH, Kim D, Park JY, Yun HJ, Suh JH. Predictors of the Treatment Response of Spontaneous Intracranial Hypotension to an Epidural Blood Patch. Medicine (Baltimore) 2016; 95(18): e3578.

Kilgore KP, Lee MS, Leavitt JA, Mokri B, Hodge DO, Frank RD*, et al.* Re-evaluating the Incidence of Idiopathic Intracranial Hypertension in an Era of Increasing Obesity. Ophthalmology 2017; 124(5): 697-700.

Kim DJ, Czosnyka Z, Keong N, Radolovich DK, Smielewski P, Sutcliffe MP*, et al.* Index of cerebrospinal compensatory reserve in hydrocephalus. Neurosurgery 2009; 64(3): 494-501; discussion -2.

Kim M, Lee EJ, Seo JH, Kim TW. Relationship of spontaneous retinal vein pulsation with ocular circulatory cycle. PLoS One 2014; 9(5): e97943.

Kim SC, Ryoo I, Sun HY, Park SW. MRI Findings of Spontaneous Intracranial Hypotension: Usefulness of Straight Sinus Distention. AJR Am J Roentgenol 2019: 1-7.

Kim WJ, Shin HY, Kim YC, Moon JY. Clinical association between brain MRI findings with epidural blood patch in spontaneous intracranial hypotension. J Neurosurg Anesthesiol 2016; 28(2): 147-52.

Kim YJ, Cho HY, Seo DW, Sohn CH, Ahn S, Lee YS*, et al.* Misdiagnosis of Spontaneous Intracranial Hypotension as a Risk Factor for Subdural Hematoma. Headache 2017; 57(10): 1593-600.

King JO, Mitchell PJ, Thomson KR, Tress BM. Manometry combined with cervical puncture in idiopathic intracranial hypertension. Neurology 2002; 58(1): 26-30.

Kinsman KA, Verdoorn JT, Luetmer PH, Clark MS, Diehn FE. Renal Contrast on CT Myelography: Diagnostic Value in Patients with Spontaneous Intracranial Hypotension. AJNR Am J Neuroradiol 2019; 40(2): 376-81.

Kolecki R, Dammavalam V, Bin Zahid A, Hubbard M, Choudhry O, Reyes M*, et al.* Elevated intracranial pressure and reversible eye-tracking changes detected while viewing a film clip. J Neurosurg 2018; 128(3): 811-8.

Kong DS, Park K, Nam DH, Lee JI, Kim JS, Eoh W*, et al.* Clinical features and long-term results of spontaneous intracranial hypotension. Neurosurgery 2005; 57(1): 91-6; discussion -6.

Kranz PG, Amrhein TJ, Choudhury KR, Tanpitukpongse TP, Gray L. Time-Dependent Changes in Dural Enhancement Associated With Spontaneous Intracranial Hypotension. AJR Am J Roentgenol 2016a; 207(6): 1283-7.

Kranz PG, Amrhein TJ, Gray L. CSF Venous Fistulas in Spontaneous Intracranial Hypotension: Imaging Characteristics on Dynamic and CT Myelography. AJR Am J Roentgenol 2017; 209(6): 1360-6.

Kranz PG, Gray L, Amrhein TJ. Spontaneous Intracranial Hypotension: 10 Myths and Misperceptions. Headache 2018; 58(7): 948-59.

Kranz PG, Gray L, Malinzak MD, Houk JL, Kim DK, Amrhein TJ. CSF-Venous Fistulas: Anatomy and Diagnostic Imaging. AJR Am J Roentgenol 2021; 217(6): 1418-29.

Kranz PG, Stinnett SS, Huang KT, Gray L. Spinal meningeal diverticula in spontaneous intracranial hypotension: analysis of prevalence and myelographic appearance. AJNR Am J Neuroradiol 2013; 34(6): 1284-9.

Kranz PG, Tanpitukpongse TP, Choudhury KR, Amrhein TJ, Gray L. How common is normal cerebrospinal fluid pressure in spontaneous intracranial hypotension? Cephalalgia 2016b; 36(13): 1209-17.

Kranz PG, Tanpitukpongse TP, Choudhury KR, Amrhein TJ, Gray L. Imaging Signs in Spontaneous Intracranial Hypotension: Prevalence and Relationship to CSF Pressure. AJNR Am J Neuroradiol 2016c; 37(7): 1374-8.

Kress BT, Iliff JJ, Xia M, Wang M, Wei HS, Zeppenfeld D*, et al.* Impairment of paravascular clearance pathways in the aging brain. Ann Neurol 2014; 76(6): 845-61.

Lai TH, Fuh JL, Lirng JF, Tsai PH, Wang SJ. Subdural haematoma in patients with spontaneous intracranial hypotension. Cephalalgia 2007; 27(2): 133-8.

Lalgudi Srinivasan H, Richetta C, Manoim N, Zipori AB, Shiran SI, Meirson H*, et al.* The role of ICP monitoring in paediatric IIH. Childs Nerv Syst 2020; 36(12): 3027-33.

Lalou AD, Asgari S, Czosnyka M, Nabbanja E, Garnett M, Czosnyka ZH. The Role of Cerebrospinal Fluid Dynamics in Normal Pressure Hydrocephalus Diagnosis and Shunt Prognostication. Acta Neurochir Suppl 2021; 131: 359-63.

Lalou AD, Czosnyka M, Donnelly J, Pickard JD, Nabbanja E, Keong NC*, et al.* Cerebral autoregulation, cerebrospinal fluid outflow resistance, and outcome following cerebrospinal fluid diversion in normal pressure hydrocephalus. J Neurosurg 2018; 130(1): 154-62.

Lang JM, Beck J, Zimmermann M, Seifert V, Raabe A. Clinical evaluation of intraparenchymal Spiegelberg pressure sensor. Neurosurgery 2003; 52(6): 1455-9; discussion 9.

Langridge B, Phillips E, Choi D. Chiari Malformation Type 1: A Systematic Review of Natural History and Conservative Management. World Neurosurg 2017; 104: 213-9.

Lee E, Kim TW, Kim JA, Kim JA, Kim H. Spontaneous Retinal Venous Pulsation in Unilateral Primary Open-angle Glaucoma With Low Intraocular Pressure. J Glaucoma 2017; 26(10): 896-901.

Lee JY, Lee MJ, Park HJ, Park JH, Jeong HJ, Oh MS*, et al.* Clinical effect of the proximity of epidural blood patch injection to the leakage site in spontaneous intracranial hypotension. Br J Neurosurg 2018; 32(6): 671-3.

Lemaire JJ, Khalil T, Cervenansky F, Gindre G, Boire JY, Bazin JE*, et al.* Slow pressure waves in the cranial enclosure. Acta Neurochir (Wien) 2002; 144(3): 243-54.

Levi V, Di Laurenzio NE, Franzini A, Tramacere I, Erbetta A, Chiapparini L*, et al.* Lumbar epidural blood patch: effectiveness on orthostatic headache and MRI predictive factors in 101 consecutive patients affected by spontaneous intracranial hypotension. J Neurosurg 2019: 1-9.

Levin BE. The clinical significance of spontaneous pulsations of the retinal vein. Arch Neurol 1978; 35(1): 37-40.

Levine DN. Spontaneous pulsation of the retinal veins. Microvasc Res 1998; 56(3): 154-65.

Levine DN, Bebie H. Phase and amplitude of spontaneous retinal vein pulsations: An extended constant inflow and variable outflow model. Microvasc Res 2016; 106: 67-79.

Li C, Raza HK, Chansysouphanthong T, Zu J, Cui G. A clinical analysis on 40 cases of spontaneous intracranial hypotension syndrome. Somatosens Mot Res 2019; 36(1): 24-30.

Li L, Gao FQ, Zhang B, Luo BN, Yang ZY, Zhao J. Overdosage of intrathecal gadolinium and neurological response. Clin Radiol 2008; 63(9): 1063-8.

Liberati A, Altman DG, Tetzlaff J, Mulrow C, Gotzsche PC, Ioannidis JP*, et al.* The PRISMA statement for reporting systematic reviews and meta-analyses of studies that evaluate health care interventions: explanation and elaboration. PLoS Med 2009; 6(7): e1000100.

Lin WC, Lirng JF, Fuh JL, Wang SJ, Chang FC, Ho CF*, et al.* MR findings of spontaneous intracranial hypotension. Acta Radiol 2002; 43: 249-55.

Liu FC, Fuh JL, Wang YF, Wang SJ. Connective tissue disorders in patients with spontaneous intracranial hypotension. Cephalalgia 2011; 31(6): 691-5.

Lochner P, Czosnyka M, Naldi A, Lyros E, Pelosi P, Mathur S*, et al.* Optic nerve sheath diameter: present and future perspectives for neurologists and critical care physicians. Neurol Sci 2019; 40(12): 2447-57.

Luetmer PH, Schwartz KM, Eckel LJ, Hunt CH, Carter RE, Diehn FE. When should I do dynamic CT myelography? Predicting fast spinal CSF leaks in patients with spontaneous intracranial hypotension. AJNR Am J Neuroradiol 2012; 33(4): 690-4.

Lundberg N. Continuous Recording and Control of Ventricular Fluid Pressure in Neurosurgical Practice. Journal of neuropathology and experimental neurology 1962; 21(3): 489.

Lutz BR, Venkataraman P, Browd SR. New and improved ways to treat hydrocephalus: Pursuit of a smart shunt. Surg Neurol Int 2013; 4(Suppl 1): S38-50.

Lyons MK, Meyer FB. Cerebrospinal Fluid Physiology and the Management of Increased Intracranial Pressure. Mayo Clinic Proceedings 1990; 65(5): 684-707.

Magnaes B. Body position and cerebrospinal fluid pressure. Part 1: clinical studies on the effect of rapid postural changes. J Neurosurg 1976a; 44(6): 687-97.

Magnaes B. Body position and cerebrospinal fluid pressure. Part 2: clinical studies on orthostatic pressure and the hydrostatic indifferent point. J Neurosurg 1976b; 44(6): 698-705.

Markey KA, Mollan SP, Jensen RH, Sinclair AJ. Understanding idiopathic intracranial hypertension: mechanisms, management, and future directions. The Lancet Neurology 2016; 15(1): 78-91.

Marmarou A, Bergsneider M, Klinge P, Relkin N, Black PM. The value of supplemental prognostic tests for the preoperative assessment of idiopathic normal-pressure hydrocephalus. Neurosurgery 2005; 57(3 Suppl): S17-28; discussion ii-v.

Marmarou A, Shulman K, LaMorgese J. Compartmental analysis of compliance and outflow resistance of the cerebrospinal fluid system. J Neurosurg 1975; 43(5): 523-34.

Martin R, Louy C, Babu V, Jiang Y, Far A, Schievink W. A two-level large-volume epidural blood patch protocol for spontaneous intracranial hypotension: retrospective analysis of risk and benefit. Reg Anesth Pain Med 2019.

Martín-Láez R, Caballero-Arzapalo H, López-Menéndez L, Arango-Lasprilla JC, Vázquez-Barquero A. Epidemiology of Idiopathic Normal Pressure Hydrocephalus: A Systematic Review of the Literature. World Neurosurg 2015; 84(6): 2002-9.

Martinez-Tejada I, Arum A, Wilhjelm JE, Juhler M, Andresen M. B waves: a systematic review of terminology, characteristics, and analysis methods. Fluids and Barriers of the CNS 2019; 16(1): 33.

Matloob SA, Toma AK, Thompson SD, Gan CL, Robertson F, Thorne L*, et al.* Effect of venous stenting on intracranial pressure in idiopathic intracranial hypertension. Acta Neurochir (Wien) 2017; 159(8): 1429-37.

Matsumae M, Sato O, Hirayama A, Hayashi N, Takizawa K, Atsumi H*, et al.* Research into the Physiology of Cerebrospinal Fluid Reaches a New Horizon: Intimate Exchange between Cerebrospinal Fluid and Interstitial Fluid May Contribute to Maintenance of Homeostasis in the Central Nervous System. Neurol Med Chir (Tokyo) 2016; 56(7): 416-41.

McCluskey G, Doherty-Allan R, McCarron P, Loftus AM, McCarron LV, Mulholland D*, et al.* Meta-analysis and systematic review of population-based epidemiological studies in idiopathic intracranial hypertension. Eur J Neurol 2018; 25(10): 1218-27.

McComb JG. Recent research into the nature of cerebrospinal fluid formation and absorption. J Neurosurg 1983; 59(3): 369-83.

McHugh JA, D'Antona L, Toma AK, Bremner FD. Spontaneous Venous Pulsations Detected With Infrared Videography. J Neuroophthalmol 2020; 40(2): 174-7.

McKeage K, Perry CM. Propofol: a review of its use in intensive care sedation of adults. CNS Drugs 2003; 17(4): 235-72.

McKee HD, Ahad MA. Spontaneous retinal venous pulsations can be present with a swollen optic disc. J Neurol Neurosurg Psychiatry 2004; 75(6): 941; author reply

Mea E, Chiapparini L, Savoiardo M, Franzini A, Bussone G, Leone M. Headache attributed to spontaneous intracranial hypotension. Neurol Sci 2008; 29 Suppl 1: S164-5.

Mea E, Chiapparini L, Savoiardo M, Franzini A, Bussone G, Leone M. Clinical features and outcomes in spontaneous intracranial hypotension: a survey of 90 consecutive patients. Neurol Sci 2009a; 30 Suppl 1: S11-3.

Mea E, Chiapparini L, Savoiardo M, Franzini A, Grimaldi D, Bussone G*, et al.* Application of IHS criteria to headache attributed to spontaneous intracranial hypotension in a large population. Cephalalgia 2009b; 29(4): 418-22.

Mea E, Savoiardo M, Chiapparini L, Casucci G, Bonavita V, Bussone G*, et al.* Headache and spontaneous low cerebrospinal fluid pressure syndrome. Neurol Sci 2007; 28 Suppl 2: S232-4.

Meadows J, Kraut M, Guarnieri M, Haroun RI, Carson BS. Asymptomatic Chiari Type I malformations identified on magnetic resonance imaging. Journal of Neurosurgery 2000; 92(6): 920.

Medina JH, Abrams K, Falcone S, Bhatia RG. Spinal imaging findings in spontaneous intracranial hypotension. AJR Am J Roentgenol 2010; 195(2): 459-64.

Meier U, Zeilinger FS, Kintzel D. Signs, Symptoms and Course of Normal Pressure Hydrocephalus in Comparison with Cerebral Atrophy. Acta Neurochirurgica 1999; 141(10): 1039-48.

Milhorat TH, Bolognese PA, Nishikawa M, Francomano CA, McDonnell NB, Roonprapunt C*, et al.* Association of Chiari malformation type I and tethered cord syndrome: preliminary results of sectioning filum terminale. Surg Neurol 2009; 72(1): 20-35.

Milhorat TH, Chou MW, Trinidad EM, Kula RW, Mandell M, Wolpert C*, et al.* Chiari I malformation redefined: clinical and radiographic findings for 364 symptomatic patients. Neurosurgery 1999; 44(5): 1005-17.

Milhorat TH, Nishikawa M, Kula RW, Dlugacz YD. Mechanisms of cerebellar tonsil herniation in patients with Chiari malformations as guide to clinical management. Acta Neurochir (Wien) 2010; 152(7): 1117-27.

Miyazawa K, Shiga Y, Hasegawa T, Endoh M, Okita N, Higano S*, et al.* CSF hypovolemia vs intracranial hypotension in “spontaneous intracranial hypotension syndrome”. Neurology 2003; 60: 941-7.

Mokri B, Hunter SF, Atkinson JL, Piepgras DG. Orthostatic headaches caused by CSF leak but with normal CSF pressures. Neurology 1998; 51(3): 786-90.

Mollan SP, Davies B, Silver NC, Shaw S, Mallucci CL, Wakerley BR*, et al.* Idiopathic intracranial hypertension: consensus guidelines on management. Journal of Neurology, Neurosurgery & Psychiatry 2018; 89(10): 1088-100.

Mollan SP, Hoffmann J, Sinclair AJ. Advances in the understanding of headache in idiopathic intracranial hypertension. Curr Opin Neurol 2019; 32(1): 92-8.

Mollan SP, Mitchell JL, Ottridge RS, Aguiar M, Yiangou A, Alimajstorovic Z*, et al.* Effectiveness of Bariatric Surgery vs Community Weight Management Intervention for the Treatment of Idiopathic Intracranial Hypertension: A Randomized Clinical Trial. JAMA Neurol 2021; 78(6): 678-86.

Mollanji R, Bozanovic-Sosic R, Zakharov A, Makarian L, Johnston MG. Blocking cerebrospinal fluid absorption through the cribriform plate increases resting intracranial pressure. Am J Physiol Regul Integr Comp Physiol 2002; 282(6): R1593-9.

Monteith TS, Kralik SF, Dillon WP, Hawkins RA, Goadsby PJ. The utility of radioisotope cisternography in low CSF/volume syndromes compared to myelography. Cephalalgia 2016; 36(13): 1291-5.

Moreno-Ajona D, McHugh JA, Hoffmann J. An Update on Imaging in Idiopathic Intracranial Hypertension. Frontiers in Neurology 2020; 11(453).

Morgan WH, Hazelton ML, Azar SL, House PH, Yu DY, Cringle SJ*, et al.* Retinal venous pulsation in glaucoma and glaucoma suspects. Ophthalmology 2004; 111(8): 1489-94.

Morgan WH, Hazelton ML, Yu DY. Retinal venous pulsation: Expanding our understanding and use of this enigmatic phenomenon. Prog Retin Eye Res 2016; 55: 82-107.

Morris PP, Black DF, Port J, Campeau N. Transverse Sinus Stenosis Is the Most Sensitive MR Imaging Correlate of Idiopathic Intracranial Hypertension. AJNR Am J Neuroradiol 2017; 38(3): 471-7.

Murakami Y, Takahashi K, Hoshi K, Ito H, Kanno M, Saito K*, et al.* Spontaneous intracranial hypotension is diagnosed by a combination of

lipocalin-type prostaglandin D synthase and brain-type transferrin in cerebrospinal fluid. Biochim Biophys Acta Gen Subj 2018; 1862(8): 1835-42.

Nabbanja E, Pickard JD, Lalou AD, Czosnyka ZH. Use of CSF infusion studies to unblock occluded hydrocephalus ventricular shunt catheters: a preliminary report of two patients. BMJ Case Rep 2018; 2018.

Nishikawa M, Sakamoto H, Hakuba A, Nakanishi N, Inoue Y. Pathogenesis of Chiari malformation: a morphometric study of the posterior cranial fossa. J Neurosurg 1997; 86(1): 40-7.

Norager NH, Olsen MH, Pedersen SH, Riedel CS, Czosnyka M, Juhler M. Reference values for intracranial pressure and lumbar cerebrospinal fluid pressure: a systematic review. Fluids Barriers CNS 2021; 18(1): 19.

Nourallah B, Zeiler FA, Calviello L, Smielewski P, Czosnyka M, Menon DK. Critical thresholds for intracranial pressure vary over time in non-craniectomised traumatic brain injury patients. Acta Neurochir (Wien) 2018; 160(7): 1315-24.

Nyaga VN, Arbyn M, Aerts M. Metaprop: a Stata command to perform meta-analysis of binomial data. Archives of Public Health 2014; 72(1): 39.

Ohtonari T, Ota S, Himeno T, Nishihara N, Sato M, Tanaka A. Excellent Outcomes of Large-Volume Epidural Blood Patch Using an Intravenous

Catheter in 15 Consecutive Cases with Cerebrospinal Fluid Leak. World Neurosurg 2018; 118: e276-e82.

Oldfield EH, Muraszko K, Shawker TH, Patronas NJ. Pathophysiology of syringomyelia associated with Chiari I malformation of the cerebellar tonsils. Implications for diagnosis and treatment. J Neurosurg 1994; 80(1): 3-15.

Oró JJ, Mueller DM. Posterior fossa decompression and reconstruction in adolescents and adults with the Chiari I malformation. Neurological Research 2011; 33(3): 261-71.

Osaka K, Handa H, Matsumoto S, Yasuda M. Development of the cerebrospinal fluid pathway in the normal and abnormal human embryos. Childs Brain 1980; 6(1): 26-38.

Pagani-Estevez GL, Cutsforth-Gregory JK, Morris JM, Mokri B, Piepgras DG, Mauck WD*, et al.* Procedural predictors of epidural blood patch efficacy in spontaneous intracranial hypotension. Reg Anesth Pain Med 2019a.

Pagani-Estevez GL, Cutsforth-Gregory JK, Morris JM, Mokri B, Piepgras DG, Mauck WD*, et al.* Procedural predictors of epidural blood patch efficacy in spontaneous intracranial hypotension. Reg Anesth Pain Med 2019b; 44: 212-20.

Park ES, Kim E. Spontaneous intracranial hypotension: clinical presentation, imaging features and treatment. J Korean Neurosurg Soc 2009; 45: 1-4.

Passi N, Degnan AJ, Levy LM. MR imaging of papilledema and visual pathways: effects of increased intracranial pressure and pathophysiologic mechanisms. AJNR Am J Neuroradiol 2013; 34(5): 919-24.

Patterson DF, Ho M-L, Leavitt JA, Smischney NJ, Hocker SE, Wijdicks EF*, et al.* Comparison of Ocular Ultrasonography and Magnetic Resonance Imaging for Detection of Increased Intracranial Pressure. Frontiers in Neurology 2018; 9(278).

Pepper J, Elhabal A, Tsermoulas G, Flint G. Symptom outcome after craniovertebral decompression for Chiari type 1 malformation without syringomyelia. Acta Neurochirurgica 2021; 163(1): 239-44.

Petersen J, Hellström P, Wikkelsø C, Lundgren-Nilsson A. Improvement in social function and health-related quality of life after shunt surgery for idiopathic normal-pressure hydrocephalus. J Neurosurg 2014; 121(4): 776-84.

Petersen LG, Petersen JC, Andresen M, Secher NH, Juhler M. Postural influence on intracranial and cerebral perfusion pressure in ambulatory neurosurgical patients. Am J Physiol Regul Integr Comp Physiol 2016; 310(1): R100-4.

Petraglia AL, Plog BA, Dayawansa S, Dashnaw ML, Czerniecka K, Walker CT*, et al.* The pathophysiology underlying repetitive mild traumatic brain

injury in a novel mouse model of chronic traumatic encephalopathy. Surg Neurol Int 2014; 5: 184.

Pickard JD, Teasdale G, Matheson M, Lindsay K, Galbraith S, Wyper D*, et al.* Intraventricular Pressure Waves — the Best Predictive Test for Shunting in Normal Pressure Hydrocephalus. 1980; Berlin, Heidelberg: Springer Berlin Heidelberg; 1980. p. 498-500.

Pimienta AL, Rimoin DL, Pariani M, Schievink WI, Reinstein E. Echocardiographic findings in patients with spontaneous CSF leak. J Neurol 2014; 261(10): 1957-60.

Piper I, Barnes A, Smith D, Dunn L. The Camino intracranial pressure sensor: is it optimal technology? An internal audit with a review of current intracranial pressure monitoring technologies. Neurosurgery 2001; 49(5): 1158-64; discussion 64-5.

Piper RJ, Kalyvas AV, Young AM, Hughes MA, Jamjoom AA, Fouyas IP. Interventions for idiopathic intracranial hypertension. Cochrane Database Syst Rev 2015; 2015(8): Cd003434.

Price DA, Grzybowski A, Eikenberry J, Januleviciene I, Verticchio Vercellin AC, Mathew S*, et al.* Review of non-invasive intracranial pressure measurement techniques for ophthalmology applications. Br J Ophthalmol 2020; 104(7): 887-92.

Qvarlander S, Malm J, Eklund A. The pulsatility curve-the relationship between mean intracranial pressure and pulsation amplitude. Physiol Meas 2010; 31(11): 1517-28.

Qvarlander S, Sundström N, Malm J, Eklund A. Postural effects on intracranial pressure: modeling and clinical evaluation. J Appl Physiol (1985) 2013; 115(10): 1474-80.

Raabe A, Czosnyka M, Piper I, Seifert V. Monitoring of intracranial compliance: correction for a change in body position. Acta Neurochir (Wien) 1999; 141(1): 31-6; discussion 5-6.

Raboel PH, Bartek J, Jr., Andresen M, Bellander BM, Romner B. Intracranial Pressure Monitoring: Invasive versus Non-Invasive Methods-A Review. Crit Care Res Pract 2012; 2012: 950393.

Rehder D. Idiopathic Intracranial Hypertension: Review of Clinical Syndrome, Imaging Findings, and Treatment. Curr Probl Diagn Radiol 2020; 49(3): 205-14.

Reinstein E, Pariani M, Bannykh S, Rimoin DL, Schievink WI. Connective tissue spectrum abnormalities associated with spontaneous cerebrospinal fluid leaks: a prospective study. Eur J Hum Genet 2013; 21(4): 386-90.

Relkin N, Marmarou A, Klinge P, Bergsneider M, Black PM. Diagnosing Idiopathic Normal-pressure Hydrocephalus. Neurosurgery 2005; 57(suppl_3): S2-4-S2-16.

Robba C, Bacigaluppi S, Cardim D, Donnelly J, Bertuccio A, Czosnyka M. Non-invasive assessment of intracranial pressure. Acta Neurol Scand 2016; 134(1): 4-21.

Rohr AC, Riedel C, Fruehauf M-C, van Baalen A, Bartsch T, Hedderich J*, et al.* MR Imaging Findings in Patients with Secondary Intracranial Hypertension. American Journal of Neuroradiology 2011; 32(6): 1021-9.

Sass C, Kosinski C, Schmidt P, Mull M, Schulz J, Schiefer J. Intrathecal saline infusion: an emergency procedure in a patient with spontaneous intracranial hypotension. Neurocrit Care 2013; 19(1): 116-8.

Schievink WI. Misdiagnosis of Spontaneous Intracranial Hypotension. Arch Neurol 2003; 60(12): 1713-8.

Schievink WI. A novel technique for treatment of intractable spontaneous intracranial hypotension: lumbar dural reduction surgery. Headache 2009; 49(7): 1047-51.

Schievink WI. Spontaneous Intracranial Hypotension. N Engl J Med 2021; 385(23): 2173-8.

Schievink WI, Chu RM, Maya MM, Johnson JP, Cohen HC. Spinal manifestations of spontaneous intracranial hypotension. J Neurosurg Spine 2013a; 18(1): 96-101.

Schievink WI, Dodick DW, Mokri B, Silberstein S, Bousser MG, Goadsby PJ. Diagnostic criteria for headache due to spontaneous intracranial hypotension: a perspective. Headache 2011; 51(9): 1442-4.

Schievink WI, Gordon OK, Tourje J. Connective tissue disorders with spontaneous spinal cerebrospinal fluid leaks and intracranial hypotension: a prospective study. Neurosurgery 2004a; 54(1): 65-70; discussion -1.

Schievink WI, Goseland A, Cunnen S. Bariatric surgery as a possible risk factor for spontaneous intracranial hypotension. Neurology 2014a; 83(20): 1819-22.

Schievink WI, Louy C. Precipitating factors of spontaneous spinal CSF leaks and intracranial hypotension. Neurology 2007; 69(7): 700-2.

Schievink WI, Maya MM, Barnard ZR, Moser FG, Jean-Pierre S, Waxman AD*, et al.* Behavioral Variant Frontotemporal Dementia as a Serious Complication of Spontaneous Intracranial Hypotension. Oper Neurosurg (Hagerstown) 2018a; 15(5): 505-15.

Schievink WI, Maya MM, Chu RM, Moser F. False localizing sign of cervico-thoracic CSF leak in spontaneous intracranial hypotension. 2015a; 84: 2445-8.

Schievink WI, Maya MM, Jean-Pierre S, Moser FG, Nuno M, Pressman BD. Rebound high-pressure headache after treatment of spontaneous intracranial hypotension: MRV study. Neurol Clin Pract 2019a; 9(2): 93-100.

Schievink WI, Maya MM, Jean-Pierre S, Nuno M, Prasad RS, Moser FG. A classification system of spontaneous spinal CSF leaks. Neurology 2016a; 87.

Schievink WI, Maya MM, Louy C. Cranial MRI predicts outcome of spontaneous intracranial hypotension. Neurology 2005a; 64: 1282-4.

Schievink WI, Maya MM, Louy C, Moser FG, Sloninsky L. Spontaneous intracranial hypotension in childhood and adolescence. J Pediatr 2013b; 163(2): 504-10.

Schievink WI, Maya MM, Louy C, Moser FG, Tourje J. Diagnostic criteria for spontaneous spinal CSF leaks and intracranial hypotension. AJNR Am J Neuroradiol 2008; 29(5): 853-6.

Schievink WI, Maya MM, Moser F, Tourje J. Spectrum of subdural fluid collections in spontaneous intracranial hypotension. J Neurosurg 2005b; 103: 608-13.

Schievink WI, Maya MM, Moser F, Tourje J, Torbati S. Frequency of spontaneous intracranial hypotension in the emergency department. J Headache Pain 2007; 8(6): 325-8.

Schievink WI, Maya MM, Moser FG, Jean-Pierre S, Nuno M. Coma: A serious complication of spontaneous intracranial hypotension. Neurology 2018b; 90(19): e1638-e45.

Schievink WI, Maya MM, Moser FG, Prasad RS, Cruz RB, Nuno M*, et al.* Lateral decubitus digital subtraction myelography to identify spinal CSF-venous fistulas in spontaneous intracranial hypotension. J Neurosurg Spine 2019b: 1-4.

Schievink WI, Maya MM, Moser FG, Simon P, Nuño M. Incidence of spontaneous intracranial hypotension in a community: Beverly Hills, California, 2006-2020. Cephalalgia 2022; 42(4-5): 312-6.

Schievink WI, Maya MM, Moser FG, Tourje J. Spectrum of subdural fluid collections in spontaneous intracranial hypotension. J Neurosurg 2005c; 103.

Schievink WI, Maya MM, Tourje J. False localizing sign of C1-2 cerebrospinal fluid leak in spontaneous intracranial hypotension. J Neurosurg 2004b; 100: 639-44.

Schievink WI, Meyer FB, Atkinson JL, Mokri B. Spontaneous spinal cerebrospinal fluid leaks and intracranial hypotension. J Neurosurg 1996; 84: 598-605.

Schievink WI, Morreale VM, Atkinson JLD, Meyer FB, Piepgras DG, Ebersold MJ. Surgical treatment of spontaneous spinal cerebrospinal fluid leaks. J Neurosurg 1998; 88.

Schievink WI, Moser FG, Maya MM. CSF–venous fistula in spontaneous intracranial hypotension. Neurology 2014b; 83(5): 472-3.

Schievink WI, Moser FG, Maya MM, Prasad RS. Digital subtraction myelography for the identification of spontaneous spinal CSF-venous fistulas. J Neurosurg Spine 2016b; 24(6): 960-4.

Schievink WI, Nuno M, Rozen TD, Maya MM, Mamelak AN, Carmichael J*, et al.* Hyperprolactinemia due to spontaneous intracranial hypotension. J Neurosurg 2015b; 122(5): 1020-5.

Schievink WI, Schwartz MS, Maya MM, Moser FG, Rozen TD. Lack of causal association between spontaneous intracranial hypotension and cranial cerebrospinal fluid leaks. J Neurosurg 2012; 116(4): 749-54.

Schrijver I, Schievink WI, Godfrey M, Meyer FB, Francke U. Spontaneous spinal cerebrospinal fluid leaks and minor skeletal features of Marfan syndrome: a microfibrillopathy. J Neurosurg 2002; 96.

Schuhmann MU, Sood S, McAllister JP, Jaeger M, Ham SD, Czosnyka Z*, et al.* Value of overnight monitoring of intracranial pressure in hydrocephalic children. Pediatr Neurosurg 2008; 44(4): 269-79.

Shankar JJ, Chakraborty S, Lum C. The venous hinge--an objective sign for the diagnosis and follow-up of treatment in patients with intracranial hypotension syndrome. Neuroradiology 2009; 51(7): 453-6.

Shofty B, Ben-Sira L, Constantini S, Freedman S, Kesler A. Optic nerve sheath diameter on MR imaging: establishment of norms and comparison of pediatric patients with idiopathic intracranial hypertension with healthy controls. AJNR Am J Neuroradiol 2012; 33(2): 366-9.

Smith JL. Whence pseudotumor cerebri? J Clin Neuroophthalmol 1985; 5(1): 55-6.

So Y, Park JM, Lee P, Kim CL, Lee C, Kim JH. Epidural blood patch for the treatment of spontaneous and iatrogenic orthostatic headache. Pain Physician 2016; 19: E1115-E22.

Spector R. Nutrient transport systems in brain: 40 years of progress. Journal of Neurochemistry 2009; 111(2): 315-20.

Spector R, Keep RF, Robert Snodgrass S, Smith QR, Johanson CE. A balanced view of choroid plexus structure and function: Focus on adult humans. Exp Neurol 2015a; 267: 78-86.

Spector R, Robert Snodgrass S, Johanson CE. A balanced view of the cerebrospinal fluid composition and functions: Focus on adult humans. Exp Neurol 2015b; 273: 57-68.

Spiegelberg A, Krause M, Meixensberger J, Seifert B, Kurtcuoglu V. Significant Association of Slow Vasogenic ICP Waves with Normal Pressure Hydrocephalus Diagnosis. Acta Neurochir Suppl 2018; 126: 243-6.

Steiner LA, Andrews PJ. Monitoring the injured brain: ICP and CBF. Br J Anaesth 2006; 97(1): 26-38.

Stephensen H, Andersson N, Eklund A, Malm J, Tisell M, Wikkelsö C. Objective B wave analysis in 55 patients with non-communicating and communicating hydrocephalus. J Neurol Neurosurg Psychiatry 2005; 76(7): 965-70.

Stovner LJ, Bergan U, Nilsen G, Sjaastad O. Posterior cranial fossa dimensions in the Chiari I malformation: Relation to pathogenesis and clinical presentation. Neuroradiology 1993; 35(2): 113-8.

Strahle J, Muraszko KM, Kapurch J, Bapuraj JR, Garton HJL, Maher CO. Chiari malformation Type I and syrinx in children undergoing magnetic resonance imaging. Journal of Neurosurgery: Pediatrics PED 2011; 8(2): 205.

Su CS, Lan MY, Chang YY, Lin WC, Liu KT. Clinical features, neuroimaging and treatment of spontaneous intracranial hypotension and magnetic resonance imaging evidence of blind epidural blood patch. Eur Neurol 2009; 61(5): 301-7.

Takahashi K, Mima T, Akiba Y. Chronic Subdural Hematoma Associated with Spontaneous Intracranial Hypotension: Therapeutic Strategies and Outcomes of 55 Cases. Neurol Med Chir (Tokyo) 2016; 56(2): 69-76.

Takai K, Niimura M, Hongo H, Umekawa M, Teranishi A, Kayahara T*, et al.* Disturbed Consciousness and Coma: Diagnosis and Management of Intracranial Hypotension Caused by a Spinal Cerebrospinal Fluid Leak. World Neurosurg 2019; 121: e700-e11.

Takeuchi N, Horikoshi T, Kinouchi H, Watanabe A, Yagi T, Mitsuka K*, et al.* Diagnostic value of the optic nerve sheath subarachnoid space in patients with intracranial hypotension syndrome. J Neurosurg 2012; 117(2): 372-7.

Tanaka Y, Tosaka M, Fujimaki H, Honda F, Yoshimoto Y. Sex- and Age-Related Differences in the Clinical and Neuroimaging Characteristics of Patients With Spontaneous Intracranial Hypotension: A Records Review. Headache 2016; 56(8): 1310-6.

Thielen KR, Sillery JC, Morris JM, Hoxworth JM, Diehn FE, Wald JT*, et al.* Ultrafast dynamic computed tomography myelography for the precise

identification of high-flow cerebrospinal fluid leaks caused by spiculated spinal osteophytes. J Neurosurg Spine 2015; 22(3): 324-31.

Thompson S, Asif H, Craven C, Haylock-Vize P, Dyson E, Chari A*, et al.* Elective ICP monitoring: how long is long enough? Fluids and Barriers of the CNS 2015; 12(Suppl 1).

Thompson SD, Coutts A, Craven CL, Toma AK, Thorne LW, Watkins LD. Elective ICP monitoring: how long is long enough? Acta Neurochir (Wien) 2017a; 159(3): 485-90.

Thompson SD, Shand Smith JD, Khan AA, Luoma AMV, Toma AK, Watkins LD. Shunting of the over 80s in normal pressure hydrocephalus. Acta Neurochir (Wien) 2017b; 159(6): 987-94.

Toma AK, Holl E, Kitchen ND, Watkins LD. Evans' index revisited: the need for an alternative in normal pressure hydrocephalus. Neurosurgery 2011; 68(4): 939-44.

Toma AK, Papadopoulos MC, Stapleton S, Kitchen ND, Watkins LD. Systematic review of the outcome of shunt surgery in idiopathic normal-pressure hydrocephalus. Acta Neurochir (Wien) 2013; 155(10): 1977-80.

Tomoda Y, Korogi Y, Aoki T, Morioka T, Takahashi H, Ohno M*, et al.* Detection of cerebrospinal fluid leakage: initial experience with three-

dimensional fast spin-echo magnetic resonance myelography. Acta Radiol 2008; 49(2): 197-203.

Tsai PH, Fuh JL, Lirng JF, Wang SJ. Heavily T2-weighted MR myelography in patients with spontaneous intracranial hypotension: a case-control study. Cephalalgia 2007; 27(8): 929-34.

Tsai YH, Chen HC, Tung H, Wu YY, Chen HM, Pan KJ*, et al.* Noninvasive assessment of intracranial elastance and pressure in spontaneous intracranial hypotension by MRI. J Magn Reson Imaging 2018; 48(5): 1255-63.

Tumani H, Huss A, Bachhuber F. Chapter 2 - The cerebrospinal fluid and barriers – anatomic and physiologic considerations. In: Deisenhammer F, Teunissen CE, Tumani H, editors. Handbook of Clinical Neurology: Elsevier; 2018. p. 21-32.

Tuncel SA, Yılmaz E, Çağlı B, Tekataş A, Çelik Y, Ünlü ME. Lumbar Opening Pressure and Radiologic Scoring in Idiopathic Intracranial Hypertension: Is There Any Correlation? Pol J Radiol 2017; 82: 701-5.

Tung H, Liao YC, Wu CC, Chang MH, Chen CC, Chen PL*, et al.* Usefulness of phase-contrast magnetic resonance imaging for diagnosis and treatment evaluation in patients with SIH. Cephalalgia 2014; 34(8): 584-93.

Vakili S, Moran D, Hung A, Elder BD, Jeon L, Fialho H*, et al.* Timing of surgical treatment for idiopathic normal pressure hydrocephalus: association between treatment delay and reduced short-term benefit. Neurosurg Focus 2016; 41(3): E2.

Van Uitert RL, Eisenstadt ML. Venous pulsations not always indicative of normal intracranial pressure. Arch Neurol 1978; 35(8): 550.

Vender J, Waller J, Dhandapani K, McDonnell D. An evaluation and comparison of intraventricular, intraparenchymal, and fluid-coupled techniques for intracranial pressure monitoring in patients with severe traumatic brain injury. J Clin Monit Comput 2011; 25(4): 231-6.

Verdoorn JT, Luetmer PH, Carr CM, Lane JI, Lehman VT, Morris JM*, et al.* Predicting High-Flow Spinal CSF Leaks in Spontaneous Intracranial Hypotension Using a Spinal MRI-Based Algorithm: Have Repeat CT Myelograms Been Reduced? AJNR Am J Neuroradiol 2016; 37(1): 185-8.

Vernooij MW, Ikram MA, Tanghe HL, Vincent AJPE, Hofman A, Krestin GP*, et al.* Incidental Findings on Brain MRI in the General Population. New England Journal of Medicine 2007; 357(18): 1821-8.

Vijay V, Mollan SP, Mitchell JL, Bilton E, Alimajstorovic Z, Markey KA*, et al.* Using Optical Coherence Tomography as a Surrogate of Measurements of

Intracranial Pressure in Idiopathic Intracranial Hypertension. JAMA Ophthalmol 2020; 138(12): 1264-71.

Vladić A, Klarica M, Bulat M. Dynamics of distribution of 3H-inulin between the cerebrospinal fluid compartments. Brain Res 2009; 1248: 127-35.

Vladić A, Strikić N, Jurčić D, Zmajević M, Klarica M, Bulat M. Homeostatic role of the active transport in elimination of [3H]benzylpenicillin out of the cerebrospinal fluid system. Life Sciences 2000; 67(19): 2375-85.

Voelz K, Kondziella D, von Rautenfeld DB, Brinker T, Lüdemann W. A ferritin tracer study of compensatory spinal CSF outflow pathways in kaolin-induced hydrocephalus. Acta Neuropathol 2007; 113(5): 569-75.

Wagshul ME, Eide PK, Madsen JR. The pulsating brain: A review of experimental and clinical studies of intracranial pulsatility. Fluids Barriers CNS 2011; 8(1): 5.

Walsh TJ, Garden JW, Gallagher B. Obliteration of retinal venous pulsations during elevation of cerebrospinal-fluid pressure. Am J Ophthalmol 1969; 67(6): 954-6.

Wan Y, Xie J, Xie D, Xue Z, Wang Y, Yang S. Clinical characteristics of 15 cases of chronic subdural hematomas due to spontaneous intracranial hypotension with spinal cerebrospinal fluid leak. Acta Neurol Belg 2016; 116(4): 509-12.

Wang M, Ding F, Deng S, Guo X, Wang W, Iliff JJ*, et al.* Focal Solute Trapping and Global Glymphatic Pathway Impairment in a Murine Model of Multiple Microinfarcts. J Neurosci 2017; 37(11): 2870-7.

Wang TY, Karikari IO, Amrhein TJ, Gray L, Kranz PG. Clinical Outcomes Following Surgical Ligation of Cerebrospinal Fluid-Venous Fistula in Patients With Spontaneous Intracranial Hypotension: A Prospective Case Series. Oper Neurosurg (Hagerstown) 2020; 18(3): 239-45.

Wang YF, Lirng JF, Fuh JL, Hseu SS, Wang SJ. Heavily T2-weighted MR myelography vs CT myelography in spontaneous intracranial hypotension. Neurology 2009; 73.

Warden KF, Alizai AM, Trobe JD, Hoff JT. Short-term continuous intraparenchymal intracranial pressure monitoring in presumed idiopathic intracranial hypertension. J Neuroophthalmol 2011; 31(3): 202-5.

Watanabe A, Horikoshi T, Uchida M, Koizumi H, Yagishita T, Kinouchi H. Diagnostic value of spinal MR imaging in spontaneous intracranial hypotension syndrome. AJNR Am J Neuroradiol 2009; 30(1): 147-51.

Watanabe K, Hashizume K, Kawaguchi M, Fujiwara A, Sasaoka N, Furuya H. Fluoroscopically guided epidural blood patch with subsequent spinal CT scans in the treatment of spontaneous cerebrospinal fluid hypovolemia. J Neurosurg 2011; 114(6): 1731-5.

Welch K. Secretion of cerebrospinal fluid by choroid plexus of the rabbit. Am J Physiol 1963; 205: 617-24.

Wiesemann E, Berding G, Goetz F, Windhagen A. Spontaneous intracranial hypotension: correlation of imaging findings with clinical features. Eur Neurol 2006; 56(4): 204-10.

Williams MA, Malm J. Diagnosis and Treatment of Idiopathic Normal Pressure Hydrocephalus. Continuum (Minneap Minn) 2016; 22(2 Dementia): 579-99.

Wong SH, White RP. The clinical validity of the spontaneous retinal venous pulsation. J Neuroophthalmol 2013; 33(1): 17-20.

Wu JW, Hseu SS, Fuh JL, Lirng JF, Wang YF, Chen WT*, et al.* Factors predicting response to the first epidural blood patch in spontaneous intracranial hypotension. Brain 2017; 140(2): 344-52.

Xia P, Hu XY, Wang J, Hu BB, Xu QL, Zhou ZJ*, et al.* Risk factors for subdural haematoma in patients with spontaneous intracranial hypotension. PLoS One 2015; 10(4): e0123616.

Xia P, Zhang SR, Zhou ZJ, Shao YQ, Hu XY. Benign paroxysmal positional vertigo in spontaneous intracranial hypotension. Neurol Res 2018; 40(10): 868-73.

Xie L, Kang H, Xu Q, Chen MJ, Liao Y, Thiyagarajan M*, et al.* Sleep drives metabolite clearance from the adult brain. Science 2013; 342(6156): 373-7.

Xu DS, Hlubek RJ, Mulholland CB, Knievel KL, Smith KA, Nakaji P. Use of Intracranial Pressure Monitoring Frequently Refutes Diagnosis of Idiopathic Intracranial Hypertension. World Neurosurg 2017a; 104: 167-70.

Xu DS, Hlubek RJ, Mulholland CB, Knievel KL, Smith KA, Nakaji P. Use of Intracranial Pressure Monitoring Frequently Refutes Diagnosis of Idiopathic Intracranial Hypertension. World Neurosurgery 2017b; 104: 167-70.

Yagi T, Horikoshi T, Senbokuya N, Murayama H, Kinouchi H. Distribution Patterns of Spinal Epidural Fluid in Patients with Spontaneous Intracranial Hypotension Syndrome. Neurol Med Chir (Tokyo) 2018; 58(5): 212-8.

Yamada S. Cerebrospinal fluid dynamics. Croat Med J 2021; 62(4): 399-410.

Yamada S, Miyazaki M, Kanazawa H, Higashi M, Morohoshi Y, Bluml S*, et al.* Visualization of cerebrospinal fluid movement with spin labeling at MR imaging: preliminary results in normal and pathophysiologic conditions. Radiology 2008; 249(2): 644-52.

Yamada S, Tsuchiya K, Bradley WG, Law M, Winkler ML, Borzage MT*, et al.* Current and emerging MR imaging techniques for the diagnosis and management of CSF flow disorders: a review of phase-contrast and time-spatial labeling inversion pulse. AJNR Am J Neuroradiol 2015; 36(4): 623-30.

Yao LL, Hu XY. Factors affecting cerebrospinal fluid opening pressure in patients with spontaneous intracranial hypotension. J Zhejiang Univ Sci B 2017; 18(7): 577-85.

Yoo HM, Kim SJ, Choi CG, Lee DH, Lee JH, Suh DC*, et al.* Detection of CSF leak in spinal CSF leak syndrome using MR myelography: correlation with radioisotope cisternography. AJNR Am J Neuroradiol 2008; 29(4): 649-54.

Yoon SH, Chung YS, Yoon BW, Kim JE, Paek SH, Kim DG. Clinical experiences with spontaneous intracranial hypotension: a proposal of a diagnostic approach and treatment. Clin Neurol Neurosurg 2011; 113(5): 373-9.

Yoshida H, Takai K, Taniguchi M. Leakage detection on CT myelography for targeted epidural blood patch in spontaneous cerebrospinal fluid leaks: calcified or ossified spinal lesions ventral to the thecal sac. J Neurosurg Spine 2014; 21(3): 432-41.

Yri HM, Jensen RH. Idiopathic intracranial hypertension: Clinical nosography and field-testing of the ICHD diagnostic criteria. A case-control study. Cephalalgia 2015; 35(7): 553-62.

Yuh WT, Zhu M, Taoka T, Quets JP, Maley JE, Muhonen MG*, et al.* MR imaging of pituitary morphology in idiopathic intracranial hypertension. J Magn Reson Imaging 2000; 12(6): 808-13.

Zada G, Pezeshkian P, Giannotta S. Spontaneous intracranial hypotension and immediate improvement following epidural blood patch placement demonstrated by intracranial pressure monitoring. Journal of Neurosurgery JNS 2007; 106(6): 1089.

Zakharov A, Papaiconomou C, Koh L, Djenic J, Bozanovic-Sosic R, Johnston M. Integrating the roles of extracranial lymphatics and intracranial veins in cerebrospinal fluid absorption in sheep. Microvasc Res 2004; 67(1): 96-104.

Zeiler FA, Donnelly J, Menon DK, Smielewski P, Hutchinson PJA, Czosnyka M. A Description of a New Continuous Physiological Index in Traumatic Brain Injury Using the Correlation between Pulse Amplitude of Intracranial Pressure and Cerebral Perfusion Pressure. J Neurotrauma 2018; 35(7): 963-74.

Zhang X, Medow JE, Iskandar BJ, Wang F, Shokoueinejad M, Koueik J*, et al.* Invasive and noninvasive means of measuring intracranial pressure: a review. Physiol Meas 2017; 38(8): R143-r82.

Zheng W, Chodobski A. The blood-cerebrospinal fluid barrier: CRC Press; 2005.